Asymmetric Synthesis of Chiral-at-Metal Complexes with Pentadentate Bis(oxazoline) Ligands

Dissertation zur Erlangung
des Doktorgrades der Naturwissenschaften (Dr. rer. nat.)
der Naturwissenschaftlichen Fakultät IV – Chemie und Pharmazie

vorgelegt von
Michael Seitz
aus Passau

2004

Diese Arbeit wurde angeleitet von Prof. Dr. O. Reiser

Promotionsgesuch eingereicht am: 24.06.2004

Tag der mündlichen Prüfung: 15.07.2004

Prüfungsausschuß: Prof. Dr. G. Schmeer (Vorsitzender)
Prof. Dr. O. Reiser (1. Gutachter)
Prof. Dr. H. Brunner (2. Gutachter)
Prof. Dr. G. Märkl (3. Prüfer)

Die vorliegende Arbeit entstand in der Zeit von November 2000 bis Juli 2004 am Lehrstuhl Prof. Dr. O. Reiser, Institut für Organische Chemie, Universität Regensburg und im Rahmen eines Auslandsaufenthaltes von Februar bis Mai 2003 in der Arbeitsgruppe von Prof. Dr. A. S. Borovik am Department of Chemistry, University of Kansas (Lawrence, USA).

Ich danke meinem Lehrer,

Herrn Prof. Dr. O. Reiser

für die interessant Themenstellung, die beständige Unterstützung in jeglicher Hinsicht und das entgegengebrachte Vertrauen.

für Jana

Table of Contents

Supporting Information (1 CD, ca. 180 MB, only available for group members):

Table of Contents

0. Preface

Symmetry is one of the most ubiquitous phenomena in our life. Normally, we are so used to it that we are often not even aware of the impact it has. For example, symmetry is often associated with beauty, most of the time unconsciously. This is true not only regarding works of art like Leonardo da Vinci´s “Vitruvian” or the Taj Mahal (Figure 0.1), but also with respect to the attractiveness of a person.

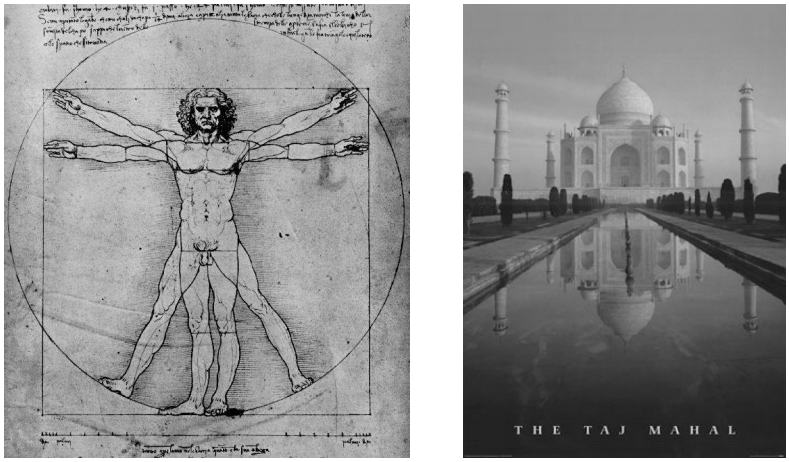

Figure 0.1. Leonardo da Vinci´s “Vitruvian” and the Taj Mahal

Besides this, symmetry is also a very successful design principle of life in general. There must be a reason why evolution chose many living things to be symmetric. Almost every higher organsim exhibits, at least on a macroscopic level, mirror-image shape. Nobody wonders, of course, why we have two eyes, two ears or two hands.

Figure 0.2. Symmetric Eastern Tiger Swallowtail

Nevertheless, the existence of a mirror-image relationship implies also a very subtle form of symmetry, namely chirality. The fact, that things can be mirror-images, but not superimposable, is an every day phenomenon. For example cars, one

“enantiomer” of which is driving in left-hand traffic countries like the UK, the other one on the roads of the rest of the world. Or our own body, where normally only one chiral form is observed, namely those with the hearts on the left side. This brings us to an astonishing phenomenon in living nature: the homochirality of life.

The “enantiopurity” of humans on a macroscopic level is reflected also in the world of submiscroscopic dimensions. In general, nature has chosen to predominantely have one form of chiral molecules. That is why (*L*)-amino acids or (*D*)-sugars are among the most important building blocks for the generation of living systems. Not only on a molecular, but also on a higher level chirality can be found e.g. in α-helices of proteins or double-stranded DNA (Figure 0.3).

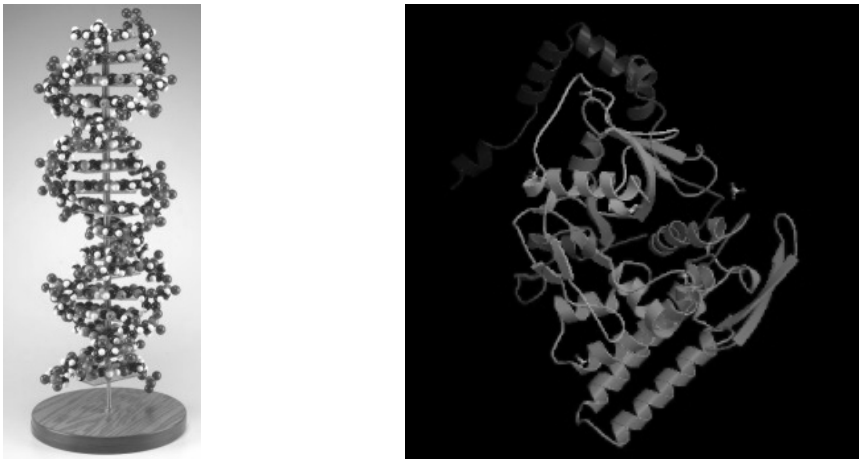

Figure 0.3. Chiral helices in nature: DNA-model and protein structure

The question of homochirality is probably closely connected to the origin of life itself. Why nature was able to prefer only one form of enantiomers is still far from being completely understood, especially because in classical physics it was long believed, that the equivalence of left and right is a given thing and this was expressed in the conservation law of parity. Only in the second half of the last century, first steps to unravel this mystery were made. An important milestone was the spectacular finding of Yang and Lee in 1956 (Nobel price 1957), that parity is not conserved in the β-decay of ^{60}Co.[1] They showed, that in principle left and right need not be equal. And indeed, nowadays it is possible to determine energy differences of enantiomeric molecules resulting from parity violation.[2] Nevertheless, the effects are normally too small to be observable, even on a microscopic level. Since Soai´s report, however, on an autocatalytic system (Scheme 0.1) that creates enantiopure molecules from almost racemic mixtures in the 90´s of the last century, we have an impression of

how this strong amplification of chiral information could have been achieved by nature on the basis of only tiny differences.[3]

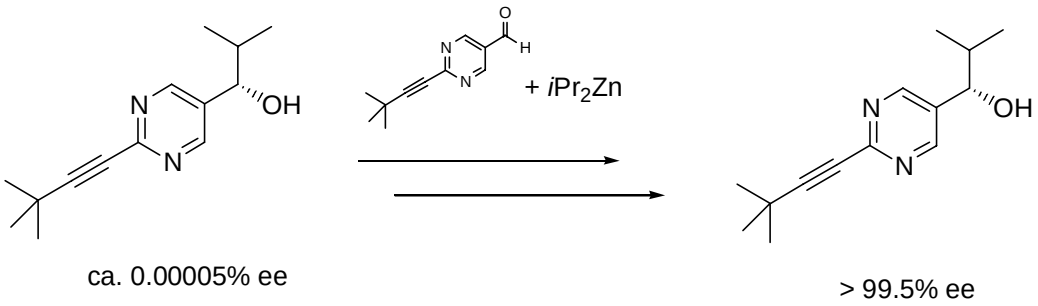

ca. 0.00005% ee

> 99.5% ee

Scheme 0.1. Soai´s discovery of autocatalytic asymmetric amplification

This is only one story in the fascinating field of chirality, but certainly one of the most important, touching the very basis of life and our view of the world. This was one of my personal motivations for this thesis, investigating the formation of certain classes of (in the best case) homochiral molecules and assemblies thereof. Maybe it can help to understand a few aspects of the always surprising nature of our world.

References:

[1] Nobel price lectures of C.N. Yang and T.D. Lee, 1957.

[2] Review: L. Keszthelyi, *Mendeleev Commun.* **2003**, *3*, 129-131.

[3] a) I. Sato, H. Urabe, S. Ishiguro, T. Shibata, K. Soai, *Angew. Chem. Int. Ed.* **2003**, *42*, 315-317 and refs. cited therein;

b) Review: D.G. Blackmond, *Proc. Natl. Acad. Sci. USA* **2004**, *101*, 5732-5736.

1. Introduction

1.1 Background

The stereoselective synthesis of only one enantiomer is a big challenge in chemistry. Different disciplines of chemistry have reached different stages of sophistication. The by far most efficient methods involving asymmetric synthesis have been developed in the area of organic chemistry.[1] Today this field is in a rather mature stage, enabling the synthesis of incredible complex chiral strucures. The availability of numerous very efficient methods culminates in perhaps the most impressive achievements, enantioselective total syntheses of natural products[2] like Longithorone A[3] (Figure 1.1) or Diazonamide A[4]

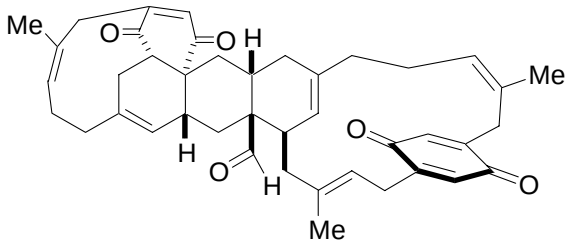

Longithorone A

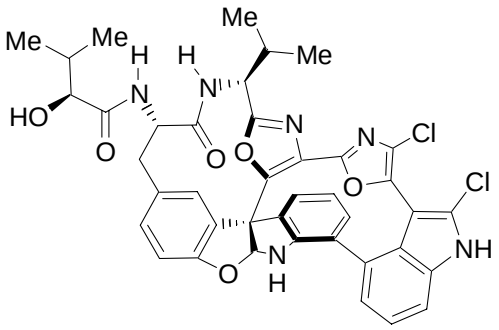

Diazonamide A

Figure 1.1. Total synthesis of complex organic molecules

The most important structural feature in chiral organic molecules is the carbon center with for different substituents (Figure 1.2).

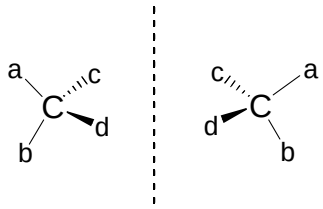

Figure 1.2. Tetrahedral C-atoms with four different substituents are stereogenic centers

Nevertheless, the existence of stereogenic carbon atoms is not sufficient for the existence of chirality, being a global property of a system. In general, the absence of an improper axis of rotation S_n is the requirement for a system to be chiral. Especially two S_n-axes are found most often, S_1 (≡ mirror plane) or S_2 (≡ center of inversion). The absence of a S_n-axis is the criterion for chirality that must be applied to the entire

system. Consequently, there are a number of other common motives besides asymmetric carbon atoms that can lead to chirality (Figures 1.3 - 1.5).

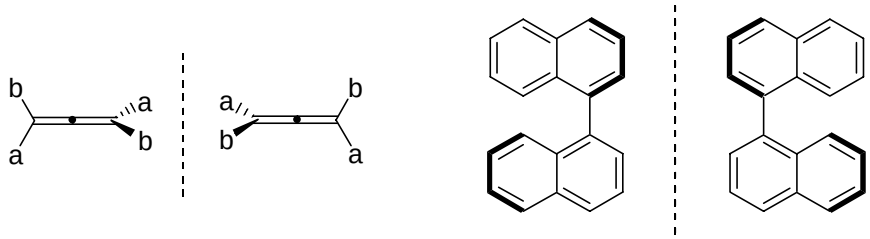

Figure 1.3. Axial chirality in allenes and binaphthyls

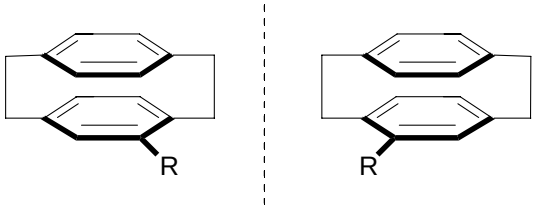

Figure 1.4. Planar chirality in paracyclophanes

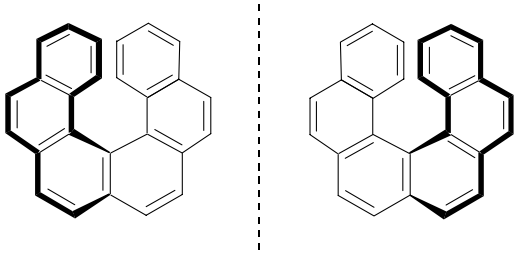

Figure 1.5 Helical chirality in helicenes

Nowadays, it is not only possible to build up chiral organic structures with stoichiometric asymmetric methodolody but also through catalysis using only substoichiometric amounts of chiral information with sometimes surprising degrees of selectivity. Many problems remain unsolved, especially with respect to industrial application. However, in principle, most of the commonly used reaction types are amenable to asymmetric catalysis.[5]

In the field of asymmetric inorganic synthesis,[6] the problem of stereoselective construction of chiral structures turns out to be more difficult. This is mainly due to the increased number of possible coordination geometries or central atoms and often also because of the lability of the ligands towards substitution. Carbon is in this respect unique among other atoms, having a strong preference for coordination numbers smaller than five and most importantly shows relative substitution and configuration stability, at least in a way to allow the isolation of defined stereoisomers

in many cases. The first breakthrough for inorganic stereochemistry was achieved by Alfred Werner as early as 1911 with the separation of enantiopure octahedral cobalt complexes (Scheme 1.1).[7]

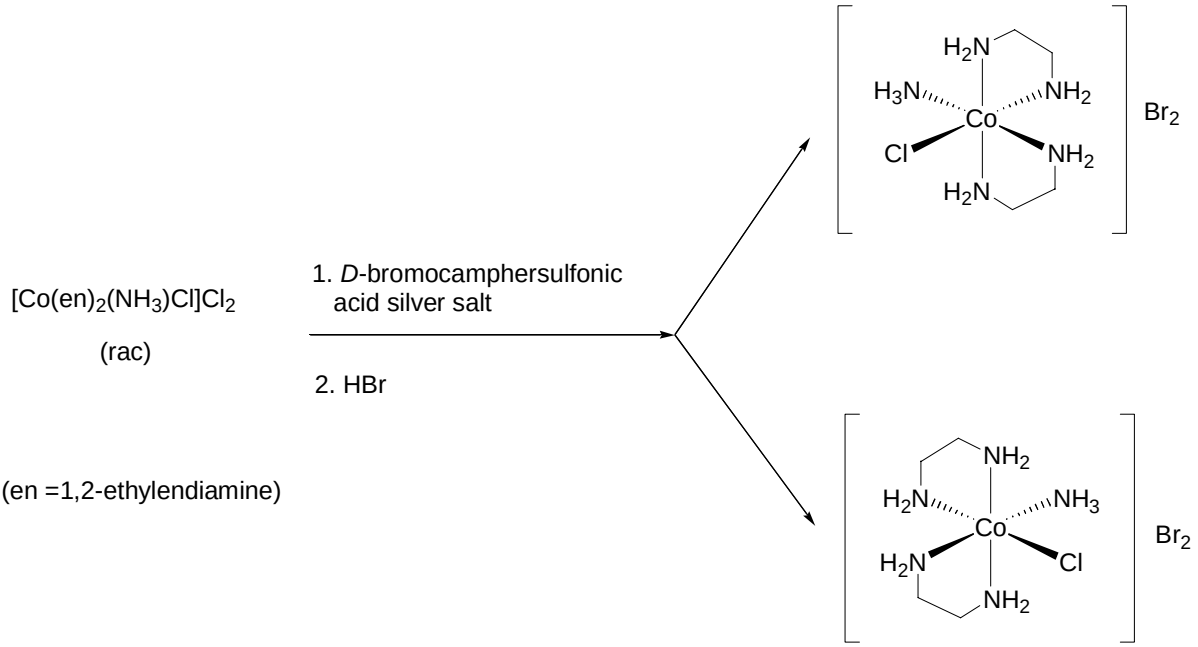

Scheme 1.1. First separation of enantiomeric metal complexes by A. Werner in 1911

Since then, many examples for these Werner-type chiral complexes have been reported. Especially octahedral metal tris-chelates $[M(ab)_3]^{n+}$ with bidentate ligand have found extensive application. With chiral, non-racemic ligands it was also possible to stereoselectively create complexes of this type with predetermination of the configuration at the metal as stereogenic center.[8] Among the most successful ligands are Zelewsky´s chiragen ligands (Scheme 1.2).[9]

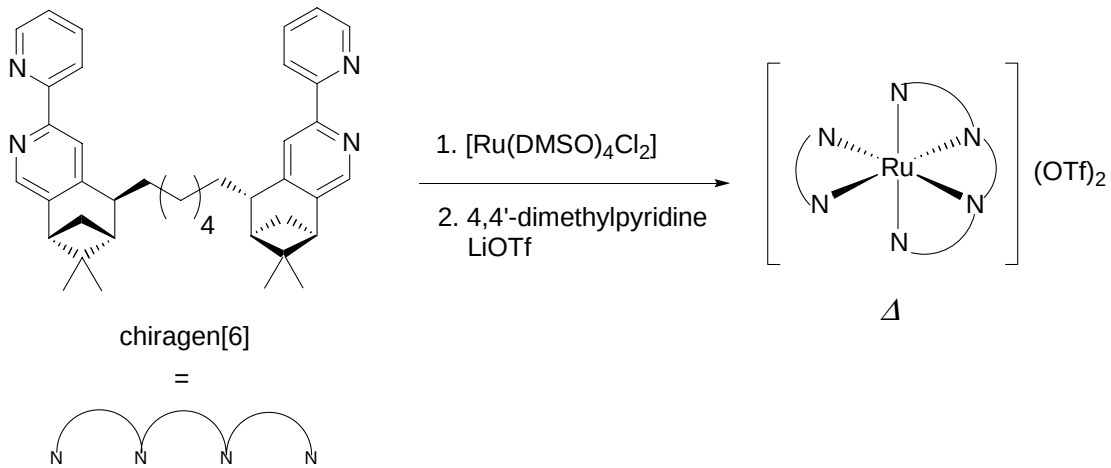

Scheme 1.2. Stereoselective formation of octahedral Ru-chiragen complexes

Besides the formation of chiral Werner-type compounds, chiral organometallic complexes have been an early subject of investigation. Soon after the discovery of ferrocene[10] in 1951, the first disubstitued chiral derivatives could be resolved, followed by a number of other reports of similar π-complexes (Figure 1.6),[11] all of which exhibit planar chirality. Compounds of this type have found numerous application in modern chemistry.

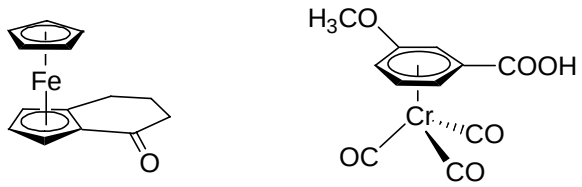

(ref. 11a) (ref. 11d)

Figure 1.6. Early examples of resolved enantiomers of planar chiral organometallic complexes

However, the occurence of chirality is not restricted to complexes with a plane as element of chirality. In 1969, the first organometallic complex was resolved with the metal as stereogenic center (Figure 1.7).[12] Since then, many other compounds of this type have been synthesized with a single stereochemical configuration.[13]

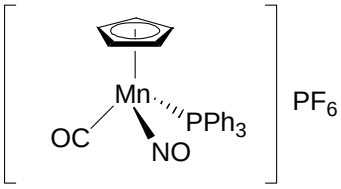

Figure 1.7. One of the first examples of resolved chiral organometallic complexes

The issue of stereochemistry becomes more and more important with the extension from mononuclear complexes to oligo- or polynuclear species, because an increasing number of stereogenic centers results in many possible diastereomeric compounds. This is one of the most important problems in supramolecular chemistry and has been dedicated a great deal of attention.[14] A complete overview of this rapidly growing field would require a multivolume treatise and goes way beyond the scope of this introduction. Nevertheless, a few selected examples should illustrate the nature of chirality in this area of reasearch, offering a potential degree of complexity comparable to organic chemistry.

Among the most prominent chiral structures in supramolecular chemistry are the so-called “helicates”.[15] This term was introduced by Lehn in 1987 (Scheme 1.3),[16] although a few examples[15a] were known before. Helicates are oligonuclear assemblies of metal ions with one or more strands of bridging organic ligands in the form of a helix. This shape introduces an element of chirality.

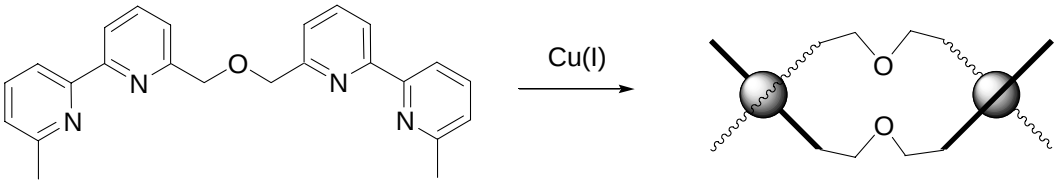

Scheme 1.3. Lehn´s first example of a “helicate”

If non-chiral ligands are employed, normally a racemic mixture is obtained. By the use of enantiomerically pure ligands, Lehn was also the first to show the asymmetric synthesis of helicates.[17]

Another fascinating area is the construction of chiral polyhedral three-dimensional structures,[18] most prominently represented by tetranuclear metal clusters with T-symmetry. The first examples were introduced by Saalfrank[19] using transition metal complexes with achiral chelating ligands. The first separation of the enantiomeric clusters from achiral ligands was accomplished by Raymond (Figure 1.8).[20] Interessingly, the clusters proved to be extraordinary stable towards racemization. Stack showed, that the use of chiral, non-racemic ligands can also lead to homochiral tetrahedral clusters, thus exhibiting complete diastereoselectivity.[21]

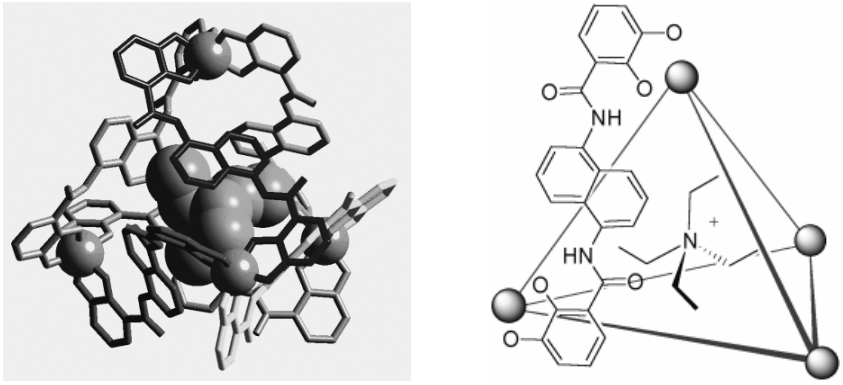

Figure 1.8. Raymond´s enantiomerically pure tetranuclear Ga-cluster (reproduced from ref. 20b).

There are many more examples for chirality in supramolecular chemistry using metal complexes,[22] too many to mention here. The wide field of topological chirality in catenanes, knots, rotaxanes, etc. also goes way beyond the limited scope of this introduction.[23]

In conclusion, the area of inorganic stereochemistry has been a rapidly evolving research subject through the last few decades. Especially, many complex chiral motives have been realized, although most of the time only as racemic mixtures. Nevertheless, the basis for the asymmetric generation of certain stereogenic elements is in most of the cases the control of the configuration at single metal centers. The development of methods for this purpose has therefore attracted more and more attention during the last years. Still, this field is far from being sufficiently explored and should hold a manifold of discoveries for the future.

1.2 Aim of this Work

The starting point for this work was the idea to design a chiral model for bleomycin,[24] a metal-containing glycooligo-peptide antibiotic capable of oxidative DNA-strand scission (Figure 1.9).

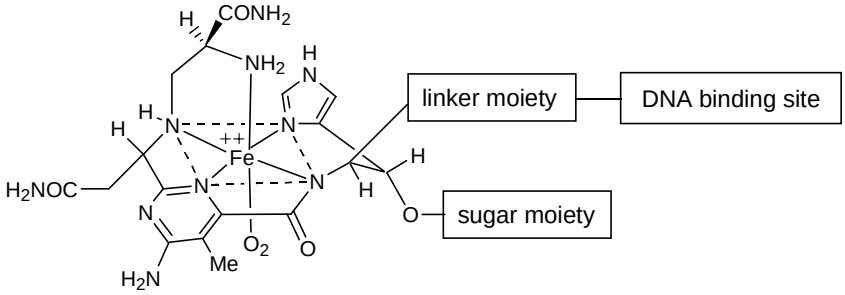

Figure 1.9. The active site of bleomycin with O_2 coordinated

This species utilizes dioxygen for the oxidative DNA-strand scission. O_2 is activated by an Fe(II)-metal-center, surrounded by five N-donors and having octahedral geometry. The activation of dioxygen at mononuclear non-heme metal centers has recently attracted great interest.[25] Therefore, a number of model systems for activated bleomycin[26] have been developed on the basis of pentadentate ligands (Figure 1.10).

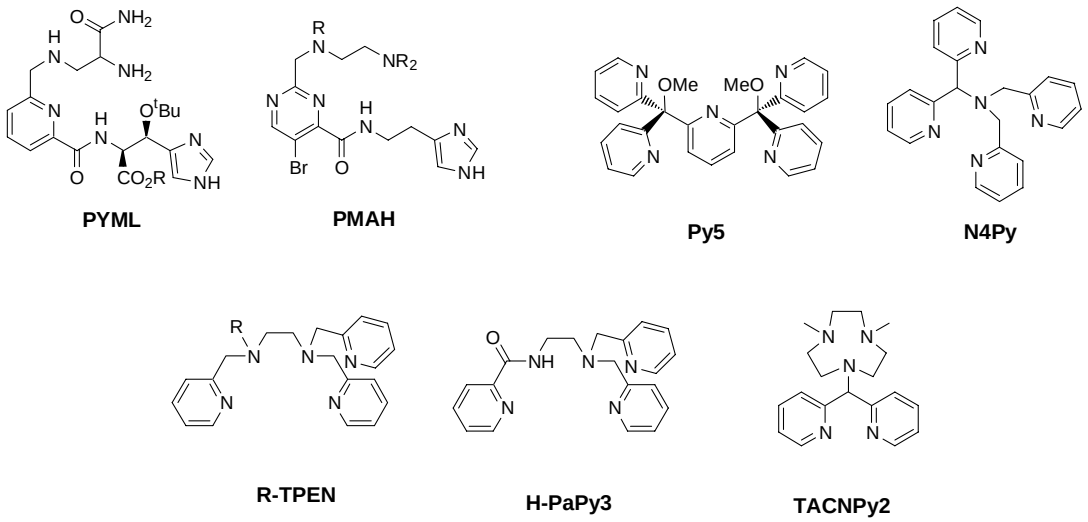

Figure 1.10. Synthetic model systems for activated bleomycin

While early attempts (like **PYML** and **PMAH**) resemble the structure of the active site of natural bleomycin very closely, the other model systems keep only the characteristic pyridine-containing five-N-donor-set. All of them are able to perform certain aspects of the bleomycin-reactivity. Nevertheless, only the deprotonated, monoanionic amide-ligands activate dioxygen in combination with Fe(II). In contrast, the Fe(III)-complexes of the other neutral ligands are usually transferred to reactive compounds by treatment with peroxo-reagents, like H_2O_2. Furthermore, besides bleomycin itself and the closely related, but not easily accessible **PYML**, no other ligand is chiral. Upon complexation of some of these ligands to a metal, the generation of stereogenic elements can be expected, but only as a racemic mixture.

The stabilization of highly reactive metal-oxo-fragments can be achieved by hydrogen bonds. The first structurally characterized iron complex containing a single terminal oxo-ligand, reported by Borovik,[27] showed a network of stabilizing hydrogen bonds (Figure 1.11).

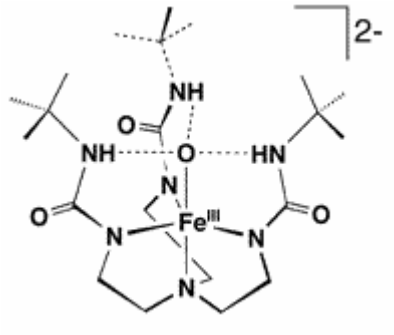

Figure 1.11. H-bonds can stabilize metal-oxo-fragments

The past research in our group has also focussed on the utilization of secondary interactions for asymmetric catalysis using bis(oxazoline) ligands with additional H-donor-groups (Scheme 1.4).[28]

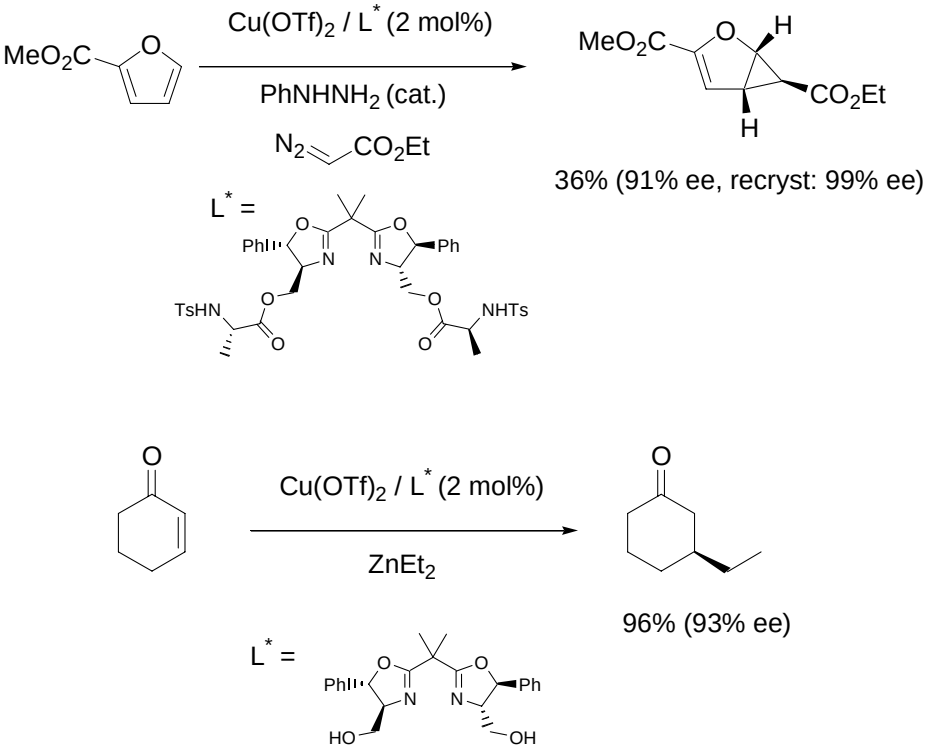

Scheme 1.4. Asymmetric catalysis via secondary interaction developed by the Reiser group.

The idea was to combine the characteristic features of bleomycin with our previous concept of chiral ligands with stabilizing secondary H-donor sites. The following requirements seemed appropriate:

- Pentadentate ligands with variable donor set, containing aromatic N-heterocycles (pyridine, pyrimidine) and providing the possibility for octahedral geometry.
- Chiral, non-racemic ligands with secondary H-donors, preferably with C_2- or higher symmetry.
- Facile synthetic accessibility of the ligands, especially regarding the source of chirality.
- Flexible assembly of the ligand structure to allow rapid variation of donor set and secondary sites.

These conditions could be met by the final design proposal of the general structure **1** (Figure 1.12).

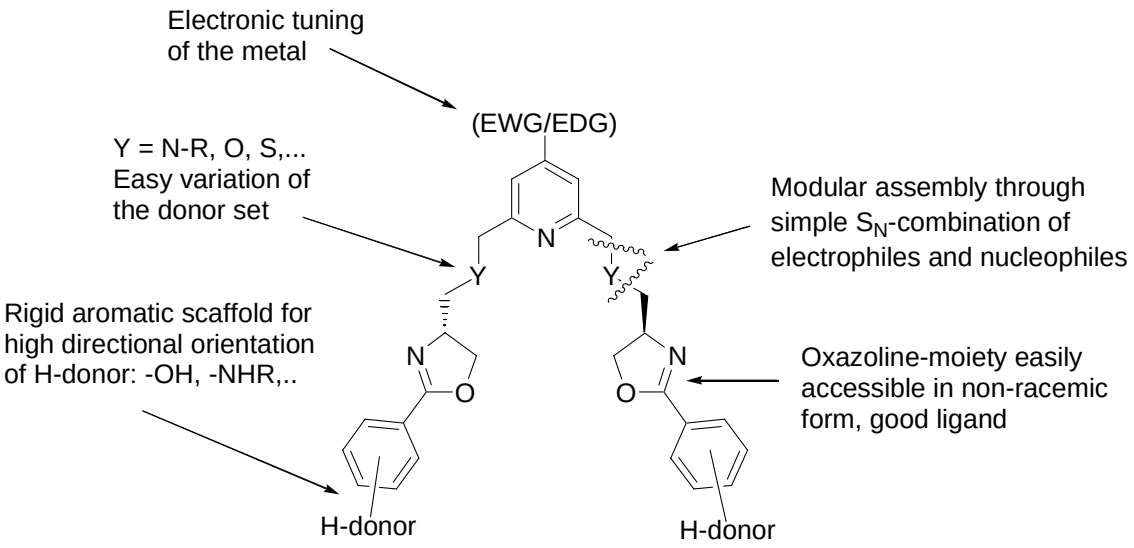

1

Figure 1.12. Our proposed design for chiral pentadentate ligands as bleomycin models.

This structural blueprint has several specific features:

- C_2-symmetry: Introduced by Kagan[29] into asymmetric catalysis, has proved to be a powerful concept.
- Oxazoline-ligands: First used by Brunner[30] in asymmetric catalysis, strongly coordinating to various metals, excellent accessibility from non-racemic amino acids
- Flexible connection of the pyridine unit and the heterocyclic oxazolines with Y: For the design of **1**, we combined the work of Newkome[31] (C_2-symmetry of cobalt complexes with his achiral pentadentate ligands) and Bernauer[32] (predetermination of metal-centered chirality with chiral, non-racemic pentadentate ligands) (Figure 1.13).

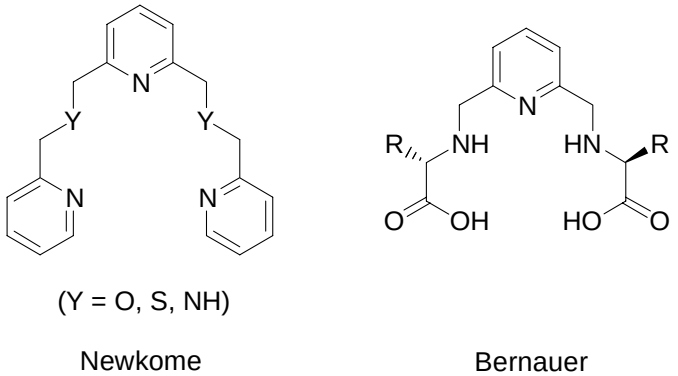

Figure 1.13. The basis of design of **1**: Newkome´s (left) and Bernauer´s ligand system (right)

- Pyridine: The electronic situation at the metal can be influenced by suitable substituents at the heteroaromatic system, as shown for the similar pyridine bis(oxazolines) by Nishiyama.[33] Furthermore, the pyridine serves as excellent chromophore for the measurement of circular dichroism (vide infra).
- Donors in benzylic position: Offer both, good possibility for connecting modular subunits by S_N-reactions and facile variation of the donor set. Provides high flexibility of the ligand which should in principle enable many coordination geometries.
- The steric as well as the electronic situation at the phenyl rings can easily be altered through suitable choice of the achiral carboxyl component of the oxazoline. Highly directed introduction of H-donors on the rigid aromatic scaffold is possible.

The corresponding metal complexes were modelled on a semi-empirical level (PM3-TM, Titan 1.0.5) to get a first hint for the coordination geometry. In the first instance this was done not to predict the exact structures but to exclude unexpected simple problems for metal complexation. The obtained complexes were encouraging, so the decision was made to hang on to this design.

The task of this work was to elucidate the basic coordination behavior and, because with complexation a couple of new stereogenic centers are introduced, the diastereoselectivity with regard to the configuration at the metal center (see 1.1). To make matters as easy as possible without losing important characteristic features, the blueprint **1** was truncated to the model system **2** (Figure 1.14).

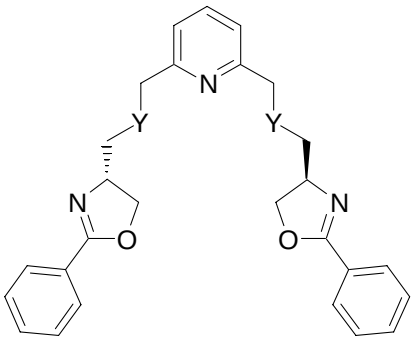

2a: Y = O
2b: Y = S
2c: Y = NMe

Figure 1.14. Model system investigated in this work

This system proved to be in in accordance with many of our expectations. Nevertheless, many surprises waited for the alert beholder along the way....

References:

[1] E.L. Eliel, S.H. Wilen, *Stereochemistry of Organic Compounds* **1994**, Wiley, New York.

[2] K.C. Nicolaou, S. Snyder, *Classics in Total Synthesis II* **2003**, Wiley-VCH, Weinheim.

[3] M.E. Layton, C.A. Morales, M.D. Shair, *J. Am. Chem. Soc.* **2002**, *124*, 773-775.

[4] K.C. Nicolaou, M. Bella, D.Y.-K. Chen, X. Huang, T. Ling, S.A. Snyder, *Angew. Chem. Int. Ed.* **2002**, *41*, 3495-3499.

[5] *Comprehensive Asymmetric Catalysis I-III (Incl. Supplement 1+2)* (Eds.: E.N. Jacobsen, A. Pfaltz, H. Yamamoto) **2004**, Springer, Heidelberg.

[6] A. Von Zelewsky, *Stereochemistry of Coordination Compounds* **1996**, Wiley, Chichester.

[7] A. Werner, *Chem. Ber.* **1911**, *44*, 1887-1899.

[8] U. Knof, A. Von Zelewsky, *Angew. Chem. Int. Ed.* **1999**, *38*, 303-322.

[9] P. Hayoz, A. Von Zelewsky, H. Stoeckli-Evans, *J. Am. Chem. Soc.* **1993**, *115*, 5111-5114.

[10] T.J. Kealy, P.L. Paulson, *Nature* **1951**, *168*, 1039-1040.

[11] a) J.B. Thomson, *Tetrahedron Lett.* **1959**, *1(6)*, 26; b) R. Riemschneider, W. Herrmann, *Ann. Chem.* **1961**, *648*, 68; c) L. Westman, K.L. Rinehart, Jr., *Acta Chem. Scand.* **1962**, *16*, 1199; d) A. Mandelbaum, Z. Neuwirth, M. Cais, *Inorg. Chem.* **1963**, *2*, 902-903.

[12] a) H. Brunner, *Angew. Chem. Int. Ed.* **1969**, *8*, 382; b) H. Brunner, H.-D. Schindler, *J. Organometal. Chem.* **1970**, *24(1)*, C7-C10.

[13] Review: H. Brunner, *Angew. Chem. Int. Ed.* **1999**, *38*, 1194-1208.

[14] a) J.-M. Lehn, *Supramolecular Chemistry, Concepts and Perspectives* **1995**, VCH, Weinheim; b) *Comprehensive Supramolecular Chemistry* (Eds.: J.L. Atwood, J.E.D. Davies, D.D. Macnicol, F. Vögtle, J.-M. Lehn, J.-P. Sauvage, M.W. Hosseini) **1996**, Pergamon, Oxford; c) *Transition Metals in Supramolecular Chemistry* (Ed.: J.-P. Sauvage) **1999**, Wiley-VCH, Weinheim; d) S. Leininger, B. Olenyuk, P. Stang, *Chem. Rev.* **2000**, *100*, 853-908.

[15] a) M. Albrecht, *Chem. Rev.* **2001**, *101*, 3457-3497; b) C. Piguet, G. Bernardinelli, G. Hopfgartner, *Chem. Rev.* **1997**, *97*, 2005-2062.

[16] J.-M. Lehn, A. Rigault, J. Siegel, J. Harrowfield, B. Chevrier, D. Moras, *Proc. Natl. Acad. Sci. USA* **1987**, *84*, 2565-2569.

[17] W. Zarges, J. Hall, J.-M. Lehn, C. Bolm, *Helv. Chim. Acta* **1991**, *74*, 1843-1852.

[18] a) D.L. Caulder, K.N. Raymond, *J. Chem. Soc., Dalton Trans.* **2000**, 1185-1200; b) T.D. Hamilton, L.R. MacGillivray, *Crystal Growth & Design* **2004**, *4*, 419-430.

[19] a) R.W. Saalfrank, A. Stark, K. Peters, H.G. Von Schnering, *Angew. Chem. Int. Ed.* **1988**, *27*, 851-853; b) R.W. Saalfrank, A. Stark, M. Bremer, H.-U. Hummel, *Angew. Chem. Int. Ed.* **1990,** *29*, 311-314.

[20] a) A.J. Terpin, M. Ziegler, D.W. Johnson, K.N. Raymond, *Angew. Chem. Int. Ed.* **2001**, *40*, 157-160; b) M. Ziegler, A.V. Davis, D.W. Johnson, K.N. Raymond, *Angew. Chem. Int. Ed.* **2003**, *42*, 665-668.

[21] E.J. Enemark, T.D.P. Stack, *Angew. Chem. Int. Ed.* **1998**, *37*, 932-935.

[22] C. Provent, A.F. Williams, *Transition Metals in Supramolecular Chemistry* (Ed.: J.-P. Sauvage) **1999**, Chapter 4 (p. 135-191), Wiley-VCH, Weinheim.

[23] a) *Molecular Catenanes, Rotaxanes and Knots: A Journey Through the World of Molecular Topology* (Eds.: J.-P. Sauvage, C. Dietrich-Buchenecker) **1999**, Wiley-VCH, Weinheim; b) D.B. Amabilino, J.F. Stoddart, *Chem. Rev.* **1995**, *95*, 2725-2829.

[24] a) J. Stubbe, J. Kozarich, W. Wu, D. E. Vanderwall, *Acc. Chem. Res.* **1996**, *29*, 322-330; b) R. M. Burger, *Struct. Bonding* **2000**, *97*, 287-303; c) L.J. Ming, *Med. Res. Rev.* **2003**, *23*, 697-762.

[25] M. Costas, M.P. Mehn, M.P. Jensen, L. Que, Jr., *Chem. Rev.* **2004**, *104*, 939-986.

[26] a) **PYML**: A. Kittaka, Y. Sugano, M. Otsuka, M. Ohno, Y. Sugiura, H. Umezawa, *Tetrahedron Lett.* **1986**, *27*, 3631-3634; b) **PMAH**: R.J. Guajardo, S.E. Hudson, S.J. Brown, P.K. Mascharak, *J. Am. Chem. Soc.* **1993**, *115,* 7971-7977; c) **Py5**: M.E. De Vries, R.M. La Crois, G. Roelfes, H. Kooijman, A.L. Spek, R. Hage, B.L. Feringa, *Chem. Commun.* **1997**, 1549-1550; d) **N4Py**: M. Lubben, A. Meetsma, E.C. Wilkinson, B.L. Feringa, L. Que, Jr., *Angew. Chem. Int. Ed.* **1995**, *34*, 1512-1514; e) **R-TPEN**: I. Bernal, I.M. Jensen, K.B. Jensen, C.J. McKenzie, H. Toftlund, J.P. Tuchagues, *J. Chem. Soc., Dalton Trans.* **1995**, 3667-3675; A.J. Simaan, F. Banse, P. Mialane, A. Boussac, S. Un, T. Kargar-Grisel, G. Bouchoux, J.-J. Girerd, *Eur. J. Inorg. Chem.* **1999**, 993-996; A. Hazell, C.J. McKenzie, L.P. Nilsen, S. Schindler, M. Weitzer, *J. Chem. Soc., Dalton Trans.* **2002**, 310-317. f) **H-PaPy3**: J.M. Rowland, M.M. Olmstead, P.K. Mascharak, *Inorg. Chem.* **2001**, *40*, 2180-2817; g) **TACNPy2**: G. Roelfes, V.

Vraymasu, K. Chen, R.Y.N. Ho, J.-U. Rohde, C. Zondervan, R.M. La Crois, E.P. Schudde, M. Lutz, A.L. Spek, R. Hage, B.L. Feringa, E. Münck, L. Que, Jr., *Inorg. Chem.* **2003**, *42*, 2639-2653.

[27] a) C.E. Macbeth, A.P. Golombek, V.G. Young, Jr., C. Yang, K. Kuczera, M.P. Hendrich, A.S. Borovik, *Science* **2000**, *289*, 938-941; b) C.E. MacBeth, R. Gupta, K.R. Mitchell-Koch, V.G. Young, Jr., G.H. Lushington, W.H. Thompson, M.P. Hendrich, A.S. Borovik, *J. Am. Chem. Soc.* **2004**, *126*, 2556-2567.

[28] a) M. Schinnerl, M. Seitz, A. Kaiser, O. Reiser, *Org. Lett.* **2001**, *3*, 4259-4262; b) M. Schinnerl, C. Böhm, M. Seitz, O. Reiser, *Tetrahedron: Asymmetry* **2003**, *14*, 765-771.

[29] H.B. Kagan, T.-P. Dang, *J. Am. Chem. Soc.* **1972**, *94*, 6429-6433.

[30] H. Brunner, U. Obermann, *Chem. Ber.* **1989**, *112*, 499-508.

[31] G.R. Newkome, V.K. Gupta, F.R. Fronczek, S. Pappalardo, *Inorg. Chem.* **1984**, *23*, 2400-2408.

[32] a) K. Bernauer, P. Pousaz, J. Porret, J. Jeanguenat, *Helv. Chim. Acta* **1988**, *71*, 1339-1348 ; b) K. Bernauer, P. Pousaz, *Helv. Chim. Acta* **1984**, *67*, 796-803.

[33] S.-B. Park, K. Murata, H. Matsumoto, H. Nishiyama, *Tetrahedron: Asymmetry* **1995**, *6*, 2487-2495.

2. Ligand Synthesis

For the assembly of the ligands **2**, a modular approach was developed. The retrosynthetic analysis (Scheme 2.1) suggests the final assembly of **2** by nucleophilic substitution.

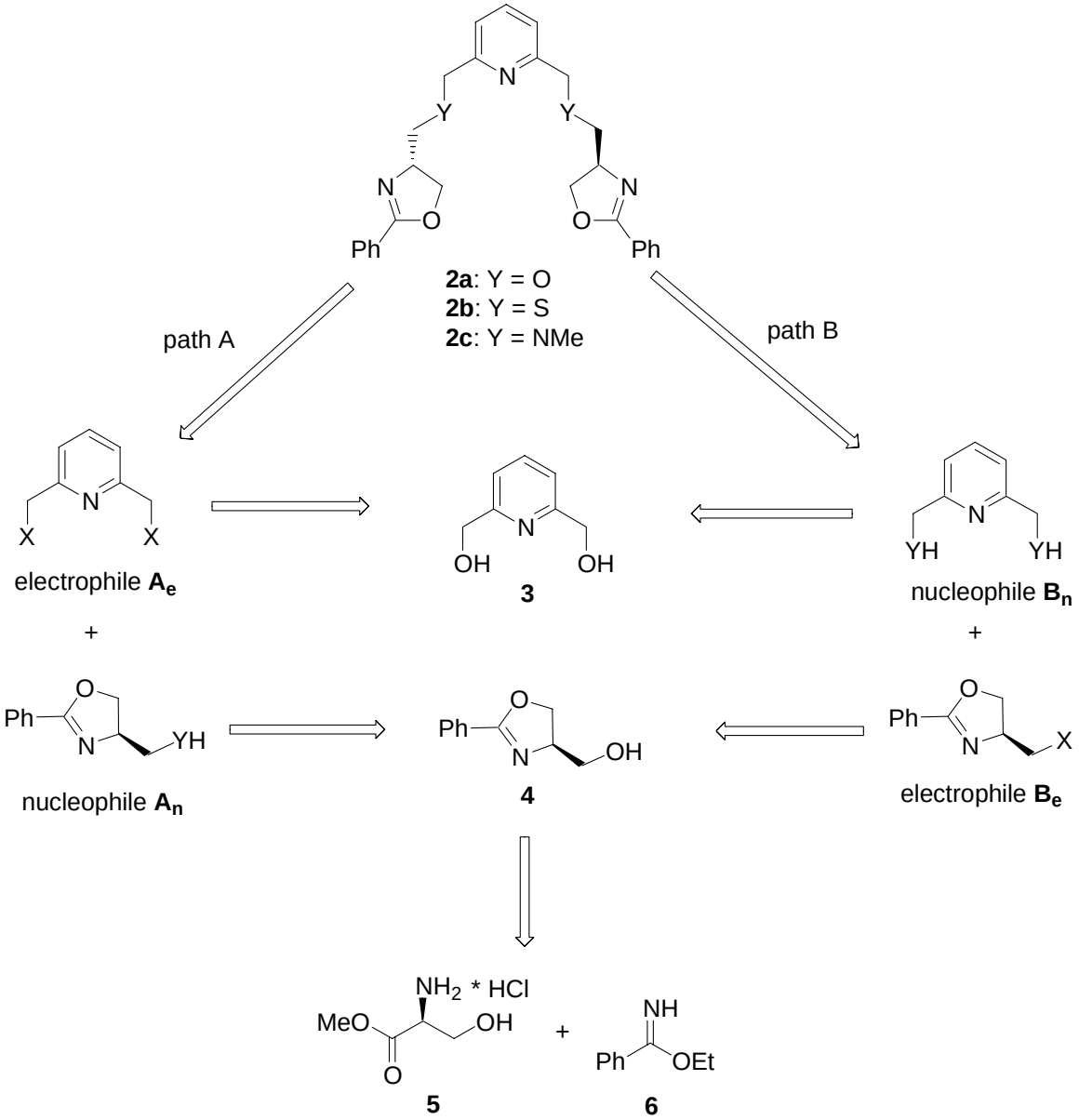

Scheme 2.1. Retrosynthesis of the ligands

For this concept, two possibilities exist. Either using the pyridine central unit as electrophile $\mathbf{A_e}$ and the oxazoline-nucleophile $\mathbf{A_n}$ (Path A) or just the other way around with nucleophilic pyridine $\mathbf{B_n}$ and oxazoline electrophile $\mathbf{B_e}$. The reactands can be derived from the same starting materials, reducing the number of steps. The pyridine components are uniformly made from commercially available diol **3** in only a

few steps in each case (vide infra). In analogy, the oxazoline building blocks are conveniently prepared from the same starting materials, namely enantiopure (*S*)-serine methyl ester hydrochlorid (**5**) and imidate **6** which are easily accessible from the corresponding nitrile. This approach is very flexible and would in principle also allow the employment of other nucleo- or electrophilic building blocks because of the generality of the final S_n2-step. For the synthesis of ligands **2**, a number of combinations was tried and the most promising reactions optimized.

2.1 Synthesis of the Pyridine Units

The central building blocks are best prepared from readily available 2,6-bis(hydroxymethyl)pyridine (**3**) (Scheme 2.2).

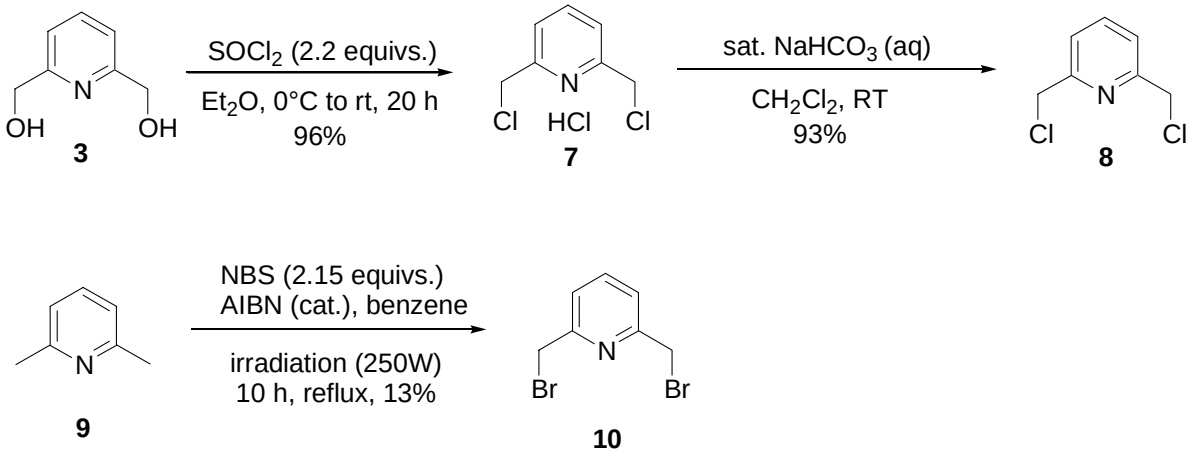

Scheme 2.2. Synthesis of the electrophilic pyridine units

Starting from diol **3**, the electrophile **8** can be obtained within two steps by a known procedure.[1] Purification is advantageously achieved without chromatography by recrystallization. Alternatively, the even more reactive bromide **10** can be synthesized from inexpensive 2,6-lutidine (**9**) by radical bromination in low yield.[2] This material must be purified by column chromatography to separate side products consisting of isomeric and higher brominated species. Furthermore, because of its high electrophilicity, traces of **10** are highly lachrymatory what makes handling unpleasant. Therefore, instead of **10** the less reactive but more convenient **8** was employed.

The synthesis of nucleophilic precursors is uniformly starting from diol **3** and involves mostly reported procedures (Scheme 2.3).

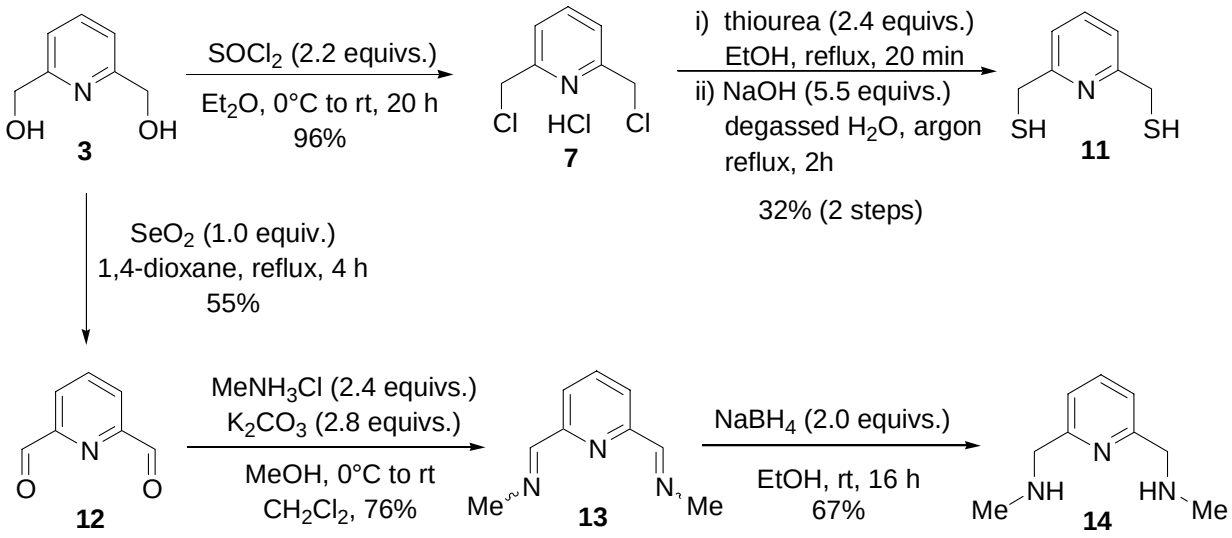

Scheme 2.3. Synthesis of the pyridine based nucleophiles

The preparation of dithiol **11** utilizes again hydrochloride **7**. It is transformed to an intermediate bis(isothiourea) derivative which is cleaved to give **11** in low yield.[1] One reason for this is its sensitivity to oxidative degradation when exposed to air. The previously unknown secondary amine **14** is prepared by a reductive amination procedure, via the bis(aldehyde) **12**[3] and diimine **13**[4] in reasonable yield. Like **11**, **14** is air-sensitive, but stable under inert N_2-atmosphere at 4°C. All steps involved in Scheme 2.3 do not require chromatographic purification, a big advantage for larger scales.

2.2 Synthesis of the Oxazoline Units

The oxazoline moiety is a very versatile functional group and its chemistry has a long standing history. In recent times, especially the group of Meyers[5] has developed a number of transformations and applications for this motive. Therefore, the synthetic route involves well established chemistry and provides straightforward access to the desired precursors (Scheme 2.4).

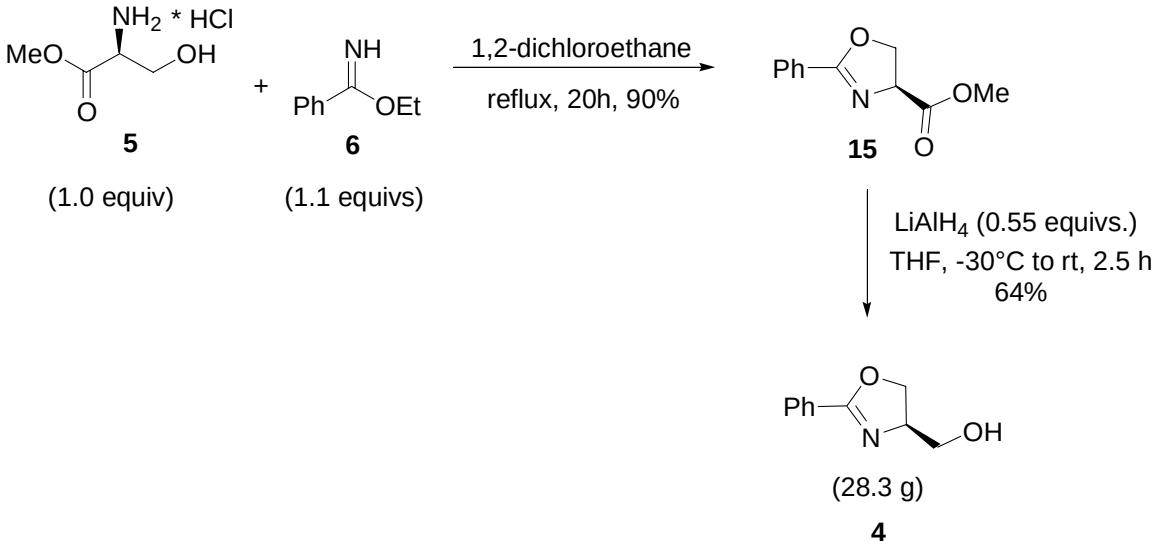

Scheme 2.4. Synthesis of the nucleophilic oxazoline units

The oxazoline ring is formed by condensation of optical pure (*S*)-serine derived methyl ester **5** and imidate **6**, prepared by acid mediated Pinner-reaction[6] of benzonitrile and EtOH. The latter very versatile method tolerates in principle a big variety of acid-stable functional groups and allows the introduction of various substituents at the aromatic system (vide supra).[7] The building block **4** is obtained by a known procedure[8] via reduction of the crude ester **15**. Instead of the reported reducing agent DIBAL-H, the less expensive $LiAlH_4$ could be used without detectable racemization but with reduced yield (90% vs. 64%). This drawback is easily acceptable in the light of cost effectiveness. In case of need, **4** could also be converted to its enantiomeric form, by a known ring opening-ring closure sequence, also reported by Meyers.[8] This is a very useful feature because of the potential synthesis of both enantiomeric ligands **2** on the basis of the excellently available natural (*S*)-serine. The reduction could be scaled up without problems employing a maximum of 250 mmol of **15**, yielding multigram amounts of **4**. Unfortunately, the product has to be purified by column chromatography, but the separation is not very difficult and can be carried out in large batches without inconvenience.

The synthesis of more nucleophilic oxazoline components was not followed, because of the potential serious problems associated with ring isomerization reactions (Scheme 2.5).

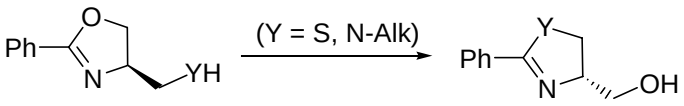

Scheme 2.5. Potential stability problems of strongly nucleophilic oxazoline units

The preparation of the oxazolines acting as electrophilic counterparts starts from **4**, minimizing the necessary overall steps once again (Scheme 2.6).

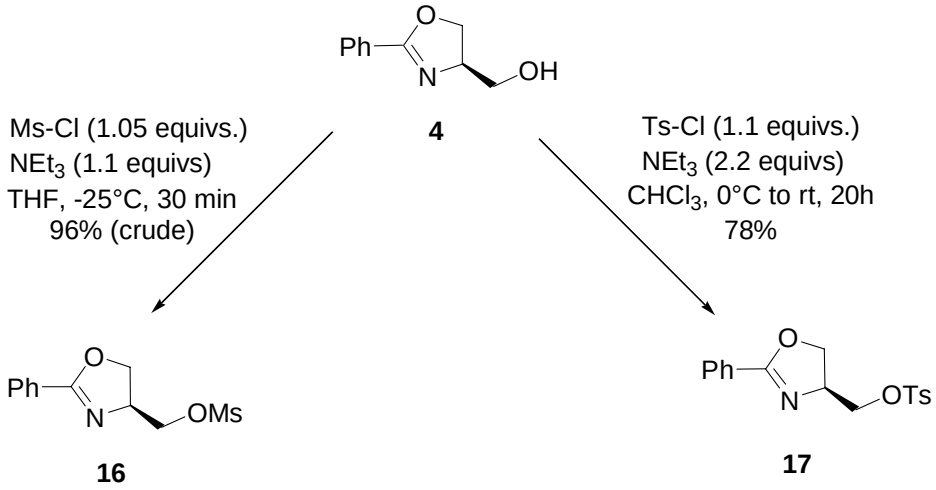

Scheme 2.6. Synthesis of electrophilic oxazoline building blocks.

From a number of possible electrophilic reactants, only the sulfonic acid ester derived **16** and **17** were prepared. The tosylate **17** was synthesized by a standard procedure reported in the literature[9] yielding an air-stable solid which can be stored for an extended period of time without degradation at ambient temperature. The more reactive, oily mesyl derivative **16**[10] can be used without purification in excellent yield but is not very stable and decomposes slowly upon standing in substance. Therefore, it is best used immediately after preparation. Chromatography as a means of purification can be avoided.

2.3 Assembly of the Ligands

With a number of building blocks in hands, the final assembly proved to be straightforward (Scheme 2.7).

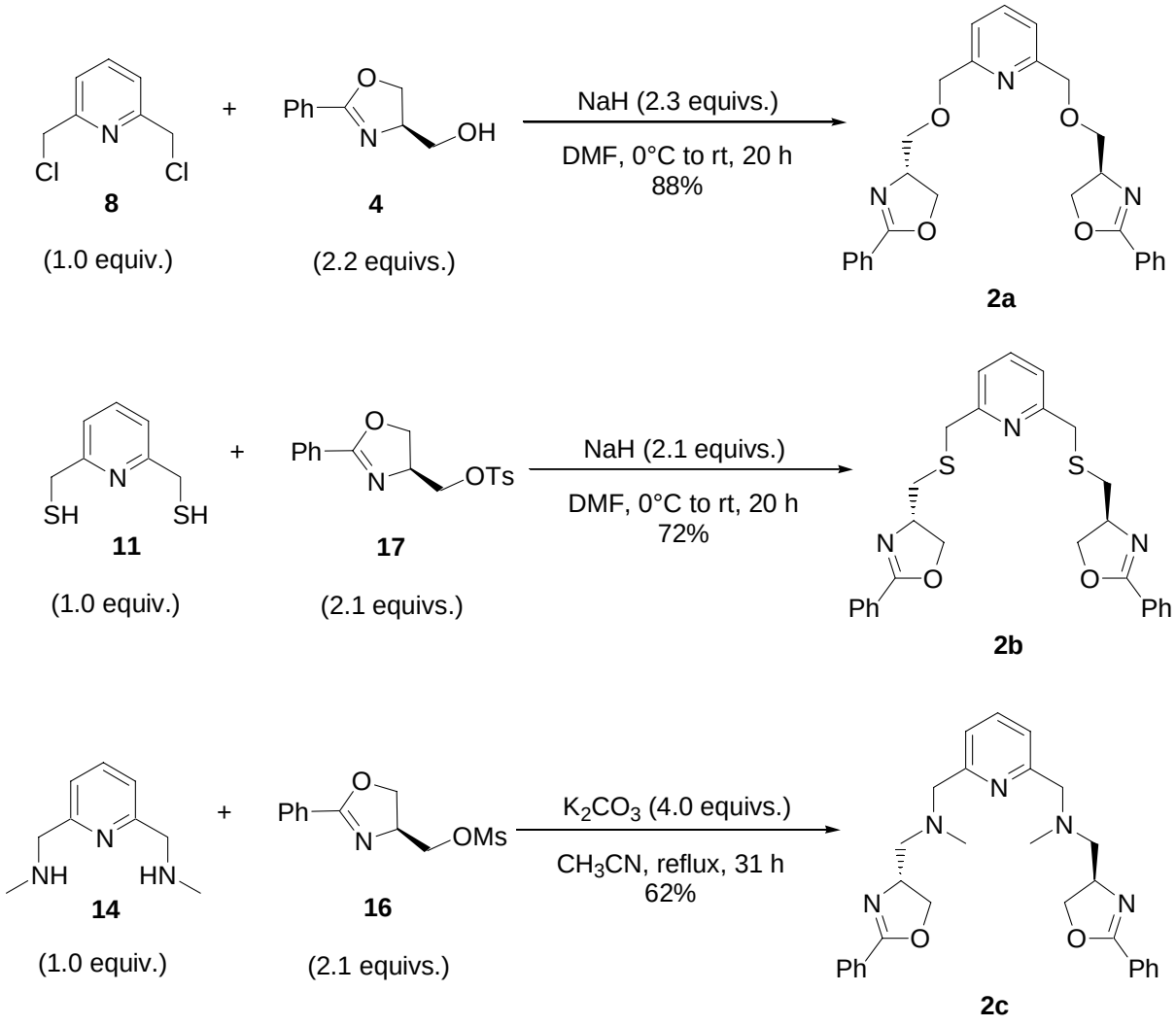

Scheme 2.7. Modular construction of ligands **2**

The general approach for **2a** and **2b** involved the increase in nucleophilicity by deprotonation of **4** and **11**. The attack at the electrophilic centers in **8** and **17** proceeded smoothly and produced the final ligands in good yields. This strategy could not be used for the assembly of **2c**. Because of the less nucleophilic character of the secondary amines in **14** compared to the alcoholate/thiolate-species, the reactive mesylate **16** had to be used instead of tosylate **17**. After a number of trials, the conditions depicted yielded **2c** in satisfactory amount. All ligands **2** have to be purified by column chromatography.

The NMR-spectra clearly show a C_2-symmetrical structure of the ligands. Ligand **2a** could also be crystallized and examined by X-ray analysis (Figure 2.1). The structural characteristics exhibit no unusual features.

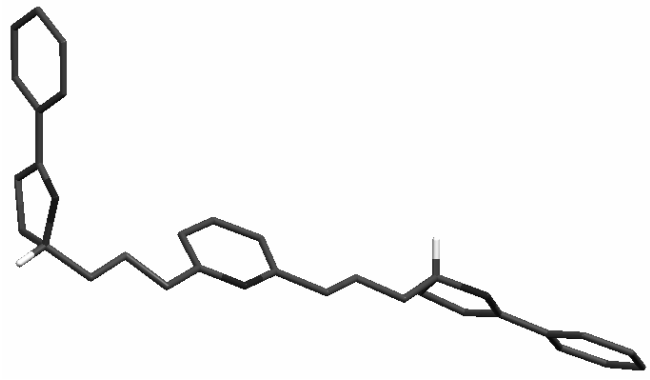

Figure 2.1. Crystal structure of ligand **2a** (hydrogens only shown at the stereogenic centers). Crystal data for **2a**: $C_{27}H_{27}N_3O_4$ (457.52); colorless rod (0.58mm*0.40mm*0.12mm); monoclinic ($P2_1$); a=4.8350(3) Å, b=11.3117(7) Å, c=21.9468(11) Å, β=92.859(6); V=1198.82(12) $Å^3$; Z=2; ρ=1.268 g/cm^3; μ=1.268 mm^{-1}; T=173(1) K; $Mo_{K\alpha}$(λ=0.71073 Å); 4.13°<θ<25.87°; 11794 reflections collected, 4534 independent, 4243 in refinement ($I \geq 2\sigma(I)$); R_1=0.0351, wR_2=0.0891, R_1(all data)=0.0373, wR_2(all data)=0.0906; absolute structure param.=0.1(7).

In conclusion, the synthesis of the desired ligands **2** proves to be straightforward and very flexible towards structural variations. Furthermore, the number of chromatographic purifications can be limited to a minimum of four (**4** and **2a-c**) making a preparation even on larger scale seem feasible. The presented strategy should also allow the facile introduction of additional functionalities for secondary interactions (vide supra).

References:

[1] With minor variations for **11**: B. Nock, H. J. Pietsch, F. Tisato, T. Maina, P. Leibnitz, H. Spies, E. Chiotellis, *Inorg. Chim. Acta* **2000**, *304(1)*, 26-32.

[2] W. Offermann, F. Vögtle, *Synthesis* **1977**, 272-273.

[3] N.W. Alcock, R.G. Kingston, P. Moore, C. Pierpoint, *J. Chem. Soc., Dalton Trans.* **1984**, 1937-1943.

[4] In analogy to: J.M. Holland, X. Liu, J.P. Zhao, F.E. Mabbs, C.A. Kilner, M. Thornton-Pett, M.A. Halcrow, *J. Chem. Soc., Dalton Trans.* **2000**, 3316-3324.

[5] T.G. Gant, A.I. Meyers, *Tetrahedron* **1994**, *50*, 2297-2360.

[6] R. Roger, D.G. Neilson, *Chem. Rev.* **1961**, *61*, 179-211.

[7] A. Kaiser, Dissertation, University of Regensburg.

[8] A.I. Meyers, W. Schmidt, M.J. McKennon, *Synthesis* **1993**, 250-262.

[9] E.V. Dehmlow, J. Vor der Brüggen, *J. Prakt. Chem.* **2000**, *342*, 502-503.

[10] J. Einsiedel, H. Hübner, P. Gmeiner, *Bioorg. Med. Chem. Lett.* **2001**, *11*, 2533-2536.

3. Complex Synthesis

The general strategy for the investigation of the coordination properties of ligands **2** was determined by the following requirements:

- **Preparation of mononuclear complexes**
  Because of the high denticity of five for **2**, only weakly coordinating anions (like ClO_4-, OTf-, BF_4-, ...) enable coordination of all ligand donors to one metal center in the range of the possible coordination numbers (especially 5,6,7...).
- **Systematic variability of certain properties**
  Especially the investigation of the influence of ionic radii and number of valence electrons under otherwise identical conditions would be desirable.
- **Relative substitution stability**
  The ligands should bind rather strong to the metal center to suppress complicating exchange processes.

Taking these preferences into account, first-row late transition metal(II) triflates and perchlorates seemed to be ideal candidates also because of several other characteristics:

- Commercial availability of all perchlorates $[M^{II}(H_2O)_6](ClO_4)_2$ (M = Mn-Zn), likewise for a number of anhydrous metal triflates (e.g. $Cu(OTf)_2$, $Zn(OTf)_2$).
- The relevance of these metals for a large number of catalytic processes, both in nature and in synthetic systems.

3.1 Perchlorate Complexes of First-Row Transition Metals

In spite of their potentially explosive nature, the perchlorate complexes turned out to be the most suitable series for our investigation. This was mainly due to the operational ease of isolation and purification. After a few unsuccessful attempts with various solvent mixtures, the following protocol was found to be suitable. Dissolving equimolar amounts of the corresponding metal precursor $[M^{II}(H_2O)_6](ClO_4)_2$ and ligand **2** separately under nitrogen atmosphere in dry THF and combining the two solutions resulted in precipitates of the desired complexes (Scheme 3.1). This

procedure allowed the facile separation of excess ligand or metal salt by simply washing the products with THF. Only in the case of Mn^{II} and ligand **2b**, no precipitate was observed and therefore this preparation was abandoned. **2c** was only used in combination with Zn^{II} due to the lack of sufficient amounts of this ligand at the beginning. Zinc in this case was chosen because of the diamagnetic behavior of the complexes, making NMR-spectroscopy possible (vide infra).

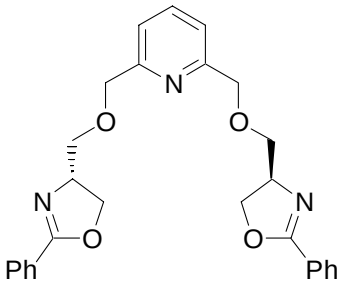

2a

$[M(H_2O)_6](ClO_4)_2$ (1.0 equiv.), THF, rt

$[Mn(\mathbf{2a})(H_2O)_2](ClO_4)_2 * THF$ (77%)
$[Fe(\mathbf{2a})(H_2O)_2](ClO_4)_2 * THF$ (43%)
$[Co(\mathbf{2a})](ClO_4)_2$ (94%)
$[Ni(\mathbf{2a})](ClO_4)_2 *H_2O * THF$ (90%)
$[Cu(\mathbf{2a})](ClO_4)_2 *H_2O * THF$ (91%)
$[Zn(\mathbf{2a})](ClO_4)_2$ (86%)

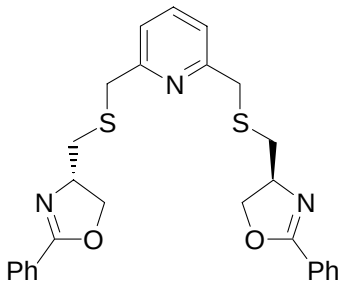

2b

$[M(H_2O)_6](ClO_4)_2$ (1.0 equiv.), THF, rt

$[Fe(\mathbf{2b})(H_2O)](ClO_4)_2 * 2\ H_2O$ (46%)
$[Co(\mathbf{2b})(THF)](ClO_4)_2 * H_2O$ (91%)
$[Ni(\mathbf{2b})](ClO_4)_2 *2\ H_2O$ (90%)
$[Cu(\mathbf{2b})](ClO_4)_2 *H_2O$ (82%)
$[Zn(\mathbf{2b})](ClO_4)_2 * H_2O$ (80%)

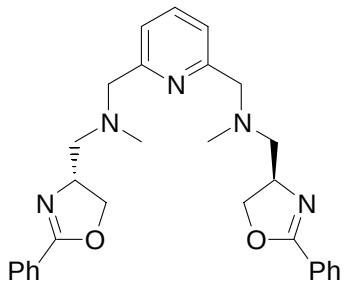

2c

$[Zn(H_2O)_6](ClO_4)_2$ (1.0 equiv.), THF, rt

$[Zn(\mathbf{2c})](ClO_4)_2 *CH_3CN * H_2O$ (60%)

Scheme 3.1. Synthesis of first-row transition metal perchlorate complexes

After simply drying the solids in vacuo, analytical pure material was obtained. All of the shown complexes were characterized by mass spectrometry to be mononuclear. Elemental analysis gave stoichiometries consistent with the formulae given above. In some cases, additional ligands like H_2O or THF could be assigned to the inner

coordination sphere of the metal on the basis of either crystal structures or predicted coordination geometries in solution (vide infra). All complexes are relative air stable solids. They are soluble in polar solvents like MeOH or CH_3CN and dissolve only very poorly in less polar media like CH_2Cl_2, EtOAc, ethers or hydrocarbons. This makes the perchlorates not ideally suited for Lewis-acid catalytic applications, because most of them desire solvents of the latter kind. In principle, anion exchange could be beneficial for the solubility problem. For the structural investigations conducted in this work, it does not constitute a problem.

3.2 Triflate Complexes of First-Row Transition Metals

The triflate anion has a few advantages compared with perchlorate. First of all, the complexes are not potentially explosive in combination with organic substances like the latter. In addition, some metal triflates are commercially available in anhydrous form, making them one of the metal precursors of choice in water sensitive catalytic processes. Last but not least, the solubility is often enhanced in comparison with perchlorates. In our case, this was not advantageous because the triflate complexes in most instances did not precipate and could not be obtained in analytically pure form by other means. On the other hand, only copper(II)- and zinc(II)-triflate can be purchased from commercial suppliers.

Because of the relevance to dioxygen activation (see introduction), iron(II) and cobalt(II) drew our attention. For this purpose, it was decided to synthesize these two metal triflates in anhydrous form by a procedure reported by Hagen for $Fe(OTf)_2$*2 CH_3CN.[1] Unfortunately, even after multiple attempts it was not possible to reproduce the protocol described. The possibility to prepare the corresponding Co(II)-triflate was also mentioned in this article. In contrast to Fe(II), the synthesis of Co(OTf)*2 CH_3CN was no problem at all (Scheme 3.2).

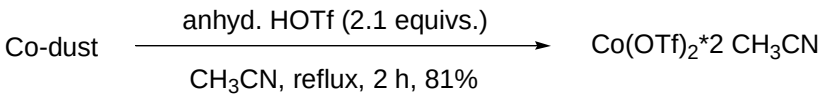

Scheme 3.2. Preparation of anhydrous Co(II)-triflate

With the triflates of divalent cobalt, copper and zinc in hand, a number of complexation attempts were conducted. Only in the case of cobalt a complex could

be obtained with ligand **2b** in analytically pure form (Scheme 3.3) following the protocol for the precipitation of the perchlorates (see section 3.1).

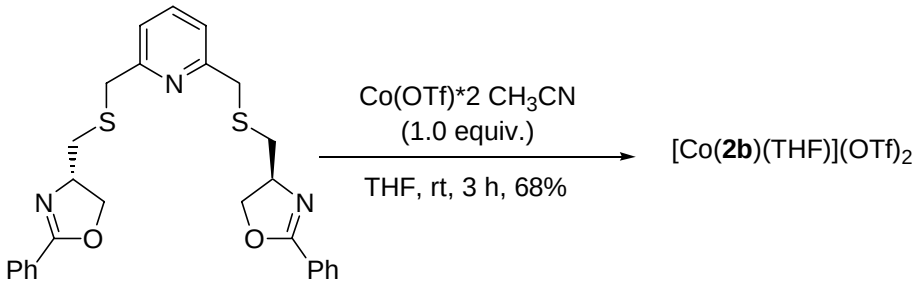

Scheme 3.3. Preparation of the Co^{II}-complex with **2b** by precipitation

Nevertheless, a few small single crystals out of these trials could be separated from the reaction mixtures and the solid state structures studied (vide infra).

3.3 Miscellaneous Complexes

To further test the complexation behavior of ligands **2**, a number of other metals were used for a number of different purposes. Since most first-row transition metals exhibit paramagnetic behavior and can therefore provide no NMR-information in this respect, the first approach was to synthesize a few additional diamagnetic complexes. In principle, this can achieved with metals of even-numbered electron configuration. Essentially, two promising classes were considered: d^{10}-species (Cu^{I} and Cd^{II}) and low-spin d^{6}-centers (Ru^{II}).

The synthesis of the cadmium(II) complexes was straightforward by applying the precipitation strategy for the first-row metals (Scheme 3.4, see also section 3.1).

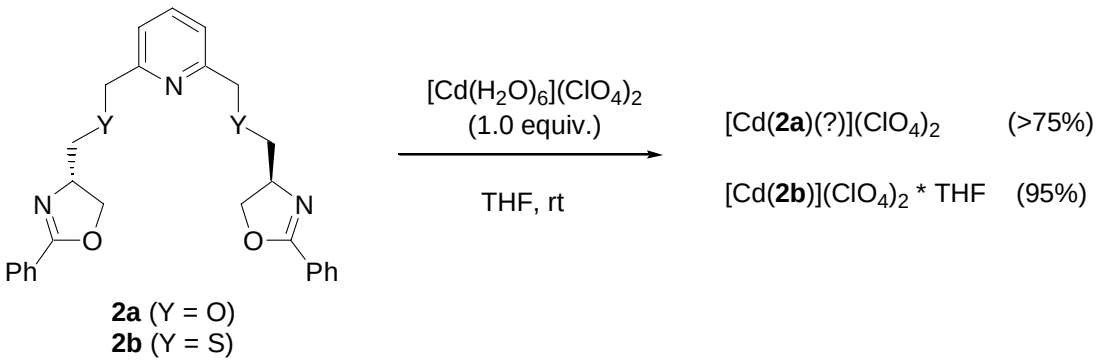

Scheme 3.4. Preparation of the Cd^{II}-perchlorate complexes

In the case of the complex with ligand **2a**, it was not possible to get a sufficient elemental analysis. Nevertheless, the conversion was almost quantitative indicated by a simple mass balance.

Starting from the copper(II) perchlorates, reduction with $NaBH_4$ yielded yellow compounds which were unambiguously identified as Cu^I-species by mass spectrometry (with **2b**) and their diamagnetic behavior (NMR) (Scheme 3.5).

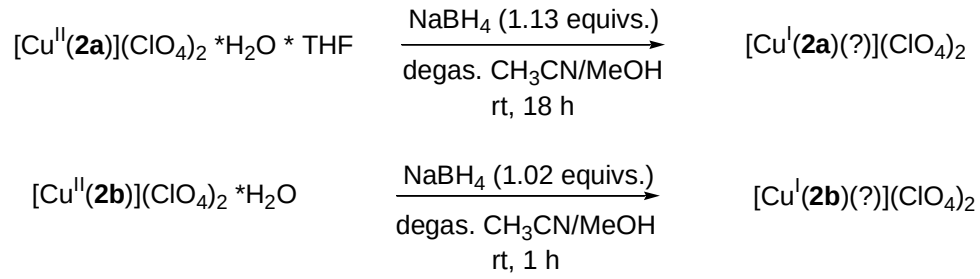

Scheme 3.5. Reductive synthesis of the copper(I) complexes

The two compounds had to be synthesized under rigorous exclusion of atmospheric dioxygen and were not isolated in substance for this reason. Short exposure of the NMR-samples to air yielded paramagnetic spectra after several hours, probably originating from reoxidized copper ions. This observation is very interesting because of the relevance of copper(I) complexes for the activation of dioxygen in nature,[2] like in the enzyme galactose oxidase or the O_2-transport protein hemocyanin in the blue blood of mollusks and arthropods. Because of the orientation of this work towards structure elucidation rather than reactivity investigation this aspect was not followed further.

The synthesis of a diamagnetic ruthenium(II) complex was tried with one of the most facile Ru^{II}-precursors, $[RuCl_2(benzene)]_2$.[3] Refluxing with ligand **2b** in an ethanolic solution and workup yielded a mixture of two species (Scheme 3.6).

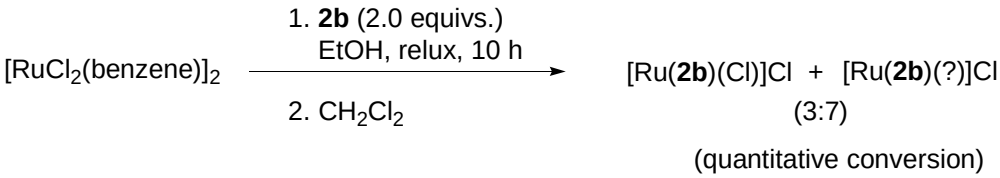

Scheme 3.6. Preparation of diamagnetic Ru^{II}-complexes

Unfortunately, it was not possible to separate the two complexes for a complete characterization. Nevertheless, it was possible to predict the nature of the two species on the basis of different analytical methods (vide infra).

The second approach for the complexation involved the testing of metals other than transition metals. As a representative of a main group element, magnesium was chosen for the availability of both $Mg(ClO_4)_2$ and $Mg(OTf)_2$. The preparation started from the perchlorate (Scheme 3.7).

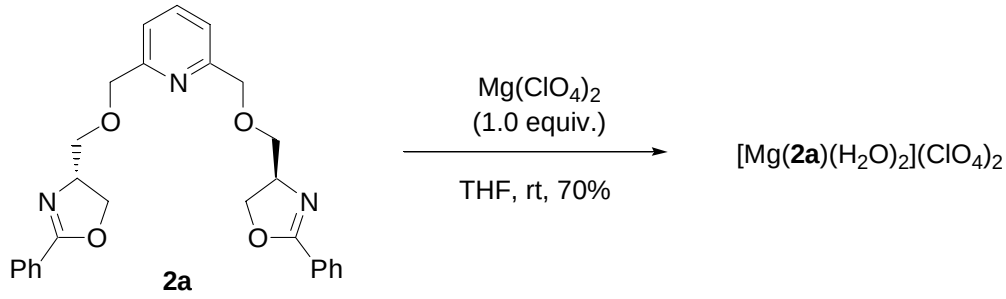

Scheme 3.7. Synthesis of the Mg^{II}-perchlorate complex with **2a**

Another class of catalysis-relevant metals are the lanthanides. To see if ligands **2** could accommodate these rather large atoms, the choice fell on ytterbium. It is the second smallest representative in the row of the trivalent ions because of the lanthanide contraction and is commercially available ($Yb(OTf)_3$). The synthesis was straightforward (Scheme 3.8).

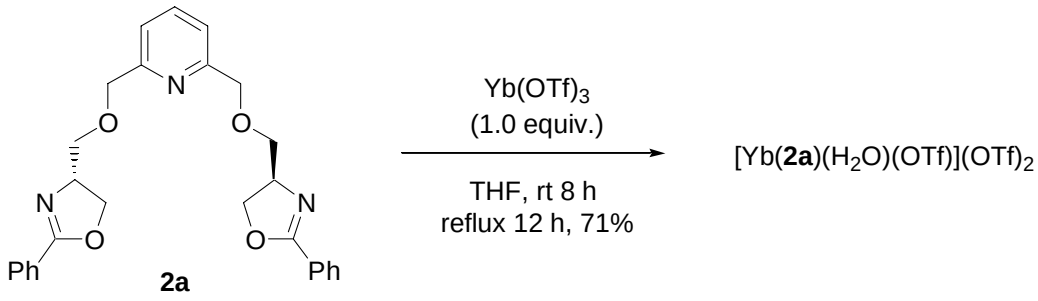

Scheme 3.8. An example for a lanthanide complex with Yb^{III}

The assigment of additional ligands to the inner coordination sphere was made on the basis of mass spectrometry.

References:

[1] K. S. Hagen, *Inorg. Chem.* **2000**, *39*, 5867-5869.

[2] a) L.M. Mirica, X. Ottenwaelder, T.D.P. Stack, *Chem. Rev.* **2004**, *104*, 1013-1045; b) E.A. Lewis, W.B. Tolman, *Chem. Rev.* **2004**, *104*, 1047-1076.

[3] M. A. Bennett, A. K. Smith, *J. Chem. Soc. Dalton Trans.* **1974**, 233-237.

4. Structural Investigations

4.1 General Considerations

This part constitutes the core of this thesis. Before the actual structure determination will be developed, a few general thoughts on this matter should be dealt with. The issue of central importance upon metal complexation with ligands **2** is the resulting stereochemistry. A great variety of possibilities can arise depending on different coordination geometries. However, there are a few invariable features in ligand arrangement because of the special geometry of **2**. The most important characteristic is the necessity for the three middle donor groups (red in Figure 4.1) of the ligands to coordinate in a meridional fashion.

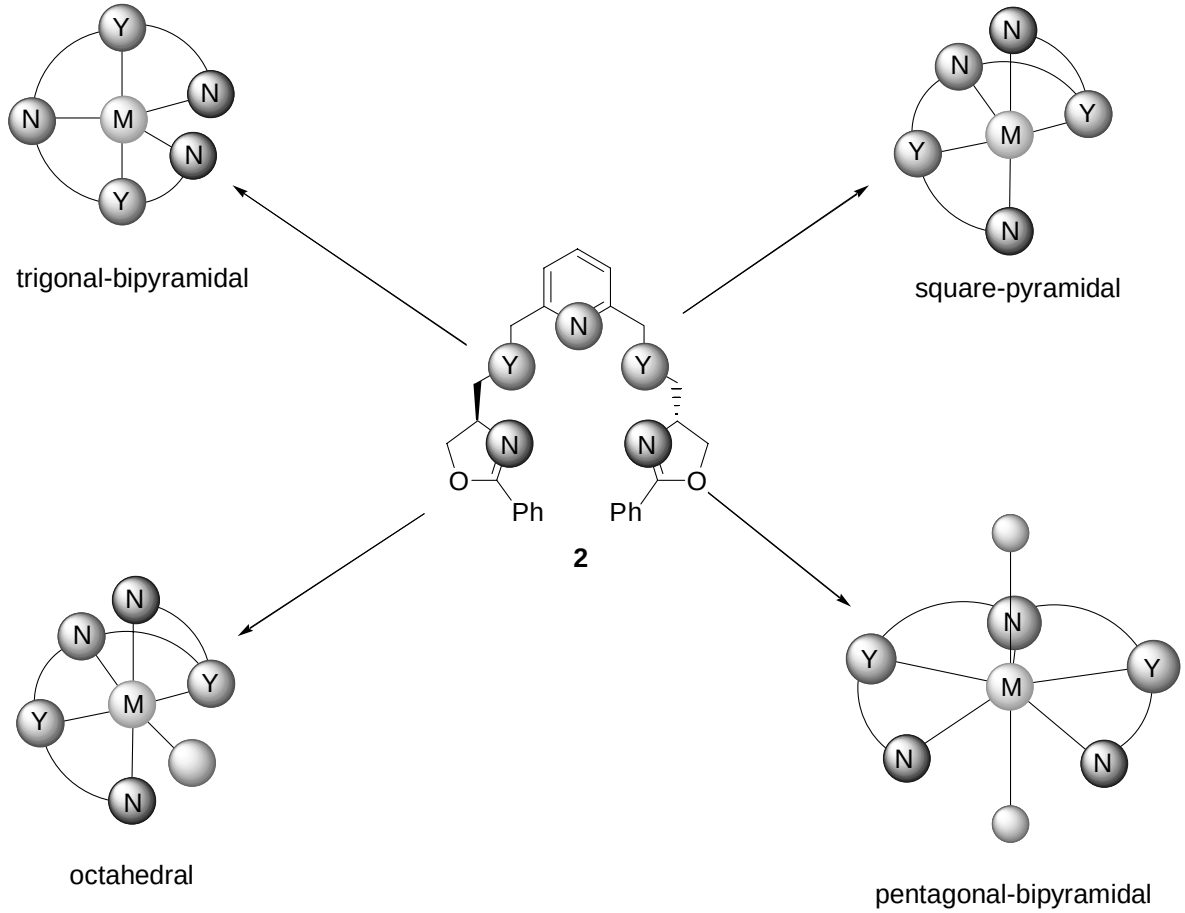

Figure 4.1. Some examples for different geometries: middle three donors (red) always meridional

This requirement is mainly due to the planarity of the pyridine ring forcing the close-by attached atoms to adopt a conformation only slightly deviating from this plane. With increasing distance from the pyridine, the oxazoline arms gain enough flexibility to take a position above or below, thereby determining the configuration at the metal

center. The octahedral geometry shall serve as illustration for these possibilities (Figure 4.2).

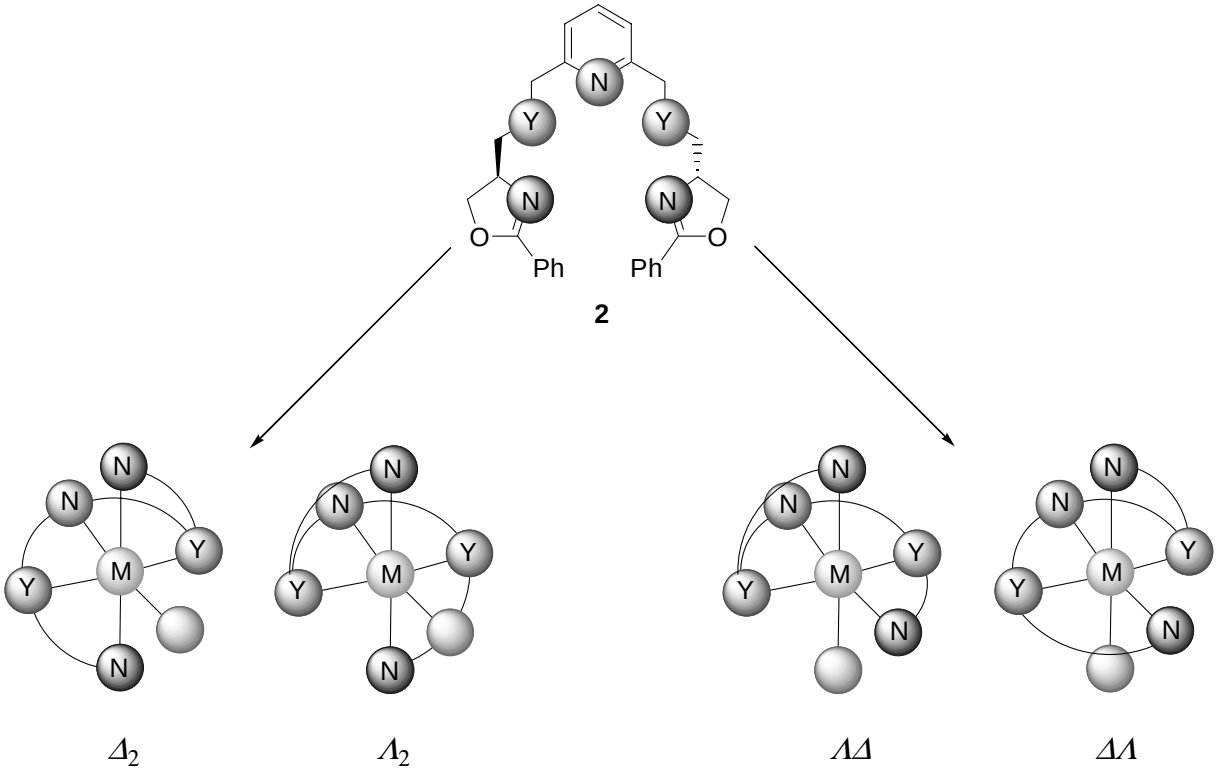

Figure 4.2. Possible isomers with ligands **2** in octahedral metal complexes

Basically, there are two principal arrangements for the two oxazoline arms. Either they can coordinate both out of the pyridine plane in opposite half spaces (Δ_2 or Λ_2) adopting positions trans to each other in the case of the octahedron. Alternatively, one arm takes a position in the plane and the other adopts an apical position ($\Lambda\Delta$ or $\Delta\Lambda$), resulting in a cis-arrangement of the oxazoline donors. These two types exist both as a pair of enantiomers. Due to the chirality of the ligands in our case, the two forms of these pairs are not enantiomeric but diastereomeric to each other.

The generation of the new stereogenic metal center in a broader sense goes hand in hand with the deviation from the plane, spanned by the three middle donors. Therefore, analoguous stereoisomeric relations hold true for other coordination geometries (Figure 4.1). The pentagonal bipyramide constitutes a special case. If all ligand donors coordinate in one planar arrangement, the resulting metal configuration should be inherently achiral. With ligands **2** (as will be seen later) the deviation from this pentagonal plane by the ligand backbone is big enough to clearly contribute to a chiral helical structure.

4.2 Solid State Structures

The elucidation of structural information in coordination chemistry is often not an easy task. Especially in transition-metal complexes the application of NMR-spectroscopy, one of the most powerful tools for structure determination, is often complicated by paramagnetic properties. Therefore, in many cases only methods like IR- or UV-spectroscopy can be applied, often only of significance in combination with other pieces of information or by comparison with known precedences. Due to these problems the commonly used approach relies on the most direct method for structure determination, single crystal X-ray analysis. In our case, it was also possible to perform a number of crystal structure analyses of the complexes synthesized. In this section only the basic structural parameters will be discussed. For a comprehensive comparison of all structures in the context of related subjects see Section 6. More detailed information on bond lengths and angles can be found in the appendix or by retrieving the corresponding cif-file from the Cambridge Crystallographic Data Centre (http://www.ccdc.cam.ac.uk).

- **$[Fe^{II}(2a)(H_2O)_2](ClO_4)_2$ *THF**

The structure of this iron(II) complex shows an unexpected pentagonal-bipyramidal geometry (Figure 4.3, Table 4.1).

Figure 4.3. Crystal structure of the cation of $[Fe^{II}(\mathbf{2a})(H_2O)_2](ClO_4)_2$ *THF (hydrogens only shown at the stereogenic carbon atoms of ligand **2a** and for the H_2O molecules)

The C_2-symmetry of the ligand is retained in the complex. The perchlorate counterions are non-coordinating. All five donor atoms of **2a** coordinate in the pentagonal plane and show bond lengths to the iron center in the usual range (Fe-N: 2.23-2.34Å, Fe-O: 2.33-2.34Å). The water molecules bind to the metal at the two axial positions and have shorter Fe-O-bond lengths (2.11-2.15Å) compared to the

ether-oxygen donors of the ligand as can be expected. Because of the phenyl rings deviating significantly from the pentagonal plane and having one single preferred orientation, the complex can be assigned a stereogenic metal center with Λ_2-configuration. Alternatively this behavior can be described as an exclusive right-handed helical arrangement of the ligand.

Table 4.1. Crystal data for iron-, cobalt- and cadmium-complexes of ligands **2**

	[Fe(**2a**)(H_2O)$_2$](ClO_4)$_2$ *THF	[Co(**2b**)(THF)](OTf)$_2$	[Co(**2c**)(H_2O)](OTf)$_2$	{[Cd(**2b**)(ClO_4)](ClO_4)}$_3$ *CH_3CN
		CCDC 216870		
formula	$C_{31}H_{39}Cl_2FeN_3O_{15}$	$C_{33}H_{35}CoF_6N_3O_9S_4$	$C_{31}H_{35}CoF_6N_5O_9S_2$	$C_{83}H_{84}Cd_3Cl_6N_{10}O_{30}S_6$
crystal app.	colorless stick	pink prism	pink block	colorless prism
mol. weight	820.40	918.81	858.69	2443.95
crystal system	orthorhombic	monoclinic	monoclinic	monoclinic
space group	$P2_12_12_1$	$P2_1$	$P2_1$	$P2_1$
a [Å]	8.2616(7)	11.481(3)	9.784(2)	9.6544(8)
b [Å]	14.0004(10)	8.809(2)	19.746(4)	17.8800(9)
c [Å]	30.790(2)	18.976(4)	9.811(2)	27.549(2)
α [°]	90	90	90	90
β [°]	90	105.688(5)	105.954(4)	97.008(10)
γ [°]	90	90	90	90
volume [Å^3]	3561.3(5)	1847.7(7)	1822.4(6)	4720.0(6)
Z	4	2	2	2
ρ [g cm^{-1}]	1.530	1.652	1.565	1.720
μ [mm^{-1}]	0.648	0.779	0.675	1.058
crystal size [mm]	0.34*0.08*0.06	0.28*0.18*0.10	0.58*0.24*0.20	0.16*0.16*0.10
temperature [K]	173(1)	100(2)	100(2)	173(1)
radiation [Å]	$Mo_{K\alpha}$ (λ = 0.71073)	$Mo_{K\alpha}$ (λ = 0.71073)	$Mo_{K\alpha}$ (λ = 0.71073)	$Mo_{K\alpha}$ (λ = 0.71073)
θ max [°]	1.97 < *θ* < 25.81	2.23 < *θ* < 25.00	2.06 < *θ* < 26.00	1.88 < *θ* < 25.87
measured reflections	30644	10392	12020	33866
independent reflections	6802	5661	6746	17358
reflections in refinement	4743, $I \geq 2\sigma(I)$	5392, $I \geq 2\sigma(I)$	6643, $I \geq 2\sigma(I)$	13828, $I \geq 2\sigma(I)$
R[a]	0.0443	0.0710	0.0317	0.0397
wR_2[b]	0.0884	0.1838	0.0800	0.0865
R[a] (all data)	0.0723	0.0733	0.0321	0.0534
wR_2 (all data)	0.0963	0.1866	0.0803	0.0913
absolute structure param.	– 0.01(2)	0.05(2)	0.008(10)	– 0.023(17)

[a] R factor definition: $R = \Sigma (||F_0| - |F_c||) / \Sigma |F_0|$. [b] SHELX-97 wR_2 factor definition: $wR_2 = [\Sigma w(F_0^2 - F_c^2)2 / \Sigma w(F_0^4)]1/2$. Weighting scheme: $w = 1 / [\sigma^2(F_0)^2 + (np)^2]$, $p = [F_0^2 + 2 F_c^2] / 3$.

Table 4.2. Crystal data for zinc-complexes of ligands **2**

	[Zn(**2a**)](ClO$_4$)$_2$	[Zn(**2a**)](OTf)$_2$ * CH$_2$Cl$_2$	[Zn(**2b**)](ClO$_4$)$_2$ *H$_2$O	[Zn(**2c**)](ClO$_4$)$_2$ *CH$_3$CN * H$_2$O
	CCDC 236254		CCDC 236253	
formula	$C_{27}H_{27}Cl_2N_3O_{12}Zn$	$C_{30}H_{29}Cl_2F_6N_3O_{10}S_2Zn$	$C_{27}H_{29}Cl_2N_3O_{11}S_2Zn$	$C_{31}H_{36}Cl_2N_6O_{10}Zn$
crystal app.	colorless prism	colorless stick	colorless prism	colorless prism
mol. weight	721.81	905.99	771.96	778.95
crystal system	monoclinic	orthorhombic	orthorhombic	orthorhombic
space group	$P2_1$	$P2_12_12_1$	$C222_1$	$C222_1$
a [Å]	8.8261(8)	8.7347(6)	14.5688(9)	11.9149(8)
b [Å]	9.9900(7)	15.2145(10)	11.4522(10)	14.3568(9)
c [Å]	16.8095(16)	26.9055(19)	18.3976(12)	19.8710(18)
α [°]	90	90	90	90
β [°]	99.692(11)	90	90	90
γ [°]	90	90	90	90
volume [Å^3]	1461.0(2)	3575.6(4)	3069.5(4)	3399.1(4)
Z	2	4	4	4
ρ [g cm^{-1}]	1.641	1.683	1.666	1.542
μ [mm^{-1}]	1.094	1.044	1.176	0.946
crystal size [mm]	0.22*0.20*0.12	0.72*0.24*0.18	0.20*0.18*0.10	0.46*0.44*0.22
temperature [K]	173(1)	173(1)	173(1)	173(1)
radiation [Å]	$Mo_{K\alpha}$ (λ = 0.71073)	$Mo_{K\alpha}$ (λ = 0.71073)	$Mo_{K\alpha}$ (λ = 0.71073)	$Mo_{K\alpha}$ (λ = 0.71073)
θ max [°]	2.34 < *θ* < 25.91	2.45 < *θ* < 25.85	2.26 < *θ* < 25.86	2.45 < *θ* < 25.86
measured reflections	20388	30057	10957	12740
independent reflections	5624	6882	2964	3279
reflections in refinement	4833, *I* ≥ 2σ(*I*)	6405, *I* ≥ 2σ(*I*)	2461, *I* ≥ 2σ(*I*)	3173, *I* ≥ 2σ(*I*)
$R^{[a]}$	0.0276	0.0377	0.0337	0.0351
$wR_2^{[b]}$	0.0561	0.0999	0.0703	0.0968
$R^{[a]}$ (all data)	0.0362	0.0411	0.0449	0.0359
wR_2 (all data)	0.0580	0.1022	0.0731	0.0974
absolute structure param.	– 0.015(8)	0.000(10)	– 0.001(16)	– 0.002(13)

[a] *R* factor definition: $R = \Sigma (||F_0| - |F_c||) / \Sigma |F_0|$. [b] SHELX-97 wR_2 factor definition: $wR_2 = [\Sigma w(F_0^2 - F_c^2)2 / \Sigma w(F_0^4)]1/2$. Weighting scheme: $w = 1 / [\sigma^2(F_0)^2 + (np)^2]$, $p = [F_0^2 + 2 F_c^2] / 3$.

- **[Co^{II}(2b)(THF)](OTf)$_2$**

As expected the structure of the cobalt(II) complex exhibits a normal, only slightly distorted octahedral geometry (Figure 4.4, Table 4.1).

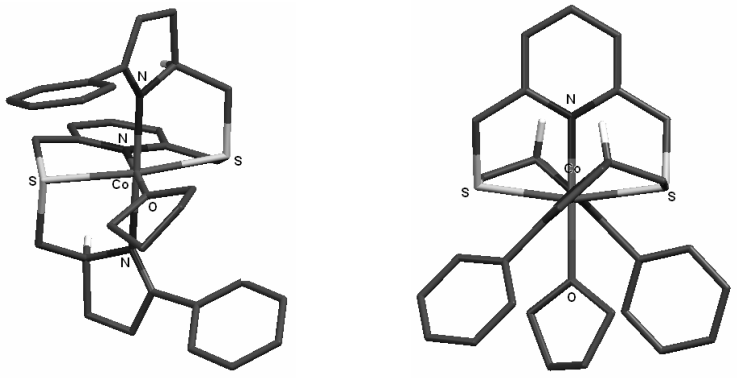

Figure 4.4. Crystal structure of the cation of [Co^{II}(**2b**)(THF)](OTf)$_2$ (CCDC No. 216870) (hydrogens only shown at the stereogenic carbon atoms of ligand **2b**)

Once more the symmetry of the ligand is conserved upon complexation yielding a Δ_2-configured species. THF is coordinating as the sixth ligand in trans-position to the pyridine ring, the triflate anions are non-coordinating. The bond lenghts are not unusual (Co-N: 2.11-2.14Å, Co-S: 2.46-2.48Å, Co-O: 2.07Å). The angles X-Co-X (X= O, S, N) vary slightly from an ideal right angle (80.6°-98.6°) or 180° (165.0°-179.7°) respectively. The two phenyl rings point away from the cobalt center and provide a rather tight chiral pocket, effectively shielding two opposite quadrants of the accessible front space of the complex.

- **[Co^{II}(2c)(H$_2$O)](OTf)$_2$**

Like in the preceeding cobalt species with thioether ligand **2b**, the Co(II)-complex with **2c** shows octahedral, almost C_2-symmetrical geometry (Figure 4.5, Table 4.1).

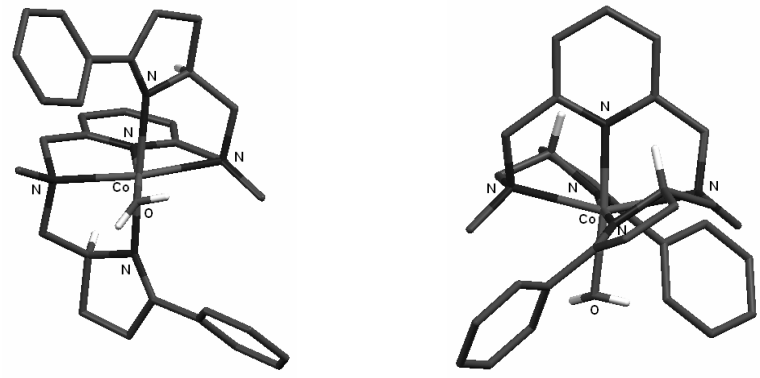

Figure 4.5. Crystal structure of the cation of [Co^{II}(**2c**)(H$_2$O)](OTf)$_2$ (hydrogens only shown at the stereogenic carbon atoms of ligand **2c**)

The distortion of this Δ_2-configured complex from a regular octahedron increases in comparison with $[Co^{II}(\mathbf{2b})(THF)]^{2+}$. The angles X-Co-X (X = O, N) vary between 77.5°-107.8° (ideally 90°) and 154.7°-176.8° (ideally 180°). The bond lenghts are similar (Co-N: 2.07-2.26Å, Co-O: 2.03Å). Besides these details the overall structures of the two cobalt complexes of **2a** and **2b** are very similar and show the same Δ_2 selectivity.

- **$[Zn^{II}(2a)](ClO_4)_2$ and $[Zn^{II}(2a)](OTf)_2*CH_2Cl_2$**

The zinc complexes with ligand **2a** show distorted trigonal-bipyramidal geometry with almost C_2-symmetry, irrespective of the nature of the counterion (ClO_4, OTf) (Figures 4.6 and 4.7, Table 4.2). Because they differ only marginally from one another the perchlorate complex will be solely discussed here.

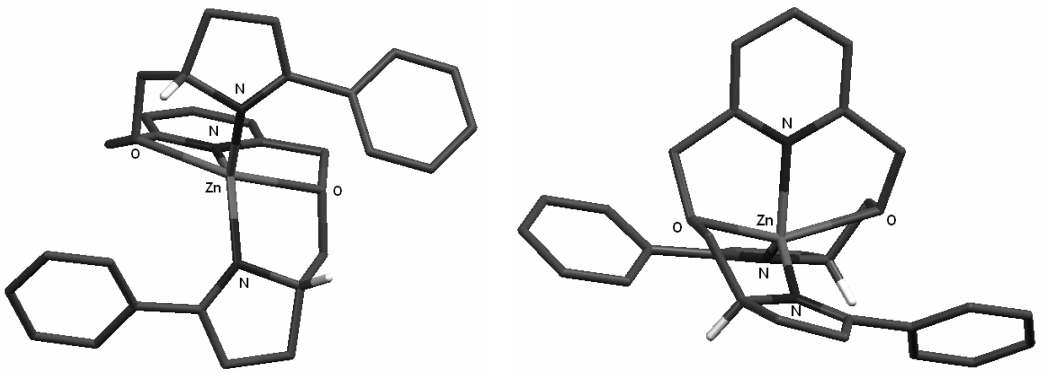

Figure 4.6. Crystal structure of the cation of $[Zn^{II}(\mathbf{2a})](ClO_4)_2$ (CCDC No. 236254) (hydrogens only shown at the stereogenic carbon atoms of ligand **2a**)

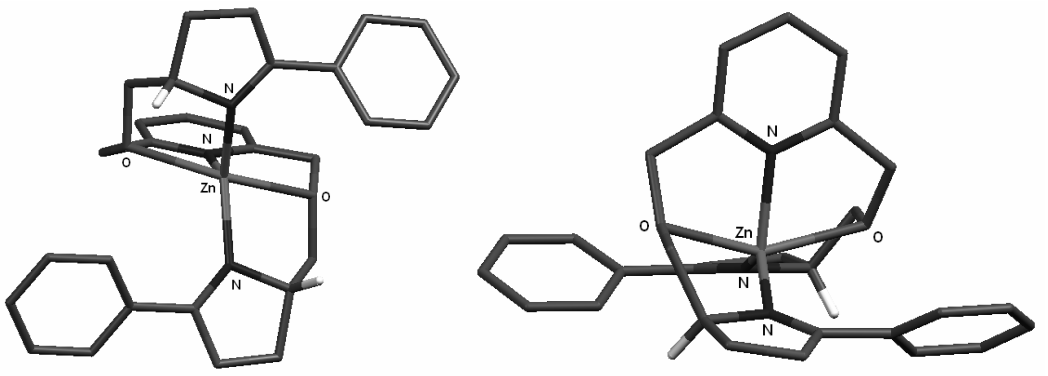

Figure 4.7. Crystal structure of the cation of $[Zn^{II}(\mathbf{2a})](OTf)_2*CH_2Cl_2$ (hydrogens only shown at the stereogenic carbon atoms of ligand **2a**)

The trigonal plane is spanned by the zinc atom and the three nitrogen donors of the pyridine and the oxazolines. They have almost equal Zn-N bond lengths (1.95-2.03Å)

and comprise angles N-Zn-N between 113.7° and 129.6° (ideally 120°). The axial positions of the ether oxygens (Zn-O: 2.22-2.28Å) are tilted from an ideal position perpendicular to the trigonal plane towards the pyridine moiety (e.g. $N_{pyridine}$-Zn-O_1 = 76.9° or $N_{pyridine}$-Zn-O_2 = 76.1°). Surprisingly, the complex favors to adopt a Λ_2-, rather than the expected Δ_2- configuration. This results in the stacking of the phenyl rings in close proximity to the rest of the ligand backbone, initially thought to exert a strong steric strain upon the complex in comparison with the Δ_2-case where the aromatic rings point away from the metal center. In consequence of this observation, steric arguments alone can not account for the stereoselectivity (vide infra).

- **$[Zn^{II}(2b)](ClO_4)_2*H_2O$**

Like the preceeding complexes the combination of Zn^{II} with ligand **2b** yields trigonal-bipyramidal species (Figure 4.8, Table 4.2).

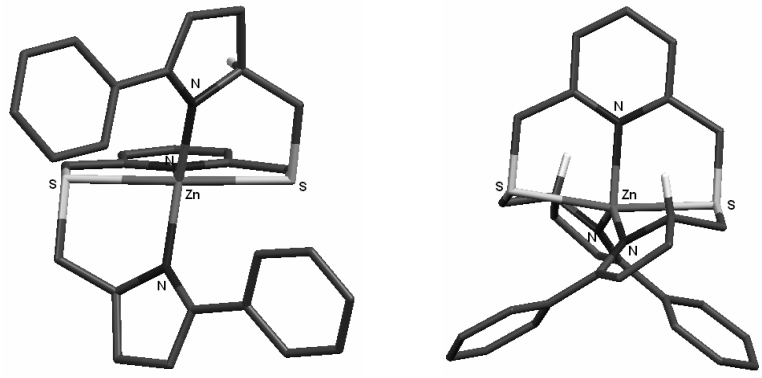

Figure 4.8. Crystal structure of the cation of $[Zn^{II}(\mathbf{2b})](ClO_4)_2*H_2O$ (CCDC No. 236253) (hydrogens only shown at the stereogenic carbon atoms of ligand **2b**)

This time the complex shows ideal C_2-symmetry but astonishingly with the opposite configuration Δ_2, where the phenyl rings are directed away from the center. The degree of distortion from the ideal trigonal-bipyramidal geometry is similar to the complexes with **2a**. Zn-N bond lengths (Zn-N: 1.98-2.10Å) are in the same range. Angular deviation is a little larger (N-Zn-N: 100.0°-139.8°) whereas the tilt of the axial thioether donors (Zn-S: 2.53Å) is only small (e.g. $N_{pyridine}$-Zn-S = 84.4°) in comparison with the ideal value of 90°. The main reason for the difference between the structures of the zinc complexes with **2a** and **2b** is the $C_{benzylic}$-Y (Y = O, S) bond length (C-O: 1.44Å vs. C-S: 1.81Å), probably also accounting for the complete reversal of stereoselectivity from Λ_2 to Δ_2.

- **$[Zn^{II}(2c)](ClO_4)_2*CH_3CN*H_2O$**

The structure of this complex resembles the corresponding species with ligand **2a** (Figure 4.9, Table 4.2).

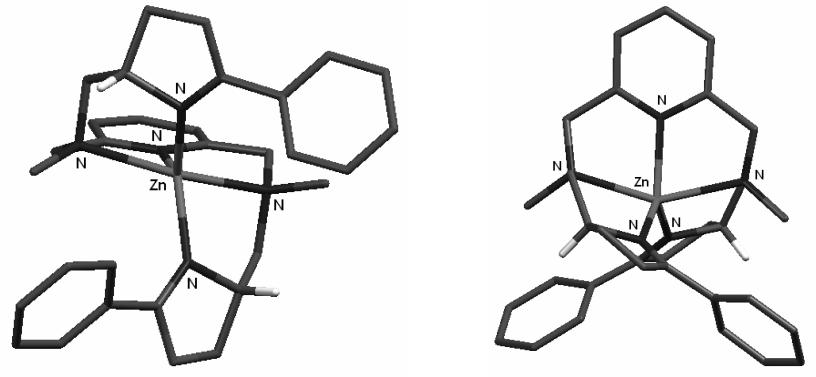

Figure 4.9. Crystal structure of the cation of $[Zn^{II}(\mathbf{2c})](ClO_4)_2*CH_3CN*H_2O$ (hydrogens only shown at the stereogenic carbon atoms of ligand **2c**)

These complexes share the trigonal-bipyramidal geometry, the idealized C_2-symmetry and most interestingly the stereoselectivity for Λ_2. The donors lying in the trigonal plane ($N_{pyridine}$, $N_{oxazoline}$) have similar Zn-N bond lengths compared to the other zinc complexes (2.03-2.11Å) and comprise angles close to the ideal value of 120° (N-Zn-N: 119.0°-122.0°). In contrast to this the tertiary amine donor nitrogens are a little further away from the zinc center (2.29Å) and are tilted with respect to the trigonal plane (e.g. N_{amine}-Zn-$N_{pyridine}$ = 75.4°). Probably the similarity in bond lengths $C_{benzylic}$-Y (Y = O, N) induce the same configurational preference for Λ_2 (C-O: 1.44Å vs. C-N: 1.48Å) (vide supra).

- **{[Cd^{II}(2b)(ClO_4)](ClO_4)}$_3$*CH_3CN**

The cadmium complex with **2b** is different from all other structures seen before. This is the only case where one of the weakly coordinating anions (perchorate) is bound to the metal center (Figure 4.10, Table 4.1).

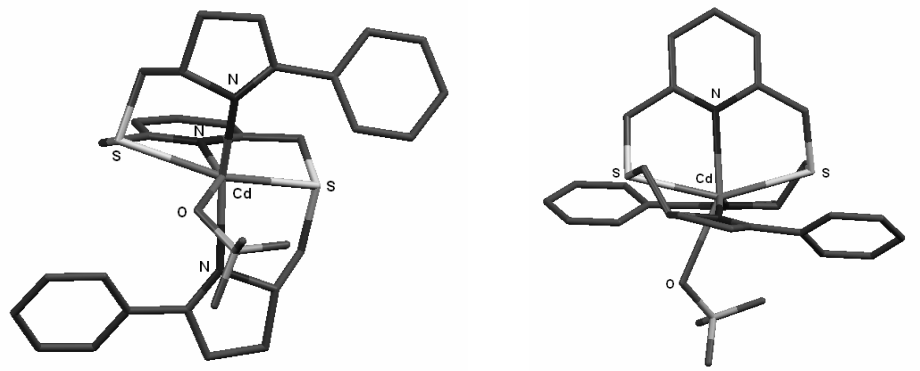

Figure 4.10. Crystal structure of one of the three unique cations of {[Cd^{II}(**2b**)(ClO_4)](ClO_4)}$_3$*CH_3CN (hydrogens only shown at the stereogenic carbon atoms of ligand **2b**)

In the unit cell three very similar unique complexes are present differing only marginally from one another. Figure 4.10 shows only one of these unique cations. The complexes exhibit a strong distortion from C_2-symmetry and all show unexpected Λ_2-configured octahedral coordination geometry. The bond lengths are rather long (Cd-N: 2.28-2.42Å, Cd-S: 2.65-2.68Å, Cd-O: 2.40-2.61Å). The strong distortion probably expresses the problem of ligand **2b** to accommodate the rather large second-row transition metal cadmium (ionic radius for six coordinate Cd^{II}: 0.95Å). Presumably, this is also the reason why the otherwise disfavored Λ_2-configuration (see Co-complexes) is the only observed stereoisomer in the solid state.

In conclusion, all solid state structures of mononuclear complexes of ligands **2** retain idealized C_2-symmetry, though sometimes slightly distorted. A number of coordination geometries are realized comprising coordination numbers between five and seven. In almost every case a single, but not uniformly preferred metal configuration is observed in the crystal. The selectivity can not be easily explained by steric arguments as initially thought. The specific properties of the individual ligands will be discussed in the context of the solution state investigations.

4.3 NMR-Spectroscopy

Nuclear magnetic resonance (NMR) spectroscopy is without doubt one of the most powerful tools for structural analysis. As mentioned before, the best results can be obtained for compounds with only paired electron spins. In this case, the subjects of investigation were the diamagnetic complexes of Cu^{I}, Zn^{II}, Cd^{II}, Ru^{II}. All other species showed paramagnetic behavior. To rule out the existence of slow isomerization reactions in solution, the samples were measured twice with an interval of at least two days. The spectra were identical in every case showing the stability of the complexes towards degradation in solution.

Before the analysis of the complexes it is useful to briefly have a look at the specific features of ligands **2** (Figure 4.11).

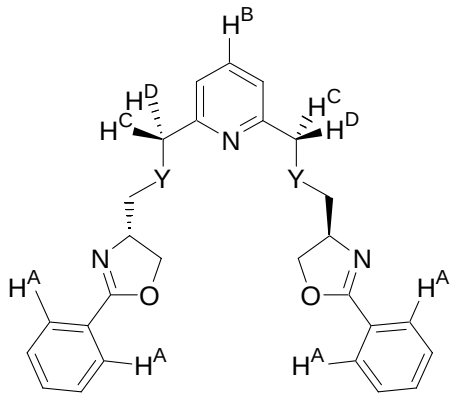

2a: Y = O
2b: Y = S
2c: Y = NMe

Figure 4.11. Domains of interest concerning NMR-spectroscopy in ligands **2**

There are a number of very diagnostic ^{1}H-signals indicating C_2-symmetry both in the free ligand as well as upon complexation. The spectra of **2a-c** are very similar. Therefore, only the ones for **2a** will be depicted (Figure 4.12). For details concerning **2b-c** see the appendix. In the aromatic region especially the signal of the protons H^B (triplet) and H^A (multiplet) are useful because of the separation from the other aromatic peaks. Due to the flexibility of the ligand arms the benzylic protons H^C/H^D show only one (broad) signal despite actually being diastereotopic. The ^{13}C-NMR spectrum shows the C_2-symmetry of **2a** (Figure 4.13).

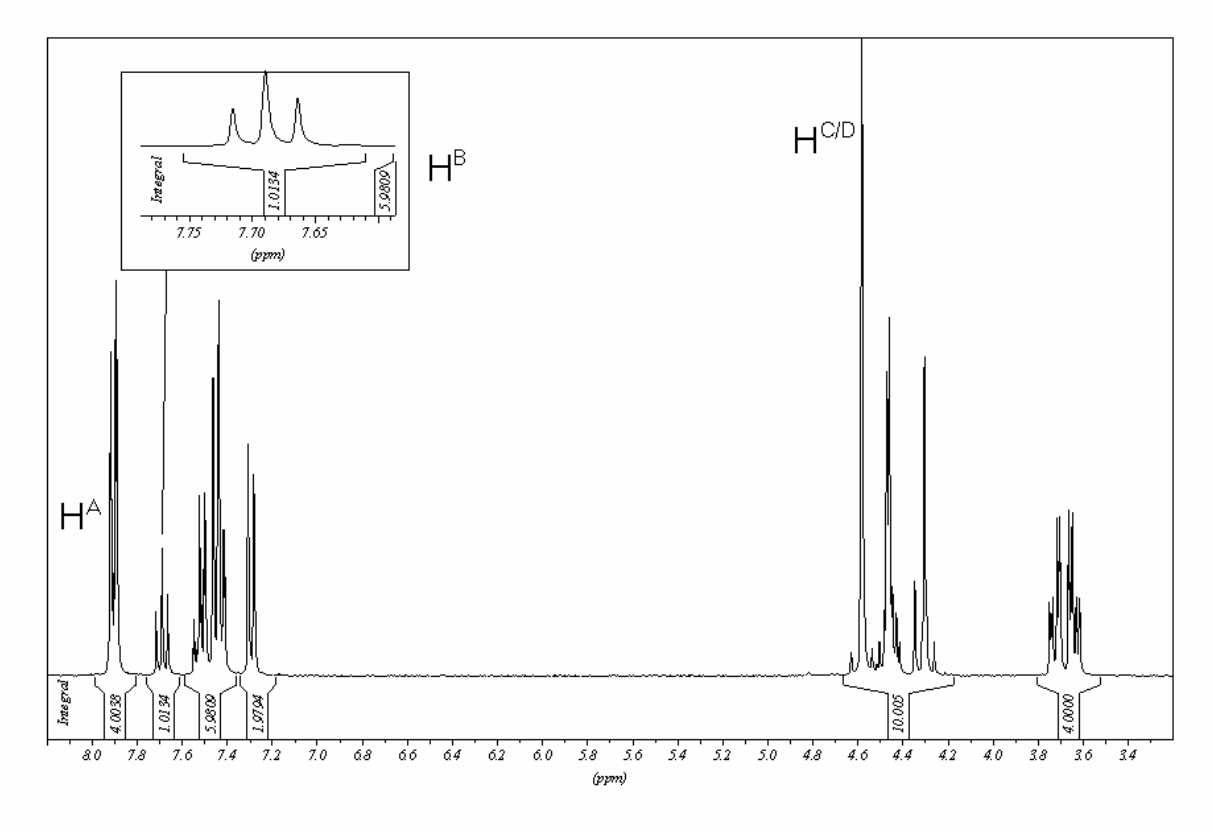

Figure 4.12. ^{1}H-NMR (300MHz, CD_3CN) spectrum of **2a** clearly showing distinguished signals

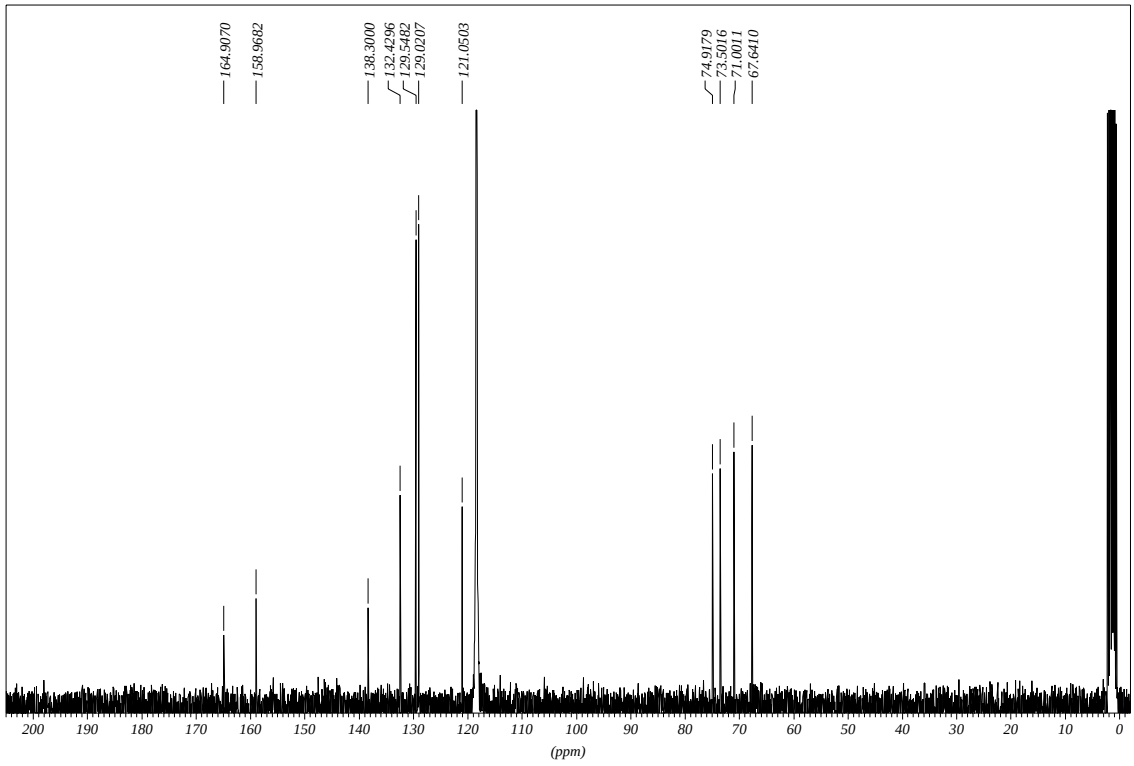

Figure 4.13. ^{13}C-NMR (75.5MHz, CD_3CN) spectrum showing the C_2-symmetry of **2a**

Upon complexation most of the proton signals are shifted to lower field. Normally H^B is the best indicator because of the strong shift to about 8.0 ppm. Because of the reduced conformational flexibility in the complexes, the benzylic protons $H^{C/D}$ split in a few cases to give two doublets with geminal coupling (J > 15Hz). These signals can sometimes not be resolved from other overlapping peak patterns. The ^{13}C-NMR spectra are very good indicators for the overall symmetry of the complexes. Once more, most of the peaks are shifted to higher ppm-values. Especially the peaks for the quarternary carbon atom C^2 in the oxazoline ring is very diagnostic. It can be assigned most unambiguously and secondly implies the binding of the oxazolines if shifted.

Table 4.4 surveys some characteristics of the isoelectronic Cu^I- and Zn^{II}-complexes along with the ones for Cd^{II}, the heavier homologue of the latter, and Ru^{II}.

Complex	**Solv.**	**Number of species**	**$\delta(H^B)_{comp}$ [ppm]**	**$\delta(H^B)_{comp}$ - $\delta(H^B)_{free}$ [ppm]**	**$\delta\ (C^2_{ox})_{comp}$ [ppm]**	**$\delta\ (C^2_{ox})_{comp}$ - $\delta\ (C^2_{ox})_{free}$ [ppm]**	**C_2-Sym.**
$[Cu^I(\mathbf{2a})(?)](ClO_4)$ * ?	$CDCl_3$	1	7.73	+ 0.08	166.1	+ 1.1	✓
$[Cu^I(\mathbf{2b})(?)](ClO_4)$ * ?	$CDCl_3$	1	7.71	+ 0.11	165.5	+ 1.0	✓
$[Zn^{II}(\mathbf{2a})](ClO_4)_2$	CD_3CN	1	8.12	+ 0.43	175.4	+ 10.5	✓
$[Zn^{II}(\mathbf{2b})](ClO_4)_2$ * H_2O	CD_3CN	1	8.08	+ 0.44	172.7	+ 8.1	✓
$[Zn^{II}(\mathbf{2c})](ClO_4)_2$ *CH_3CN * H_2O	CD_3CN	≥ 2	-	-	-	-	?
$[Cd^{II}(\mathbf{2a})(?)](ClO_4)_2$	CD_3CN	1	8.02	+ 0.33	170.5	+ 5.6	✓
$[Cd^{II}(\mathbf{2b})](ClO_4)_2$ * THF	CD_3CN	?	broad	-	broad	-	?

Table 4.4. Comparison of the Cu^I-, Zn^{II}- and Cd^{II}-complexes with **2a-c** (for the complete spectra see the appendix)

As example the spectra of [Zn(**2a**)]$(ClO_4)_2$ are shown in Figure 4.14.

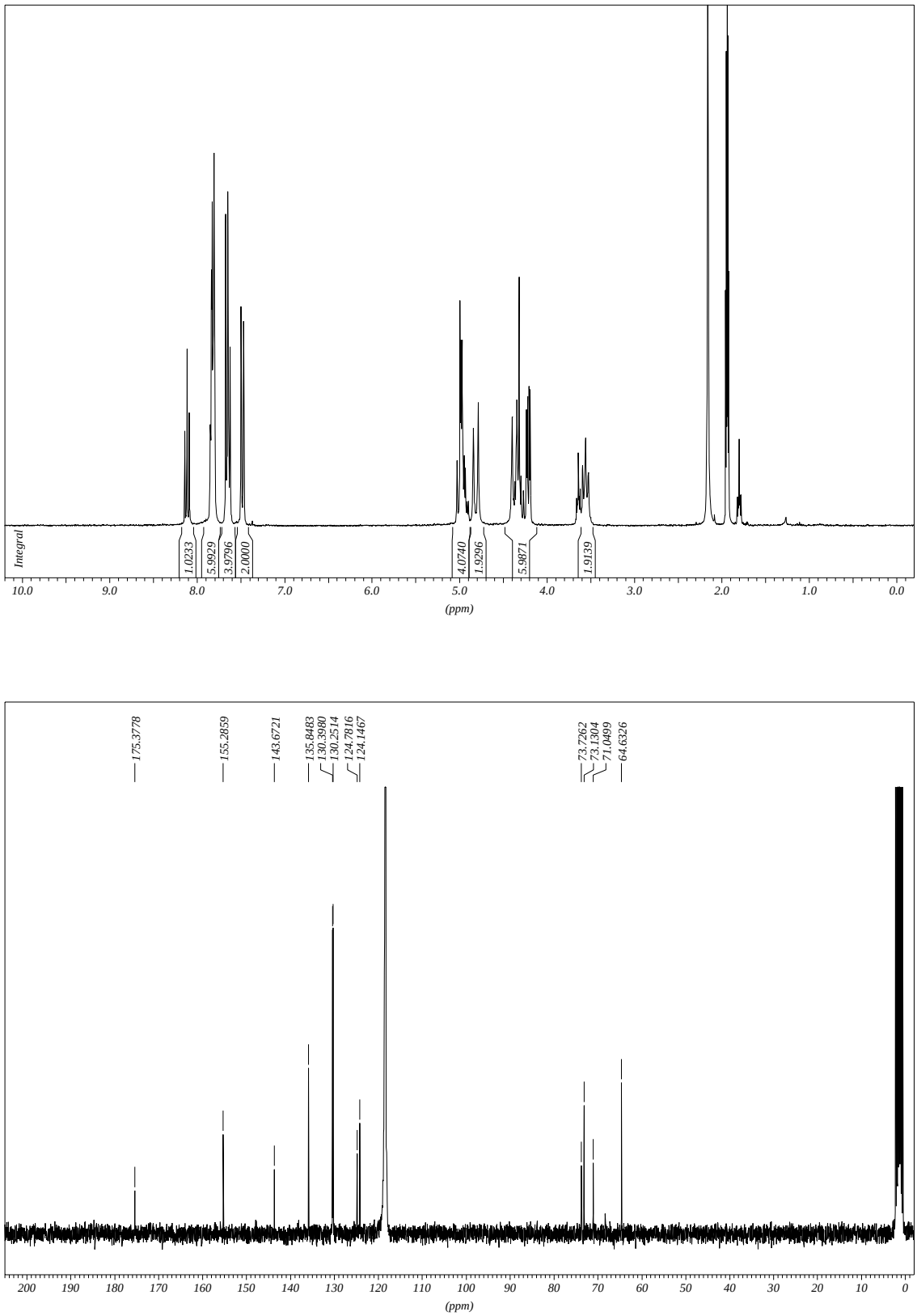

Figure 4.14. ^{1}H-NMR (300 MHz, CD_3CN) and ^{13}C-NMR (75.5 MHz, CD_3CN) spectra of [Zn(**2a**)]$(ClO_4)_2$

As can be seen from Table 4.4, the complexation behavior of ligands **2a** and **2b** with Cu^{I} and Zn^{II} is very similar. In these cases only one single species can be observed, indicating completely stereoselective complex formation. Both ligands show almost identical shifts for certain signals (H^{B} and C^{2} of the oxazoline ring) indicating a very close structural relationship. Metals with d^{10} electron configuration are relative indifferent towards special coordination geometries because of the lack of ligand field stabilization energy. With respect to zinc(II), a trigonal-bipyramidal arrangement like in the solid state is very likely. Concerning the copper(I) species nothing is known about the crystal structure. Therefore, the assignment to one specific coordination geometry is highly speculative. Nevertheless, a trigonal-bipyramidal geometry in analogy to the isoelectronic Zn^{II}-complexes is presumably the best guess, also supported by the isostructural relationsship between Cu^{II} and Zn^{II} as indicated by CD-spectroscopy (vide infra).

The combination of zinc(II) with ligand **2c** yields spectra with more than one species, in contrast to the solid state where only one complex could be observed. Their nature could not be clarified. This behavior has to be attributed to the additional methyl groups at the connecting tertiary amines exerting a strong steric strain on the ligand backbone upon complexation. This strain which has the biggest effect in the very crowded trigonal-bipyramide (see solid state) is probably relieved in solution by dissociation of one ligand arm from the metal center.

In the case of Cd^{II} only the complex with **2a** exhibits well-defined behavior. With **2b** very broad proton spectra are obtained, indicating exchange processes and/or major configurational changes in solution. This is one more hint that **2b** is not a suitable ligand for large metals like cadmium, as could also be seen in the strong distortion of the crystal structure of $[Cd(\mathbf{2b})(ClO)_4]^{+}$. Ligand **2a** has the much smaller donor atom oxygen instead of sulfur and very probably adopts a pentagonal-bipyramidal geometry (see CD-spectroscopy) which apparently has the ability to accommodate much larger cations than **2b**.

Special cases are the very probably octahedral Ru^{II}-complexes with **2b**. NMR clearly shows two independent C_2-symmetrical species (ratio 7:3) as could be shown by complete correlation of the spectra. Therefore, only Δ_2 or Λ_2 are possible configurations. This problem could in principle be solved by one of the two following proposals:

- Two homochiral complexes are present only distinguished by the sixth external ligand (Cl, CH_2Cl_2, etc.).
- The two species are Δ_2-[Ru(**2b**)Cl]$^+$ and Λ_2-[Ru(**2b**)Cl]$^+$.

Molecular modelling of the two latter isomers of [Ru(**2b**)Cl]$^+$ indicates the greater stability of the Δ_2-configuration by ca. 3 kcal/mol, mainly because of the steric interaction of the phenyl rings with the ligand backbone disfavoring Λ_2 (Figure 4.15).

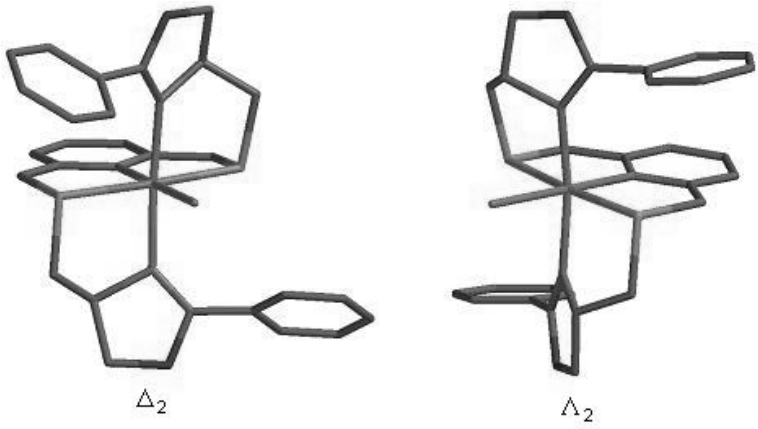

Figure 4.15. Molecular modelling of [Ru(**2b**)Cl]$^+$ (PM3-TM, Titan 1.05, Schrödinger Inc.)

This would mean that regardless of the two possibilities proposed above the more stable diasteromer (Δ) is present in excess anyway. The importance of this for the interpretation of the CD-spectra and particularly for the correlation to the absolute configuration will become obvious later.

4.4 CD-Spectroscopy

The measurement of circular dichroism (CD) has proved to be a very valuable tool for the examination of conformational changes in chiral assemblies. It could be used with great success for the investigation of secondary structures of peptides. This is mainly done by comparison of a given spectrum with known characteristic signal patterns (Figure 4.16).

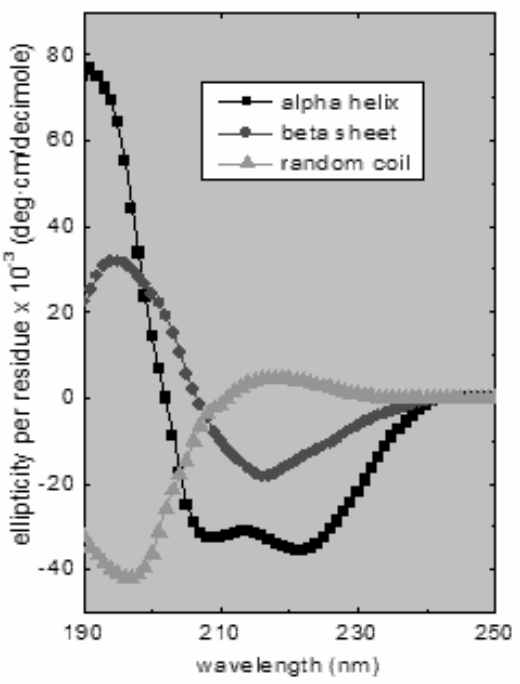

Figure 4.16. Characteristic CD signals for certain secondary structures in proteins

Such a reference system could also be an extremely useful tool for our ligand system, because it would allow the determination of solution state structures of unknown metal complexes of **2** with regard to coordination geometry and absolute configuration.

In the special case of ligand system **2**, an empirical method for the rationalization of CD-signals on the basis of sector rules for the pyridine chromophore has been reported by Palmer.[1] These rules for the n-π*-transition have been used for their subject of investigation, metal complexes of macrocyclic pyridine crown ether **18** (Figure 4.17). Likewise they apply for ligand system **2**.

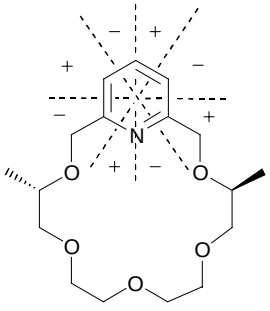

18

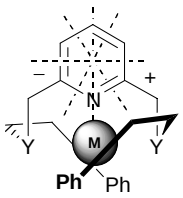

schematic representation
of metal complexes with **2**

Figure 4.17. Pyridine crown ether **18** and proposed sector rules for n→π*-transitions by Palmer et al. (+ und – correspond to the sign of the CD-signal for the presence of substituents *above* the pyridine ring. *Below* this plane the signs are inverted.)

If the sector rules are employed for the prediction of CD-signals in our case, the octahedral Δ_2-configuration on the right of Figure 4.17 would yield a positive sign for the n-π^*-transition. This is because the right arm is placed above the pyridine plane in the sector indicated with "+". The left arm is located below this plane beneath the sector given a "– ". A positive sign is resulting due to the fact that signs are inverted under the pyridine plane, a consequence of the C_2-symmetry.

Nevertheless, these sector rules can often not fully describe the spectral properties because they only take into account the pyridine chromophore rather than the contribution from the overall shape. In general, they give a good hint but not more. The spectra of most of the complexes show patterns of a complexity that can not be explained by this simple sector model. Nevertheless, in some cases good agreement could be found.

Before the measurement of the CD-spectra the corresponding UV absorption spectra were collected for all compounds in question. Table 4.5 shows the position of the maxima of the n-π*-transition. This absorption can be observed as a peak on the higher wavelength side of the very intense π-π*-bands, often only as a shoulder (Figure 4.18).

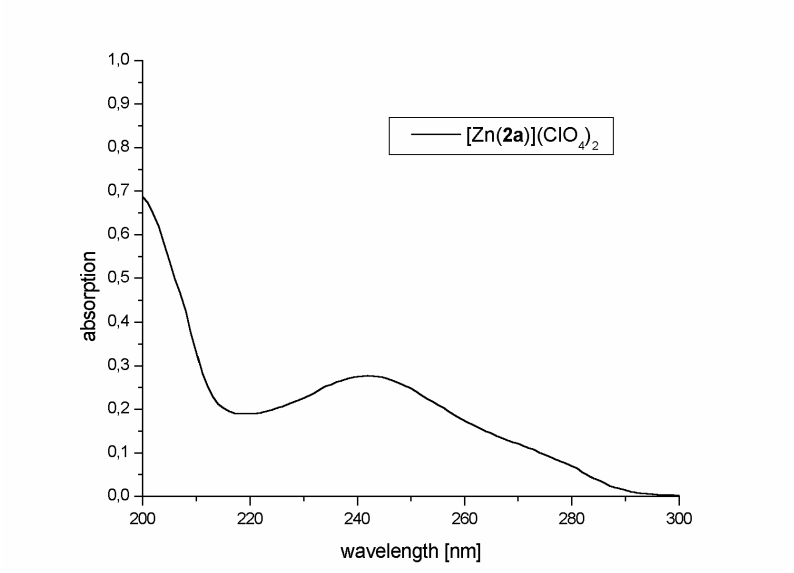

Figure 4.18. Typical UV-spectrum of complexes with **2** (in this case [Zn(**2a**)]$(ClO_4)_2$)

Complex	λ_{max}(n-π*) [nm]	Complex	λ_{max}(n-π*) [nm]	Complex	λ_{max}(n-π*) [nm]
[Mn(**2a**)$(H_2O)_2$]$(ClO_4)_2$ *THF	244	-			
[Fe(**2a**)$(H_2O)_2$]$(ClO_4)_2$ *THF	242	[Fe(**2b**)(H_2O)]$(ClO_4)_2$ *2 H_2O	222		
[Co(**2a**)]$(ClO_4)_2$	238	[Co(**2b**)(THF)]$(ClO_4)_2$ *H_2O	231	[Co(**2c**)(H_2O)]$(OTf)_2$	232
[Ni(**2a**)]$(ClO_4)_2$ *H_2O*THF	247	[Ni(**2b**)]$(ClO_4)_2$ *2 H_2O	230		
[Cu(**2a**)]$(ClO_4)_2$ *H_2O*THF	245	[Cu(**2b**)]$(ClO_4)_2$ *H_2O	244		
[Zn(**2a**)]$(ClO_4)_2$	242	[Zn(**2b**)]$(ClO_4)_2$ *H_2O	267	[Zn(**2c**)]$(ClO_4)_2$ *H_2O*CH_3CN	241
[Cd(**2a**)(?]$(ClO_4)_2$	243	[Cd(**2b**)]$(ClO_4)_2$ *THF	237		
[Mg(**2a**)$(H_2O)_2$]$(ClO_4)_2$	244	[Co(**2b**)(THF)]$(OTf)_2$	231		

Table 4.5. Position of n-π*-band of complexes with **2**

As can be seen, the usual peak wavelength varies between 230nm and 250nm. The only exception is the zinc complex with ligand **2b** having the maximum at 267nm. It is not clear why this is the case.

CD-spectra were recorded in the range from 200nm to 300nm of ca. 10^{-4} M solutions in CH_3CN (see NMR-solvent: CD_3CN) in 1mm cylindrical cuvettes. The solutions were stored for one week and the measurements repeated to exclude slow isomerization reactions or degradation. Like with the NMR-samples no change could be observed in comparison to the initial spectra. The free ligands show no detectabe CD-signals in the region of the n-π^*-transition. Therefore, the observed signals can be unambiguously attributed to the corresponding complexes.

- **Complexes with Ligand 2a**

Figure 4.19 shows the CD-spectra of all complexes $[M^{II}(\mathbf{2a})(X)]^{2+}$.

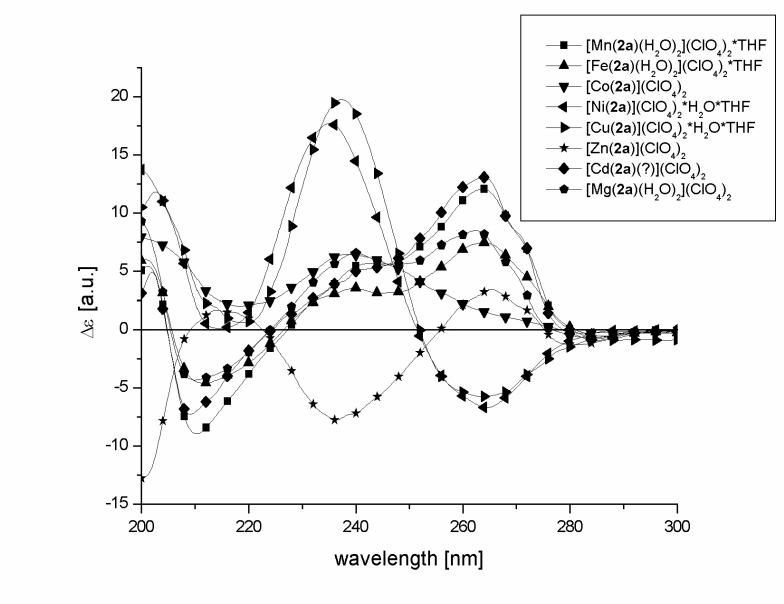

Figure 4.19. CD-spectra of complexes of **2a**

Out of the many spectra two repeating patterns can be extracted. The first group is populated by the complexes of manganese, iron, cadmium and magnesium (Figure 4.20).

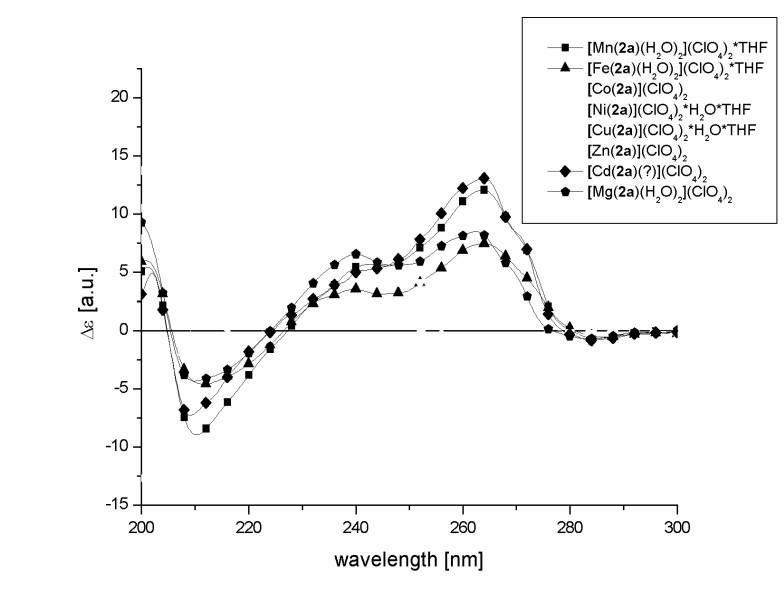

Figure 4.20. CD-spectra of Mn^{II}-, Fe^{II}-, Cd^{II}- and Mg^{II}-complexes with **2a**

The four patterns differ only very slightly from each other. For the iron species the crystal structure shows Λ_2–pentagonal-bipyramidal geometry. From the solutions of

Cd^{II} with **2a** C_2-symmetry can be deduced. Taking these facts together the probability for all these complexes to be Λ_2–pentagonal-bipyramidal also in solution is very high.

The second group consists of nickel(II), copper(II) and zinc(II) (Figure 4.21).

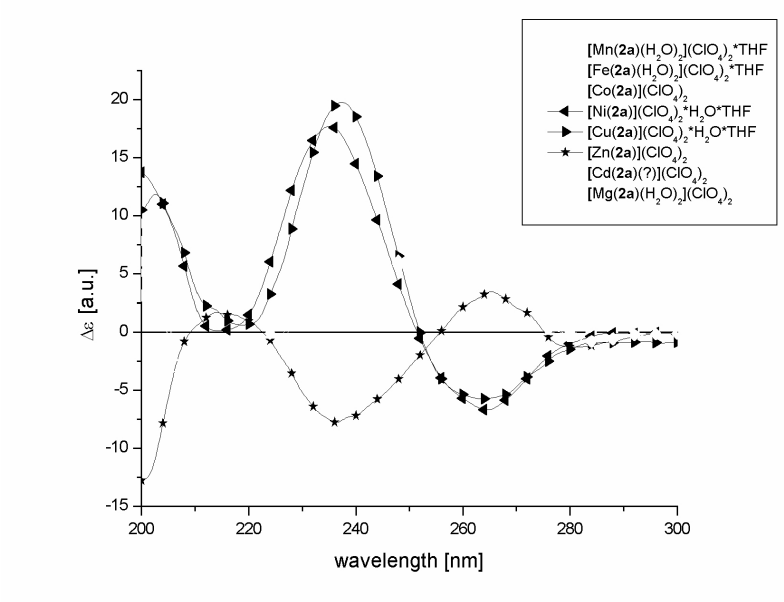

Figure 4.21. CD-spectra of Ni^{II}-, Cu^{II}- and Zn^{II}-complexes with **2a**

These signals also exhibit a high degree of similarity. The zinc(II) complex is known to be a Λ_2-configured trigonal-bipyramide (X-ray) and to exist only as one form in solution (NMR). Therefore it is very likely that the solid state structure is retained in solution. In consequence, nickel(II) and copper(II) should be Δ_2–species with trigonal-bipyramidal geometry because of the mirror-image behavior of the CD-spectrum of zinc(II) indicating an almost enantiomeric relationship. It is interesting to note that simply by exchanging the metal, two pseudo-enantiomeric complexes can be prepared from the same ligand with the same stereo-information.

The case of cobalt(II) remains unclear because further structural information and an appropriate comparison like for the other complexes is not available.

- **Complexes with Ligand 2b**

CD-spectra of $[M^{II}(\mathbf{2b})(X)]^{2+}$ are given in Figure 4.22.

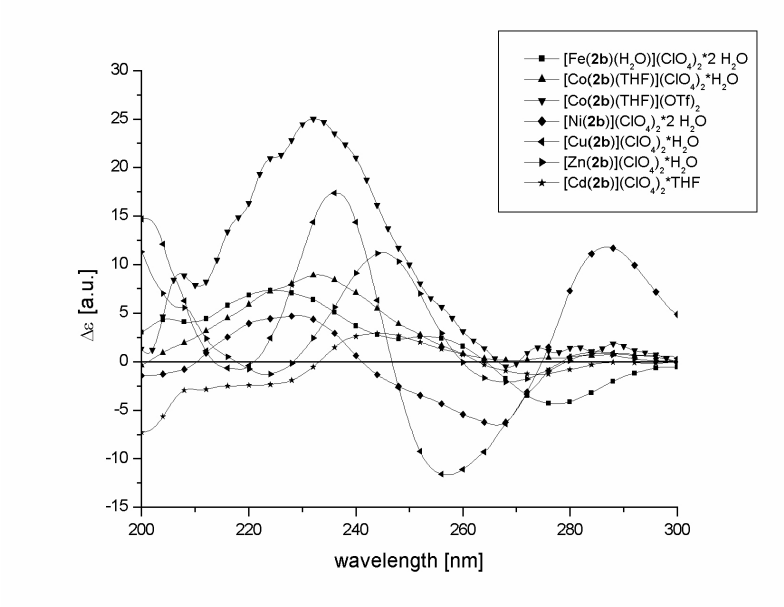

Figure 4.22. CD-spectra of complexes of **2b**

The spectra show less similarity among each other compared with the ones for **2a** but still a few characteristic patterns can be extracted. The spectra for copper(II) and zinc(II) with **2b** resemble very strongly their counterparts with ligand **2a** which were trigonal-bipyramidal (Figure 4.23).

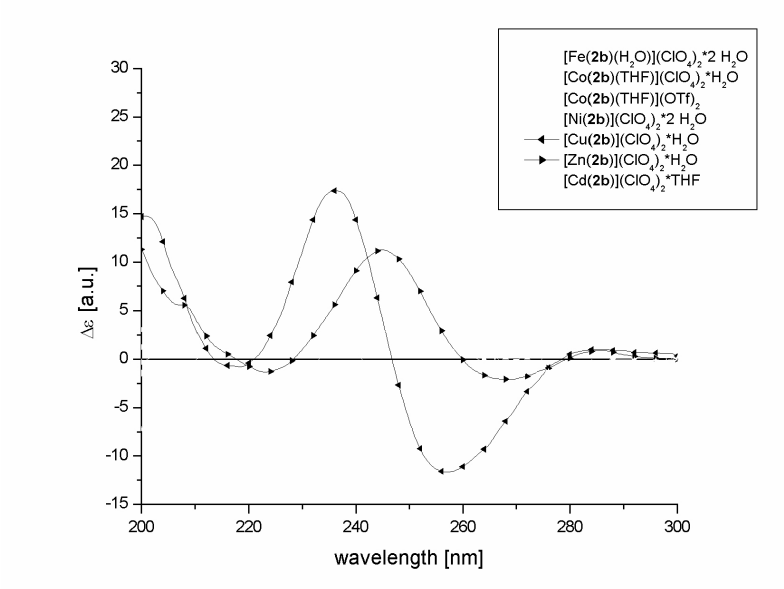

Figure 4.23. CD-spectra of Cu^{II}- and Zn^{II}-complexes with **2b**

In the case of $[Zn(\mathbf{2b})]^{2+}$ the solid state structure shows exactly this geometry with Δ_2-configuration and forms upon dissolving in CH_3CN only one species (NMR). The assignment of Δ_2 also for the solutions of Cu^{II} and Zn^{II} is in complete agreement with the mirror-image CD-spectrum of the opposite configured $[Zn(\mathbf{2a})]^{2+}$ (vide supra). Again it is a noteworthy finding that exchanging the two isosteric ligands **2a** and **2b** forms pseudo-enantiomers upon complexation with zinc(II). Only two donor atoms have to be altered for this purpose.

Also very interesting are the spectra of cobalt(II) and iron(II) (Figure 4.24).

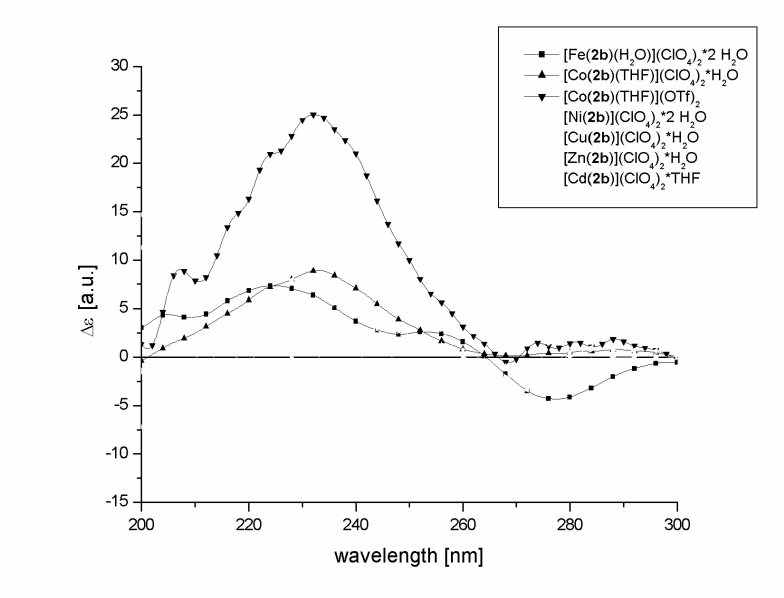

Figure 4.24. CD-spectra of Fe^{II}- and Co^{II}-complexes with **2b**

In this case, a very characteristic broad peak from ca. 200nm to 260nm can be observed, clearly distinguished from the other coordination geometries discussed above. Cobalt(II) exhibits Δ_2-octahedral geometry in the solid state. As predicted with the sector rules introduced above a positive CD-band is observed. Here the assigment is relative unambiguous because of the simplicity of the signal set. Another hint is the CD-spectrum of the two octahedral ruthenium(II)-species in comparison to Co^{II} (Figure 4.25), also showing a net spectrum with positive signals only. As discussed earlier this is due to the predominance of the Δ_2-configuration and is one more indication for the retention of the solid state Co^{II}-structure in solution.

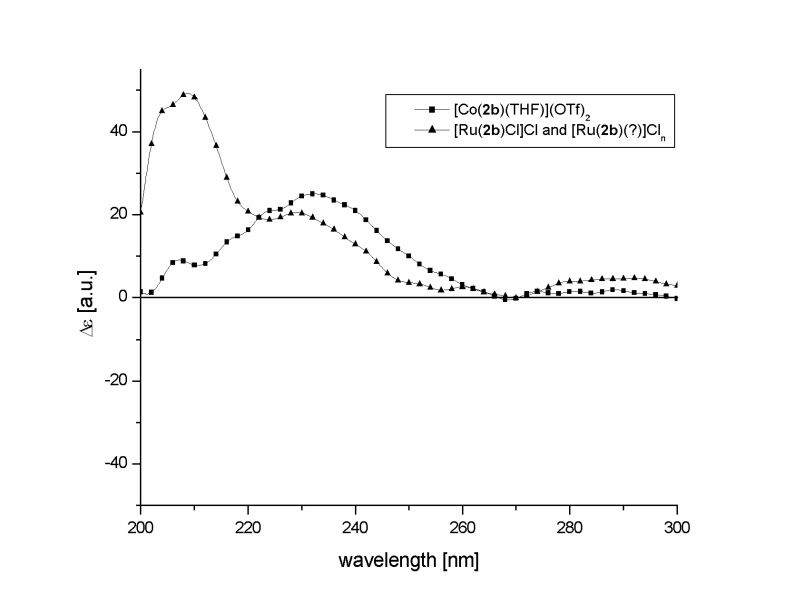

Figure 4.25. Comparison of the Ru^{II}- and the Co^{II}-CD-spectra with **2b**

The spectra of Ni^{II} and Cd^{II} could not be interpreted. In the case of Cd^{II} this is not very surprising in the light of the existence of probably more than one species in solution (NMR).

- **Complexes with Ligand 2c**

Finally, the CD-spectra of the two complexes with **2c** are shown in Figure 4.26.

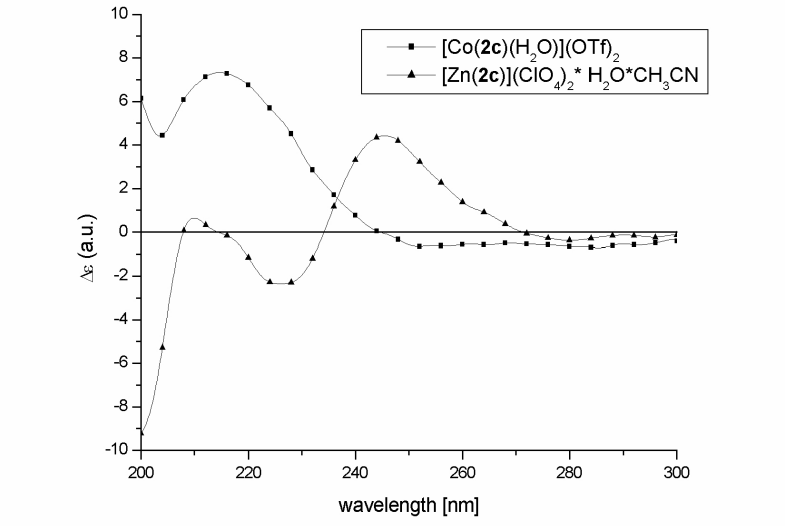

Figure 4.26. CD-spectra of [Co(**2c**)(H_2O)]($OTf)_2$ and [Zn(**2c**)]$(ClO_4)_2$*H_2O*CH_3CN

The spectrum of the zinc complex is as expected not well-defined because more than one species is present in solution (NMR). The Co^{II}-complex in contrast exhibits a nice Δ_2- octahedral pattern (vide supra) as was seen in the crystal structure.

In conclusion, most of the metal complexes with **2** could be assigned to one specific coordination geometry and a determined configuration in solution by comparison and further information from NMR and X-ray. The cases where it was known from prior findings that no defined structures form upon dissolving did indeed stand out because of their strange behavior regarding CD-spectra. In almost every case the solid and the solution state structures are similar.

References:

[1] R.B. Dyer, R.A. Palmer, R.G. Ghirardelli, J.S. Bradshaw, B.A. Jones, *J. Am. Chem. Soc.* **1987**, *109*, 4780-4786.

5 Multinuclear Assemblies

5.1 Introduction

The subject of investigation so far was the stereoselectivity of mononuclear complexes with ligands **2**. A different approach is the controlled construction of multinuclear chiral structures, important especially in the field of supramolecular chemistry (see Section 1). Rapidly emerging classes of polymeric metal-containing structures are on the one hand so-called "coordination polymers"[1] (infinitely extending metal-ligand assemblies with bridging organic ligands) and on the other "inorganic-organic hybrid polymers"[2] (metal-centers, modified by organic ligands and connected by inorganic bridges). Although these fields have experienced tremendous attention over the last years, the asymmetric synthesis of chiral structures has been devoted relatively little effort. One of the most prominent chiral structures is the helix. Enantiopure, one-dimensional helices have been reported for coordination polymers in a few instances.[1] In contrast, the domain of inorganic-organic hybrid polymers has seen only very recently a first example of the generation of an enantiopure one-dimensional helical chain.[3]

In our case the pentagonal-bipyramidal geometry seemed ideally suited for the construction of one-dimensional polymeric chains because of the orientation of the two apical coordination sites perpendicular to the pentagonal plane and lying on one straight line. The best candidate on the metal part with this geometry soon was realized to be Cd^{II} (in combination with ligand **2a**), known for its tendency to form halogen bridged one- or two-dimensional polymeric structures.[4]

5.2 Synthesis and Structural Analysis

The procedure for the preparation involved refluxing cadmium(II) halides with ligand **2a** in methanol (Scheme 5.1).

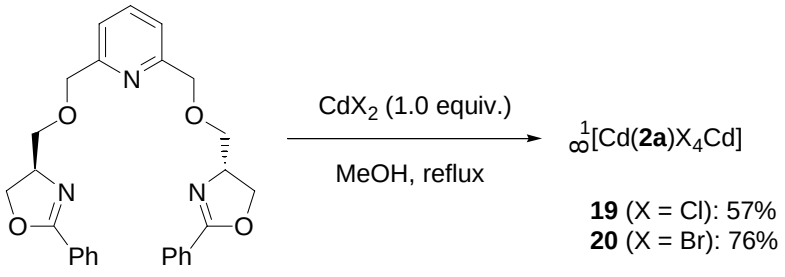

2a

Scheme 5.1. Synthesis of the polymeric cadmium species

The polymeric nature of the products was very likely because of their very low solubility. The exact structure remained at first unclear, of course. After collecting as much analytical data as possible, the following facts were known:

- Elemental analysis: Ligand to CdX_2 = 1 : 2
- Mass spectrometry: Main species $[Cd(\mathbf{2a})X]^+$ and $[CdX_3]^-$
- ^{1}H-NMR (CD_3CN): very low solubility but clearly one C_2-symmetrical species
- CD-spectroscopy (CH_3CN):

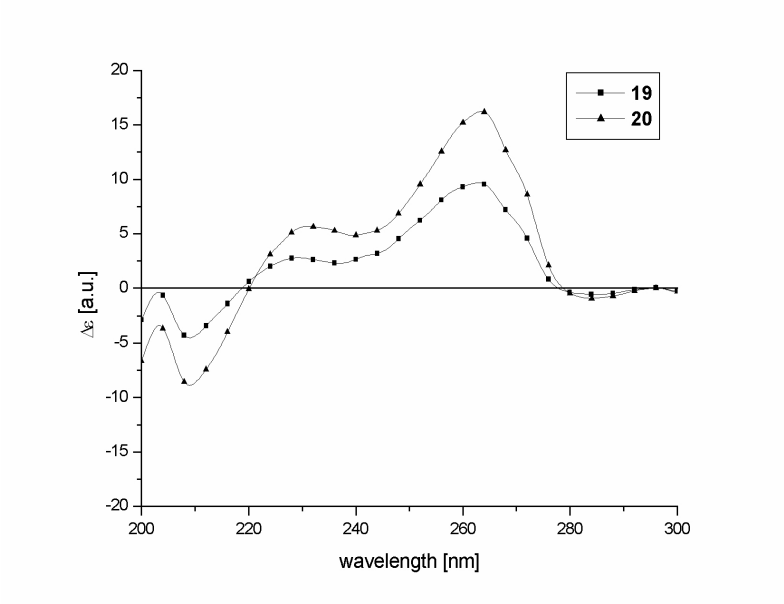

→ Λ_2-pentagonal-bipyramidal

All these findings finally gave an idea of the underlying design principle. Noteworthy is especially the role of CD-spectroscopy which gives an accurate prediction of the coordination geometry as well as the absolute configuration. This demonstrates the power of the approach developed in the last section.

Finally it was possible to grow single crystals suitable for X-ray analysis by slow vapor-diffusion of Et_2O into a saturated solution of the Cd-species in CH_3CN. The structure determination completely confirmed the prediction (Figure 5.1, Table 5.1)

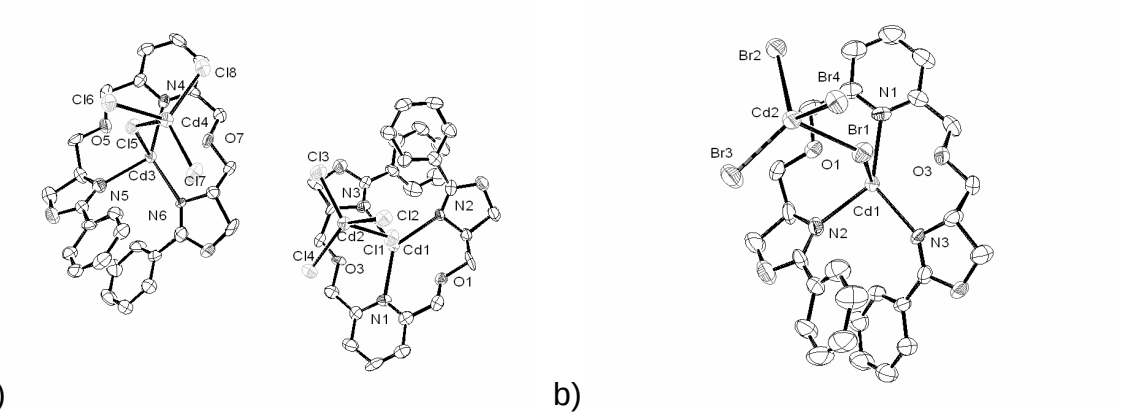

a) b)

Figure 5.1. Crystal structures of the asymmetric units of a) **19** and b) **20** (hydrogen atoms omitted for clarity)

Table 5.1. Crystal data for cadmium complexes **19** and **20**

	$_\infty$[Cd(2a)Cl$_4$Cd] (19)	**$_\infty$[Cd(2a)Br$_4$Cd] (20)**
formula	$C_{27}H_{27}Cd_2Cl_4N_3O_4$	$C_{27}H_{27}Br_4Cd_2N_3O_4$
crystal appearance	colorless stick	colorless prism
mol. weight	824.24	1001.94
crystal system	monoclinic	orthorhombic
space group	$P2_1$	$P2_12_12_1$
a [Å]	8.6650(9)	9.0518(7)
b [Å]	12.2190(8)	12.5611(7)
c [Å]	29.130(3)	29.0084(15)
α [°]	90	90
β [°]	95.297(12)	90
γ [°]	90	90
volume [Å ^{3}]	3071.0(5)	3298.3(4)
Z	4	4
ρ [g cm^{-1}]	1.783	2.018
μ [mm^{-1}]	1.770	6.170
crystal size [mm]	0.20*0.05*0.03	0.12*0.10*0.10
temperature [K]	173(1)	173(1)
radiation [Å]	$Mo_{K\alpha}$ (λ = 0.71073)	$Mo_{K\alpha}$ (λ = 0.71073)
θ max [°]	1.81 < *θ* < 25.87	2.14 < *θ* < 25.86
measured reflections	31456	23444
independent reflections	11538	6341
reflections in refinement	7944, $I \geq 2\sigma(I)$	4401, $I \geq 2\sigma(I)$
R[a]	0.0313	0.0344
wR_2[b]	0.0575	0.0634
R[a] (all data)	0.0560	0.0588
wR_2 (all data)	0.0620	0.0684
abs. structure param.	0.00(3)	– 0.011(14)

[a] R factor definition: $R = \Sigma (||F_o| - |F_c||) / \Sigma |F_o|$. [b] SHELX-97 wR_2 factor definition: $wR_2 = [\Sigma w(F_o^2 - F_c^2)2 / \Sigma w(F_o^4)]1/2$. Weighting scheme: $w = 1 / [\sigma^2(F_o)^2 + (np)^2]$, $p = [F_o^2 + 2 F_c^2] / 3$.

The structures of **19** and **20** are very similar and follow the same design principles. Both consist of unprecedented one-dimensional chains of pentagonal-bipyramidal coordinated Cd-centers, connected by only slightly distorted tetrahedral CdX_4 units via bridging halogens (Figure 5.2). All bond lengths and angles are in the normal range. An obvious difference between the two structures is the increase in the helical pitch (**19**: 8.67Å vs. **20**: 9.05Å), resulting from the different bridging X-Cd bond length (Cd-Cl: 2.503-2.601Å vs. Cd-Br: 2.636-2.729Å).

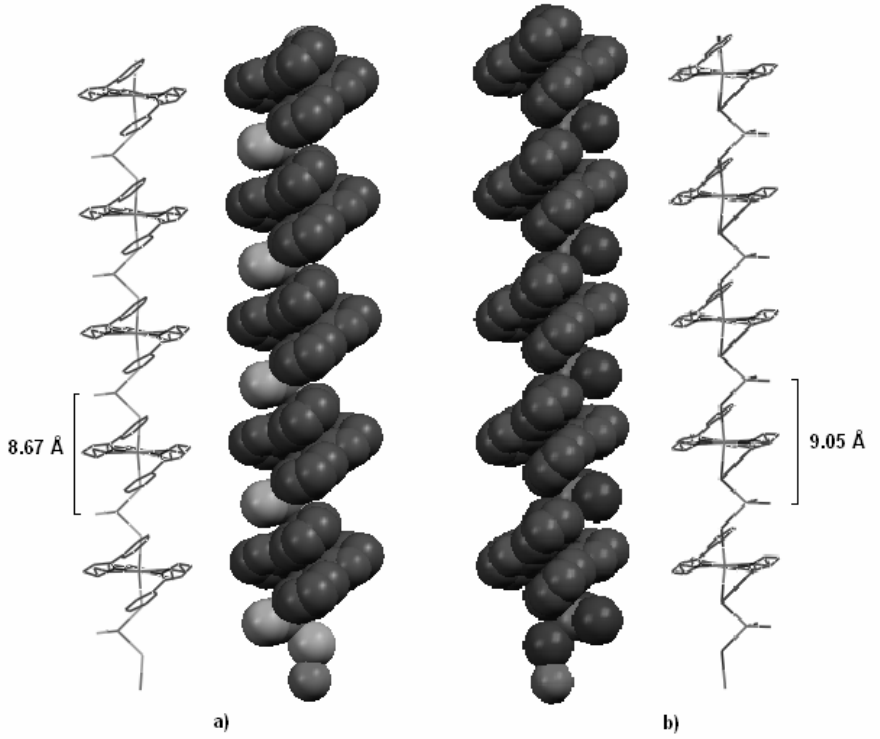

Figure 5.2. 1D-chain subunits of a) **19** and b) **20**

In the case of **19**, two unique chains can be distinguished, differing only very slightly from each other. Essentially they can be regarded as almost identical, like in **20**, where only one chain can be found. Regarding stereochemistry, only Λ_2-configured metal centers are present, yielding exclusively *P*-helical chains. The stacking of the individual chains is parallel to each other and to the crystallographic axis a, thereby creating a highly directed, helically ordered assembly. In both compounds, every other chain is stacked upside down, resulting in a deviation of the connecting Cd-tetrahedra alternately to the right and to the left with respect to the mirror-plane bisecting the pyridine ring. Obviously, this does not change the overall helicity of the assembly. These columns are ordered in a zig-zag-fashion (in the plane normal to

the axis a) (Figure 5.3) and each neighboring chain is shifted by half of the helix pitch (normal to axis b) (Figure 5.4).

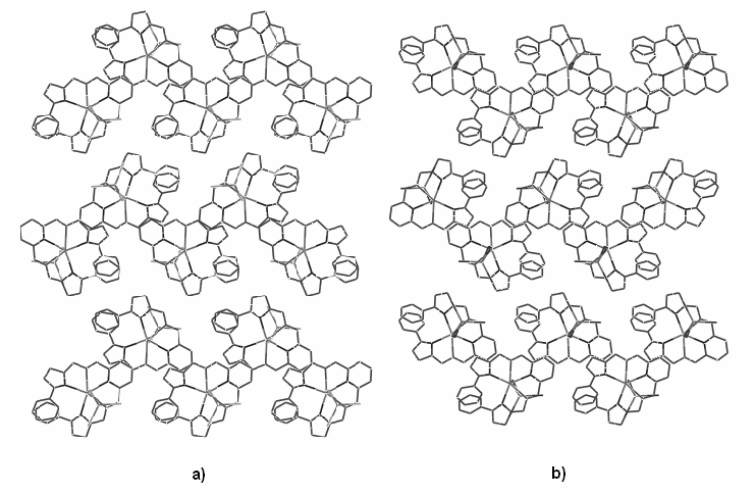

Figure 5.3. View normal to the crystallographic axis a for a) **19** and b) **20**

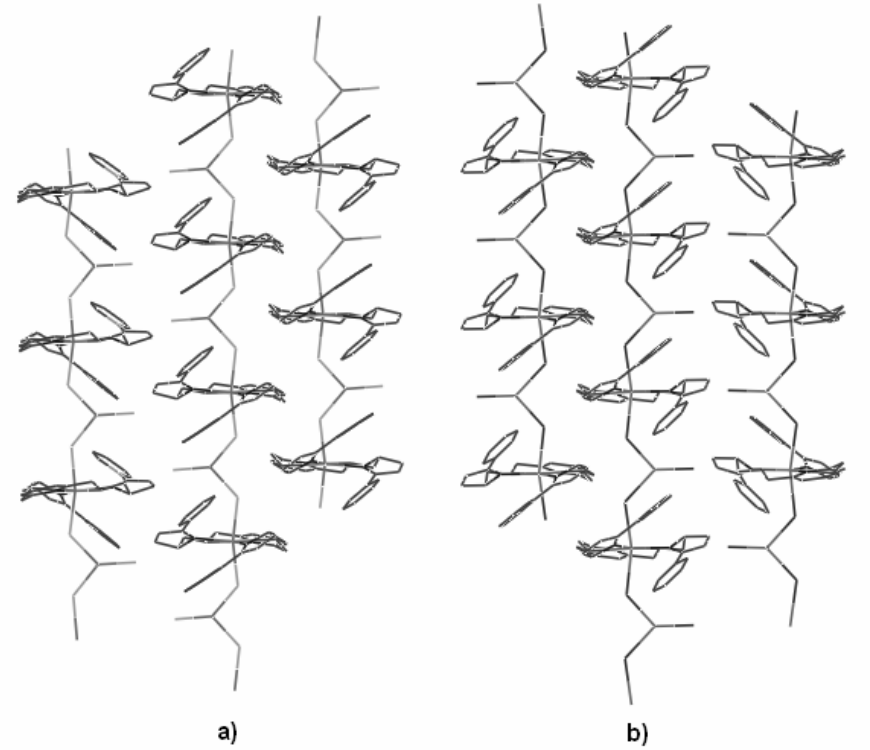

Figure 5.4. View normal to the crystallographic axis b for a) **19** and b) **20**

In conclusion, it could be shown that ligand **2a** is capable of inducing helical topology in inorganic-organic hybrid polymers with unprecedented design and complete stereoselectivity. This constitutes the first example of homochiral, non-racemic, one-dimensional helices with an extended network of bridging halogens. Furthermore, the structure elucidation before X-ray analysis demonstrates the predictive power of CD-spectroscopy for this purpose.

References:

[1] Reviews: a) C. Janiak, *J. Chem. Soc., Dalton Trans.* **2003**, 2781-2804; b) S. Kitagawa, R. Kitaura, S.-I. Noro, *Angew.Chem. Int. Ed.* **2004**, *43*, 2334-2375. Selected very recent examples: a) R. Wang, L. Xu, X. Li, Y. Li, Q. Shi, Z. Zhou, M. Hong, A.S.C. Chan, *Eur. J. Inorg. Chem.* **2004**, 1595-1599; b) S.P. Anthony, T.P. Radhakrishnan, *Chem. Commun.* **2004**, 1058-1059; c) U. Siemeling, I. Scheppelmann, B. Neumann, A. Stammler, H.-G. Stammler, J. Frelek, *Chem. Commun.* **2003**, 2236-2237; d) N. Niklas, F. Hampel, R. Alsfasser, *Chem. Commun.* **2003**, 1586-1587; e) A.N. Khlobystov, M.T. Brett, A.J. Blake, N.R. Champness, P.M.W. Gill, D.P. O'Neill, S.J. Teat, C. Wilson, M. Schröder, *J. Am. Chem. Soc.* **2003**, *125*, 6753-6761.

[2] Reviews: a) P.M. Forster, A.K. Cheetham, *Topic*s in Catalysis **2003**, *24(1-4)*, 79-86; b) P.J. Hagrman, D. Hagrman, J. Zubieta, *Angew. Chem. Int. Ed.* **1999**, *38*, 2638-2684.

[3] E.V. Anokhina, A.J. Jacobson, *J. Am. Chem. Soc.* **2004**, *126*, 3044-3045.

[4] F.A. Cotton, G.W. Wilkinson, C.A. Murillo, *Advanced Inorganic Chemistry,* Wiley-Interscience, New York **1999** (6th edition).

6 Results and Discussion

The structural characteristics for ligands **2** are summarized in Tables 6.1-6.3. The depicted polyhedron for an individual metal indicates the proposed geometry in solution and in the solid state, as deduced from X-ray analysis, NMR- and CD-spectroscopy (vide supra). The preference for a single configuration is indicated by the proper descriptor. If solid and solution state structures differ from each other or more than one species is formed, this is also stated.

Solid and Solution State Structures (X-Ray/NMR/CD) 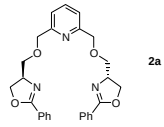 **2a**					
^{25}Mn 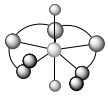 Λ_2	**^{26}Fe** 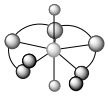 Λ_2	**^{27}Co** ?	**^{28}Ni**  Δ_2	**^{29}Cu**  Δ_2	**^{30}Zn**  Λ_2
^{43}Tc	**^{44}Ru**	**^{45}Rh**	**^{46}Pd**	**^{47}Ag**	**^{48}Cd** 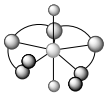 Λ_2

Table 6.1. Structures of transition-metal complexes with ligand **2a**

Solid and Solution State Structures (X-Ray/NMR/CD) 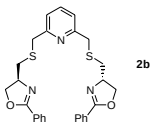 **2b**					
^{25}Mn	**^{26}Fe**  Δ_2	**^{27}Co**  Δ_2	**^{28}Ni** ?	**^{29}Cu**  Δ_2	**^{30}Zn**  Δ_2
^{43}Tc	**^{44}Ru**  $\Delta_2 > \Lambda_2$	**^{45}Rh**	**^{46}Pd**	**^{47}Ag**	**^{48}Cd**  not uniform

Table 6.2. Structures of transition-metal complexes with ligand **2b**

Solid and Solution State Structures (X-Ray/NMR/CD) 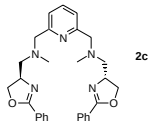 2c					
^{25}Mn	^{26}Fe	^{27}Co  Δ_2	^{28}Ni	^{29}Cu	^{30}Zn  not uniform
^{43}Tc	^{44}Ru	^{45}Rh	^{46}Pd	^{47}Ag	^{48}Cd

Table 6.3. Structures of transition-metal complexes with ligand **2c**

6.1 Comparison by Coordination Geometry

- **Pentagonal-Bipyramidal**

Metal complexes with coordination number (CN) seven[1] are rather rare and represent only approximately 1.8% of the reported structures for transition metal complexes (Cambridge Structural Database).[1d] Among the transition metals, this CN is not evenly distributed and is found predominantly with second and third-row elements of the early transition metals (Figure 6.1).

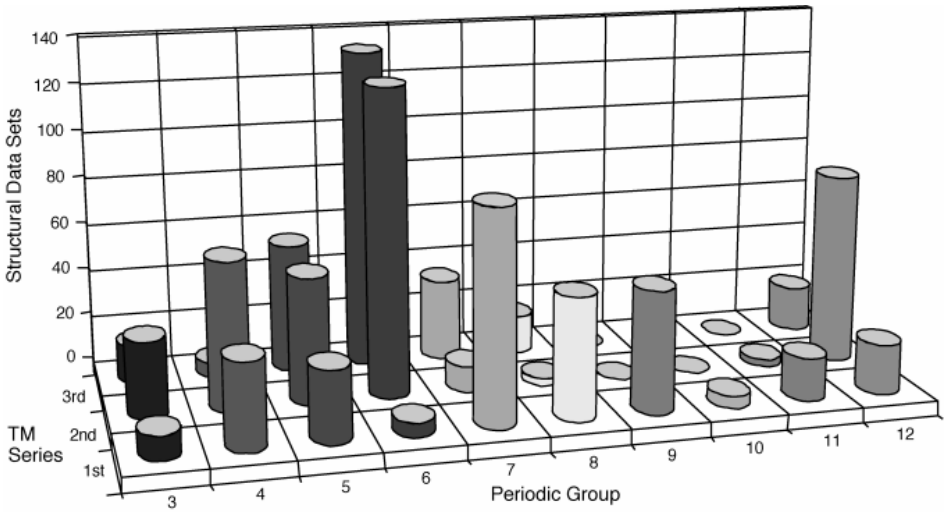

Figure 6.1. Distribution of σ-heptacoordinate complexes through the transition metal series (reproduced from ref. 1d)

For the 3d-metal series, CN seven is usually found only with multidentate ligands and is dominated by the pentagonal-bipyramide. Typically, pentadentate ligands with a strong conformational preference for a coplanar coordination mode of the five donor groups are employed, for example macrocyclic ligands (like **21**[2]) or ligands of the imine- or hydrazone-type (like **22**[3]) derived from 2,6-diacetylpyridine (Figure 6.2).

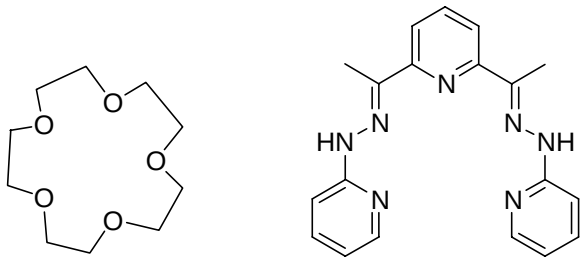

21 **22**

Figure 6.2. Typical ligands for the induction of pentagonal-bipyramidal geometry

For pentagonal-bipyramidal coordination geometries, the existence of stereogenic elements other than stereogenic carbon atoms in the ligand is connected to the deviation of certain parts of the ligand from the pentagonal plane (vide supra). This behavior is realized in a few cases, manifesting itself in a helical twist of the two ligand halves in order to release steric repulsion of the two ends of the ligand arms.[4] If the ligand itself bears no chiral information, this helical arrangement is formed as a racemic mixture.

Exclusive formation of right-handed helices is observed for ligand **2a** upon complexation with Mg^{II}, Mn^{II}, Fe^{II} and Cd^{II} (vide supra). Although a relative small number of precedences of pentagonal-bipyramidal complexes with topologically linear ligands (see Figure 6.1) have been reported with these metals,[5] this complete stereoselectivity has to the best of my knowledge not been reported for a pentagonal-bipyramidal system, both in mononuclear as well as in polynuclear assemblies.

- **Octahedral**

The octahedron is probably the most important coordination polyhedron for metal complexes. Therefore, the focus in the stereoselective synthesis of chiral-at-metal compounds always has been on this coordination geometry. A large number of these complexes have been reported with a great variety of different ligands.[6]

Octahedral complexes are also formed with ligands **2b** (Fe^{II}, Co^{II}, Ru^{II}, Cd^{II}) and **2c** (Co^{II}) (Tables 6.2-6.3). In the case of pentadentate chelators, Bernauer´s ligands **23**

and **24** (Figure 6.3.) are known to show complete diastereoselectivity upon complexation in many instances.[7]

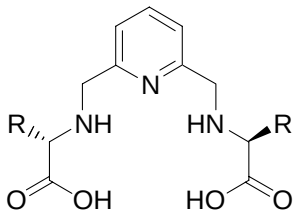

23

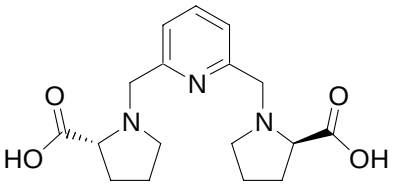

24

Figure 6.3. Bernauer´s pentadentate ligands

Therefore, the selectivity observed with the closely related ligands **2** is not surprising. However, the reversal of the configuration observed for the cobalt (Δ_2) and the cadmium (Λ_2) complexes with **2b** in the solid state structures is rather unusual. This phenomenon has its origin probably in the change of ionic radii (octahedral Co^{2+}: 0.75Å vs. octahedral Cd^{2+}: 0.95Å), but remains largely unexplained. However, as has been observed by NMR-spectroscopy (vide supra), the Cd^{II}-complex with **2b** shows not a single species in solution. Therefore, the significance of this finding is questionable with respect to stereoselectivity.

- **Trigonal-Bipyramidal**

Metal complexes with coordination number five are usually not ideally suited for high configurational stability because of the tendency for pseudo-rotation and/or dissociative/associative ligand exchange processes leading to favorable tetrahedral or octahedral species. The employment of multidentate ligands is often advantageous in this respect, suppressing these reactions to a great extent. However, because of the problems mentioned above, the stereoselective synthesis of e.g. trigonal-bipyramidal complexes with the metal as stereogenic center is still a challenging task. Predetermination of chirality with this coordination geometry is preferentially encountered with tripodal ligands.[8] Only three examples with topologically linear ligands have been reported.[9]

Trigonal-bipyramidal complexes are formed upon complexation with all ligands **2**, especially with the late transition metals Ni^{II} (**2a**), Cu^{II} (**2a**-**2b**) and Zn^{II} (**2a**-**2c**). This coordination geometry is not unusual for these metals and has been observed in numerous racemic cases before.[10] Complete stereoselection is observed in zinc(II) complexes with ligands **2a** (Λ_2) and **2b** (Δ_2), in the solid state as well as in solution.

This configurational reversal has up to date only been encountered with the employment of enantiomeric (trivial) or diastereomeric ligands.[9b] Only the exchange of two (non-stereogenic) donor atoms (O vs. S) is sufficient for this purpose. This phenomenon has not been encountered so far. Maybe the closest analogy can be seen in the cobalt complexes of ligands **25** and **26** (Figure 6.4). While **25** forms octahedral Δ_2-Co^{III}-complexes, **26** gives rise to a mixture of cobalt(III) complexes, in which one species was identified to possess the Λ_2-configuration.[11]

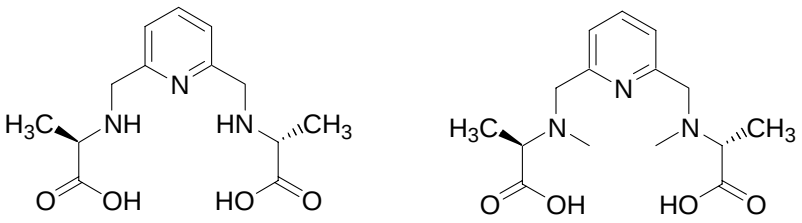

25 **26**

Figure 6.4. Bernauer`s ligands giving rise to two opposite configurations

Interestingly, the trigonal-bipyramidal zinc complex with ligand **2c** gives also a mixture of species in solution as determined by NMR. Perhaps this has to be attributed to the presence of the tertiary amine donor, both in **2c** and in **26**. Especially in the highly crowded trigonal-bipyramidal zinc complex with **2c**, the additional methyl group is probably exerting a strong steric strain upon the ligand backbone. This steric repulsion, although not strong enough to make pentacoordination of the ligand impossible in the crystal structure, is likely to be avoided in solution by dissociation of one arm from the metal.

6.2 Comparison by Ligands

- **Ligand 2a**

As Table 6.1 shows, ligand **2a** favors the formation of either pentagonal-bipyramidal (Mn^{II}, Fe^{II}, Cd^{II}) or trigonal-bipyramidal (Ni^{II}, Cu^{II}, Zn^{II}) complexes. While the first coordination geometry is uniformly formed with complete Λ_2-selectivity, the latter case exhibits a reversal in configuration from Δ_2 (Ni, Cu) to Λ_2 (Zn). This phenomenon goes largely unexplained. Why the usually often favored octahedron was never observed, also remains unclear. **2a** is able to accommodate rather large cations like Cd^{II} or Yb^{III}.

- **Ligand 2b**

The survey in Table 6.2 clearly demonstrates the strong preference of **2b** to form Δ_2-species with first-row transition metals, either in an octahedral fashion (Fe^{II}, Co^{II}) or by adopting the trigonal-bipyramide (Cu^{II}, Zn^{II}). With elements of the second row (Ru^{II}, Cd^{II}), the stereoselectivity especially in solution apparantly drops. This is probably because of the difficulty of **2b** to accomodate these large cations. In comparison with **2a**, this would not be surprising because of the increased van-der-Waals-radius by exchanging oxygen with sulfur, making the binding cavity smaller.

- **Ligand 2c**

Due to the small number of examples with **2c**, only statements on the basis of limited experimental evidence can be made. The coordination behavior (Table 6.3) seems similar to the one for **2b**, although the stereoselectivity for the zinc complex is reversed (Λ_2) in the solid state. This selectivity resembles more the characteristics for **2a**. As has been stated before, the additional methyl group could prove to be a serious problem because of the potential build-up of steric strain resulting in lowering the configurational preference (vide supra).

References:

[1] a) M.G.B. Drew, *Progr. Inorg. Chem.* **1977**, *23*, 67-210; b) D.L. Kepert, *Progr. Inorg. Chem.* **1979**, *25*, 41-144; c) M. Melnik, P. Sharrock, *Coord. Chem. Rev.* **1985**, *65*, 49-85; d) D. Casanova, P. Alemany, J.M. Bofill, S. Alvarez, *Chem. Europ. J.* **2003**, *9*, 1281-1295.

[2] J.L. Atwood, P.C. Junk, *Polyhedron* **2000**, *19*, 85-91 and refs cited therein.

[3] D. Wester, G.J. Palenik, *J. Chem. Soc., Chem. Commun.* **1975**, 74-75.

[4] For example: E.C. Constable, J.V. Walker, D.A. Tocher, M.A.M. Marcus, *J. Chem. Soc., Chem. Commun.* **1992**, 768-771.

[5] Selected examples:

Mg^{II}: a) K.M. Park, I. Yoon, J. Seo, Y.H. Lee, S.S. Lee, *Acta Crystallogr.* **2001**, *E57*, m154-m156;

Mn^{II} + Fe^{II}: b) G.J. Palenik, D.W. Wester, *Inorg. Chem.* **1978**, *17*, 864-870; c) M.G.B. Drew, J. Nelson, S.M. Nelson, *J. Chem. Soc., Dalton Trans.* **1981**, 1685-1690;

Cd^{II}: d) M. Fondo, A. Sousa, M.R. Bermejo, A. Garcia-Deibe, A. Sousa-Pedrares, O.L. Hoyos, M. Helliwell, *Eur. J. Inorg. Chem.* **2002**, 703-710.

[6] Review: a) U. Knof, A. Von Zelewsky, *Angew. Chem. Int. Ed.* **1999**, *38*, 303-322; selected very recent examples: b) S.G. Telfer, X.-J. Yang, A.F. Williams, *J. Chem. Soc., Dalton Trans.* **2004**, 699-705; c) C. Hamann, A. Von Zelewsky, A. Neels, H. Stoeckli-Evans, *J. Chem. Soc., Dalton Trans.* **2004**, 402-406.

[7] a) K. Bernauer, P. Pousaz, J. Porret, J. Jeanguenat, *Helv. Chim. Acta* **1988**, *71*, 1339-1348 ; b) K. Bernauer, P. Pousaz, *Helv. Chim. Acta* **1984**, *67*, 796-803.

[8] a) Y.-H. Chiu, O. dos Santos, J.W. Canary, *Tetrahedron* **1999**, 12069-12078; b) A. Abufarag, H. Vahrenkamp, *Inorg. Chem.* **1995**, *34*, 3279-3284; c) J.W. Canary, C.S. Allen, J.M. Castagnetto, Y. Wang, *J. Am. Chem. Soc.* **1995**, *117*, 8484-8485; d) W.A. Nugent, R.L. Harlow, *J. Am. Chem. Soc.* **1994**, *116*, 6142-6148.

[9] a) Casella, M.E. Silver, J.A. Ibers, *Inorg. Chem.* **1984**, *23*, 1409-1418; b) O. Mamula, A. von Zelewsky, T. Bark, H. Stoeckli-Evans, A. Neels, G. Bernardinelli, *Chem. Eur. J.* **2000**, *6*, 3575-3585; c) C.J. Sanders, P.N. O'Shaughnessy, P. Scott, *Polyhedron*, **2003**, *22*, 1617-1625.

[10] Review: *Comprehensive Coordination Chemistry II, Volume 6: Transition Metal Groups 9-12* (Ed.: D.E. Fenton) **2004**, Elsevier, Oxford.

[11] K. Bernauer, H. Stoeckli-Evans, D. Hugi-Cleary, H.J. Hilgers, H. Abd-el-Khalek, J. Porret, J.-J. Sauvain, *Helv. Chim. Acta* **1992**, *75*, 2327-2339.

7 Summary

In the course of this thesis, the following results could be obtained:

- **Development of a facile modular synthesis for the preparation of the new ligand system 2**

  The procedures for the assembly of **2a-c** could be optimized for the preparation of multigram quantities of these ligands. The validity of the modular approach has been demonstrated and will allow rapid variation of the ligands in the future. The set of building blocks can easily be expanded because of the generality of the final assembly step.

- **Experimental simple preparation and purification of a large number of different metal complexes of ligand system 2**

  Especially the perchlorate complexes proved to be accessible in analytically pure form by an easy precipitation strategy without the need for additional purification steps.

- **Generation of a predictive model for complex properties in solution using CD-spectroscopy**

  This constitutes the main finding of this work. It is now possible for ligand system **2** to assign coordination geometry and configurational preference for unknown metal complexes in solution solely from the information obtained by CD-measurements as demonstrated for the polymeric cadmium species (see Section 5). This holds true for a set of very important coordination polyhedra including the octahedron, the trigonal-bipyramide and the pentagonal-bipyramide (Figure 7.1). With this respect it could be almost as valuable as in the case of elucidation of the secondary structure of proteins by CD-spectroscopy. It has to be emphasized that the benefit is not to complete missing crystal structures but rather to have proper information about the solution behavior of certain species. This could prove to be very important for the rationalization of reactivity and selectivity with respect to application in asymmetric catalysis. For most known catalytic systems employed today, few or sometimes nothing is definitely known in solution, mostly relying on mere speculation.

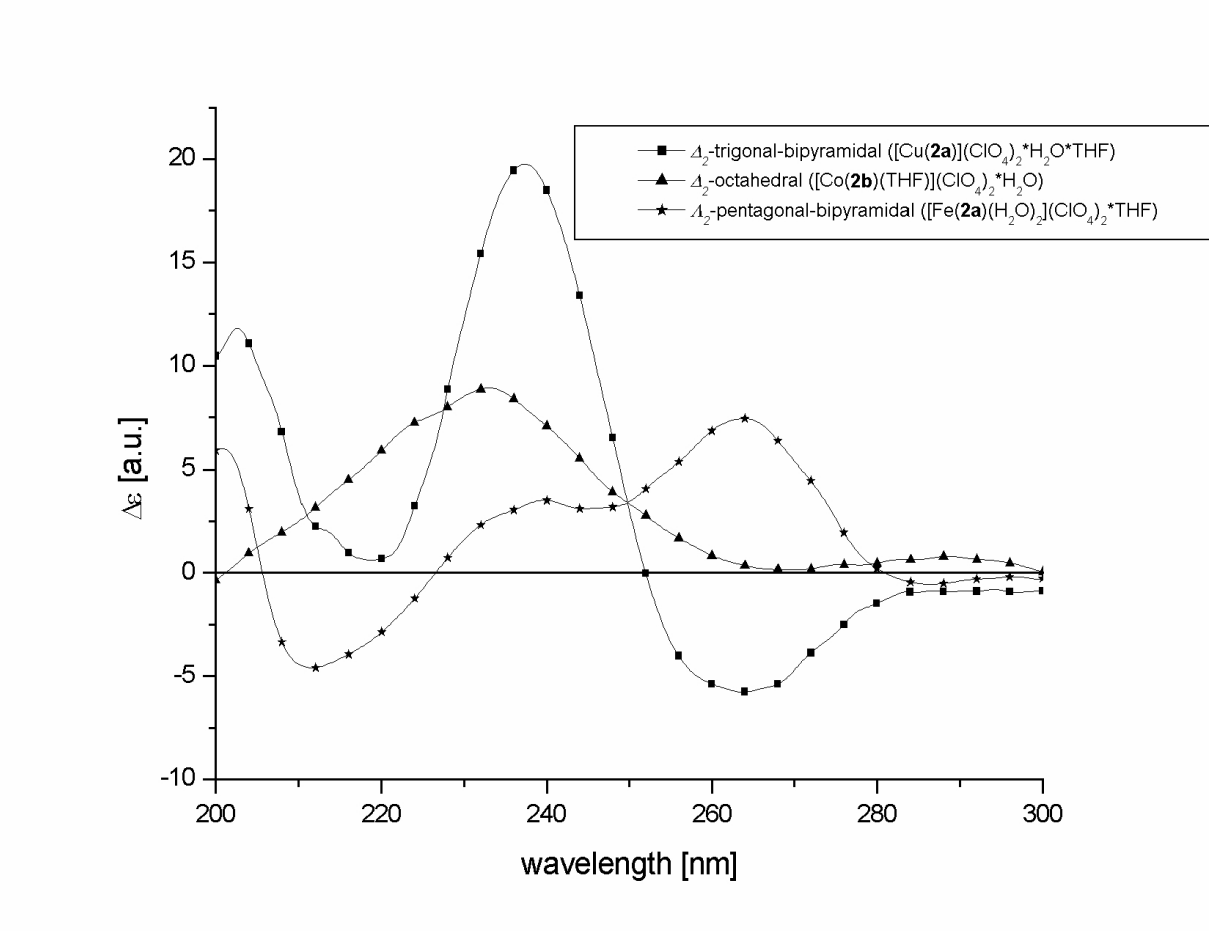

Figure 7.1. Characteristic CD-patterns for specific coordination geometries

- **Stereoselective synthesis of both pseudo-enantiomers of zinc complexes from ligands with only one stereochemistry**

  Up to date only the employment of enantiomeric (trivial) or diastereomeric ligands (vide supra) is suitable for the generation of complexes with opposite configuration at the metal center. With ligands **2** it could be shown that the completely stereoselective construction of trigonal-bipyramidal zinc(II) complexes (which is also rather rare using topologically linear ligands) with **2a** and **2b** leads to pseudo-enantiomeric complexes in the solid (Figure 7.2) and the solution state (Figure 7.3). In this case, only the exchange of two donor atoms (O vs. S) is necessary for this purpose. This phenomenon was to the best of my knowledge not observed before.

Figure 7.2. Pseudo-enantiomeric crystal structures of $[Zn(\mathbf{2a})]^{2+}$ and $[Zn(\mathbf{2b})]^{2+}$

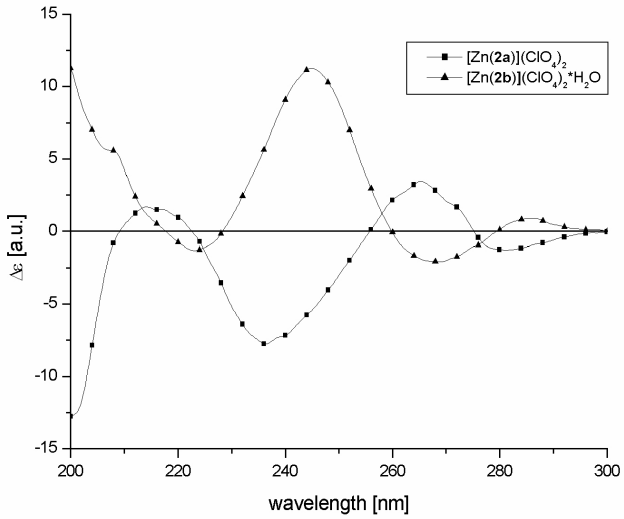

Figure 7.3. Mirror-image relationship of the CD-spectra of $[Zn(\mathbf{2a})](ClO_4)_2$ and $[Zn(\mathbf{2b})](ClO_4)_2{*}H_2O$

- **Stereoselective synthesis of both pseudo-enantiomers of metal complexes from only one ligand by solely exchanging the metal**

  This phenomenon is related to the preceeding finding. It could be shown that with ligand **2a**, both pseudo-enantiomeric forms of trigonal-bipyramidal complexes are accessible in solution simply by varying the metal from Ni^{II}/Cu^{II} (Δ_2) to Zn^{II} (Λ_2) (Figure 7.4).

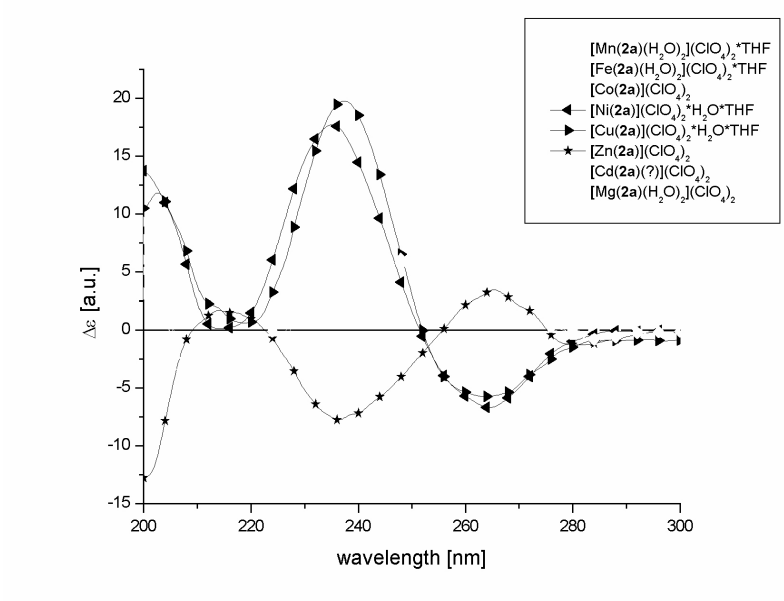

Figure 7.4. Configurational switch observed for the CD-spectra of [(Ni or Cu)(**2a**)]$(ClO_4)_2$*H_2O*THF and [Zn(**2a**)]$(ClO_4)_2$

The same could be shown for the solid state structures of (distorted) octahedral complexes of **2b** with Co^{II} (Δ_2) and Cd^{II} (Λ_2) (Figure 7.5). However, this statement can not be extended for the solution state because of the presence of more than one species for the cadmium complex.

Figure 7.5. Pseudo-enantiomeric crystal structures of [Co(**2b**)(THF)]$^{2+}$ and [Cd(**2b**)(ClO_4)]$^{+}$

- **Unprecedented determination of helical chirality in pentagonal-bipyramidal coordination compounds**

This phenomenon has been observed in a number of metal complexes of ligand **2a**, both in mononuclear (Mg^{II}, Mn^{II}, Fe^{II}, Cd^{II}) (Figure 7.6) as well as in polynuclear assemblies (Cd^{II}) (Figure 7.7). Besides the fact that this coordination geometry itself is rather unusual, the predetermination of helical chirality in

complexes of this kind has to the best of my knowledge not been reported up to date.

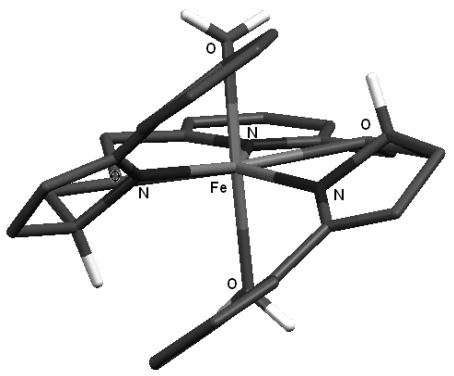

Figure 7.6. Pentagonal-bipyramidal coordination geometry in the crystal structure $[Fe(\mathbf{2a})(H_2O)_2]^{2+}$ with exclusively right-handed helicity

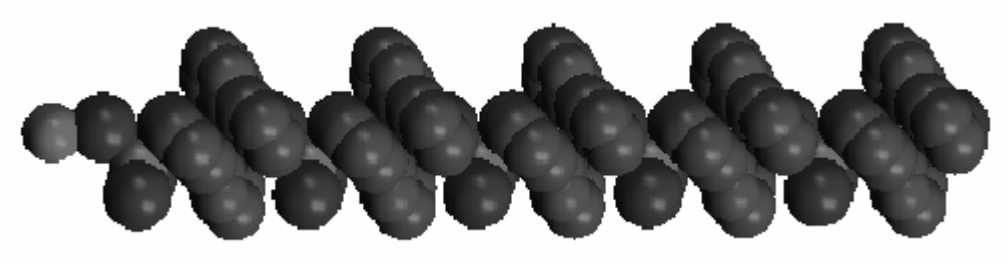

Figure 7.7. Selective right-handed helix formation in one-dimensional polymeric $_{\infty}[Cd(\mathbf{2a})Br_4Cd]$

8 Experimental Section

8.1 General

Where indicated, reactions were carried out under a dry, oxygen-free atmosphere of N_2 using Schlenk-technique. Commercially available reagents were used as received. DMF, CH_3CN and CH_2Cl_2 were distilled over P_4O_{10} and stored under N_2 over molecular sieves 3Å. EtOH and MeOH were dried over Mg and stored under N_2. THF, 1,4-dioxane and Et_2O were dried with Na/benzophenone and stored over Na-wire under N_2. EtOAc, CH_2Cl_2, MeOH and hexanes for chromatographic separations were distilled before use. For column chromatography silica gel Geduran 60 (Merck, 0.063-0.200 mm) was used. TLC-analysis was done on silica gel 60 F_{254} (Merck) coated on aluminium sheets.

NMR-spectra were recorded on Bruker Avance 300 (^{1}H: 300 MHz, ^{13}C: 75.5 Mhz) and Bruker Avance 600 (^{1}H: 600 MHz) with TMS as internal standard. IR-spectroscopy was done on a Mattson Genesis Series FT-IR (sample preparation as indicated). X-ray analysis was performed by the Crystallography Laboratory (University of Regensburg, M. Zabel, S. Stempfhuber) and the Crystallography Laboratory (University of Kansas, D. R. Powell). Elemental analysis (Heraeus elementar vario EL III) and mass spectrometry (Finnigan ThermoQuest TSQ 7000) were done by the Central Analytical Laboratory (Universität Regensburg). CD-spectra were recorded on a Jasco J-710 spectropolarimeter using ca. 10^{-4}M CH_3CN-solutions (HPLC-grade) in 1mm-cuvettes (cylindrical).

8.2 Ligand Synthesis

2,6-Pyridinedicarboxylic acid dimethyl ester

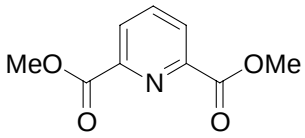

100.0 g (598.4 mmol) 2,6-pyridinedicarboxylic acid were suspended in 700 mL MeOH and treated cautiously with 5.0 mL conc. sulfuric acid. The mixture was heated to reflux for 5 h. The product crystallized upon cooling to room temperature, was collected on a Büchner-funnel and washed with 50 mL MeOH and Et_2O. After drying in vacuo the product was obtained as a colorless solid (104.3 g, 89%).

M.p. 122-124°C. ^{1}H-NMR (300 MHz, $CDCl_3$): δ = 8.32 (d, *J* = 7.9 Hz, 2 H), 8.04 (t, *J* = 7.7 Hz, 1 H), 4.04 (s, 6 H). ^{13}C-NMR (75.5 MHz, $CDCl_3$): δ = 165.0, 148.2, 138.3, 128.0, 53.2.

2,6-Bis(hydroxymethyl)pyridine (3)

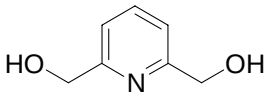

A suspension of 34.30 g (175.7 mmol, 1.0 eq.uivs.) 2,6-pyridinedicarboxylic acid dimethyl ester in 470 mL dry EtOH was cooled in an ice-bath and treated with 31.05 g (820.7 mmol, 4.67 equivs.) $NaBH_4$ in portions. A reflux-condenser with a drying tube was placed on the flask and the mixture was stirred for 1 h at 0°C. The ice-bath was removed and stirring was continued until the exothermic reaction had ceased. (If the reaction gets too vigorous, the flask should be cooled with a cold water-bath.) After further stirring for 3 h at ambient temperature, the mixture was refluxed for 10 h. The solvent was removed in vacuo, the residue was treated with 120 mL acetone and the mixture refluxed for 1 h. The solvent was evaporated again and 120 mL saturated aqueous K_2CO_3-solution was added. Heating for 1 h under reflux was followed by removing the solvent under vacuum. The residue was dissolved in 470 mL water and the solution was extracted continously in a liquid-liquid-extractor overnight to yield 20.42 g (84%) of a colorless solid.

M.p. 114-115°C. ^{1}H-NMR (300 MHz, DMSO-d_6): δ = 7.76 (t, *J* = 7.7 Hz, 1 H), 7.30 (d, *J* = 7.7 Hz, 2 H), 5.34 (t, *J* = 5.8 Hz, 2 H), 4.51 (d, *J* = 5.8 Hz, 4 H). ^{13}C-NMR (75.5 MHz, DMSO-d_6): δ = 160.7, 136.9, 118.0, 64.1.

2,6-Bis(bromomethyl)pyridine (10)

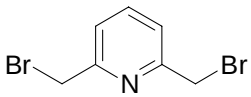

To a suspension of 24.61 g (138.3 mmol, 2.15 equivs.) N-bromosuccinimide in 220 mL dry benzene was added 6.90 g (64.4 mmol, 1.0 equivs.) 2,6-lutidine und 130 mg AIBN. The mixture was heated slowly until the reaction started. After most of the vigorous boiling had subsided the mixture was irradiated with a 250W-light bulb and heated to reflux for 10 h. After evaporation of the solvent the residue was taken up in a minimum of hexanes, the suspension filtered and the filtrate reduced under vacuum. The remaining solid was subjected to column chromatography (SiO_2, hexanes/EtOAc 10:1, R_f = 0.22). The product was obtained as a slightly brown solid (2.23 g, 13%). (CAUTION: The title compound and every byproduct are very lachrymatory! Avoid contact with skin!)

M.p. 87-88°C. ^{1}H-NMR (300 MHz, $CDCl_3$): δ = 7.69 (t, *J* = 7.7 Hz, 1 H), 7.36 (d, *J* = 7.7 Hz, 2 H), 4.52 (s, 4 H). ^{13}C-NMR (75.5 MHz, $CDCl_3$): δ = 156.7, 138.1, 122.8, 33.5.

2,6-Bis(chloromethyl)pyridine Hydrochloride (7)

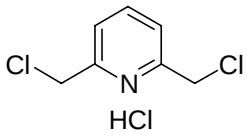

To a suspension of 2.11 g (15.2 mmol, 1.0 equivs.) 2,6-bis(hydroxymethyl)pyridine (**3**) in 15 mL dry Et_2O (cooled to 0°C) was added a solution of 2.43 mL (33.4 mmol, 3.97 g, 2.2 equivs.) $SOCl_2$ in 3 mL Et_2O. After complete addition the mixture was stirred at 0°C for one hour, before the ice-bath was removed and stirring was continued at ambient temperature for 20 hours. The white solid was collected, washed with Et_2O and dried under reduced pressure. The product was obtained as a colorless solid (3.05 g, 96%).

M.p. 151-152°C. ^{1}H-NMR (300 MHz, DMSO-d_6): δ = 12.61 (br s, 1 H), 7.95 (t, *J* = 7.7 Hz, 1 H), 7.56 (d, *J* = 7.7 Hz, 2 H), 4.81 (s, 4 H). ^{13}C-NMR (75.5 MHz, DMSO-d_6): δ = 155.7, 139.2, 123.0, 45.9.

2,6-Bis(chloromethyl)pyridine (8)

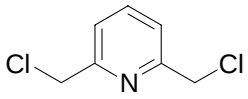

3.56 g (16.8 mmol) 2,6-bis(chloromethyl)pyridine hydrochloride (**7**) were suspended in 60 mL CH_2Cl_2. Saturated aqueous $NaHCO_3$ (60 mL) was added slowly and the phases were separated. The aqueous phase was extracted with 2*30 mL CH_2Cl_2 and the combined organic phases dried over Na_2SO_4. After evaporation of the solvent the residue was recrystallized from n-hexane to yield 2.75 g (93%) product as a colorless solid.

M.p. 74-75 °C. ^{1}H-NMR (300 MHz, $CDCl_3$): δ = 7.77 (t, *J* = 7.7 Hz, 1 H), 7.44 (d, *J* = 7.7 Hz, 2 H), 4.67 (s, 4 H). ^{13}C-NMR (75.5 MHz, $CDCl_3$): δ = 156.4, 138.1, 122.1, 46.4.

2,6-Bis(carbamimidoylsulfanylmethyl)pyridine Trihydrochloride

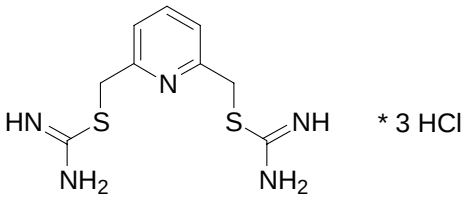

To a solution of 5.00 g (23.5 mmol, 1.0 equivs.) 2,6-bis(chloromethyl)pyridine hydrochlorid (**7**) in 100 mL EtOH was added 4.30 g (56.5 mmol, 2.4 equivs.) thiourea and the mixture was refluxed for 20 min. After cooling down to ambient temperature the solid was collected and washed with EtOH and Et_2O. Drying under reduced pressure yielded 7.46 g (87%) of a fine colorless solid.

M.p. > 200 °C. ^{1}H-NMR (300 MHz, D_2O): δ = 7.94 (t, *J* = 7.9 Hz, 1 H), 7.51 (d, *J* = 7.9 Hz, 2 H), 4.53 (s, 4 H). ^{13}C-NMR (75.5 MHz, D_2O): δ = 170.8, 154.3, 140.8, 123.6, 35.6. IR (KBr): $\tilde{\nu}$ = 3280 cm^{-1}, 3080, 3000, 2870, 2590, 1653, 1612, 1435, 1279, 1228, 1178, 1066, 937, 819, 683. MS (ESI, H_2O/CH_3CN): *m/z* (%) = 255.7 (65), 217.6 (38), 215.7 (100), 197.6 (32). $C_9H_{16}Cl_3N_5S_2$ (364.75): calc. C 29.64, H 4.42, N 19.20; found C 29.61, H 4.50, N 19.10.

2,6-Bis(mercaptomethyl)pyridine (11)

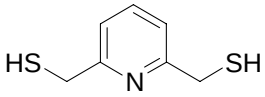

Under Ar 7.46 g (20.5 mmol, 1.0 equiv.) 2,6 Bis(carbamimidoylsulfanylmethyl)-pyridine Trihydrochloride were dissolved in 20 mL degassed water and 4.50 g (112.5 mmol, 5.5 equivs.) NaOH were added. The solution was refluxed for 2 h and after cooling down to room temperature, the pH was adjusted to approx. 8 with degassed 1 M HCl. The mixture was transferred to a Schlenk-separatory funnel, set under Ar, and the aqueous phase was extracted with 3*30 mL degassed $CHCl_3$. The organic phases were collected under Ar. The combined organic layers were dried (Na_2SO_4) and evaporated under reduced pressure. Kugelrohr-distillation (p = 0.04 mbar, heating 130°C) yielded 1.30 g (37%) of the product as an air-sensitive slightly yellow oil, that was stored under N_2 at 4°C.

^{1}H-NMR (300 MHz, $CDCl_3$): δ = 7.62 (t, *J* = 7.7 Hz, 1 H), 7.21 (d, *J* = 7.7 Hz, 2 H), 3.82 (d, *J* = 8.0 Hz, 4 H), 2.03 (t, *J* = 8.0 Hz, 2 H). ^{13}C-NMR (75.5 MHz, $CDCl_3$): δ = 159.9, 137.8, 120.5, 30.8.

Ethyl benzimidate (6)

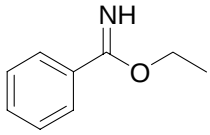

42.46 g (228.7 mmol) Ethyl benzimidate hydrochloride were suspended in 200 mL CH_2Cl_2. 300 mL sat. aqueous $NaHCO_3$ was added slowly and the phases were separated. The aqueous phase was extracted with 4*125 mL CH_2Cl_2, the combined organic phases dried over Na_2SO_4 and concentrated. The remaining crude product was distilled (bp 96-97°C / 4 hPa) to yield 29.69 g (87%) colorless liquid.

^{1}H-NMR (300 MHz, $CDCl_3$): δ = 7.78 – 7.68 (m, 2 H), 7.65 – 7.51 (br s, 1 H), 7.48 – 7.32 (m, 3 H), 4.32 (q, 2 H, *J* = 7.0 Hz), 1.41 (t, 3 H, *J* = 7.0 Hz). ^{13}C-NMR (75.5 MHz, $CDCl_3$): δ = 167.8, 132.9, 130.8, 128.4, 126.7, 61.8, 14.2.

(*S*)-4-Methoxycarbonyl-2-phenyl-oxazoline (15)

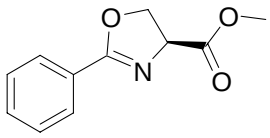

Under N_2 a flask was charged with 28.07 g (188.2 mmol, 1.0 equivs.) ethyl benzimidate (**6**), 32.20 g (207.0 mmol, 1.1 equivs.) (S)-serine methyl ester hydrochloride (**5**) and 550 mL dry 1,2-dichloroethane. The mixture was refluxed for 20 h, filtered and the solvent was removed in vacuo. The oily residue was dissolved in Et_2O, filtered again and the filtrate was evaporated. The crude product (34.70 g, 90%) was obtained as a colorless oil, that could be used for the next step without purification.

$[\alpha]_D^{20}$ = +120.1 (c = 2.1, $CHCl_3$). ^{1}H-NMR (300 MHz, $CDCl_3$): δ = 8.01 – 7.94 (m, 2 H), 7.53 – 7.36 (m, 3 H), 4.95 (dd, 1 H, *J* = 10.6, 7.9 Hz), 4.69 (dd, 1 H, *J* = 8.7, 7.9 Hz), 4.59 (dd, 1 H, *J* = 10.6, 8.7 Hz), 3.81 (s, 3 H). ^{13}C-NMR (75.5 MHz, $CDCl_3$): δ = 171.6, 166.2, 131.8, 128.6, 128.3, 126.9, 69.5, 68.6, 52.7.

(*R*)-4-Hydroxymethyl-2-phenyl-oxazoline (4)

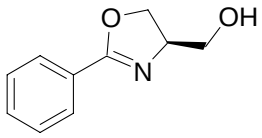

A 2000mL-two-necked-nitrogen-flask equipped with a thermometer and a 100mL-dropping funnel was charged with 5.21 g (137.2 mmol, 0.55 equivs.) $LiAlH_4$, set under N_2 and 450 mL dry THF. The suspension was cooled with dry ice/acetone to -35°C and a solution of 51.18 g (249.4 mmol, 1.0 equivs.) (*S*)-4-methoxycarbonyl-2-phenyl-oxazoline (**15**) in 80 mL THF was added dropwise in the course of 45 min so that the temperature did not rise above -30°C. After complete addition the mixture was allowed to reach 0°C and stirred in an ice-bath for 30 min. The 100mL-dropping funnel was replaced by a bigger one (1000 mL) and a solution of 300 g sodium potassium tartrate in 600 mL water was added very carefully. The yellow mixture was stirred at ambient temperature for additional 2 h and extracted with 4*200 mL EtOAc. The combined organic layers were dried (Na_2SO_4) and evaporated. The residue was purified by column chromatography (SiO_2, EtOAc, R_f = 0.31). The product was obtained as a colorless solid (28.28 g, 64%).

M.p. 97-98 °C. $[\alpha]_D^{20}$ = +54.4 (c = 1.3, EtOH). ^{1}H-NMR (300 MHz, $CDCl_3$): δ = 7.83 – 7.71 (m, 2 H), 7.46 – 7.36 (m, 1 H), 7.35 – 7.22 (m, 2 H), 4.52 – 4.30 (m, 3 H), 3.98 (dd, *J* = 11.7, 2.9 Hz, 1 H), 3.9 – 3.5 (br s, 1 H), 3.66 (dd, *J* = 11.7, 3.7 Hz, 1 H). ^{13}C-NMR (75.5 MHz, $CDCl_3$): δ = 165.5, 131.4, 128.24, 128.19, 127.1, 69.2, 68.1, 63.6.

(*S*)-2-Phenyl-4-tosyloxymethyl-oxazoline (17)

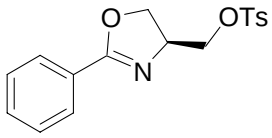

To a solution of 15.00 g (84.65 mmol, 1.0 equivs.) (*R*)-4-hydroxymethyl-2-phenyl-oxazoline (**4**) and 26.0 mL (186.2 mmol, 18.84 g, 2.2 equivs.) dry NEt_3 in 80 mL dry $CHCl_3$ under N_2 and at 0°C was added dropwise a solution of 17.75 g (93.12 mmol, 1.1 equivs.) tosyl chloride in 80 mL dry $CHCl_3$. The mixture was stirred at ambient temperature for 20 h, washed with 2*30 mL water, 30 mL sat. $NaHCO_3$ and 30 mL water. The organic layer was dried (Na_2SO_4) and evaporated. The crude product was recrystallized from 2-propanol yielding 21.74 g (78%) slightly yellow solid.

M.p. 107-111 °C. $[\alpha]_D^{20}$ = +56.6 (c = 1.0, EtOH). ^{1}H-NMR (300 MHz, $CDCl_3$): δ = 7.86 – 7.79 (m, 2 H), 7.77 – 7.69 (m, 2 H), 7.49- 7.20 (m, 2 H), 4.55 – 4.38 (m, 2 H), 4.33 – 4.19 (m, 2 H), 4.05 – 3.96 (m, 1 H), 2.39 (s, 3 H). ^{13}C-NMR (75.5 MHz, $CDCl_3$): δ = 166.0, 145.0, 132.5, 131.8, 129.9, 128.4, 128.3, 128.0, 127.0, 70.8, 69.8, 65.1, 21.7.

(*S*)-2-Phenyl-4-mesyloxymethyl-oxazoline (16)

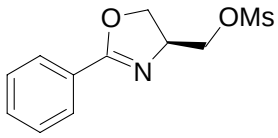

Under N_2 3.01 g (17.0 mmol, 1.0 equivs.) (*R*)-4-hydroxymethyl-2-phenyl-oxazoline (**4**) were dissolved in 40 mL dry THF and cooled to -25°C external temperature. 2.60 µL (18.7 mmol, 1.89 g, 1.1 equivs.) dry NEt_3 and 1.38 mL (17.8 mmol, 2.04 g, 1.05 equivs.) mesyl chloride were added subsequently. The mixture was stirred at -25°C for 30 min, before water (50 mL) and CH_2Cl_2 (80 mL) were added. The organic layer was separated, dried ($MgSO_4$) and the solvent evaporated under reduced pressure. The crude yellow oil (4.17 g, 96%) was used for the subsequent steps without further purification. An analytical sample was obtained by column chromatography (flash-SiO_2, hexanes / EtOAc 1:1).

$[\alpha]_D^{20}$ = +54.5 (c = 1.56, CH_2Cl_2). ^{1}H-NMR (300 MHz, $CDCl_3$): δ = 8.00 – 7.88 (m, 2 H), 7.57 – 7.36 (m, 3 H), 4.69 – 4.49 (m, 2 H), 4.47 – 4.30 (m, 3 H), 3.03 (s, 3 H). ^{13}C-NMR (75.5 MHz, $CDCl_3$): δ = 166.1, 131.9, 128.5, 128.4, 127.0, 70.4, 69.3, 65.4, 37.6. IR (film): $\tilde{\nu}$ = 3080, 3040, 2980, 2950, 2920, 1728, 1645, 1603, 1580, 1496, 1452, 1356, 1277, 1242, 1174, 1061, 1025, 961, 833, 786, 695. MS (DCI, NH_3): *m/z* (%) = 258.2 (9), 257.2 (20), 256.1 (100). HRMS (EI): calcd for $C_{11}H_{13}NO_4S$ $[M]^+$ 255.0565, found 255.0565.

Pyridine-2,6-dicarbaldehyde (12)

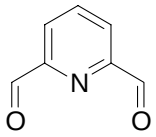

A solution of 7.50 g (53.9 mmol, 1.0 equivs.) 2,6-bis(hydroxymethyl)pyridine (**3**) and 5.98 g (53.9 mmol, 1.0 equivs.) SeO_2 in 120 mL dry 1,4-dioxane was refluxed for 4 hours. The dark mixture was filtered hot and the solvent removed. The remaining solid was taken up in CH_2Cl_2 and passed over a short column of silica. After washing the silica with CH_2Cl_2, the filtrate was reduced to yield a slightly yellow solid. This crude product was broken up and suspended in n-hexane (30 mL). After stirring for one hour, the solid was collected and washed with n-hexane. The product was obtained as a very slightly pink solid (4.00 g, 55%).

M.p. 124-126°C. ^{1}H-NMR (300 MHz, $CDCl_3$): δ = 10.18 (s, 2 H), 8.23 – 8.05 (m, 3 H). ^{13}C-NMR (75.5 MHz, $CDCl_3$): δ = 192.3, 153.0, 138.4, 125.3.

2,6-Bis(methyliminomethyl)pyridine (13)

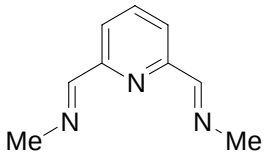

A solution of 3.95 g (58.4 mmol, 2.4 equivs.) methylamine hydrochloride in MeOH (100 mL) was cooled to 0°C and treated with 9.42 g (68.2 mmol, 2.8 equivs.) K_2CO_3. After stirring for one hour in an ice-bath 3.29 g (24.3 mmol, 1.0 equivs.) pyridine-2,6-dicarbaldehyde (**12**) was added. The mixture was stirred at ambient temperature for further three hours and the solvent evaporated. The solid residue was taken up in 150 mL CH_2Cl_2 and the suspension stirred for one hour. After filtering off the solid, the solvent was evaporated to yield a yellow oil (2.97 g, 76%). No further purification of the product was necessary for the next step.

^{1}H-NMR (300 MHz, $CDCl_3$): δ = 8.31, 8.32 (2 s, 2 H), 7.85 (d, *J* = 7.7 Hz, 2 H), 7.68 (t, *J* = 7.7 Hz, 1 H), 3.48, 3.47 (2 s, 6 H). ^{13}C-NMR (75.5 MHz, $CDCl_3$): δ = 163.0, 154.2, 137.0, 121.9, 48.0.

2,6-Bis(N-methylaminomethyl)pyridine (14)

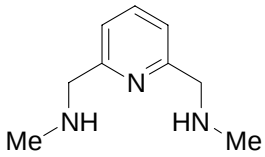

To a solution of 2.62 g (16.3 mmol, 1.0 equivs.) 2,6-bis(methyliminomethyl)pyridine (**13**) in dry EtOH (40 mL) was added 1.23 g (32.6 mmol, 2.0 equivs.) $NaBH_4$ in portions. The solution was stirred for 16 hours and water (40 mL) was added cautiously. This solution was extracted with 3*40 mL CH_2Cl_2, the combined organic phases dried ($MgSO_4$) and the solvent evaporated. The residue was distilled (bp 97-100°C / 0.08 mbar) to yield a yellow oil (1.81 g, 67%), that was stored under nitrogen at 4°C.

^{1}H-NMR (300 MHz, $CDCl_3$): δ = 7.60 (t, *J* = 7.6 Hz, 1 H), 7.16 (d, *J* = 7.6 Hz, 2 H), 3.85 (s, 4 H), 2.48 (s, 6 H), 1.78 (br s, 2 H). ^{13}C-NMR (75.5 MHz, $CDCl_3$): δ = 159.3, 136.7, 120.4, 57.2, 36.2. MS (DCI, NH_3): *m/z* (%) = 167.2 (10), 166.2 (100. HRMS (EI): calcd for $C_9H_{14}N_3$ $[M-H]^+$ 164.1188, found 164.1189.

Ligand 2a

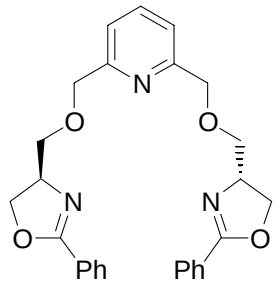

13.86 g (78.2 mmol, 2.2 equivs.) (*R*)-4-hydroxymethyl-2-phenyl-oxazoline (**4**) were dissolved in 200 mL dry DMF under N_2 and cooled to 0°C. 3.27 g (81.8 mmol, 2.3 equivs.) NaH-suspension (60% in mineral oil) were added in portions and the mixture was stirred for 15 min. 6.26 g (35.6 mmol, 1.0 equiv.) 2,6-bis(chloromethyl)pyridine (**8**) were added as a solid and the ice-bath was removed. Stirring was continued at ambient temperature for 20 h. 200 mL water and 150 mL CH_2Cl_2 were added cautiously and the phases were separated. The aqueous layer was extracted with 2*150 mL CH_2Cl_2. The combined organic layers were washed with 3*100 mL water and dried (Na_2SO_4). After removal of the solvent in vacuo the residue was purified by column chromatography (SiO_2, EtOAc to EtOAc / MeOH 24:1) to yield 14.37 g (88%) of a colorless solid.

M.p. 68-69 °C. $[\alpha]_D^{20}$ = +62.5 (c = 0.80, CH_2Cl_2). ^{1}H-NMR (300 MHz, $CDCl_3$): δ = 8.00 – 7.86 (m, 4 H), 7.65 (t, *J* = 7.7 Hz, 1 H), 7.51 – 7.35 (m, 6 H), 7.31 (d, *J* = 7.7 Hz, 2 H), 4.68 (s, 4 H), 4.61 – 4.46 (m, 4 H), 4.41 – 4.34 (m, 2 H), 3.88 – 3.80 (m, 2 H), 3.66 – 3.58 (m, 2 H). ^{13}C-NMR (75.5 MHz, $CDCl_3$): δ = 165.0, 157.7, 137.2, 131.4, 128.31, 128.30, 127.6, 120.0, 74.2, 72.9, 70.5, 66.4. ^{1}H-NMR (300 MHz, CD_3CN): δ = 7.95 – 7.84 (m, 4 H), 7.69 (t, *J* = 7.7 Hz, 1 H), 7.56 – 7.38 (m, 6 H), 7.30 (d, *J* = 7.7 Hz, 2 H), 4.58 (s, 4 H), 4.52 – 4.40 (m, 4 H), 4.36 – 4.24 (m, 2 H), 3.76 – 3.59 (m, 4 H). ^{13}C-NMR (75.5 MHz, CD_3CN): δ = 164.9, 159.0, 138.3, 132.4, 129.5, 129.0,

121.1, 74.9, 73.5, 71.0, 67.6. IR (KBr): $\tilde{\nu}$ = 3060 cm^{-1}, 3040, 2985, 2958, 2947, 2936, 1642, 1591, 1577, 1493, 1467, 1460, 1446, 1356, 1345, 1289, 1252, 1242, 1130, 1076, 1059, 1025, 970, 955, 922, 785, 608. MS (DCI, NH_3): *m/z* (%) = 459.2 (25), 458.1 (100). $C_{27}H_{27}N_3O_4$ (457.52): calc. C 70.88, H 5.95, N 9.18; found C 70.73, H 5.93, N 9.04.

Ligand 2b

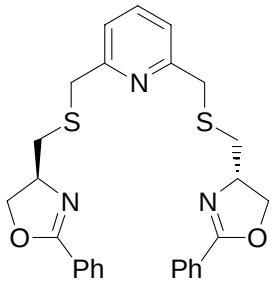

2.12 g (12.4 mmol, 1.0 equivs.) 2,6-bis(mercaptomethyl)pyridine (**11**) were dissolved in 100 mL dry DMF under N_2 and cooled to 0°C. 1.04 g (26.0 mmol, 2.1 equivs.) NaH-suspension (60% in mineral oil) was added in portions and the mixture was stirred for until the evolution of hydrogen had ceased. 8.60 g (26.0 mmol, 2.1 equivs.) (*S*)- 2-phenyl-4-tosyloxymethyl-oxazoline (**17**) was added as a solid and the ice-bath was removed. Stirring was continued at ambient temperature overnight. 100 mL water and 200 mL CH_2Cl_2 were added and the phases were separated. The organic layer was extracted with 4*100 mL water and dried ($MgSO_4$). After removal of the solvent in vacuo the residue was purified by column chromatography (SiO_2, hexanes / EtOAc 1:1 to hexanes / EtOAc 3:7) to yield 4.36 g (72%) of a slightly yellow oil, that solidified after several days to give a waxy slightly brown solid.

M.p. 59-61 °C. $[\alpha]_D^{20}$ = +21.6 (c = 1.16, CH_2Cl_2). ^{1}H-NMR (300 MHz, $CDCl_3$): δ = 7.98 – 7.85 (m, 4 H), 7.60 (t, *J* = 7.7 Hz, 1 H), 7.53 – 7.32 (m, 6 H), 7.25 (d, *J* = 7.7 Hz, 2 H), 4.57 – 4.39 (m, 4 H), 4.29 – 4.15 (m, 2 H), 3.89 (s, 4 H), 2.94 (dd, *J* = 13.3, 4.8 Hz, 2 H), 2.65 (dd, *J* = 13.3, 7.8 Hz, 2 H) . ^{13}C-NMR (75.5 MHz, $CDCl_3$): δ = 164.5, 158.2, 137.4, 131.5, 128.3 (2 peaks), 127.6, 121.4, 72.0, 66.5, 38.3, 36.6. ^{1}H-NMR (300 MHz, CD_3CN): δ = 7.94 – 7.80 (m, 4 H), 7.64 (t, *J* = 7.7 Hz, 1 H), 7.55 – 7.35 (m, 6 H), 7.23 (d, *J* = 7.7 Hz, 2 H), 4.55 – 4.35 (m, 4 H), 4.20 – 4.05 (m, 2 H), 3.85 (s, 4 H), 2.84 (dd, *J* = 13.4, 5.2 Hz, 2 H), 2.72 (dd, *J* = 13.4, 6.6 Hz, 2 H) . ^{13}C-NMR (75.5 MHz, CD_3CN): δ = 164.6, 159.7, 138.6, 132.4, 129.5, 129.0, 128.9, 122.3, 72.7, 67.7, 38.8, 37.2. IR (film): $\tilde{\nu}$ = 3074, 2978, 2930, 2910, 1970, 1912, 1820, 1731, 1646, 1589, 1573, 1495, 1453, 1418, 1360, 1306, 1264, 1177, 1084, 1063, 1029, 967, 909, 818, 782, 751, 694. MS (ESI): *m/z* (%) = 491.2 (34), 490.1 (100). HRMS (EI): calcd for $C_{27}H_{27}N_3O_2S_2$ $[M]^+$ 489.1545, found 489.1541.

Ligand 2c

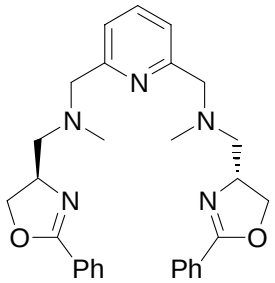

Under N_2 a solution of 1.11 g (4.35 mmol, 2.1 equivs.) (*S*)-2-phenyl-4-mesyloxymethyl-oxazoline (**16**) in 20 mL dry CH_3CN was added dropwise to a solution of 342 mg (2.07 mmol, 1.0 equiv.) 2,6-bis(N-methylaminomethyl)pyridine (**14**) in 10 mL dry CH_3CN. 1.14 g (8.28 mmol, 4.0 equivs.) K_2CO_3 were added and the mixture was heated to reflux for 31 h. After cooling down the suspension was filtered and the solvent evaporated. The residue was purified by column chromatography (SiO_2,CH_2Cl_2 / MeOH 19:1) to give 623 mg (62%) of a yellow oil, that eventually solidified after a few weeks.

$[\alpha]_D^{20}$ = -14.6 (c = 0.84, MeOH), $[\alpha]_{436}^{20}$ = -26.2 (c = 0.84, MeOH); ^{1}H-NMR (300 MHz, $CDCl_3$): δ = 7.98 – 7.84 (m, 4 H), 7.59 (t, *J* = 7.7 Hz, 1 H), 7.50 – 7.33 (m, 6 H), 7.30 (d, *J* = 7.7 Hz, 2 H), 4.56 – 4.38 (m, 4 H), 4.32 – 4.17 (m, 2 H), 3.81 (d, *J* = 14.3 Hz, 2 H), 3.68 (d, *J* = 14.3 Hz, 2 H), 2.90 – 2.74 (m, 2 H), 2.66 – 2.47 (m, 2 H), 2.37 (s, 6 H). ^{13}C-NMR (75.5 MHz, $CDCl_3$): δ = 164.2, 158.7, 136.8, 131.3, 128.3, 128.2, 127.8, 121.2, 72.0, 65.4, 64.5, 62.1, 43.5. IR (film): $\tilde{\nu}$ = 3420, 3076, 2952, 2908, 2845, 2810, 1970, 1910, 1820, 1645, 1578, 1494, 1450, 1352, 1291, 1253, 1177, 1156, 1138, 1084, 1053, 1025, 963, 930, 910, 867, 782, 696. MS (DCI, NH_3): *m/z* (%) = 485.3 (27), 484.2 (100), 337.1 (7). HRMS (EI): calcd for $C_{29}H_{33}N_5O_2$ $[M]^+$ 483.2634, found 483.2635.

8.3 Complex Synthesis

Caution: Although no problems were encountered with the complexes described in the following procedures, perchlorates are potential explosives and should be handled with care!

$[Mn(2a)(H_2O)_2](ClO_4)_2$ * THF

Under N_2 403 mg (1.11 mmol, 1.0 equiv.) $Mn(ClO_4)_2$*6 H_2O and 509 mg (1.11 mmol, 1.0 equiv.) $N(ON)_2$ were dissolved separately in 10 mL dry THF each. The ligand solution was transferred to the metal salt. Precipitation of a colorless solid started immediately. After 3 h this was collected on a membrane filter (Schleicher & Schuell, RC-L 58, 0.2 µm), washed with THF and dried in vacuo to yield 699 mg (77%) colorless solid.

M.p. > 200 °C. MS (ESI, CH_3CN): *m/z* (%) = 255.9 [47, [Mn(**2a**)]$^{2+}$), 276.5 (100, [Mn(**2a**)(CH_3CN)]$^{2+}$), 458.1 (34, [H**2a**]$^{+}$), 611.1 (8, [Mn(**2a**)(ClO_4)]$^{+}$). $C_{31}H_{39}Cl_2MnN_3O_{15}$ (819.50): calc. C 45.43, H 4.80, N 5.13; found C 45.24, H 4.84, N 5.24.

[Fe(2a)(H_2O)$_2$](ClO_4)$_2$ * THF

Under N_2 51.2 mg (141 µmol, 1.0 equiv.) Fe(ClO_4)$_2$*6 H_2O and 64.5 mg (141 µmol, 1.0 equiv.) N(ON)$_2$ were dissolved separately in 5 mL dry THF each. The ligand solution was transferred to the metal salt. Very few of a brown oil separated almost immediatelly. The supernatant solution was decanted and left overnight without stirring at ambient temperature. A colorless solid separated and was collected on a membrane filter (Schleicher & Schuell, RC-L 58, 0.2 µm), washed with Et_2O and dried in vacuo to yield 50 mg (43%) colorless needles, which were suitable for X-ray-diffraction.

M.p. 117-119°C (decomp.). MS (ESI, CH_3CN): *m/z* (%) = 256.4 (17, [Fe(**2a**)]$^{2+}$), 458.1 (100, [H**2a**]$^{+}$). $C_{31}H_{39}Cl_2FeN_3O_{15}$ (820.40): calc. C 45.38, H 4.79, N 5.12; found C 45.20, H 4.70, N 5.02.

[Co(2a)](ClO_4)$_2$

Under N_2 226 mg (616 µmol, 1.0 equiv.) Co(ClO_4)$_2$*6 H_2O and 282 mg (616 mmol, 1.0 equiv.) N(ON)$_2$ were dissolved separately in 10 mL dry THF each. The ligand solution was transferred to the metal salt. Precipitation of a purple oil started immediately. After 3 h the supernatant solution was decanted. The oily residue was treated with 10 mL dry THF, followed by decanting. This was repeated twice. After drying the residual purple, sticky material overnight in vacuo yielded a purple solid (414 mg, 94%).

M.p. > 200°C. MS (ESI, CH_3CN): *m/z* (%) = 257.9 (100, [Co(**2a**)]$^{2+}$), 278.5 (10, [Co(**2a**)(CH_3CN)]$^{2+}$), 458.1 (8, [H**2a**]$^{+}$), 615.1 (17, [Co(**2a**)(ClO_4)]$^{+}$. $C_{27}H_{27}Cl_2CoN_3O_{12}$ (715.35): calc. C 45.33, H 3.80, N 5.87; found C 45.17, H 3.98, N 5.75.

[Ni(2a)](ClO_4)$_2$ * H_2O * THF

Under N_2 226 mg (619 µmol, 1.0 equiv.) Ni(ClO_4)$_2$*6 H_2O and 283 mg (619 mmol, 1.0 equiv.) N(ON)$_2$ were dissolved separately in 10 mL dry THF each. The ligand solution was transferred to the metal salt. Precipitation of a turquoise oil started immediately. After 3 h the supernatant solution was decanted. The oily residue was treated with 10 mL dry THF, followed by decanting. This was repeated twice. After drying the residual purple, sticky material overnight in vacuo yielded a turquoise solid (446 mg, 90%).

M.p. 168-173°C (decomp.). MS (ESI, CH_3CN): *m/z* (%) = 257.4 (20, [Ni(**2a**)]$^{2+}$), 278.0 (100, [Ni(**2a**)(CH_3CN)]$^{2+}$), 458.1 (22, [H**2a**]$^{+}$), 614.1 (100, [Ni(**2a**)(ClO_4)]$^{+}$. $C_{31}H_{37}Cl_2N_3NiO_{14}$ (805.24): calc. C 46.24, H 4.63, N 5.22 ; found C 46.19, H 4.76, N 5.29.

[Cu(2a)]$(ClO_4)_2$ * H_2O * THF

Under N_2 230 mg (620 µmol, 1.0 equiv.) $Cu(ClO_4)_2$*6 H_2O and 284 mg (620 mmol, 1.0 equiv.) $N(ON)_2$ were dissolved separately in 10 mL dry THF each. The ligand solution was transferred to the metal salt. Precipitation of a blue oil started immediately. After 3 h the supernatant solution was decanted. The oily residue was treated with 10 mL dry THF, followed by decanting. This was repeated twice. After drying the residual purple, sticky material overnight in vacuo yielded a light blue solid (456 mg, 91%).

M.p. 166-172°C (decomp.). MS (ESI, CH_3CN): *m/z* (%) = 260.0 (98, $[Cu(\mathbf{2a})]^{2+}$), 280.5 (100, $Cu(\mathbf{2a})(CH_3CN)]^{2+}$), 458.2 (12, $[H\mathbf{2a}]^+$), 520.1 (98, $[Cu(\mathbf{2a})]^+$), 619.2 (79, $[Cu(\mathbf{2a})(ClO_4)]^+$). $C_{31}H_{37}Cl_2CuN_3O_{14}$ (810.09): calc. C 45.96, H 4.60, N 5.19; found C 45.78, H 4.73, N 5.26.

[Cu^I(2a)(?)](ClO_4) *(?)

Under N_2 115 mg (142 µmol, 1.0 equiv.) $[Cu(N(ON)_2)](ClO_4)_2$ * H_2O * THF was dissolved in dry CH_3CN/MeOH (10mL:20mL). The blue solution was degassed by three freeze(N_2)-thaw(vaccum)-cycles and 6.0 mg (160 µmol, 1.13 equivs.) $NaBH_4$ were added. The color changed from light blue to red-brown and a brown solid precipitated. After stirring the solution for 18 h at ambient temperature, the solvent was removed under vacuum from the yellow solution. The residue was suspended in 1 mL degassed $CDCl_3$ and the mixture was filtered through a plug of cotton under N_2 into a NMR-tube, which was sealed against atmospheric oxygen. In contrast to the corresponding Cu^{II}-complex, being paramagnetic, the title compound exhibited diamagnetic behavior.

^{1}H-NMR (300 MHz, $CDCl_3$): δ = 8.31 (d, *J* = 7.4 Hz, 4 H), 7.73 (t, *J* = 7.7 Hz, 1 H), 7.65 – 7.39 (m, 6 H), 7.21 (d, *J* = 7.7 Hz, 2 H), 4.97 – 4.75 (m, 4 H), 4.63 (d, *J* = 15.6 Hz, 2 H), 4.47 (d, *J* = 15.6 Hz, 2 H), 4.19 – 3.95 (m, 4 H), 3.32 – 3.11 (m, 2 H). ^{13}C-NMR (75.5 MHz, $CDCl_3$): δ = 166.1, 155.8, 138.3, 133.0, 129.0, 128.6, 125.0, 123.1, 70.9, 70.4, 69.1, 66.9.

After exposure of this solution to the atmosphere for 5 min and closing the NMR-tube again, the solution turned green in a matter of seconds and a green precipitate formed after several hours. ^{1}H-NMR shows paramagnetic behavior again. Due to this reactivity, no further caracterization was carried out.

[Zn(2a)]$(ClO_4)_2$

Under N_2 49.0 mg (132 µmol, 1.0 equiv.) $Zn(ClO_4)_2$*6 H_2O and 60.2 mg (132 µmol, 1.0 equiv.) $N(ON)_2$ were dissolved separately in 5 mL dry THF each. The ligand solution was transferred to the metal salt. Precipitation of the complex started immediately upon addition. The mixture was stirred at ambient temperature for 1 h. The precipitate was collected on a membrane filter (Schleicher & Schuell, RC-L 58, 0.2 µm), washed with THF and dried in vacuo to yield 82 mg (86%) of a colorless solid, that was essentially pure. Crystals suitable for X-Ray-diffraction were obtained by diffusion of Et_2O into a solution of the title compound in CH_3CN.

M.p. > 200°C. ^{1}H-NMR (300 MHz, CD_3CN): δ = 8.12 (t, *J* = 7.9 Hz, 1 H), 7.88 – 7.75 (m, 6 H), 7.70 – 7.59 (m, 4 H), 7.48 (d, *J* = 7.9 Hz, 2 H), 5.06 – 4.88 (m, 4 H), 4.81 (d, *J* = 16.2 Hz, 2 H), 4.44 – 4.16 (m, 6 H), 3.60 – 3.48 (m, 2 H). ^{13}C-NMR (75.5 MHz, CD_3CN): δ = 175.4, 155.3, 143.7, 135.8, 130.4, 130.3, 124.8, 124.1, 73.7, 73.1, 71.0, 64.6. MS (ESI, CH_3CN): *m/z* (%) = 260.4 (100, [Zn(**2a**)]$^{2+}$), 458.1 (82, [**2a**]$^{+}$), 620.1 (7, [Zn(**2a**)(ClO_4)]$^{+}$). $C_{27}H_{27}Cl_2N_3O_{12}Zn$ (721.81): calc. C 44.93, H 3.77, N 5.82; found C 45.01, H 3.99, N 5.87.

[Cd(2a)(?)](ClO_4)$_2$

Under N_2 233 mg (555 µmol, 1.0 equiv.) $Cd(ClO_4)_2$*6 H_2O and 254 mg (555 µmol, 1.0 equiv.) $N(ON)_2$ were dissolved separately in 10 mL dry THF each. The ligand solution was transferred to the metal salt. Precipitation of the complex started immediately upon addition. The mixture was stirred at ambient temperature for 1 h. The precipitate was collected on a membrane filter (Schleicher & Schuell, RC-L 58, 0.2 µm), washed with THF, Et_2O and dried in vacuo to yield 427 mg (%) of a colorless solid.

M.p. > 200°C. ^{1}H-NMR (300 MHz, CD_3CN): δ = 8.02 (t, *J* = 7.8 Hz, 1 H), 7.62 – 7.50 (m, 2 H), 7.48 – 7.30 (m, 10 H), 5.10 – 4.85 (m, 6 H), 4.69 (dd, *J* = 10.4, 9.3 Hz, 2 H), 4.29 – 4.15 (m, 4 H), 3.81 (dd, *J* = 11.1, 8.4 Hz, 2 H), 3.69 – 3.55 (m, 4 H, THF), 1.85 – 1.72 (m, 4 H, THF). ^{13}C-NMR (75.5 MHz, CD_3CN): δ = 170.5, 154.9, 140.8, 134.1, 129.8, 129.1, 125.7, 122.8, 73.2, 70.4, 70.3, 68.4, 65.9, 26.3. MS (ESI, CH_3CN): *m/z* (%) = 285.0 (80, [Cd(**2a**)]$^{2+}$), 305.6 (100, [Cd(**2a**)(CH_3CN)]$^{2+}$), 458.1 (37, [H**2a**]$^{+}$), 670.1 (13, [Cd(**2a**)(ClO_4)]$^{+}$). No sufficient elemental analysis could be obtained.

[Mg(2a)(H_2O)$_2$](ClO_4)$_2$

Under N_2 267 mg (1.20 mmol, 1.0 equiv.) $Mg(ClO_4)_2$ * x H_2O and 547 mg (1.20 mmol, 1.0 equiv.) $N(ON)_2$ were dissolved separately in 10 mL dry THF each. The ligand solution was transferred to the metal salt. The solution was stirred at ambient temperature for 4 h, before the solvent was removed in vacuo. The slightly yellow residue was treated with 20 mL dry Et_2O and the suspension was stirred vigorously for 1 h. The solid was collected, washed with dry Et_2O and dried under reduced pressure to yield a slightly yellow solid (596mg, 70%).

M.p. 110-123°C (decomp.). ^{1}H-NMR (300 MHz, CD_3CN): very broad signals. MS (ESI, CH_3CN): *m/z* (%) = 240.5 (37, [Mg(**2a**)]$^{2+}$), 261.0 (100, [Mg(**2a**)(CH_3CN)]$^{2+}$), 458.1 (83, [H**2a**]$^{+}$), 580.1 (15, [Mg(**2a**)(ClO_4)]$^{+}$). No sufficient elemental analysis could be obtained.

[Fe(2b)(H_2O)](ClO_4)$_2$ * 2 H_2O

Under N_2 103 mg (283 µmol, 1.0 equiv.) $Fe(ClO_4)_2$*6 H_2O and 138 mg (283 µmol, 1.0 equiv.) $N(SN)_2$ were dissolved separately in 3 mL dry, degassed THF each. The ligand solution was transferred to the metal salt. Precipitation of the complex started immediately upon addition. The mixture was stirred at ambient temperature for 1 h. The supernatant solution was decanted and the residue was treated with 10 mL dry, degassed THF, followed by decanting. This was repeated twice and the residual brown solid was dried in vacuo to yield 104 (46%) mg of the Fe-complex that was stored under N_2.

M.p. > 100°C (decomp.). MS (ESI, CH_3CN): *m/z* (%) = 272.4 (100, $[Fe(\mathbf{2b})]^{2+}$), 293.0 (6, $[Fe(\mathbf{2b})(CH_3CN)]^{2+}$), 490.1 (13, $[H\mathbf{2b}]^{+}$), 644.1 (8, $[Fe(\mathbf{2b})(ClO_4)]^{+}$). $C_{27}H_{33}Cl_2FeN_3O_{13}S_2$ (798.45): calc. C 40.62, H 4.17, N 5.26; found C 40.70, H 4.01, N 5.00.

$[Co(2b)(THF)](ClO_4)_2 * H_2O$

Under N_2 66.7 mg (182 µmol, 1.0 equiv.) $Co(ClO_4)_2*6\ H_2O$ and 89.0 mg (182 µmol, 1.0 equiv.) $N(SN)_2$ were dissolved separately in 5 mL dry THF each. The ligand solution was transferred to the metal salt. Precipitation of the complex started immediately upon addition. The mixture was stirred at ambient temperature for 1 h. The precipitate was collected on a membrane filter (Schleicher & Schuell, RC-L 58, 0.2 µm), washed with THF and dried in vacuo to yield 138 mg (91%)

M.p. > 100°C (decomp.). MS (ESI, CH_3CN): *m/z* (%) = 273.9 (100, $[Co(N(SN)_2)]^{2+}$), 490.1 (8, $N(SN)_2^{+}$), 647.0 (5, $[Fe(N(SN)_2)(ClO_4)]^{+}$). $C_{31}H_{37}Cl_2CoN_3O_{12}S_2$ (837.61): calc. C 44.45, H 4.45, N 5.02; found C 44.59, H 4.25, N 5.19.

$[Ni(2b)](ClO_4)_2 * 2\ H_2O$

Under N_2 62.3 mg (170 µmol, 1.0 equiv.) $Ni(ClO_4)_2*6\ H_2O$ and 83.4 mg (170 µmol, 1.0 equiv.) $N(SN)_2$ were dissolved separately in 5 mL dry THF each. The ligand solution was transferred to the metal salt. Precipitation of the complex started immediately upon addition. The mixture was stirred at ambient temperature for 20 h. The precipitate was collected on a membrane filter (Schleicher & Schuell, RC-L 58, 0.2 µm), washed with THF and dried in vacuo to yield 120 mg (90%)

M.p. > 179°C (decomp.). MS (ESI, CH_3CN): *m/z* (%) = 273.4 (100, $[Ni(N(SN)_2)]^{2+}$), 294.0 (12, $[Ni(N(SN)_2)(CH_3CN)]^{2+}$), 490.1 (25, $N(SN)_2^{+}$), 646.1 (7, $[Ni(N(SN)_2)(ClO_4)]^{+}$). $C_{27}H_{31}Cl_2N_3NiO_{12}S_2$ (783.28): calc. C 41.40, H 3.99, N 5.36; found C 41.67, H 4.08, N 5.14.

$[Cu(2b)](ClO_4)_2 * H_2O$

Under N_2 195 mg (526 µmol, 1.0 equiv.) $Cu(ClO_4)_2*6\ H_2O$ and 258 mg (526 µmol, 1.0 equiv.) $N(SN)_2$ were dissolved separately in 10 mL dry THF each. The ligand solution was transferred to the metal salt. Precipitation of the complex started immediately upon addition. The mixture was stirred at ambient temperature for 1 h, before 20 mL dry n-pentane was added. The precipitate was collected on a membrane filter (Schleicher & Schuell, RC-L 58, 0.2 µm), washed with THF and dried in vacuo to yield 333 mg (82%)

M.p. > 200°C. MS (ESI, CH_3CN): *m/z* (%) = 275.9 (100, $[Cu(N(SN)_2)]^{2+}$), 390.8 (40), 490.0 (2, $[N(SN)_2]^{+}$), 552.1 (35, $[Cu^{I}(N(SN)_2)]^{+}$). $C_{27}H_{29}Cl_2CuN_3O_{11}S_2$ (770.12): calc. C 42.11, H 3.80, N 5.46; found C 41.89, H 3.70, N 5.39.

$[Cu^{I}(2b)(?)](ClO_4)$

Under N_2 115 mg (93 µmol, 1.0 equiv.) $[Cu(N(SN)_2)](ClO_4)_2 * H_2O$ was dissolved in dry CH_3CN/MeOH (5mL:10mL). The green solution was degassed by three freeze(N_2)-thaw(vaccum)-cycles and after complete dissolution 3.5 mg (93 µmol,

1.02 equivs.) $NaBH_4$ were added. The color changed from deep green to light-green, yellow, orange-brown. After 1 h a bright yellow color had developed again. The solvent was removed under vacuum. The residue was suspended in 1 mL degassed $CDCl_3$ and the mixture was filtered through a plug of cotton under N_2 into a NMR-tube, which was sealed against atmospheric oxygen. In contrast to the corresponding Cu^{II}-complex, being paramagnetic, the title compound exhibited diamagnetic behavior.

^{1}H-NMR (300 MHz, $CDCl_3$): δ = 8.09 (d, *J* = 7.1 Hz, 4 H), 7.71 (t, *J* = 7.7 Hz, 1 H), 7.49 – 7.19 (m, 8 H), 4.90 – 4.69 (m, 4 H), 4.40 – 4.10 (m, 8 H), 2.53 (dd, *J* = 14.4, 10.6 Hz, 2 H), 1.09 (dd, *J* = 10.6, 5.5 Hz, 2 H). ^{13}C-NMR (75.5 MHz, $CDCl_3$): δ = 165.5, 156.5, 138.6, 132.7, 128.8, 128.3, 125.5, 123.6, 72.3, 66.6, 38.7, 38.5. MS (ESI, CH_3CN): *m/z* (%) = 552.1 (100, [Cu(**2b**)]$^+$). MS (-ESI, CH_3CN): *m/z* (%) = 751.9 ([Cu(N(SN)$_2$](ClO$_4$)$_2$]$^-$).

After exposure of this solution to the atmosphere for 5 min and closing the NMR-tube again, the solution turned green in a matter of hours and a green precipitate formed after several days.

[Zn(2b)](ClO$_4$)$_2$ * H$_2$O

Under N_2 193.5 mg (520 µmol, 1.0 equiv.) Zn(ClO$_4$)$_2$*6 H$_2$O and 254.4 mg (520 µmol, 1.0 equiv.) N(SN)$_2$ were dissolved separately in 10 mL dry THF each. The ligand solution was transferred to the metal salt. Precipitation started immediately upon addition. The mixture was stirred at ambient temperature for 1 h and 15 mL dry Et_2O were added. The creamy, slightly sticky solid was collected on a membrane filter (Schleicher & Schuell, RC-L 58, 0.2 µm), washed with THF and dried in vacuo to yield 323 mg (80%) of a colorless solid, that was essentially pure. Crystals suitable for X-Ray-diffraction were obtained by diffusion of Et_2O into a solution of the title compound in CH_3CN.

M.p. > 200°C. ^{1}H-NMR (300 MHz, CD_3CN): δ = 8.08 (t, *J* = 7.7 Hz, 1 H), 7.95 – 7.84 (m, 4 H), 7.83 – 7.75 (m, 2 H), 7.74 – 7.63 (m, 4 H), 7.58 (d, *J* = 7.7 Hz, 2 H), 4.98 – 4.83 (m, 2 H), 4.59 – 4.16 (m, 8 H), 3.30 (dd, *J* = 14.3, 3.6 Hz, 2 H), 2.93 – 2.73 (m, 2 H). ^{13}C-NMR (75.5 MHz, CD_3CN): δ = 172.7, 156.2, 142.9, 135.7, 130.7, 129.8, 125.8, 125.7, 74.6, 65.3, 38.5, 38.2. MS (ESI, CH_3CN): *m/z* (%) = 276.4 (100, [Zn(**2b**)]$^{2+}$), 490.1 (39, [H**2b**]$^+$), 654.1 (9, [Zn(**2b**)(ClO$_4$)]$^+$). $C_{27}H_{29}Cl_2N_3O_{11}S_2Zn$ (771.96): calc. C 42.01, H 3.79, N 5.44; found C 42.73, H 3.45, N 5.21.

[Cd(2b)](ClO$_4$)$_2$ * THF

Under N_2 52.2 mg (124 µmol, 1.0 equiv.) Cd(ClO$_4$)$_2$*6 H$_2$O and 60.9 mg (124 µmol, 1.0 equiv.) N(SN)$_2$ were dissolved separately in 4 mL dry THF each. The ligand solution was transferred to the metal salt. Precipitation of the complex started immediately upon addition. The mixture was stirred at ambient temperature for 1 h. The precipitate was collected on a membrane filter (Schleicher & Schuell, RC-L 58, 0.2 µm), washed with THF, Et_2O and dried in vacuo to yield 103 mg (95%) of a light orange solid.

M.p. 162-167°C (decomp.). ^{1}H-NMR (300 MHz, CD_3CN): broad signals. MS (ESI, CH_3CN): *m/z* (%) = 301.1 (100, $[Cd(\mathbf{2b})]^{2+}$), 321.6 (12, $[Cd(\mathbf{2b})(CH_3CN)]^{2+}$), 490.1 (7, $[H\mathbf{2b}]^{+}$), 702.1 (7, $[Cd(\mathbf{2b})(ClO_4)]^{+}$). $C_{31}H_{35}CdCl_2N_3O_{11}S_2$ (873.07): calc. C 42.19, H 4.19, N 4.99; found C 42.65, H 4.04, N 4.81.

$[Zn(2c)](ClO_4)_2 * CH_3CN * H_2O$

Under N_2 27.0 mg (72.6 µmol, 1.0 equiv.) $Zn(ClO_4)_2$*6 H_2O and 35.1 mg (72.6 µmol, 1.0 equiv.) $N(NN)_2$ were dissolved separately in 2 mL dry THF each. The ligand solution was transferred to the metal salt. Precipitation started immediately upon addition. The mixture was stirred at ambient temperature for 1 h. The slightly yellow solid was collected on a membrane filter (Schleicher & Schuell, RC-L 58, 0.2 µm), washed with THF and dried in vacuo. Crystals of $[Zn(N(NN)_2)](ClO_4)_2$ * 2 CH_3CN, suitable for X-Ray-diffraction, were obtained by diffusion of Et_2O into a solution of the title compound in CH_3CN. Upon exposure to air, the crystals replace one CH_3CN-molecule by H_2O to yield 35 mg (60%) of the title compound as colorless prisms.

M.p. > 200 °C. ^{1}H-NMR (300 MHz, CD_3CN): for spectrum see appendix. MS (ESI, CH_3CN): *m/z* (%) = 273.5 (100, $[Zn(\mathbf{2c})]^{2+}$). $C_{31}H_{38}Cl_2N_6O_{11}Zn$ (806.96): calc. C 46.14, H 4.75, N 10.41; found C 46.28, H 4.75, N 10.08.

$Co(OTf)_2$*2 CH_3CN

The following procedure was carried out under a dry atmosphere of N_2 using Schlenk-technique. 935 mg (15.9 mmol, 1.0 equivs.) cobalt (Aldrich, >99.9%, <100 mesh) were suspended in 16 mL anhydrous CH_3CN. The mixture was cooled to 0°C and 5.0 g (33.3 mmol, 2.1 equivs.)) triflic acid (Merck-Schuchardt, >98%) were added dropwise in the course of 3 min. The icebath was removed and stirring was continued for 30 min. After heating the mixture for 2 h under reflux the solvent and excess triflic acid were removed under reduced pressure. The solid was dissolved in dry CH_3CN and residual cobalt was removed by filtration through a pad of Celite 535 (Fluka). The resulting red solution was concentrated under reduced pressure until crystallization began. The solid was redissolved by adding a minimum amount of dry CH_3CN. This solution was layered with approximately twice the volume of dry Et_2O and allowed to stand at room temperature for two days. The formed slightly sticky crystals were collected , washed with Et_2O and dried in vacuo to constant weight to give a pink amorphous powder (5.67g, 81%), that was stored under N_2.

IR (nujol): $\tilde{\nu}$ = 3172 cm^{-1}, 2726, 2675, 2319, 2292, 1310, 1213, 1185, 1039, 722, 642, 516. MS (ESI, CH_3CN): *m/z* (%) = 330.8 (100, $[Co(CH_3CN)_3(OTf)]^{+}$), 289.7 (74, $[Co(CH_3CN)_2(OTf)]^{+}$). $C_6H_6CoF_6N_2O_6S_2$ (439.18): calc. C 16.41, H 1.38, N 6.38, S 14.60; found C 16.63, H 1.47, N 6.61, S 14.46.

$[Co(2b)(THF)](OTf)_2$

The following procedure was carried out under a dry atmosphere of N_2 using Schlenk-technique. 113 mg (231 µmol, 1.0 equivs.) $N(SN)_2$ and 101 mg (231 µmol, 1.0 equivs.) $Co(OTf)_2$*2 CH_3CN were dissolved separately in 2.5 mL dry THF each. The Co-solution was added to the ligand-solution. A pink solid formed almost immediately. The mixture was stirred for additional 3 h. The solid was collected and washed with dry THF. Drying the complex under reduced pressure yielded a pink

solid (145 mg, 68%). Single-crystals suitable for X-ray analysis were obtained by vapour-diffusion of Et_2O into a CH_3CN-solution of the title compound.

IR (nujol): $\tilde{\nu}$ = 3162 cm^{-1}, 2725, 2672, 1304, 1154, 1122, 1028, 967, 722, 636. MS (ESI, CH_3CN): *m/z* (%) = 274.1 (100, $[Co(\mathbf{2b})]^{2+}$). $C_{33}H_{35}CoF_6N_3O_9S_4$ (918.81): calc. C 43.14, H 3.84, N 4.57, S 13.96; found C 43.04, H 3.80, N 4.60, S 13.98.

{Ru[N(SN)$_2$]Cl}Cl and {Ru[N(SN)$_2$]CH$_2$Cl$_2$}Cl$_2$

Under N_2 a Schlenk-flask was charged with 55.7 mg (111 µmol, 1.0 equivs.) $[RuCl_2(benzene)]_2$ and 15 mL anhydrous EtOH were added. The suspension was treated with 109.1 mg (222.7 µmol, 2.0 equivs.) $N(SN)_2$ and the mixture was heated to reflux for 10 h. After cooling down to ambient temperature the solvent was removed in vacuo (4 h) and the residue was taken up in 5 mL dry CH_2Cl_2. The resulting yellow-brown solution was passed through a pad of Celite 535 (Fluka) and the solvent was removed under reduced pressure again to yield 161 mg of a dark-yellow solid that consisted of two symmetric diamagnetic Ru^{II}-complexes as shown by ^{1}H-NMR.

^{1}H-NMR (600 MHz, $CDCl_3$): a) [Ru(**2b**)(?)]Cl_n: δ = 8.27 (d, *J* = 7.3 Hz, 4 H), 7.72 – 7.34 (m, 9 H), 5.30 (s, 2 H), 4.98 (d, *J* = 18.0 Hz, 2 H), 4.82 – 4.69 (m, 2 H), 4.06 – 3.94 (m, 2 H), 3.76 (d, *J* = 18.0 Hz, 2 H), 3.59 – 3.37 (m, 4 H), 2.51 – 2.41 (m, 2 H); b) [Ru(**2b**)Cl]Cl: δ = 8.00 (d, *J* = 7.5 Hz, 4 H), 7.72 – 7.34 (m, 9 H), 4.82 – 4.69 (m, 2 H), 4.54 (d, *J* = 17.0 Hz, 2 H), 4.30 – 4.20 (m, 2 H), 4.06 – 3.94 (m, 2 H), 3.28 – 3.20 (m, 2 H), 3.08 (d, *J* = 17.0 Hz, 2 H), 1.82 – 1.72 (m, 2 H). MS (ESI, CH_3CN): *m/z* (%) = 315.6 (8, $[Ru(\mathbf{2b})(CH_3CN)]^{2+}$), 626.2 (100, $[Ru(\mathbf{2b})Cl]^{+}$).

[Yb(2a)(H$_2$O)(OTf)](OTf)$_2$

Under N_2 289 mg (466 µmol, 1.0 equiv.) $Yb(OTf)_3$ and 213 mg (466 µmol, 1.0 equiv.) $N(ON)_2$ were dissolved separately in 5 mL dry THF each. The ligand was transferred to the metal and the resulting colorless solution was stirred at ambient temperature for 8 h. After refluxing the mixture for 12 h, the orange solution was cooled down and the solvent was removed in vacuo. The residue was treated with 25 mL dry Et_2O and stirred vigorously for 1 h. The solid was collected, washed with dry Et_2O and dried under reduced pressure to yield 363 mg (71%) of a light orange solid.

M.p. > 100°C (decomp.). MS (ESI, CH_3CN): *m/z* (%) = 344.2 (36, $[Yb(\mathbf{2a})(OH)(CH_3CN)]^{2+}$), 398.7 (66, $[Yb(\mathbf{2a})(H_2O)(OTf)]^{2+}$), 419.2 (54, $[Yb(\mathbf{2a})(H_2O)(OTf)(CH_3CN)]^{2+}$), 458.2 (100, $[\mathbf{2a}]^{+}$), 797.1 (18, $[Yb(\mathbf{2a})(OH)(OTf)]^{+}$), 947.1 (18, $[Yb(\mathbf{2a})(H_2O)\ (OTf)_2]^{+}$). $C_{30}H_{29}F_9N_3O_{14}\ S_3Yb$ (1095.79): calc. C 32.88, H 2.67, N 3.83; found C 32.51, H 2.90, N 3.83.

$_\infty$[Cd(2a)Cl$_4$Cd] (19)

Under N_2 a mixture of 319 mg (1.58 mmol, 1.0 equiv.) $CdCl_2{*}H_2O$ and 725 mg (1.58 mmol, 1.0 equiv.) **2a** in 20 mL dry MeOH was refluxed for 3 h. After cooling down to ambient temperature, the formed white precipitate was collected, washed with cold dry MeOH and dried in vacuo to yield 368 mg (57%) of a colorless solid. Crystals

suitable for X-ray-analysis were obtained by diffusion of Et_2O into a solution of the title compound in CH_3CN (Note: The title compound was only sparingly soluble in CH_3CN. Therefore no ^{13}C-NMR could be obtained.)

M.p. > 200 °C. ^{1}H-NMR (300 MHz, CD_3CN): δ = 7.94 (t, *J* = 7.8 Hz, 1 H), 7.75 – 7.59 (m, 4 H), 7.53 – 7.17 (m, 8 H), 5.10 – 4.87 (m, 6 H), 4.64 (dd, *J* = 10.4, 9.1 Hz, 2 H), 4.20 – 4.04 (m, 4 H), 3.73 (dd, *J* = 11.0, 8.5 Hz, 2 H). MS (ESI, CH_3CN): *m/z* (%) = 458.1 (58, [**2a**]$^+$), 606.1 (100, [Cd(**2a**)Cl]$^+$). MS (-ESI, CH_3CN): *m/z* (%) = 218.3 (100, $[CdCl_3]^-$). $C_{27}H_{27}Cd_2Cl_4N_3O_4$ (824.14): calc. C 39.35, H 3.30, N 5.10; found C 39.35, H 3.40, N 5.17.

$_\infty$[Cd(2a)Br$_4$Cd] (20)

Under N_2 a mixture of 344 mg (1.26 mmol, 1.0 equiv.) $CdBr_2$ and 578 mg (1.26 mmol, 1.0 equiv.) **2a** in 10 mL dry MeOH was refluxed for 1 h. After cooling down to ambient temperatur, the white solid was collected, washed with dry, cold MEOH and dried in vacuo to yield 478 mg (76%) of a colorless solid. Crystals suitable for X-ray-analysis were obtained by diffusion of Et_2O into a solution of the title compound in CH_3CN

M.p. > 200°C. ^{1}H-NMR (300 MHz, CD_3CN): δ = 7.95 (t, *J* = 7.9 Hz, 1 H), 7.75 – 7.59 (m, 4 H), 7.54 – 7.43 (m, 2 H), 7.38 (d, *J* = 7.9 Hz, 2 H), 7.33 – 7.20 (m, 4 H), 5.08 – 4.87 (m, 6 H), 4.65 (dd, *J* = 10.4, 9.1 Hz, 2 H), 4.22 – 4.05 (m, 4 H), 3.76 (t, *J* = 11.0, 8.5 Hz, 2 H). ^{13}C-NMR (75.5 MHz, CD_3CN): δ = 169.2, 155.2, 140.3, 133.5, 130.3, 128.7, 126.2, 122.7, 73.6, 70.7, 70.1, 66.2. MS (ESI, CH_3CN): *m/z* (%) = 458.1 (46, [**2a**]$^+$), 480.1 (100, [Na(**2a**)]$^+$), 558.1 (11, [Cd_3Br_4(**2a**)]$^{2+}$), 594.1 (6), 650.0 (5, [Cd(**2a**)Br]$^+$). MS (-ESI, CH_3CN): *m/z* (%) = 440.4 (100). $C_{27}H_{27}Br_4$ $Cd_2N_3O_4$ (1001.94): calc. C 32.37, H 2.72, N 4.19; found C 32.37, H 2.61, N 4.56.

9 Appendix

9.1 NMR-Spectra

2,6-Pyridinedicarboxylic acid dimethyl ester

^{1}H-NMR (300 MHz, $CDCl_3$)

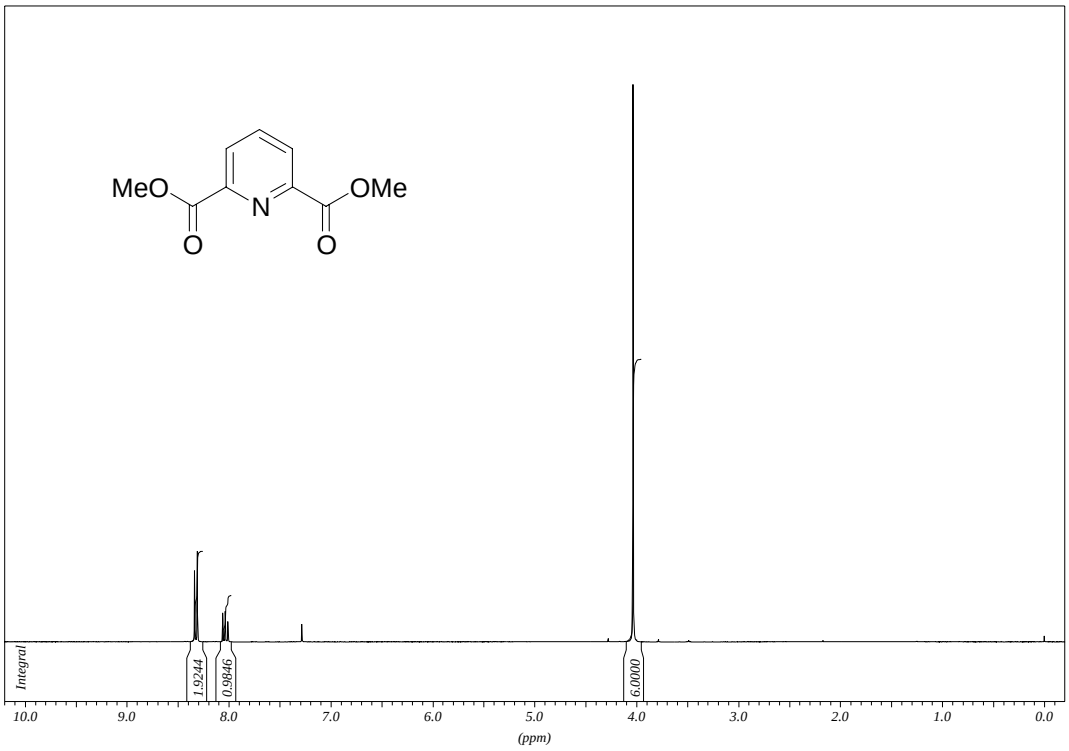

^{13}C-NMR (75.5 MHz, $CDCl_3$)

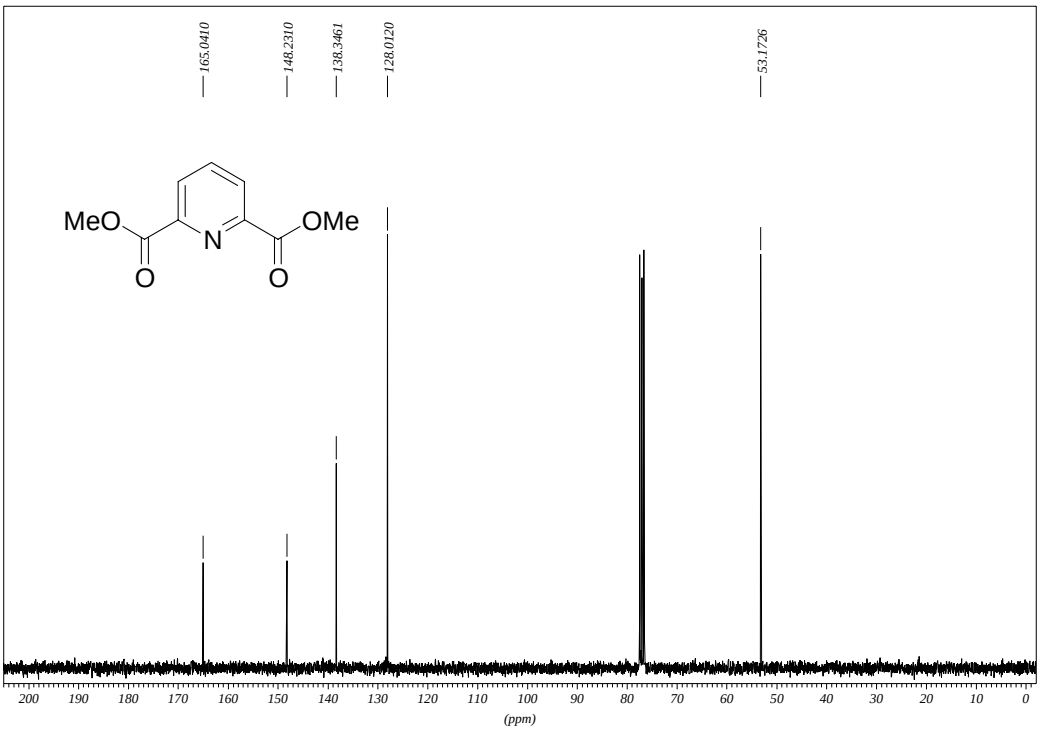

2,6-Bis(hydroxymethyl)pyridine (3)

^{1}H-NMR (300 MHz, DMSO-d_6)

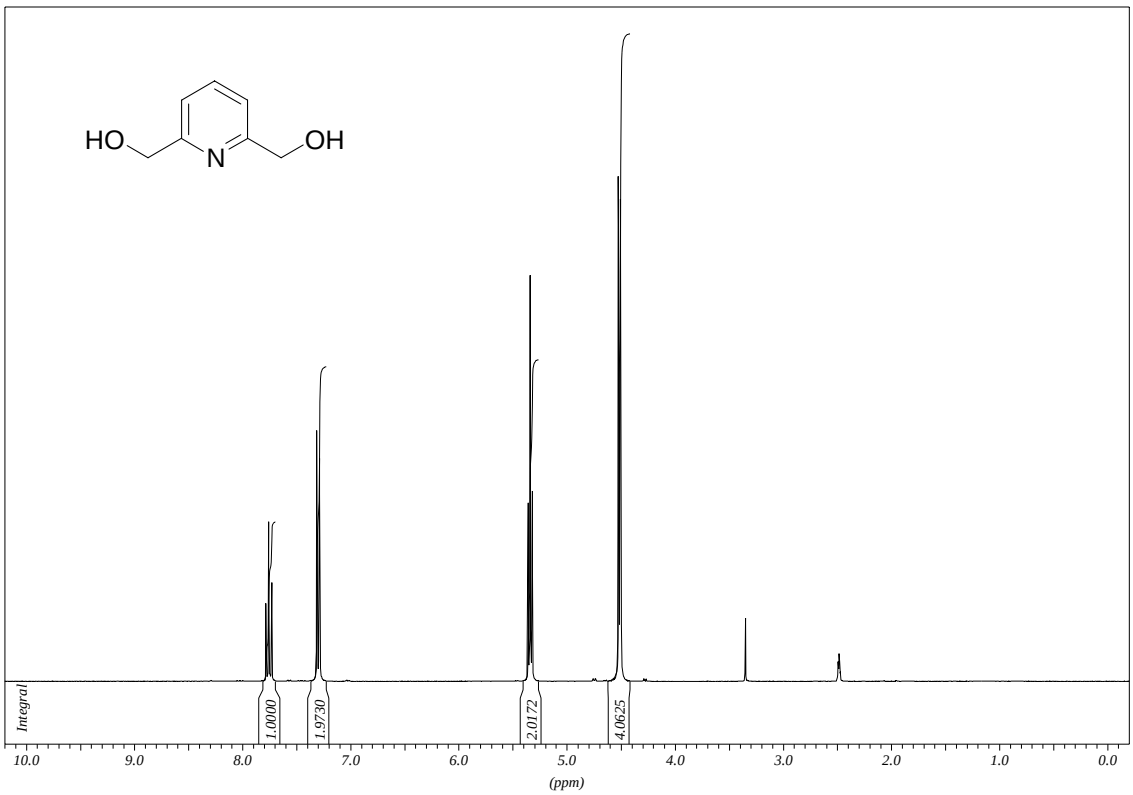

^{13}C-NMR (300 MHz, DMSO-d_6)

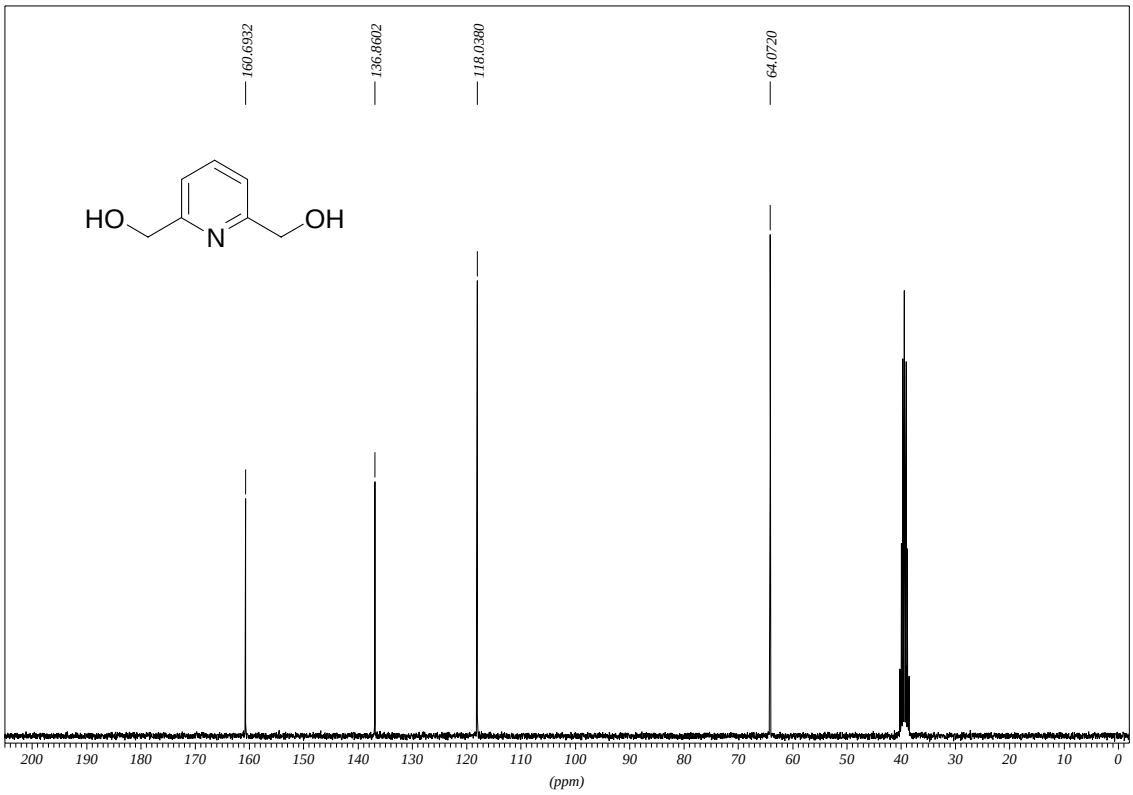

2,6-Bis(bromomethyl)pyridine (10)

^{1}H-NMR (300 MHz, $CDCl_3$)

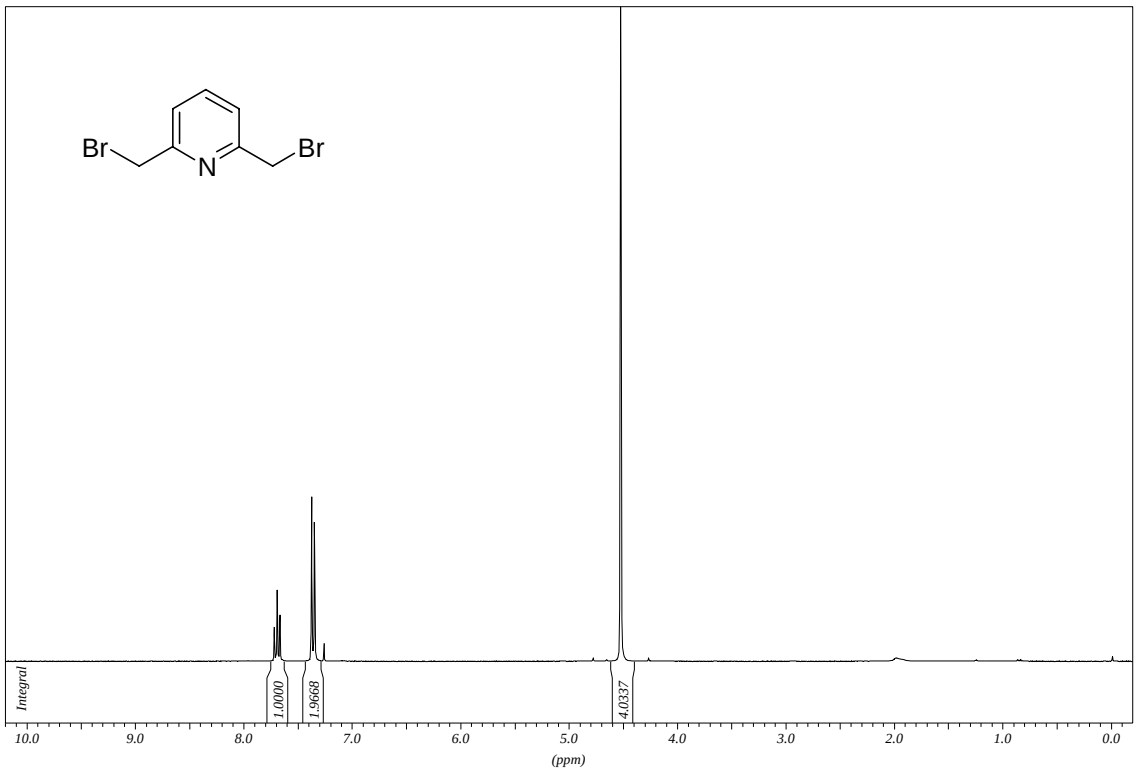

^{13}C-NMR (75.5 MHz, $CDCl_3$)

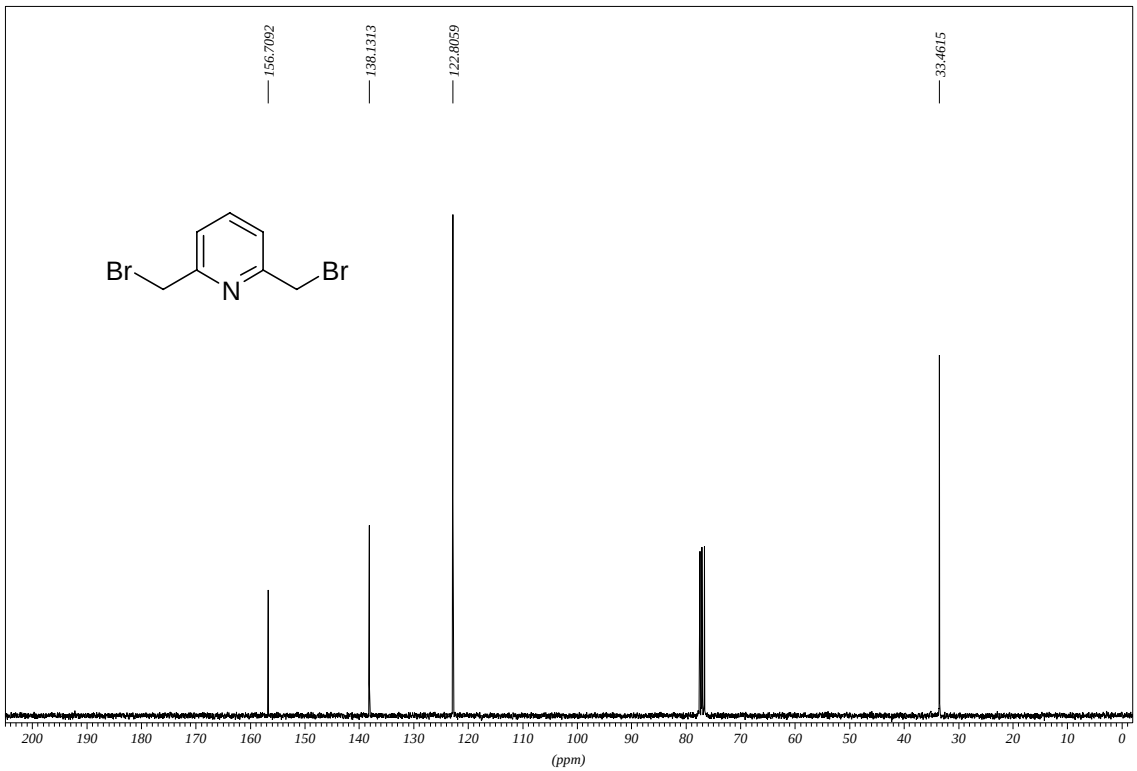

2,6-Bis(chloromethyl)pyridine Hydrochloride (7)

^{1}H-NMR (300 MHz, DMSO-d_6)

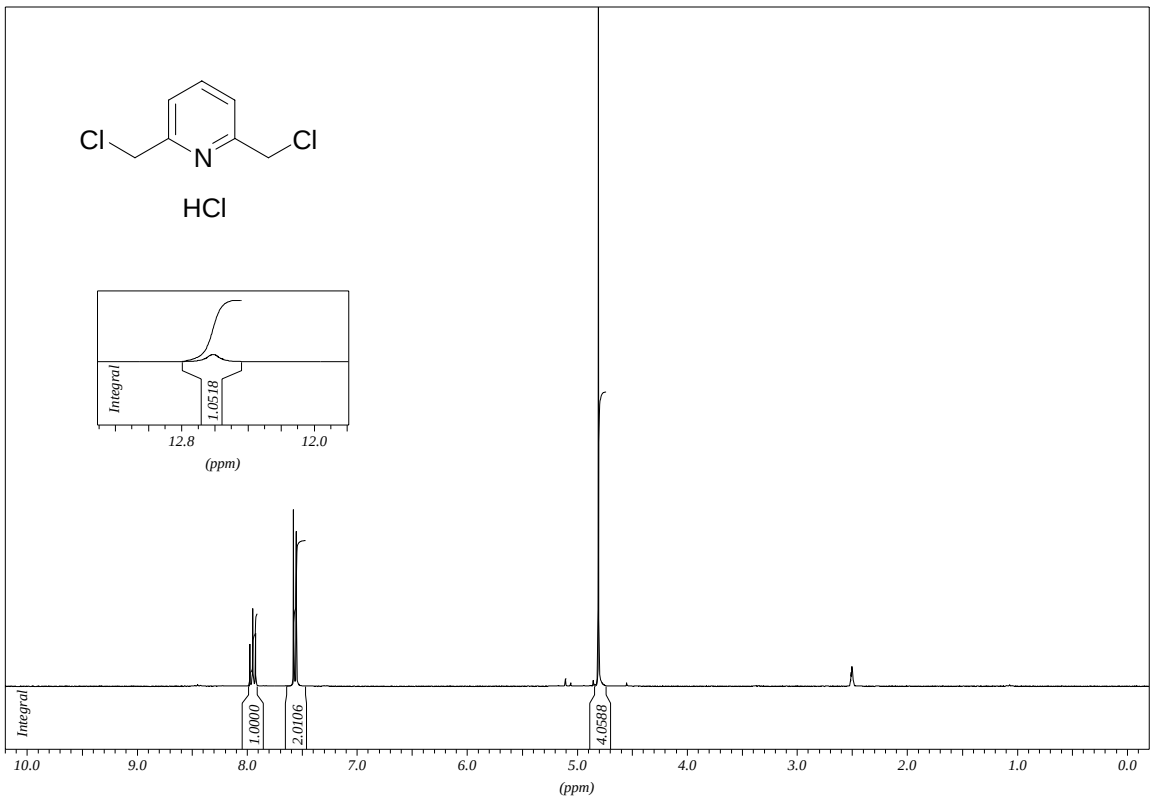

^{13}C-NMR (75.5 MHz, DMSO-d_6)

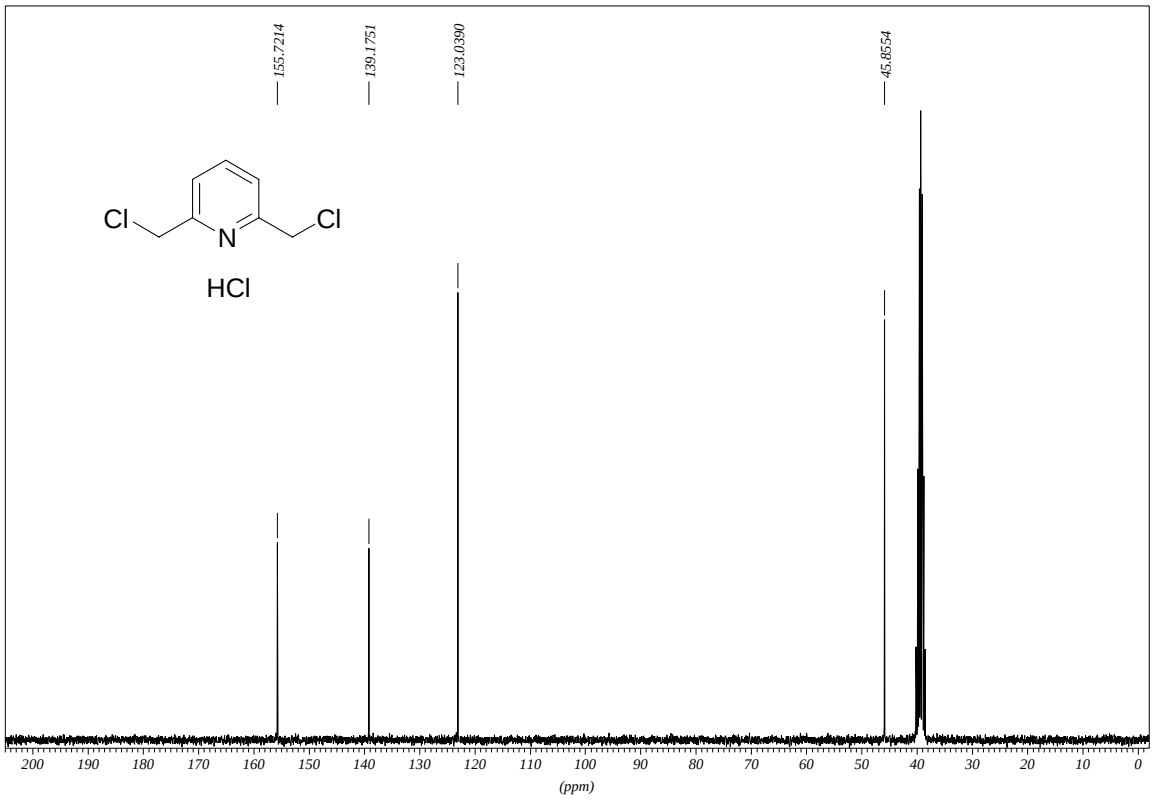

2,6-Bis(chloromethyl)pyridine (8)

^{1}H-NMR (300 MHz, $CDCl_3$)

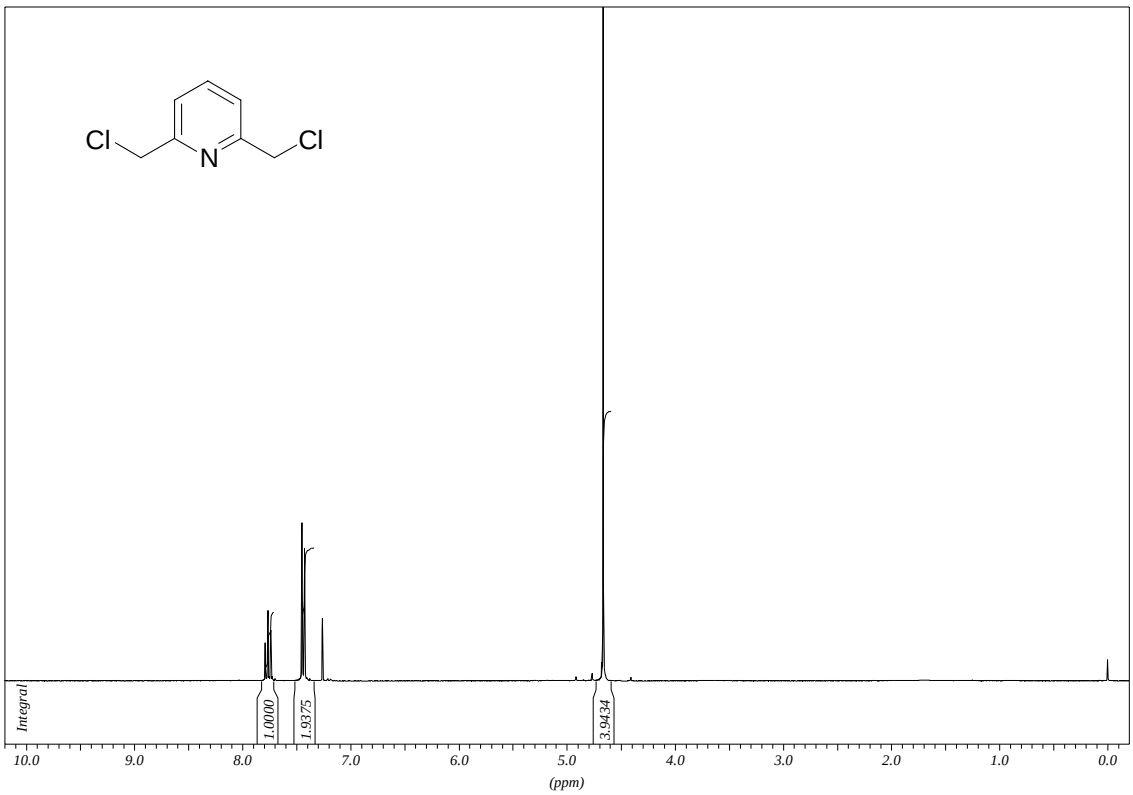

^{13}C-NMR (75.5 MHz, $CDCl_3$)

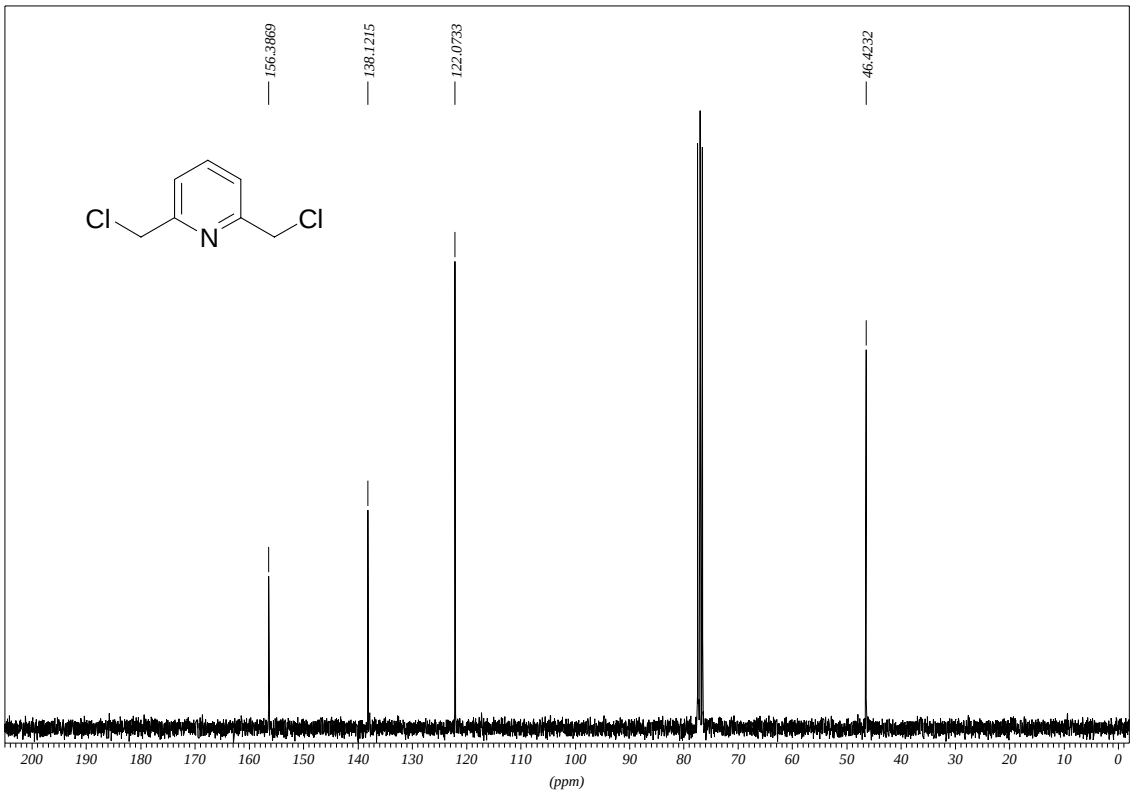

2,6-Bis(carbamimidoylsulfanylmethyl)pyridine Trihydrochloride

^{1}H-NMR (300 MHz, D_2O)

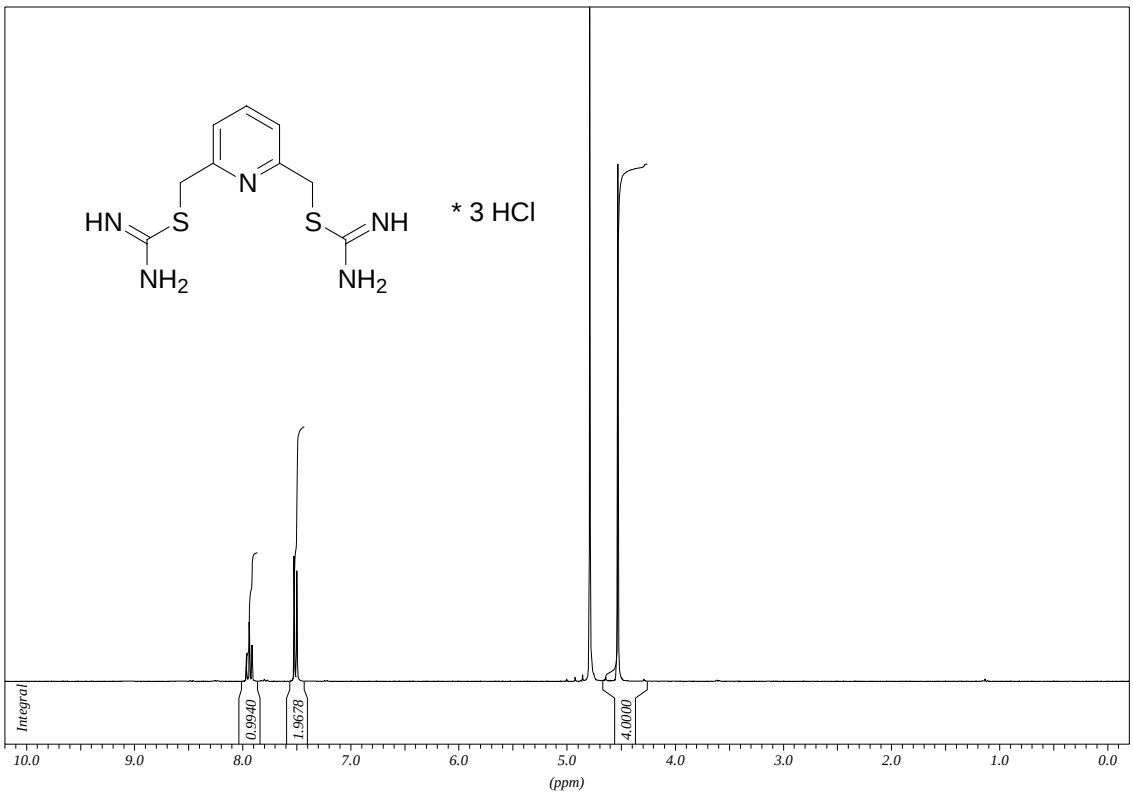

^{13}C-NMR (75.5 MHz, D_2O)

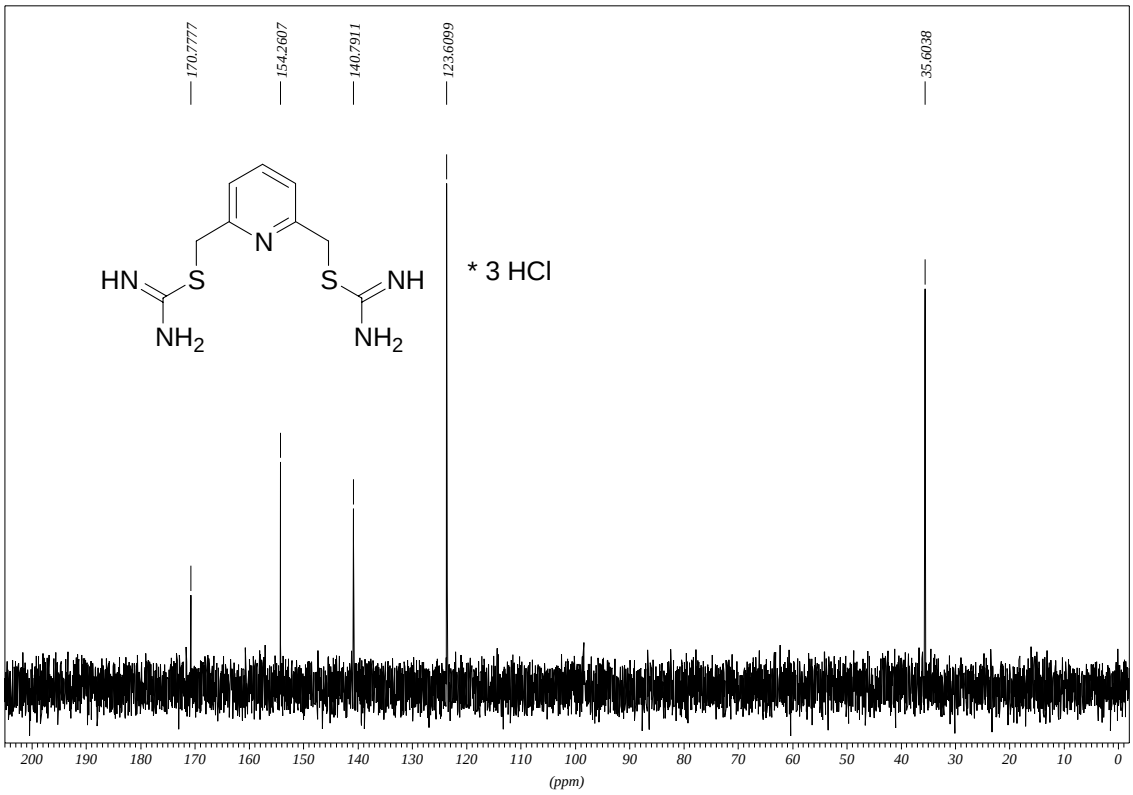

2,6-Bis(mercaptomethyl)pyridine (11)

^{1}H-NMR (300 MHz, $CDCl_3$)

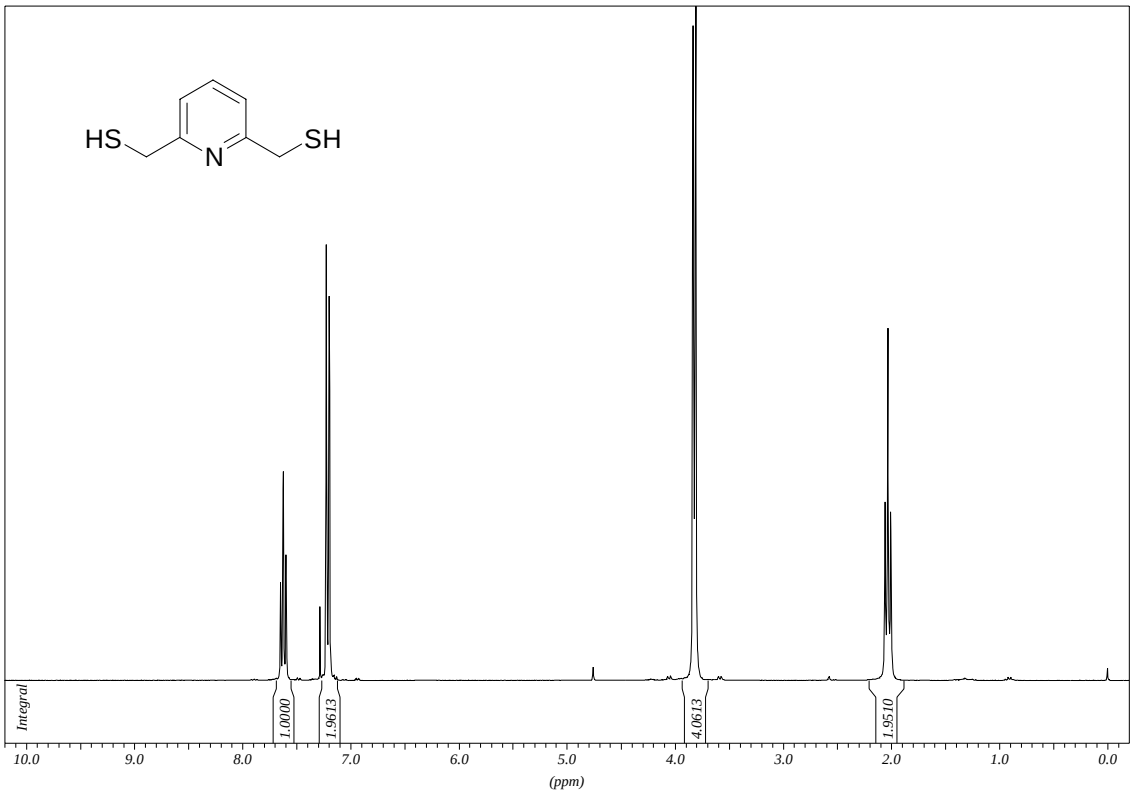

^{13}C-NMR (75.5 MHz, $CDCl_3$)

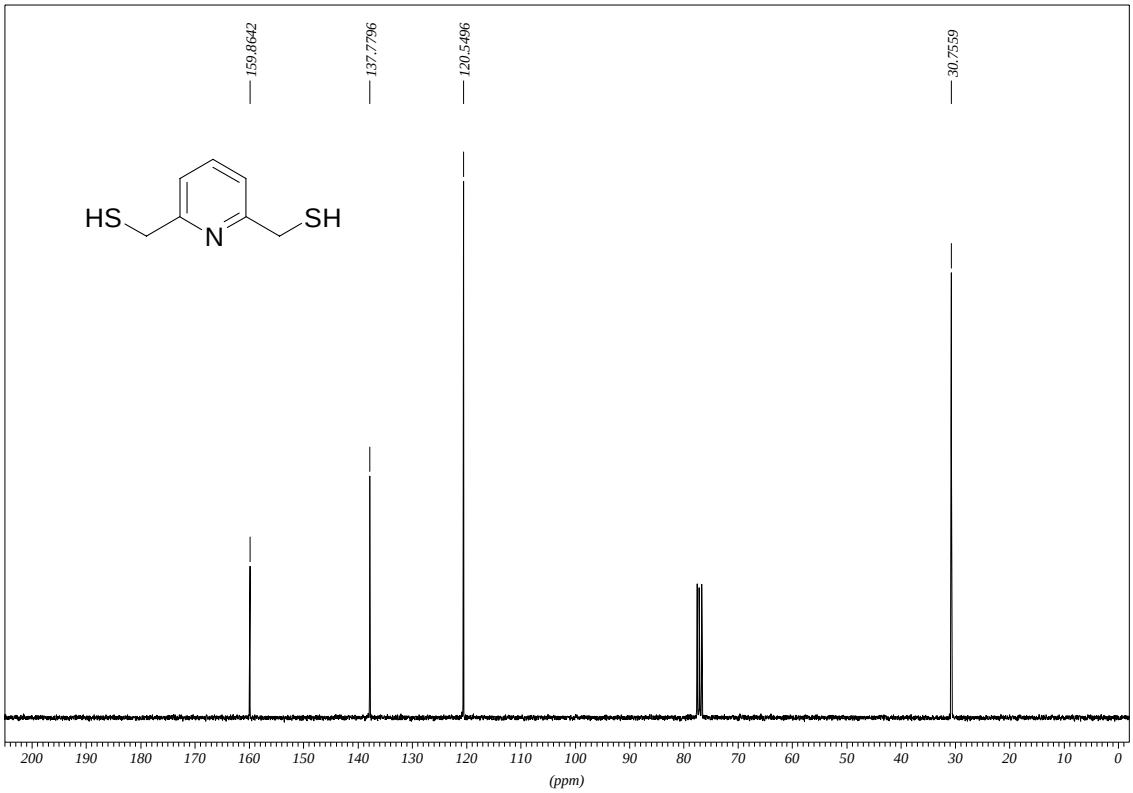

Ethyl benzimidate (6)

^{1}H-NMR (300 MHz, $CDCl_3$)

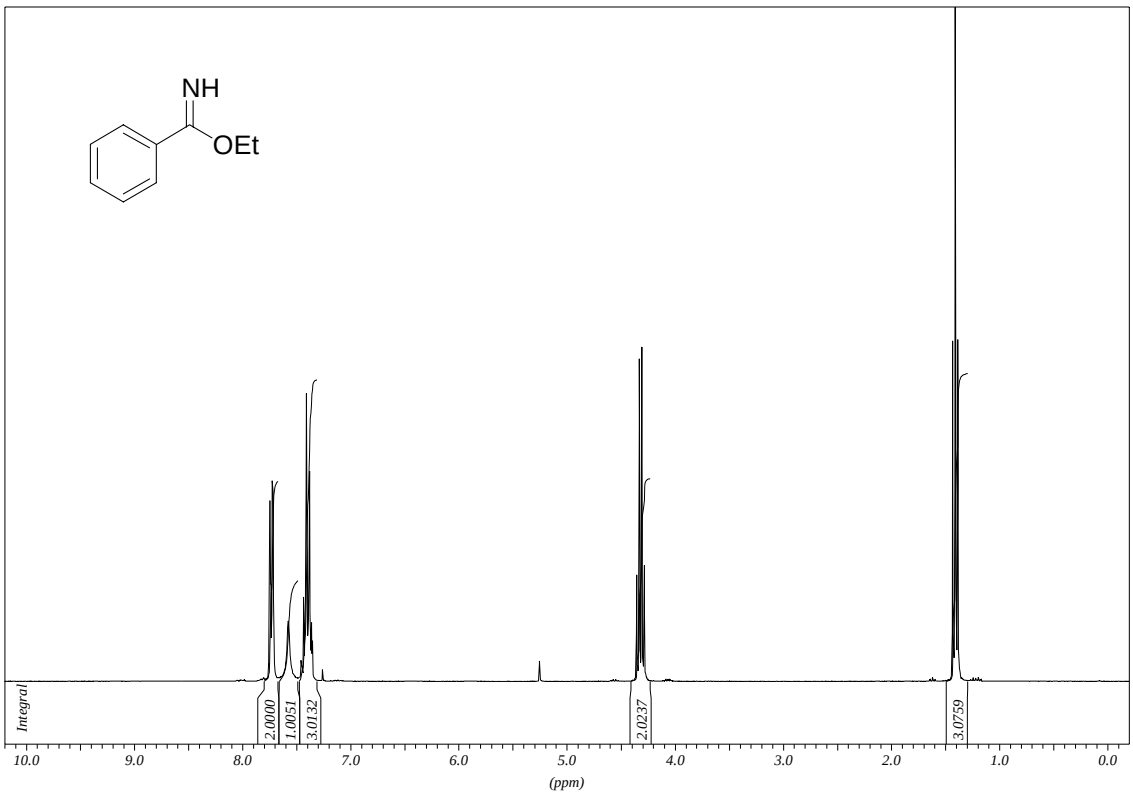

^{13}C-NMR (75.5 MHz, $CDCl_3$)

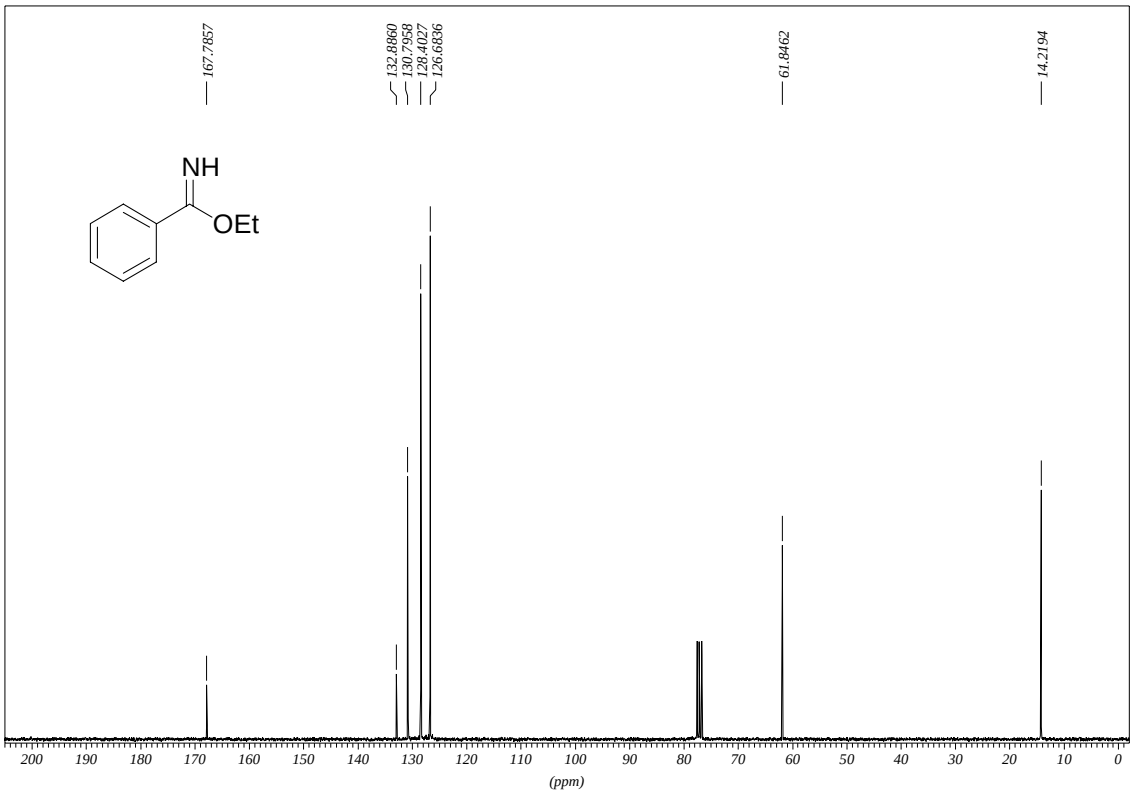

(*S*)-4-Methoxycarbonyl-2-phenyl-oxazoline (15)

^{1}H-NMR (300 MHz, $CDCl_3$)

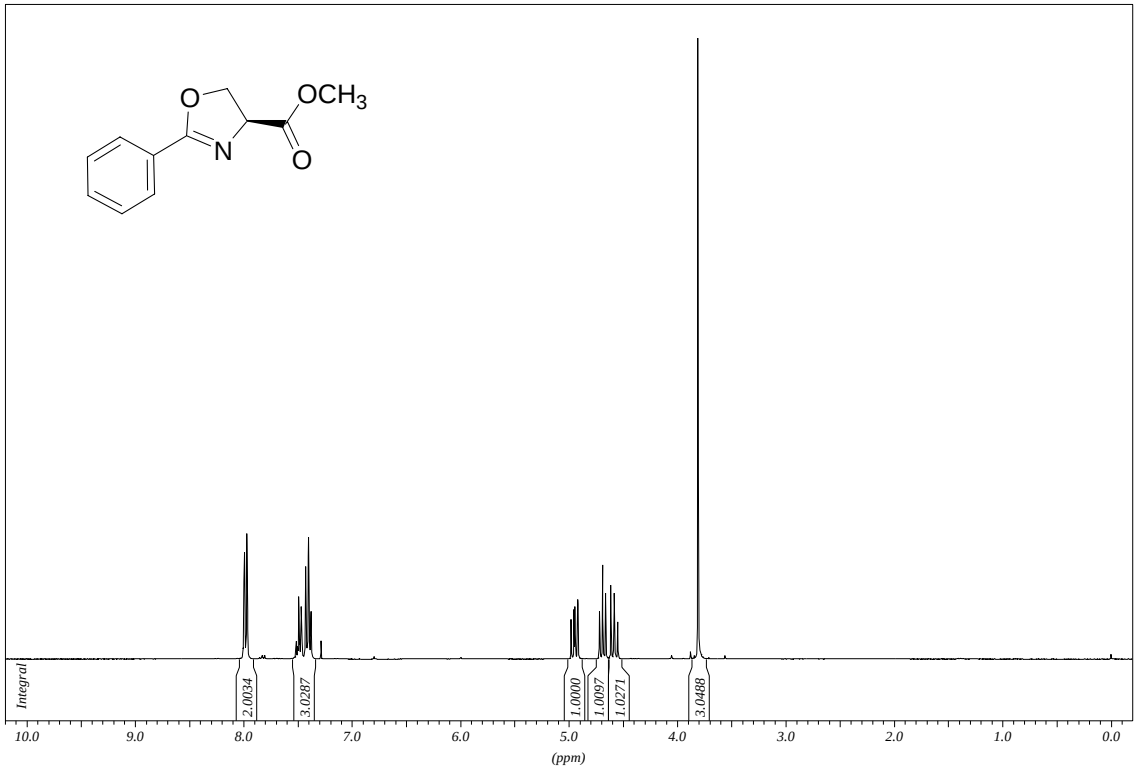

^{13}C-NMR (75.5 MHz, $CDCl_3$)

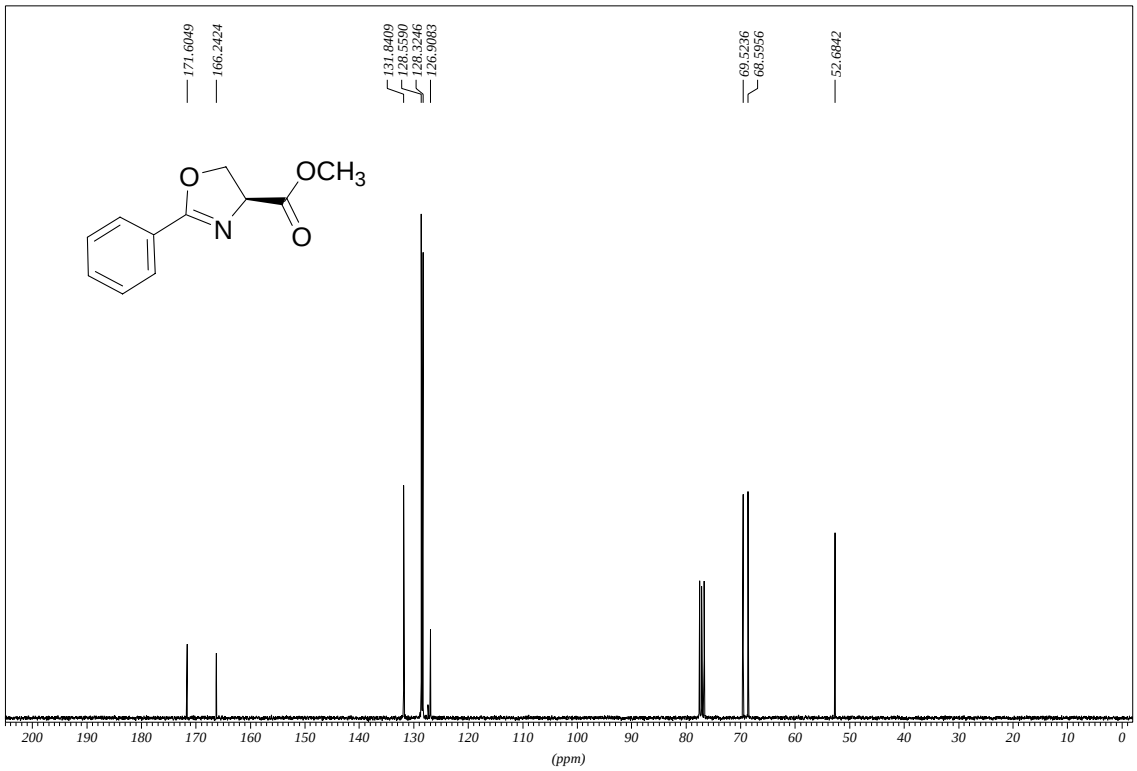

(*R*)-Hydroxymethyl-2-phenyl-oxazoline (4)

^{1}H-NMR (300 MHz, $CDCl_3$)

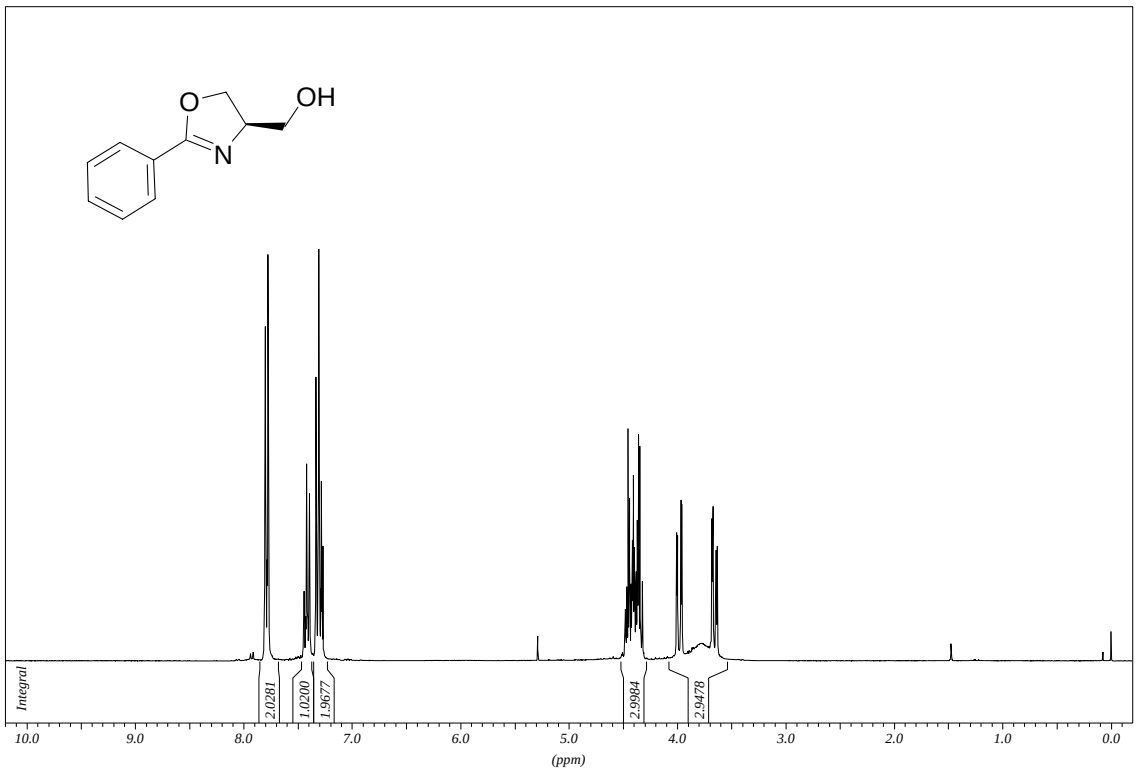

^{13}C-NMR (75.5 MHz, $CDCl_3$)

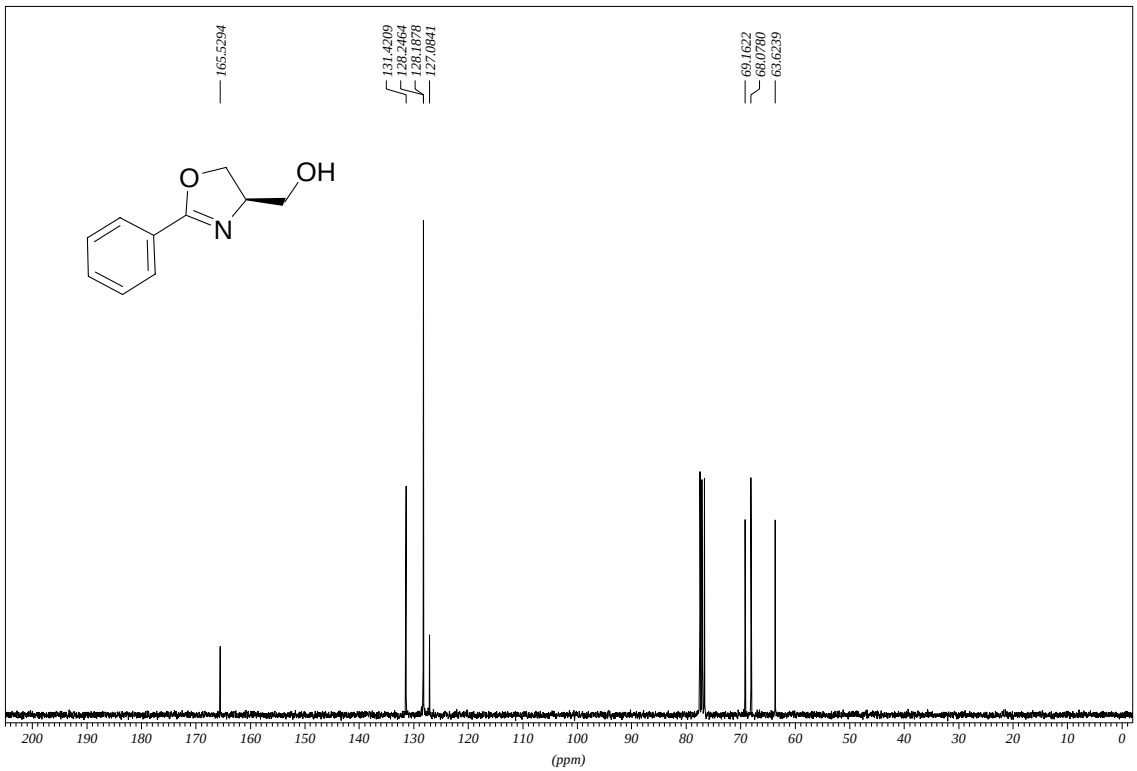

(*S*)-2-Phenyl-4-tosyloxymethyl-oxazoline (17)

^{1}H-NMR (300 MHz, $CDCl_3$)

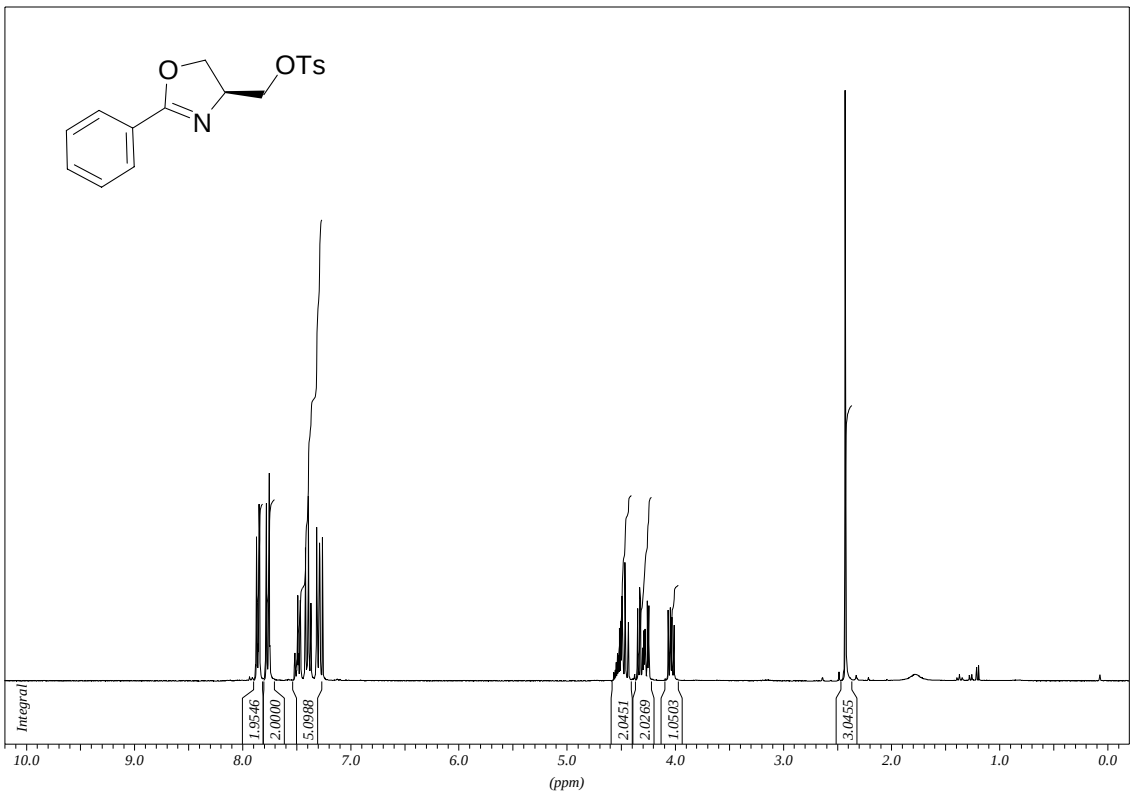

^{13}C-NMR (75.5 MHz, $CDCl_3$)

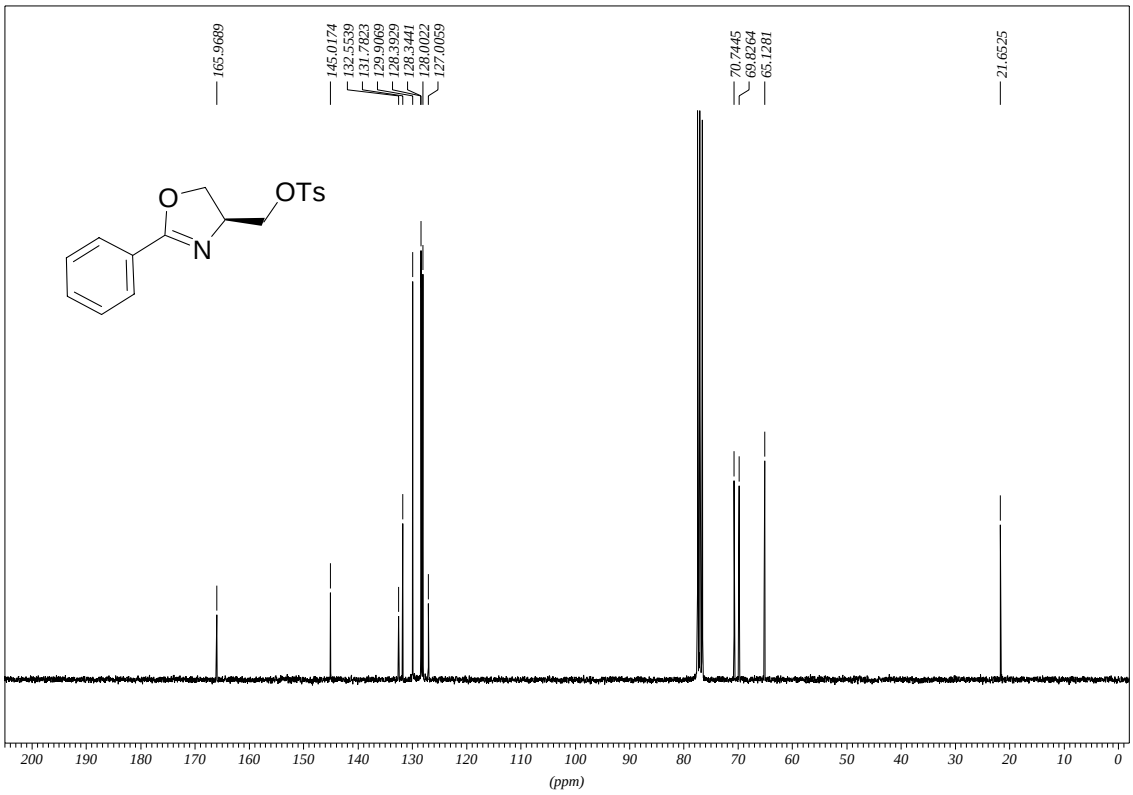

(*S*)-2-Phenyl-4-mesyloxymethyl-oxazoline (16)

^{1}H-NMR (300 MHz, $CDCl_3$)

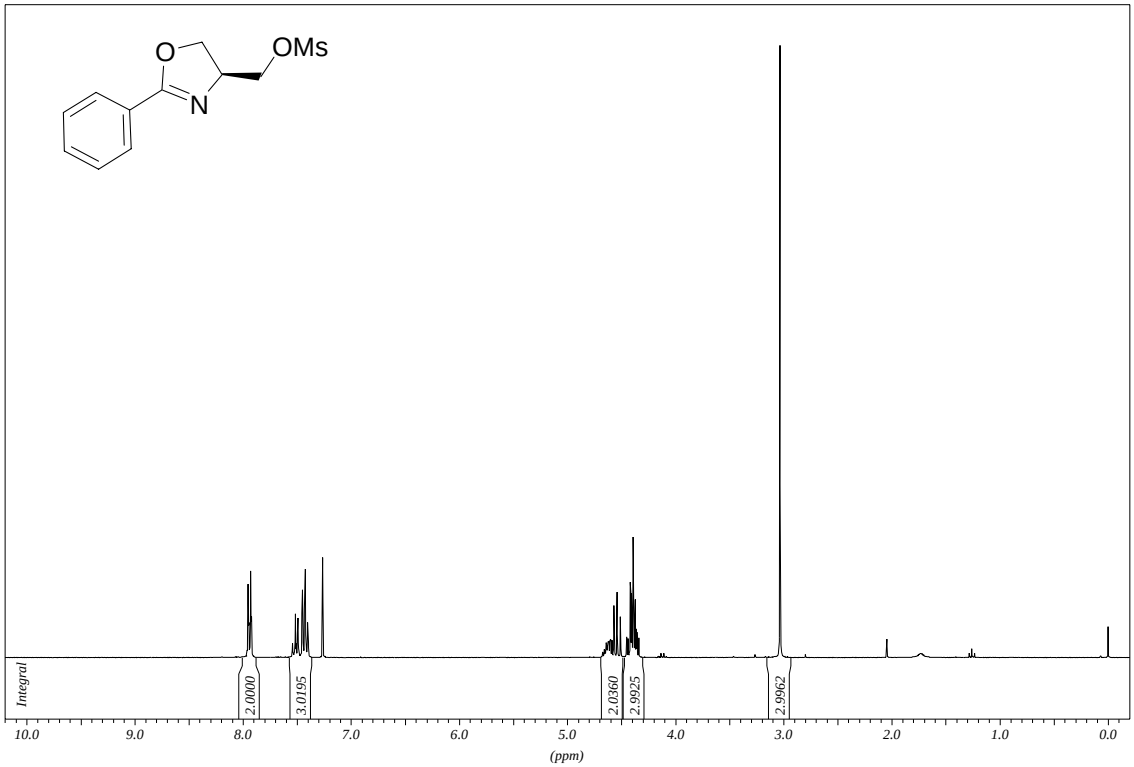

^{13}C-NMR (75.5 MHz, $CDCl_3$)

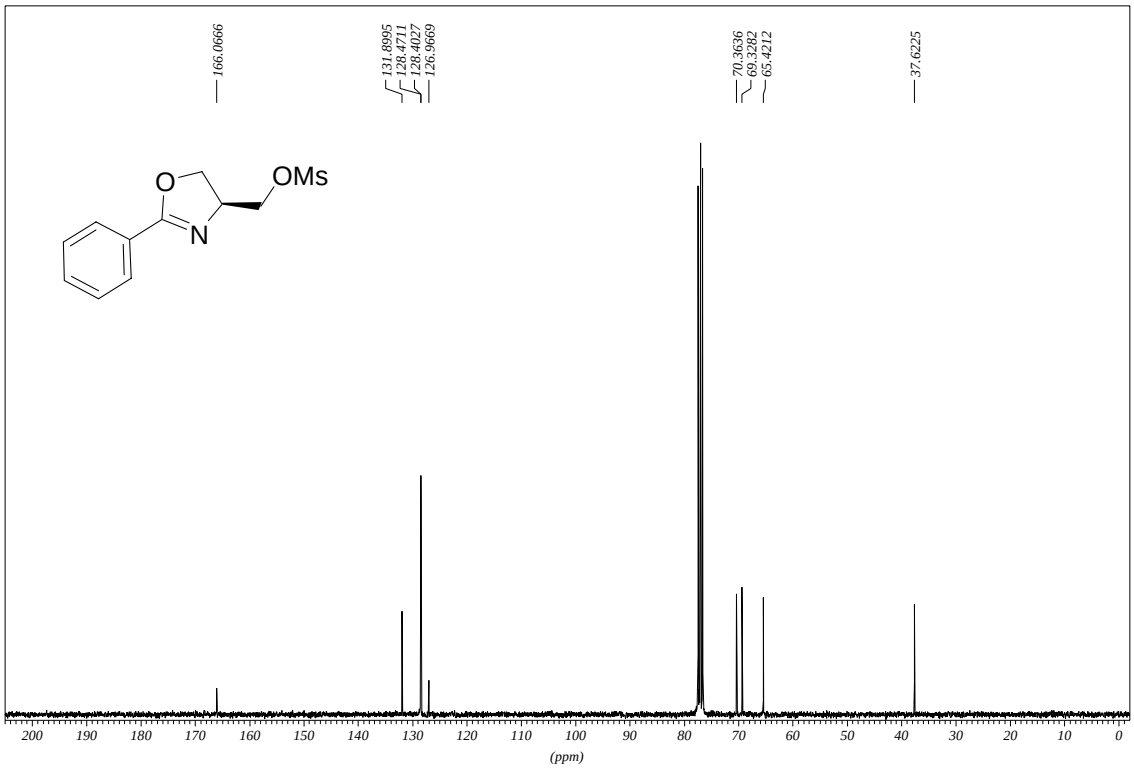

Pyridine-2,6-dicarbaldehyde (12)

^{1}H-NMR (300 MHz, $CDCl_3$)

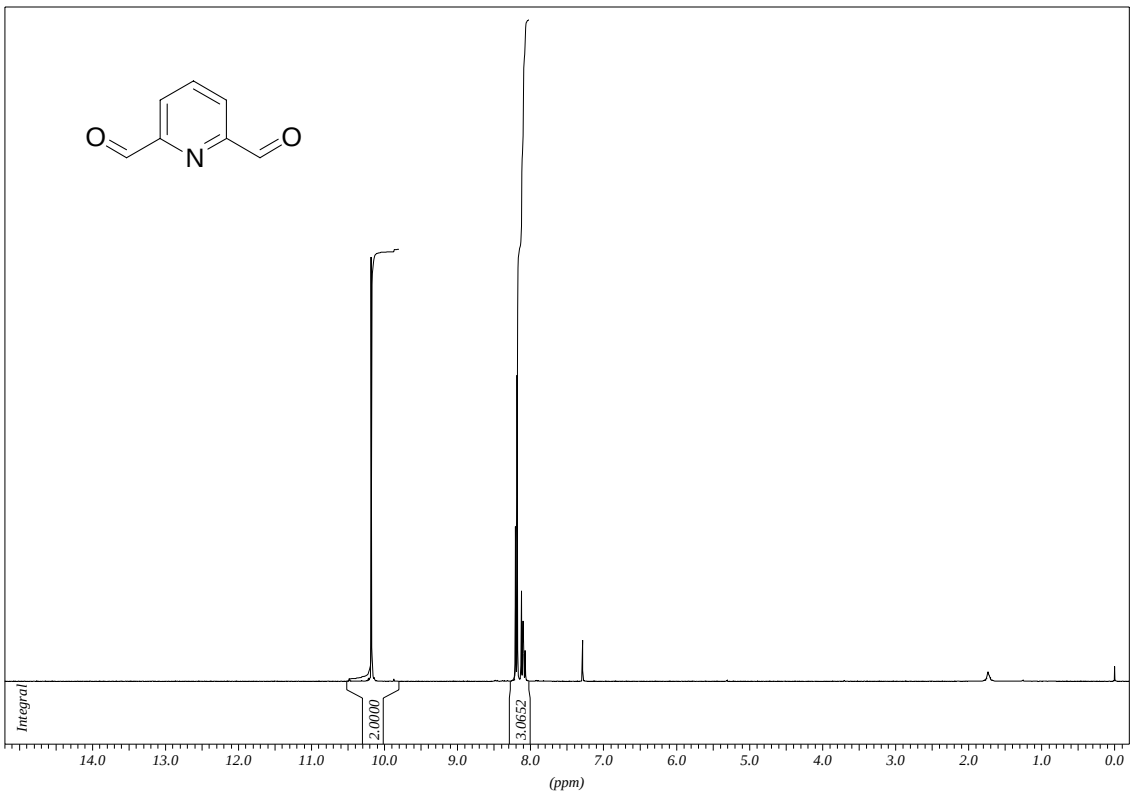

^{13}C-NMR (75.5 MHz, $CDCl_3$)

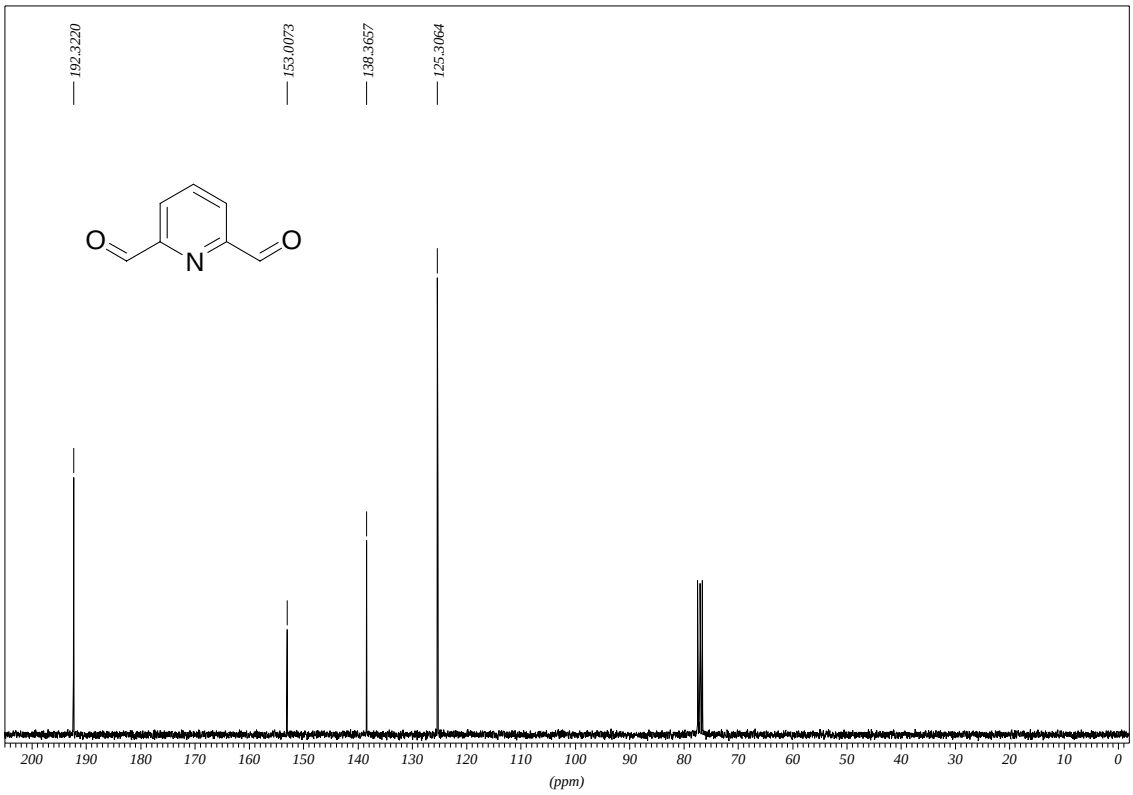

2,6-Bis(methyliminomethyl)pyridine (13)

^{1}H-NMR (300 MHz, $CDCl_3$)

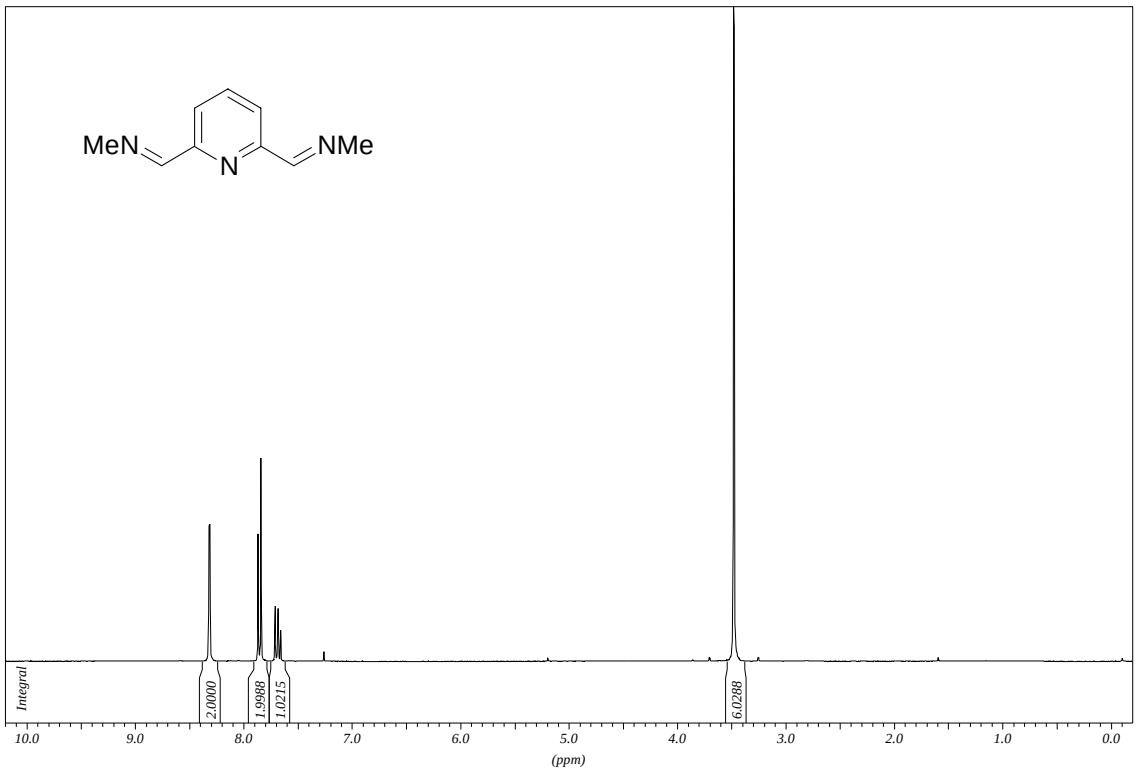

^{13}C-NMR (75.5 MHz, $CDCl_3$)

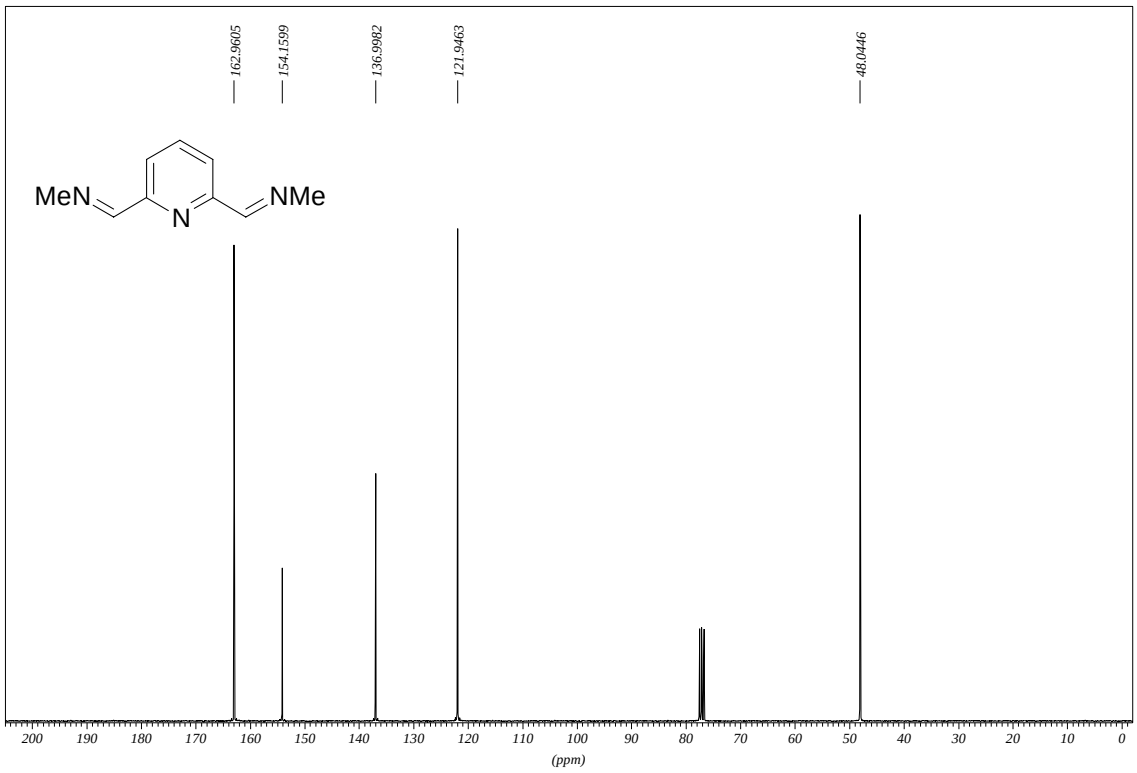

2,6-Bis(*N*-methylaminomethyl)pyridine (14)

^{1}H-NMR (300 MHz, $CDCl_3$)

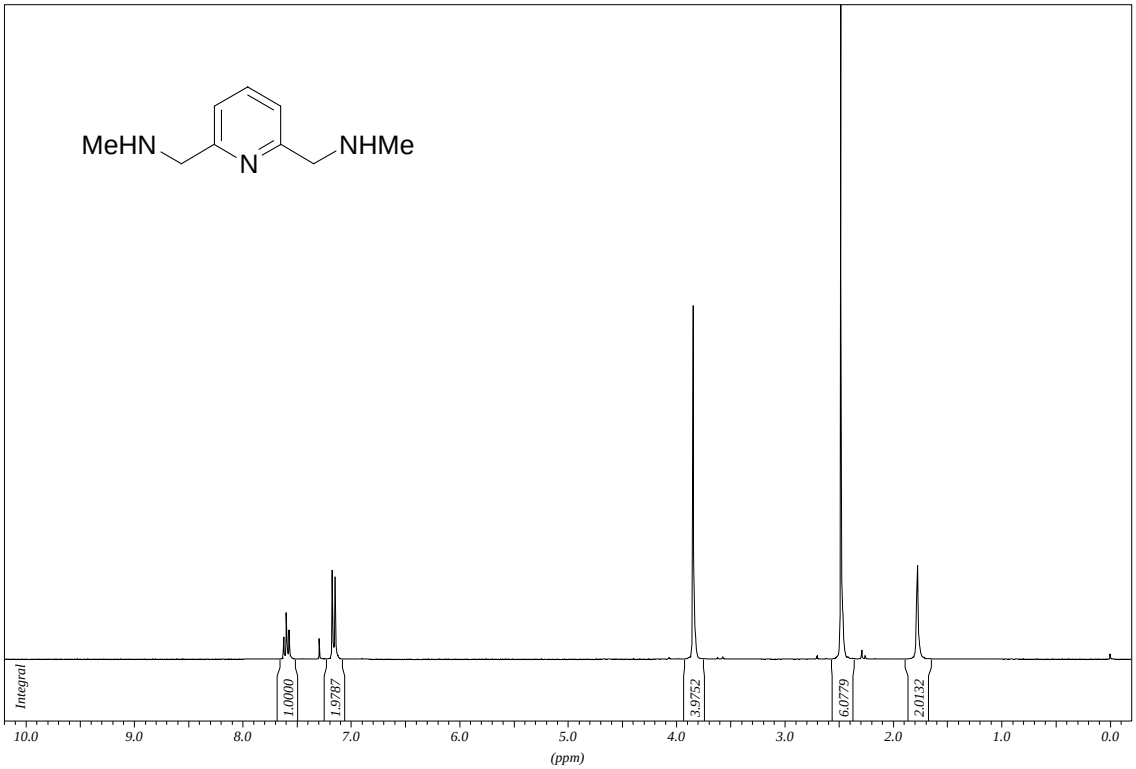

^{13}C-NMR (75.5 MHz, $CDCl_3$)

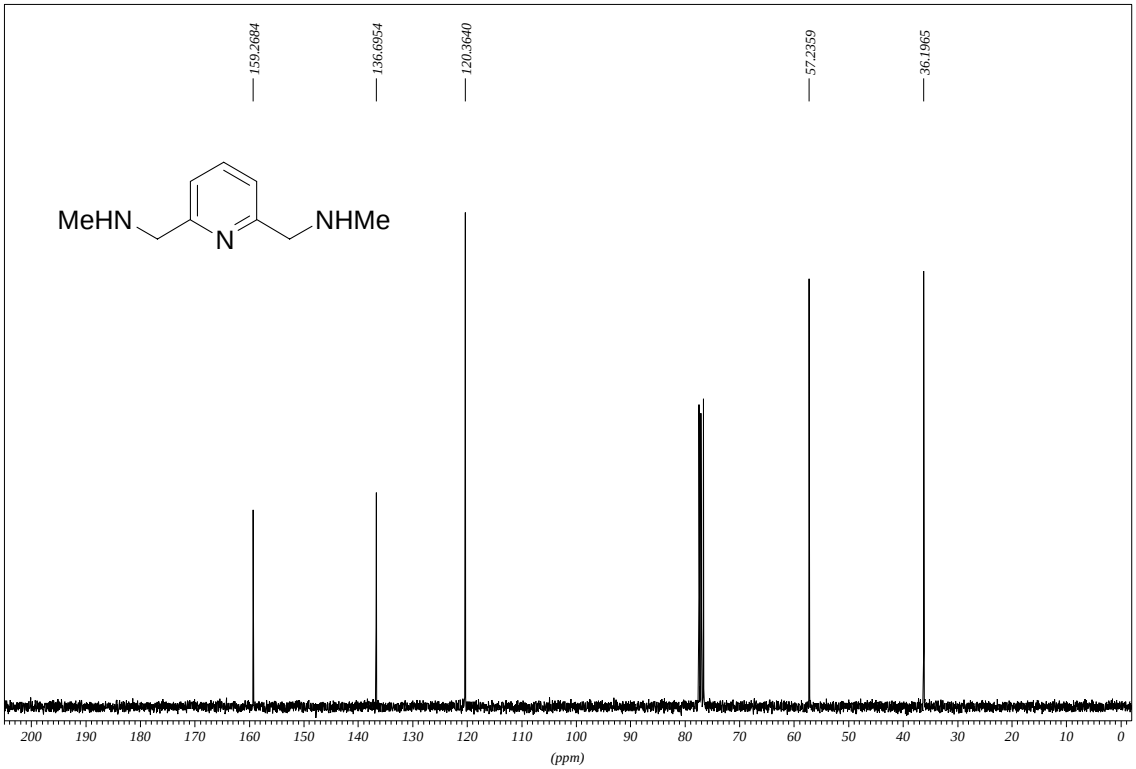

Ligand 2a

^{1}H-NMR (300 MHz, $CDCl_3$)

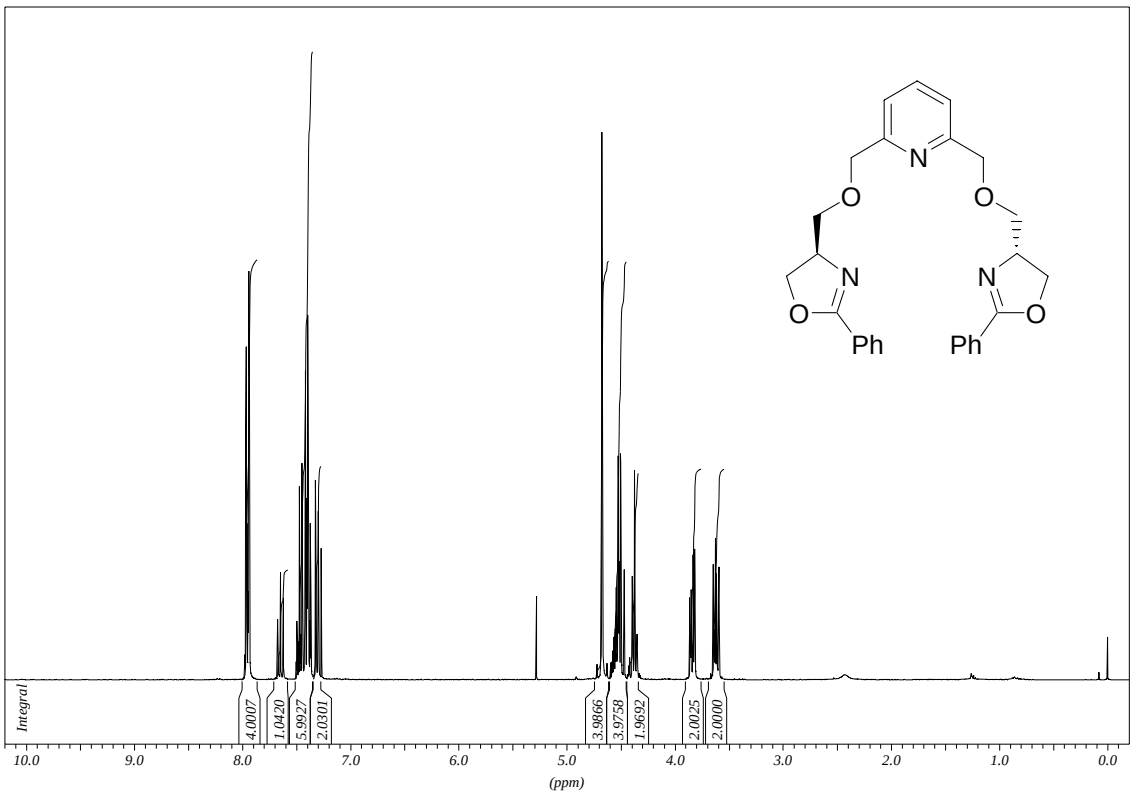

^{13}C-NMR (75.5 MHz, $CDCl_3$)

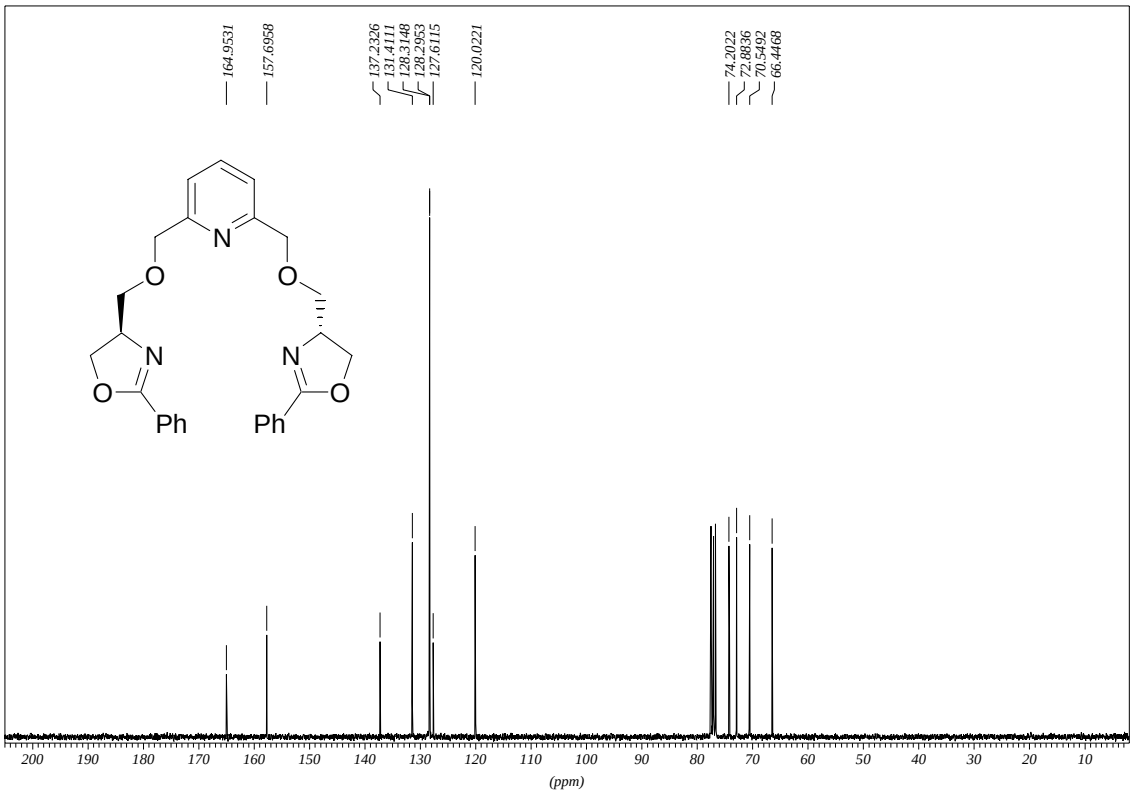

Ligand 2a

^{1}H-NMR (300 MHz, CD_3CN)

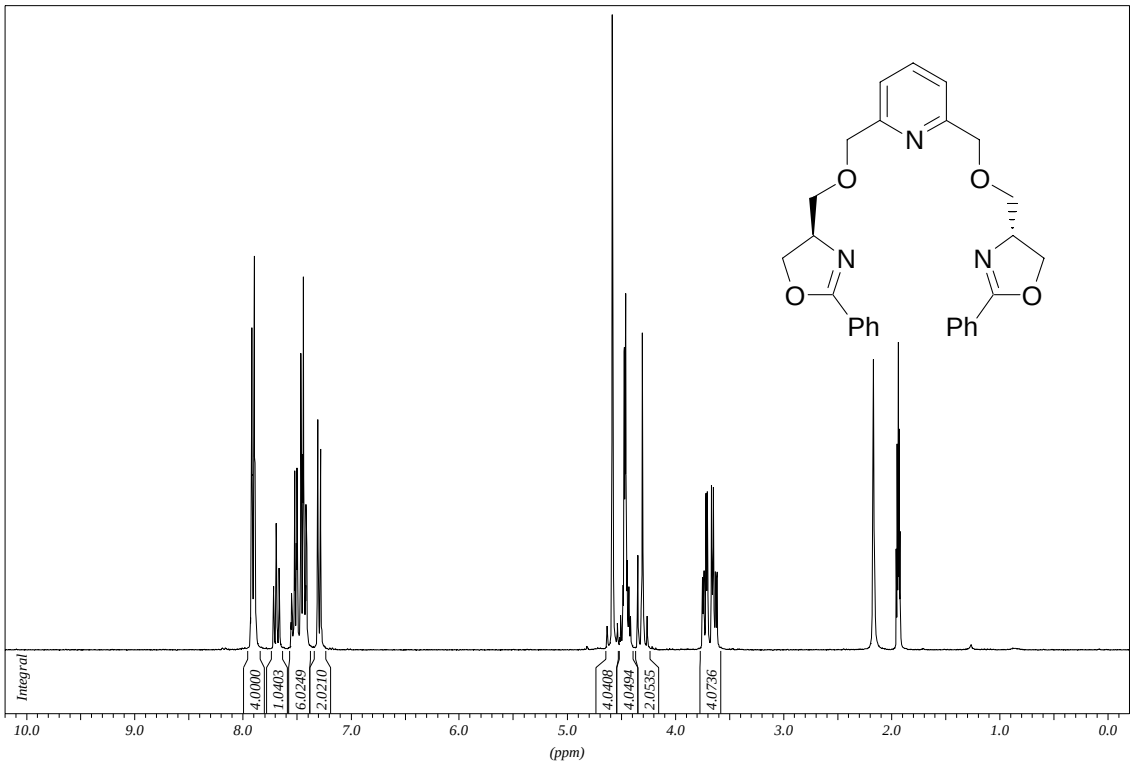

^{13}C-NMR (75.5 MHz, CD_3CN)

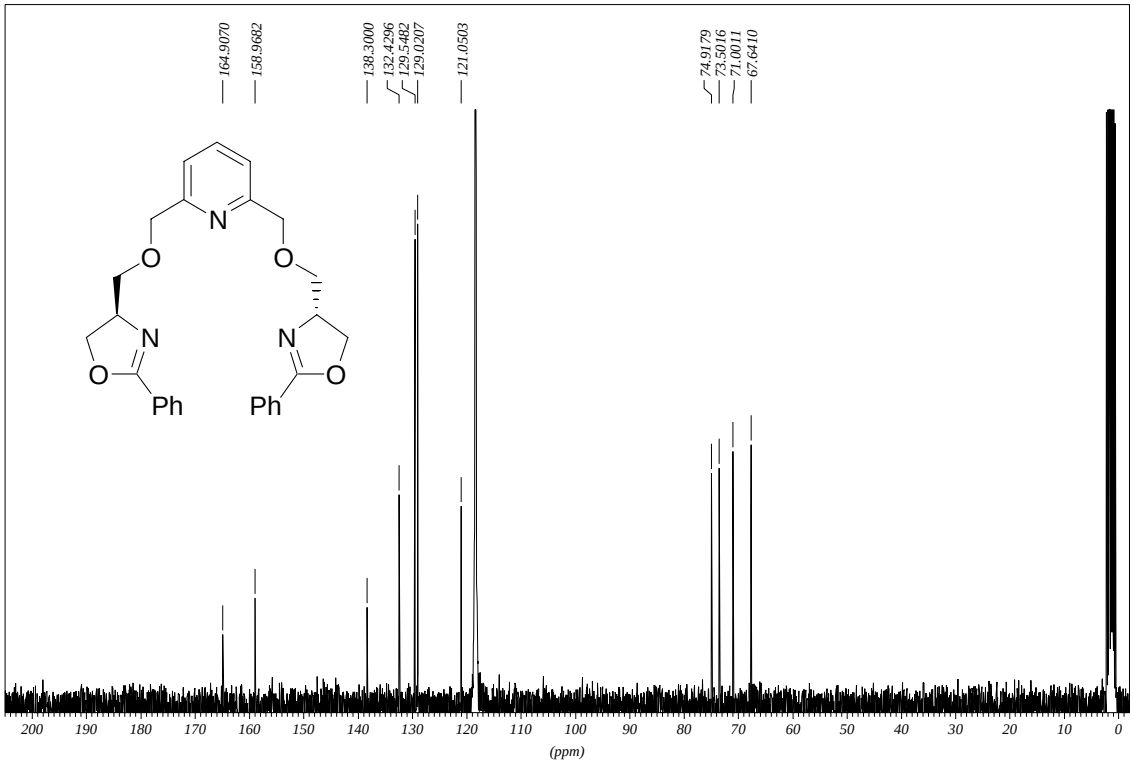

Ligand 2b

^{1}H-NMR (300 MHz, $CDCl_3$)

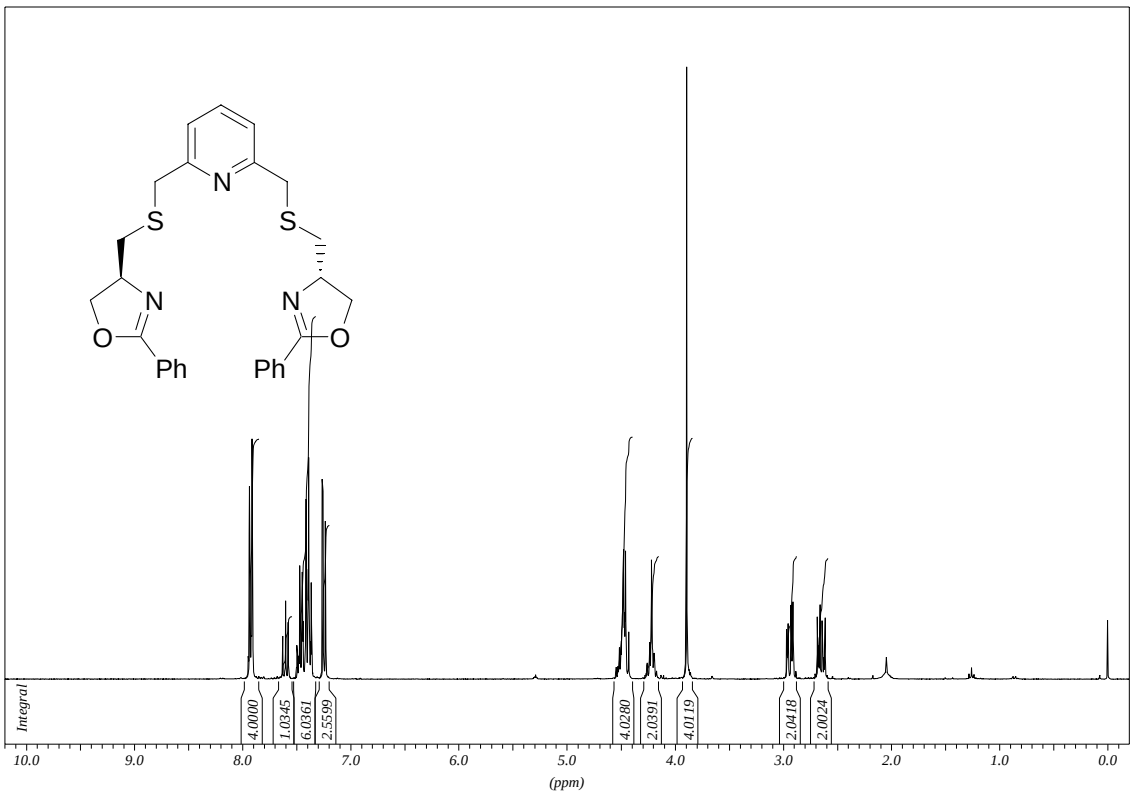

^{13}C-NMR (75.5 MHz, $CDCl_3$)

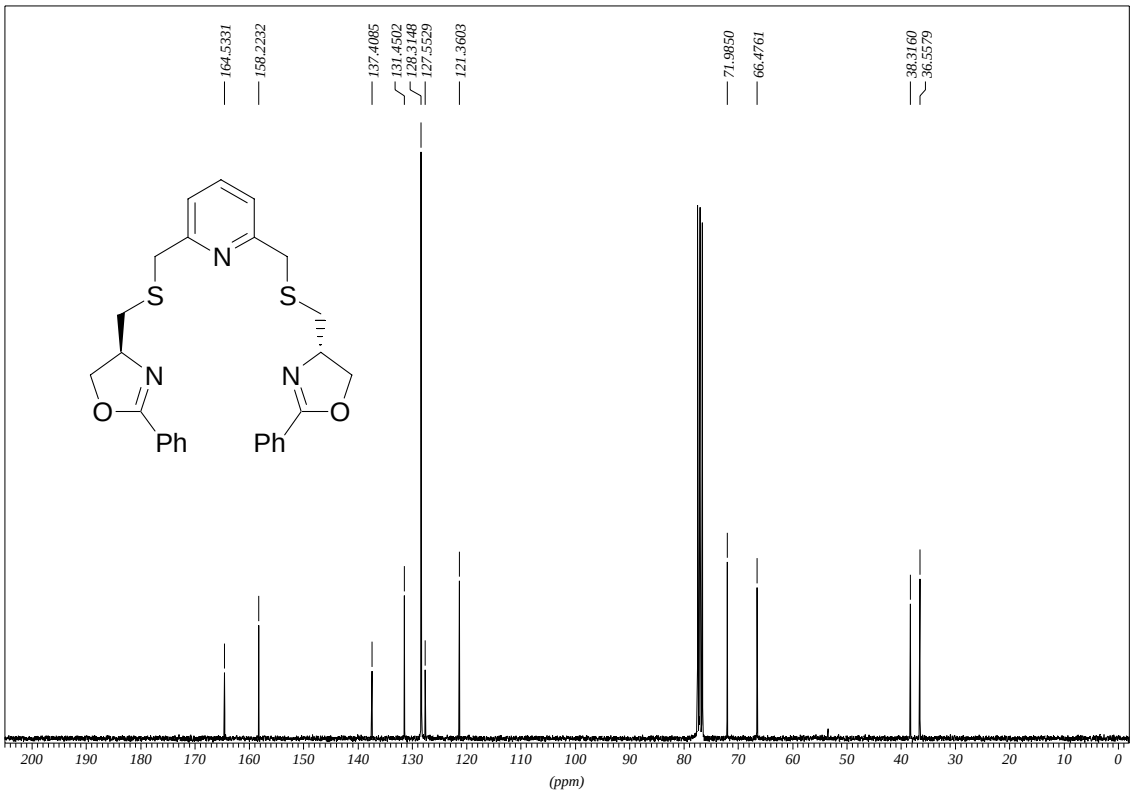

Ligand 2b

^{1}H-NMR (300 MHz, CD_3CN)

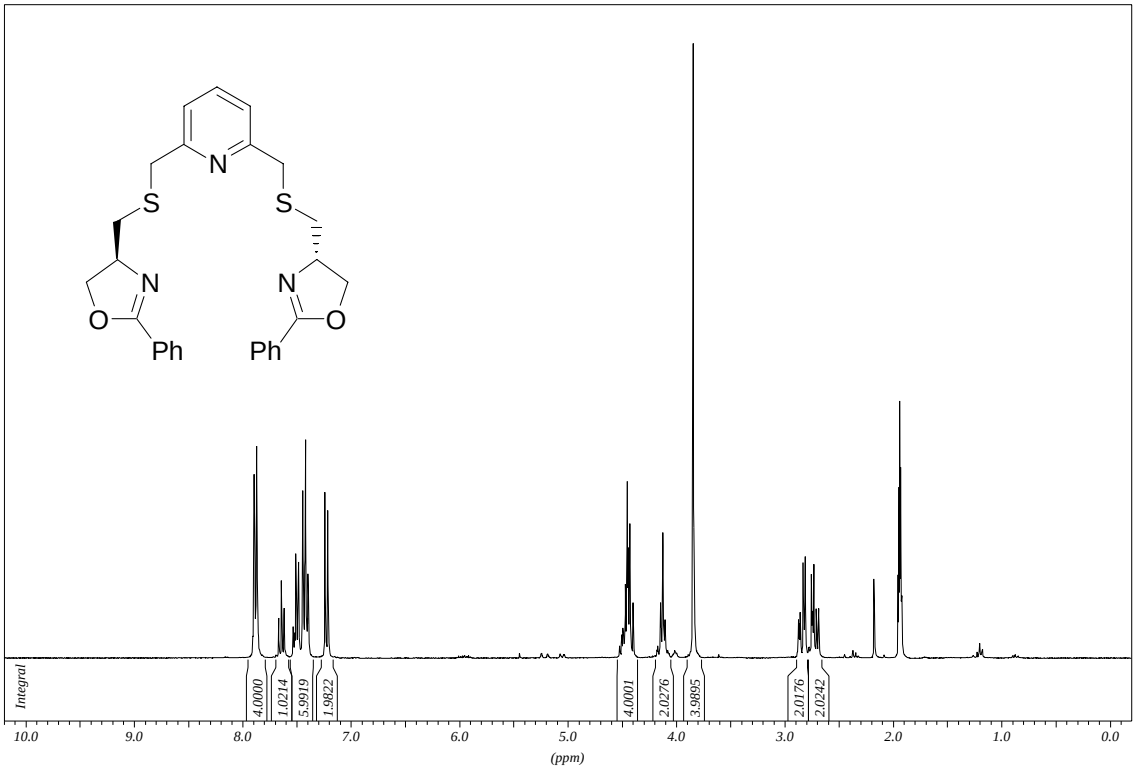

^{13}C-NMR (75.5 MHz, CD_3CN)

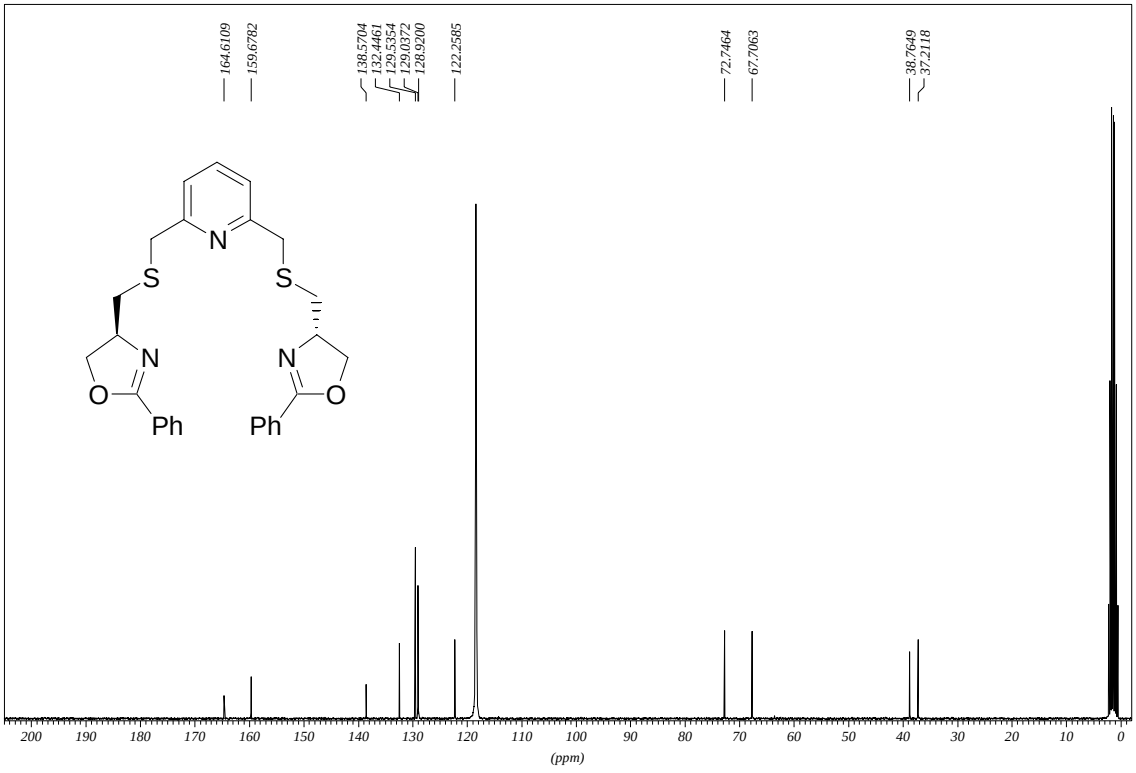

Ligand 2c

^{1}H-NMR (300 MHz, $CDCl_3$)

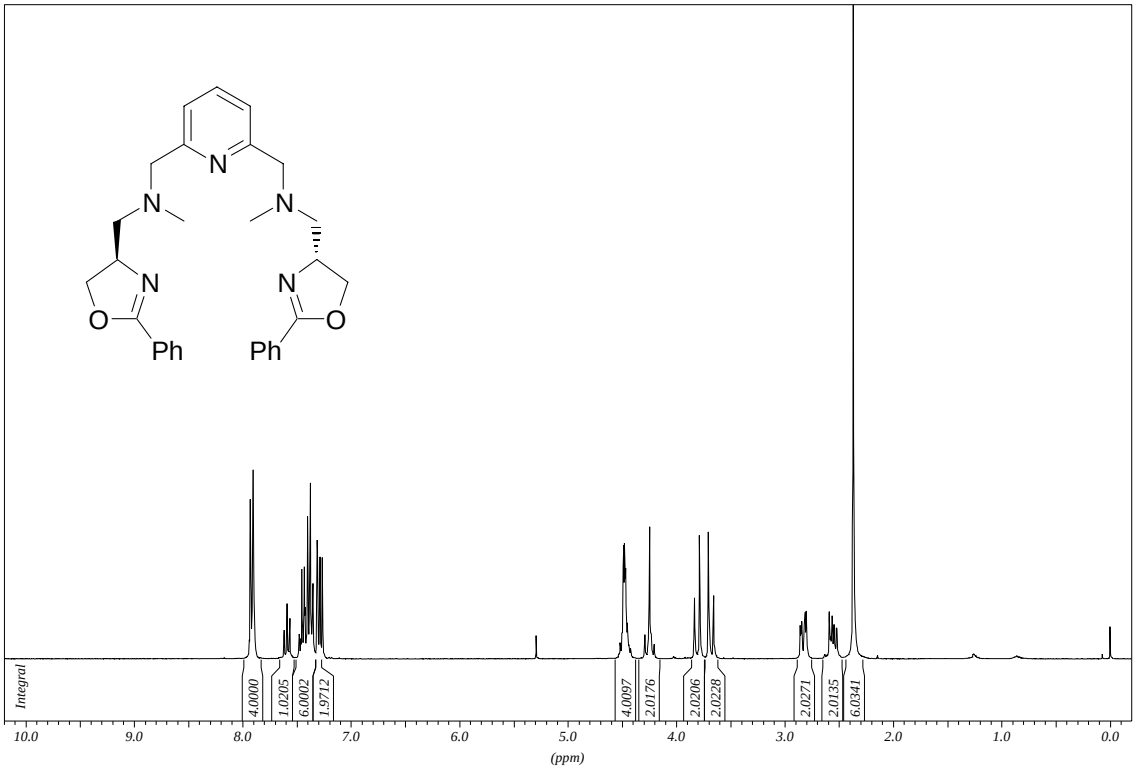

^{13}C-NMR (75.5 MHz, $CDCl_3$)

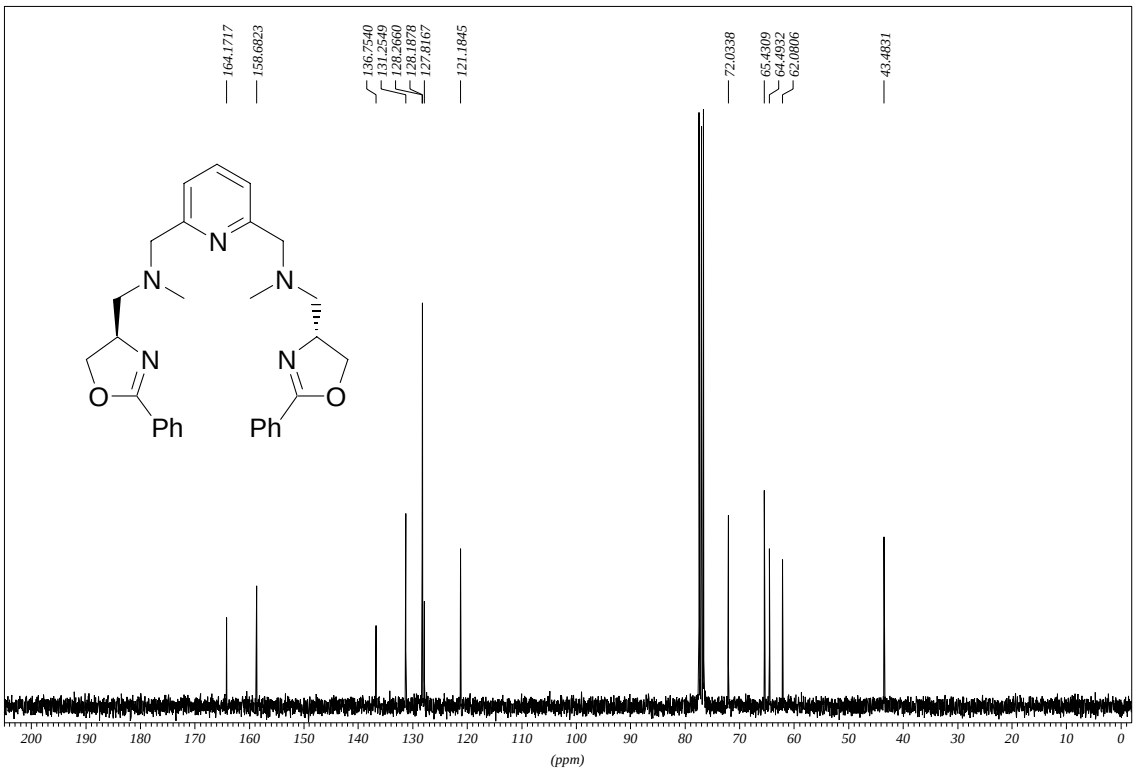

Ligand 2c

^{1}H-NMR (300 MHz, CD_3CN)

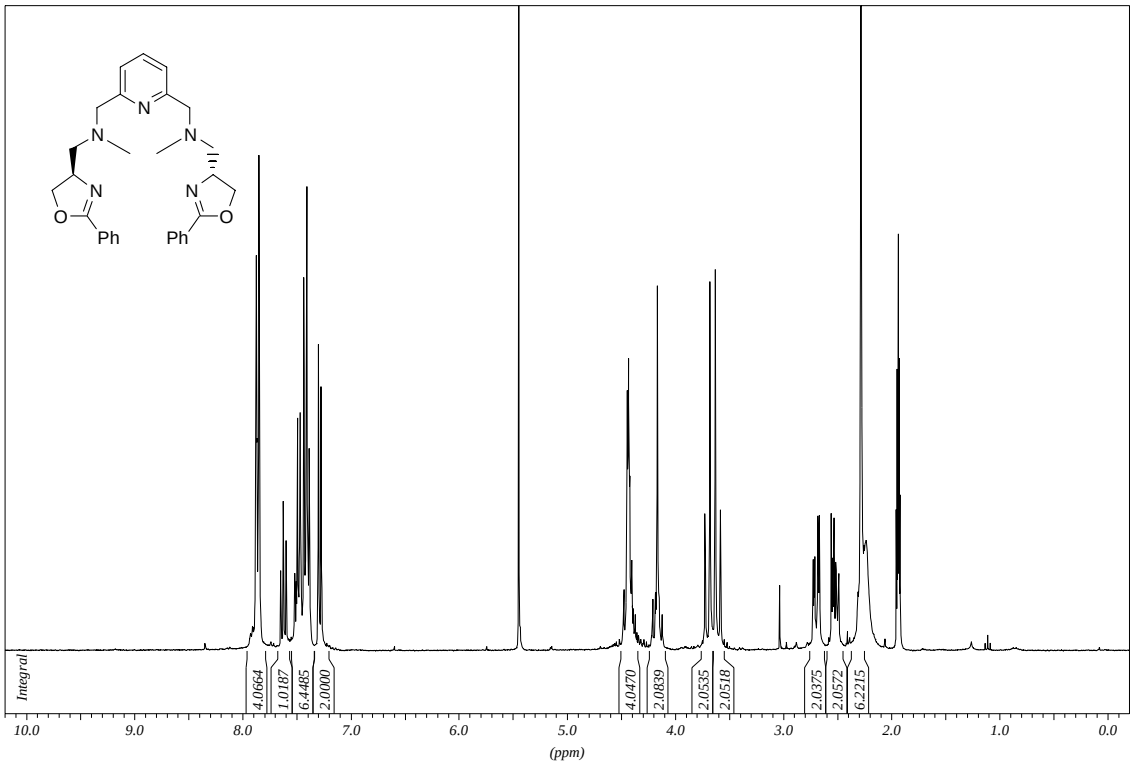

^{13}C-NMR (75.5 MHz, CD_3CN)

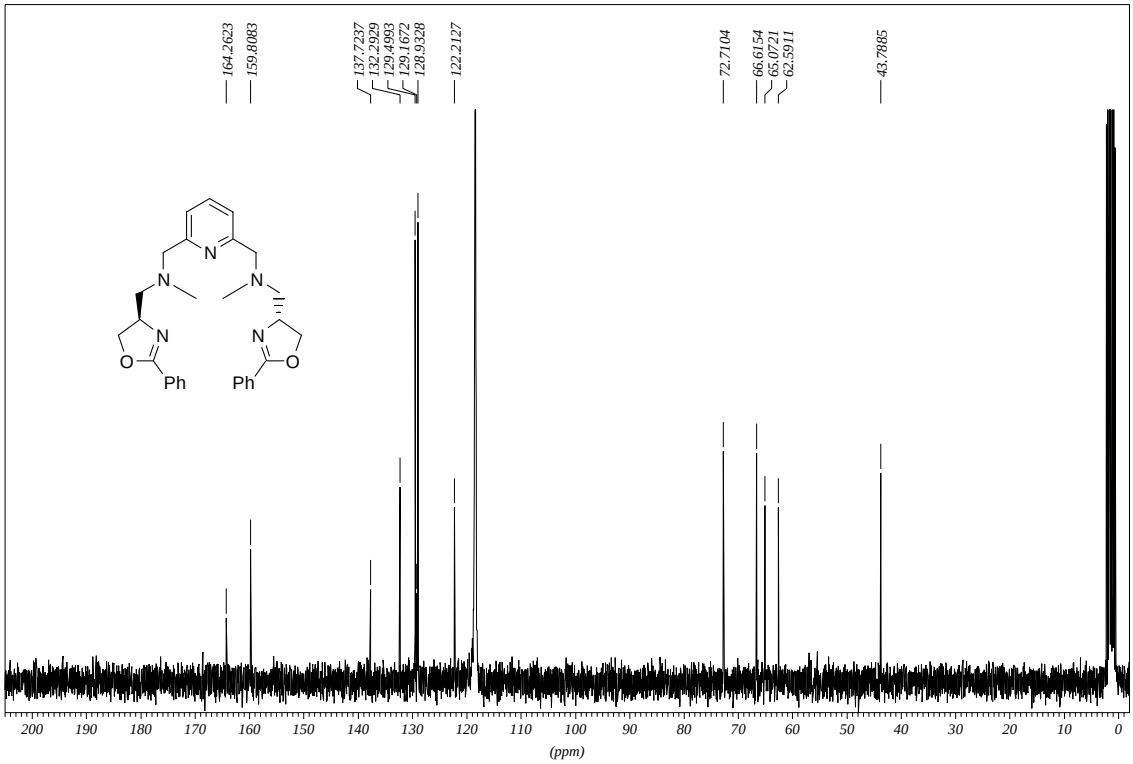

$[Cu^{I}(2a)(?)](ClO_4)$

^{1}H-NMR(300 MHz, $CDCl_3$)

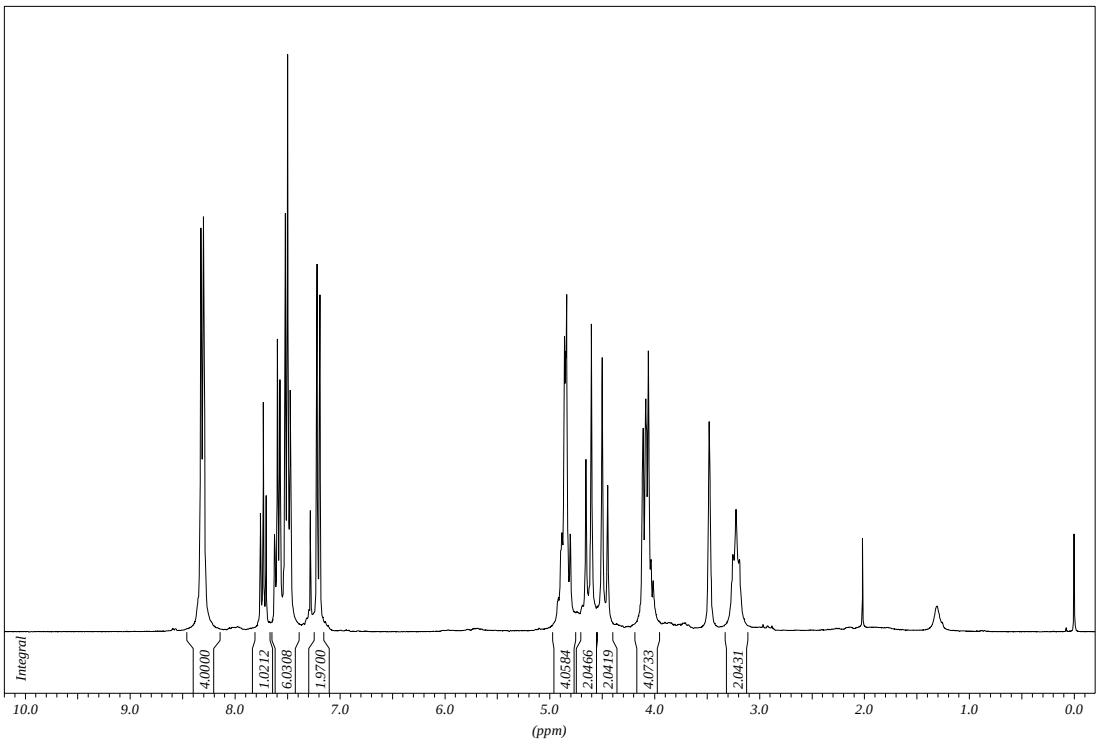

^{13}C-NMR (75.5 MHz, $CDCl_3$)

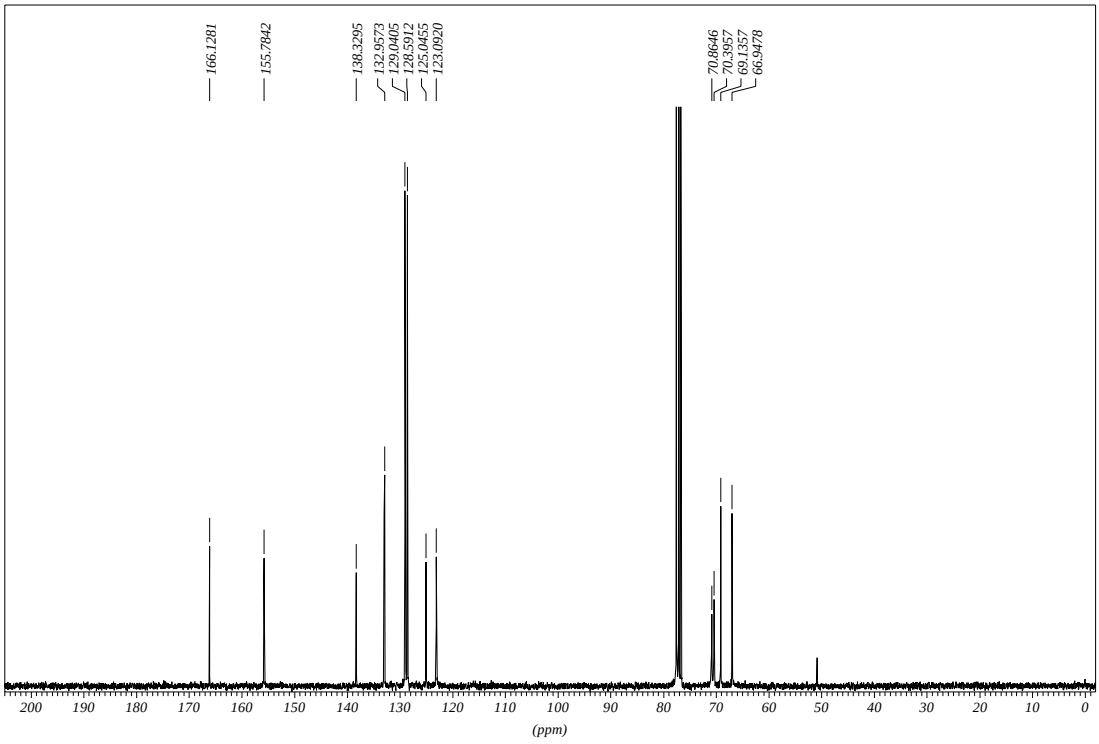

$[Cu^{I}(2b)(?)](ClO_4)$

^{1}H-NMR(300 MHz, $CDCl_3$)

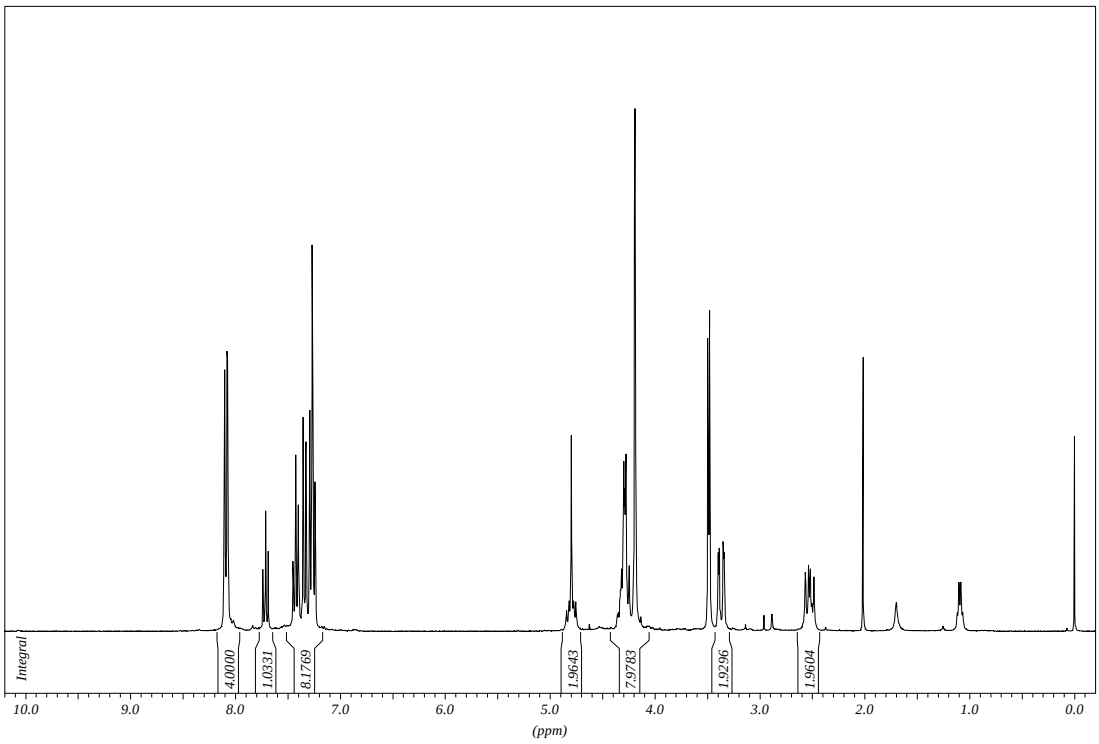

^{13}C-NMR (75.5 MHz, $CDCl_3$)

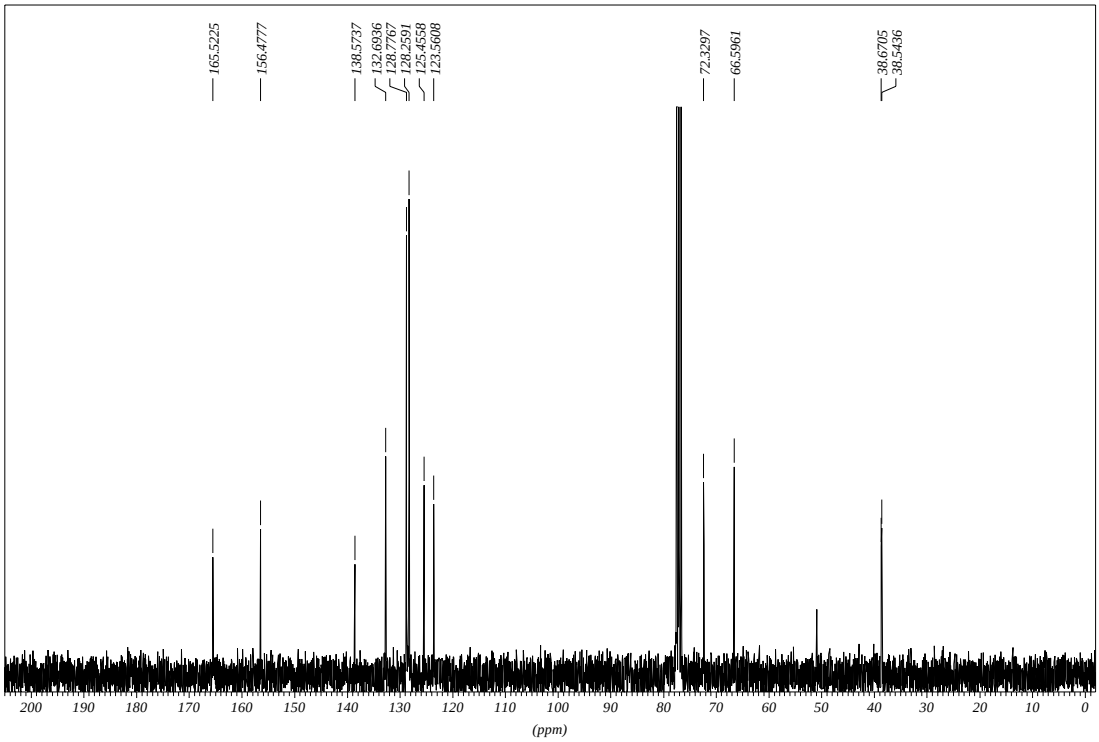

$[Zn^{II}(2a)](ClO_4)_2$

^{1}H-NMR (300 MHz, CD_3CN)

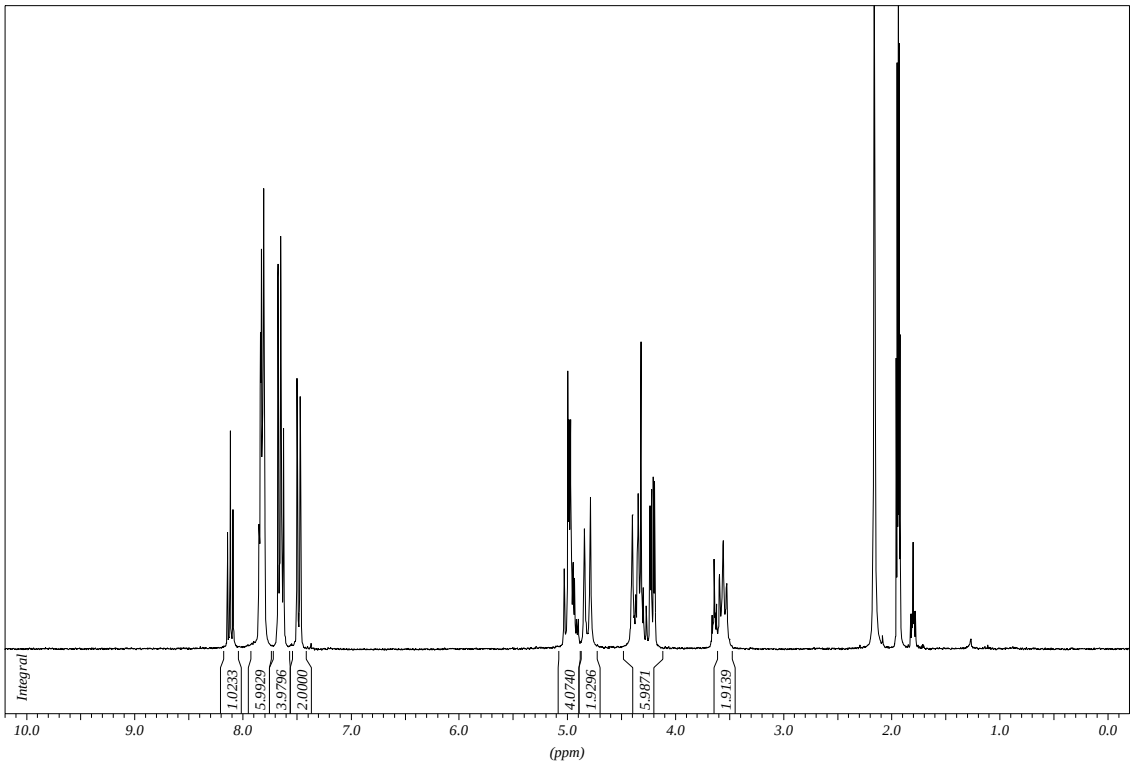

^{13}C-NMR (75.5 MHz, CD_3CN)

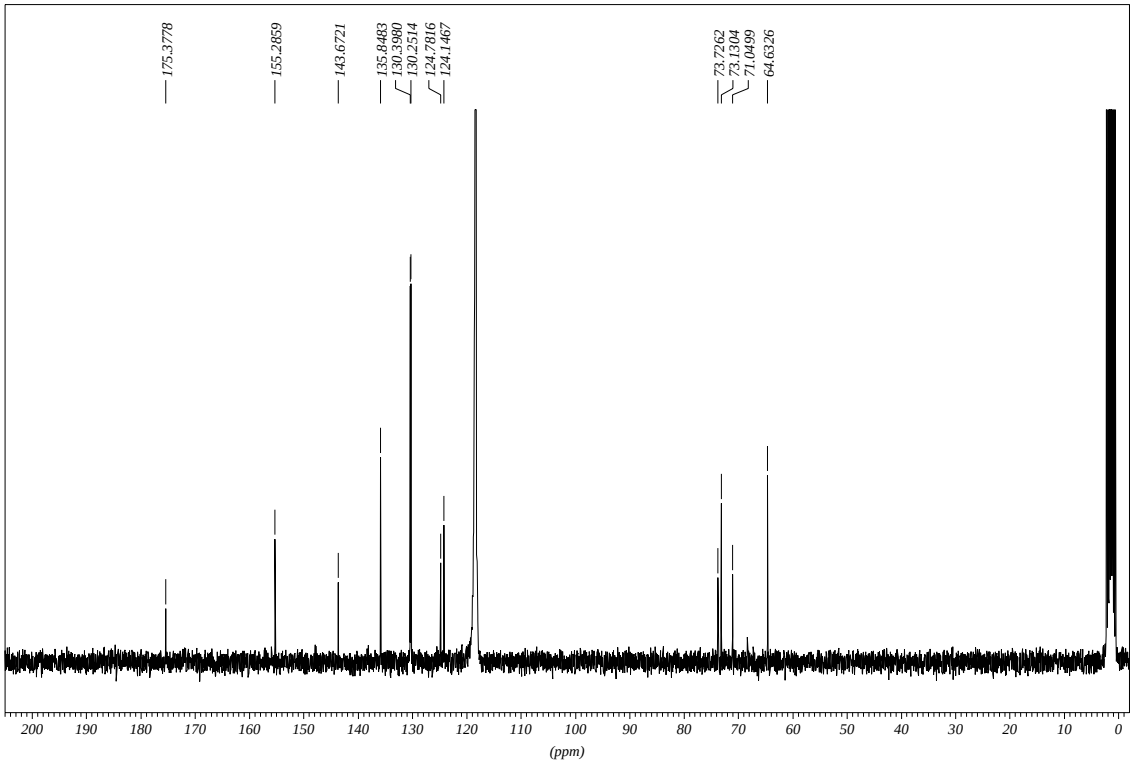

$[Zn^{II}(2b)](ClO_4)_2*H_2O$

^{1}H-NMR (300 MHz, CD_3CN)

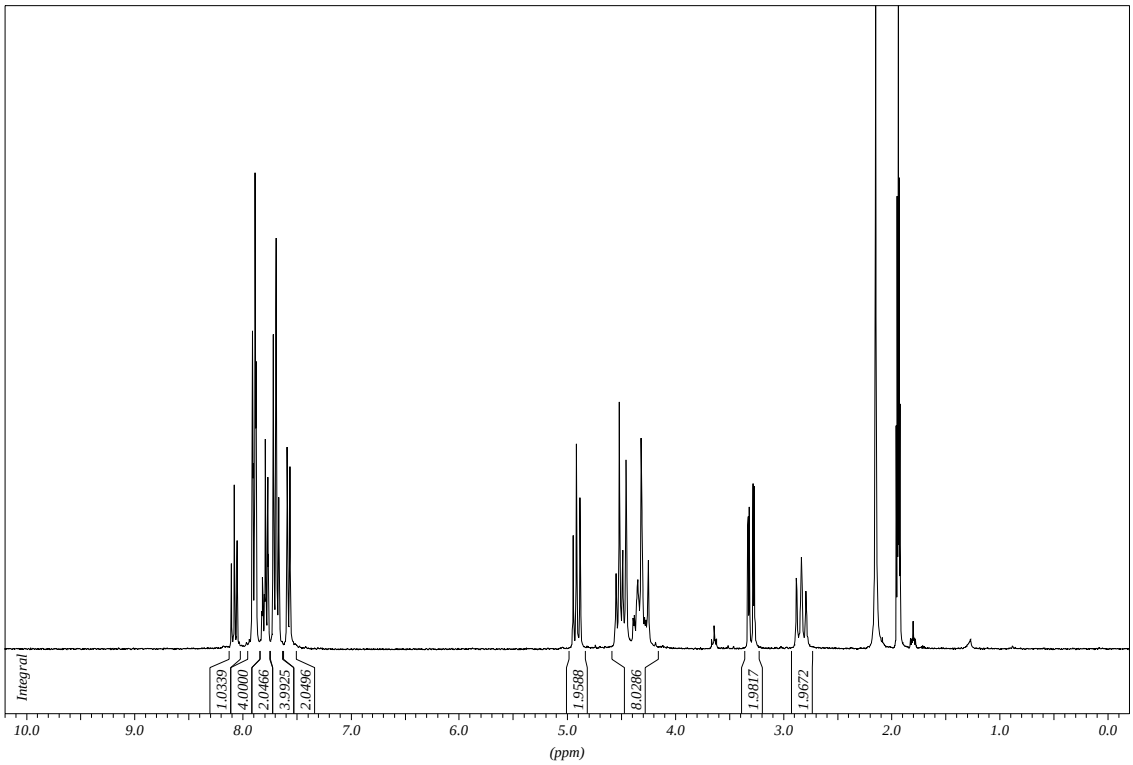

^{13}C-NMR (75.5 MHz, CD_3CN)

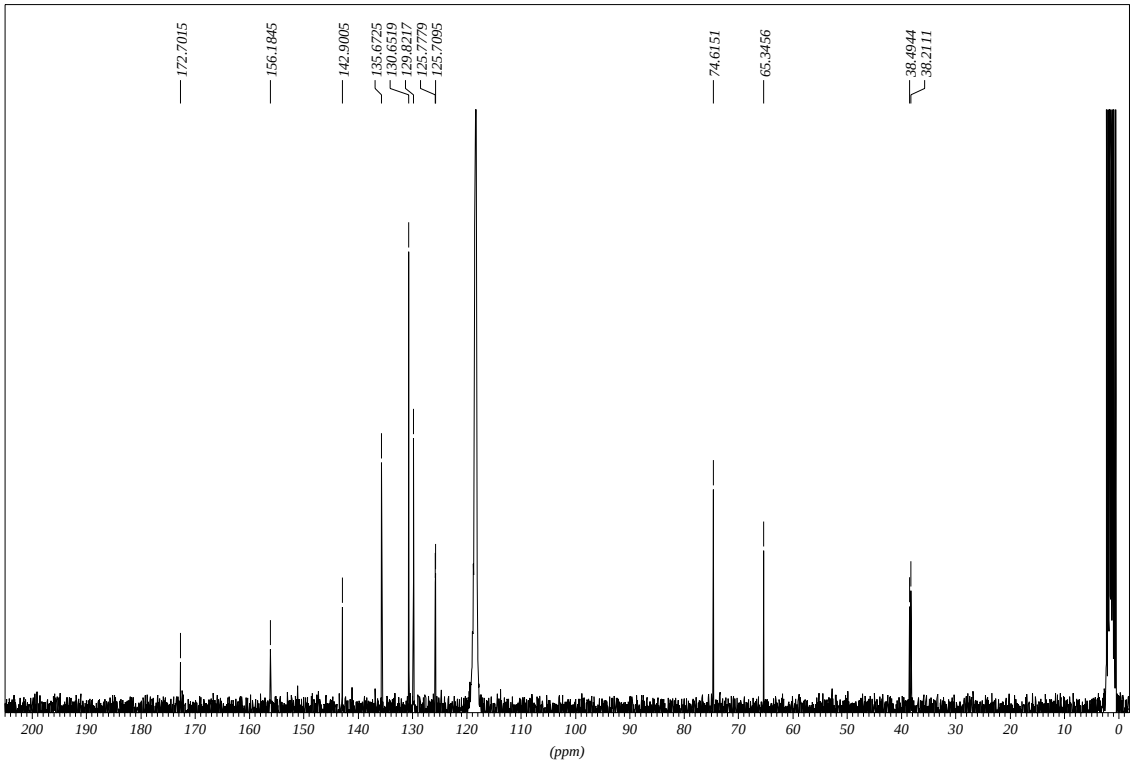

Zn^{II}(2c)]$(ClO_4)_2$*H_2O*CH_3CN

^{1}H-NMR (300 MHz, CD_3CN)

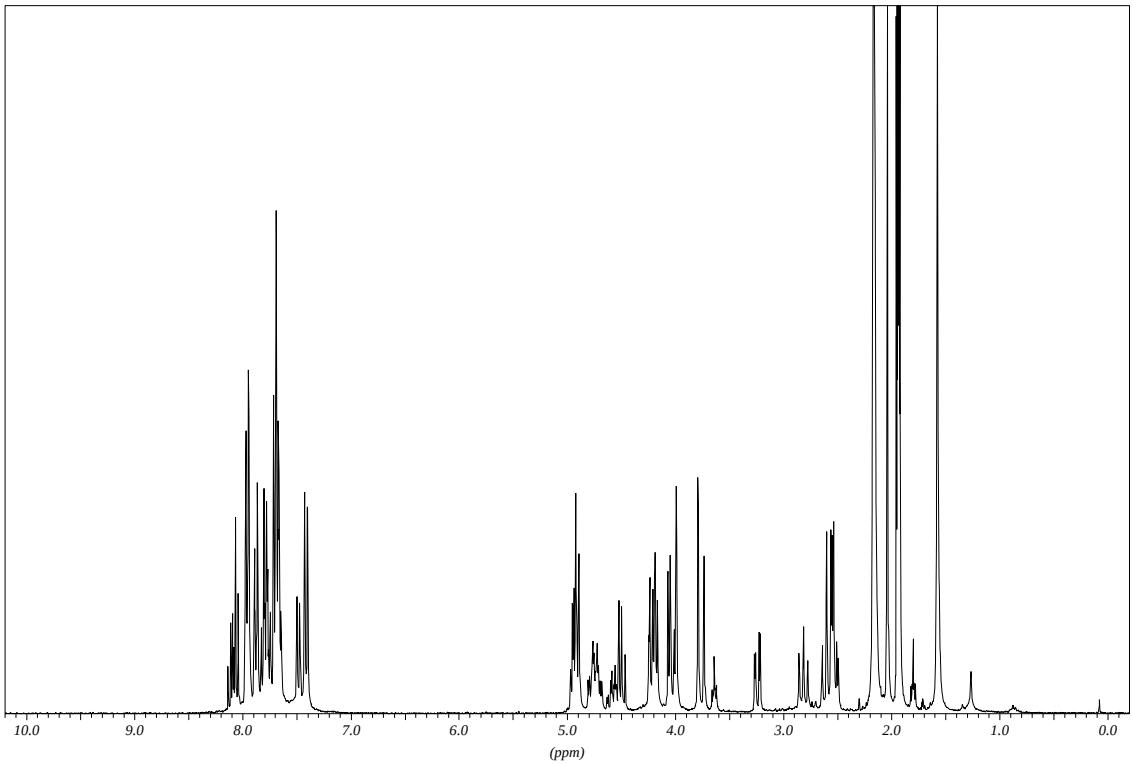

$[Cd^{II}(2a)(?)](ClO_4)_2$

^{1}H-NMR (300 MHz, CD_3CN)

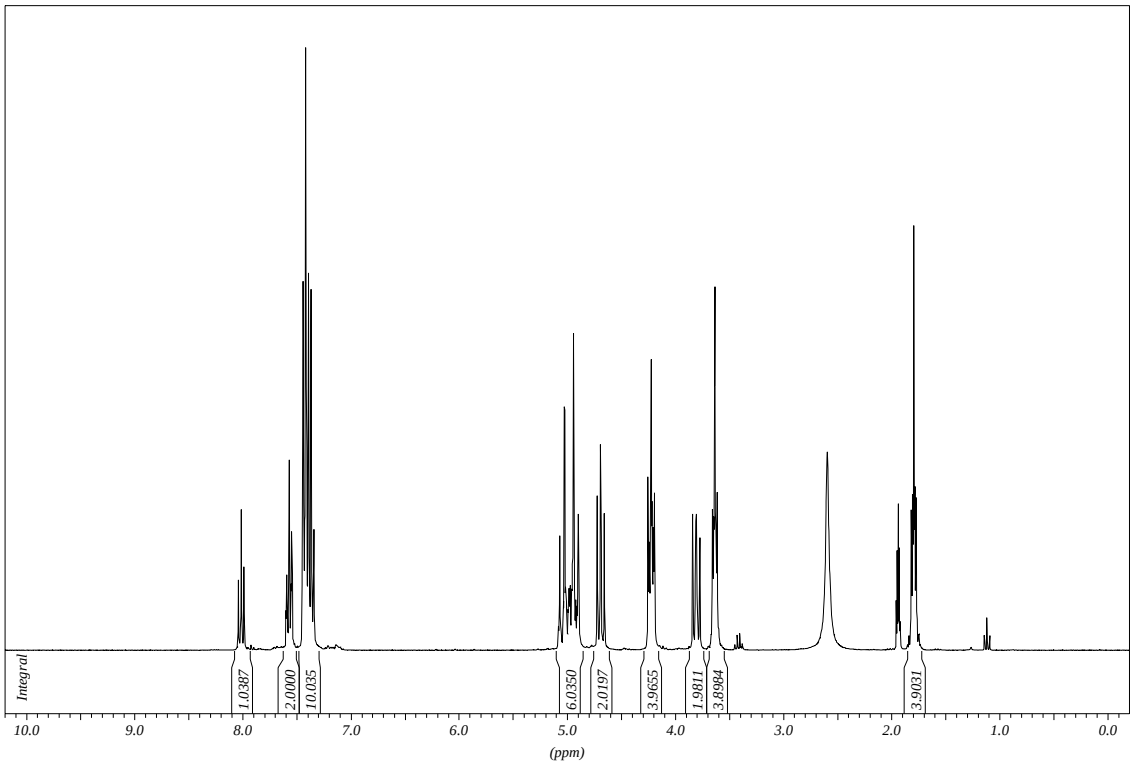

^{13}C-NMR (75.5 MHz, CD_3CN)

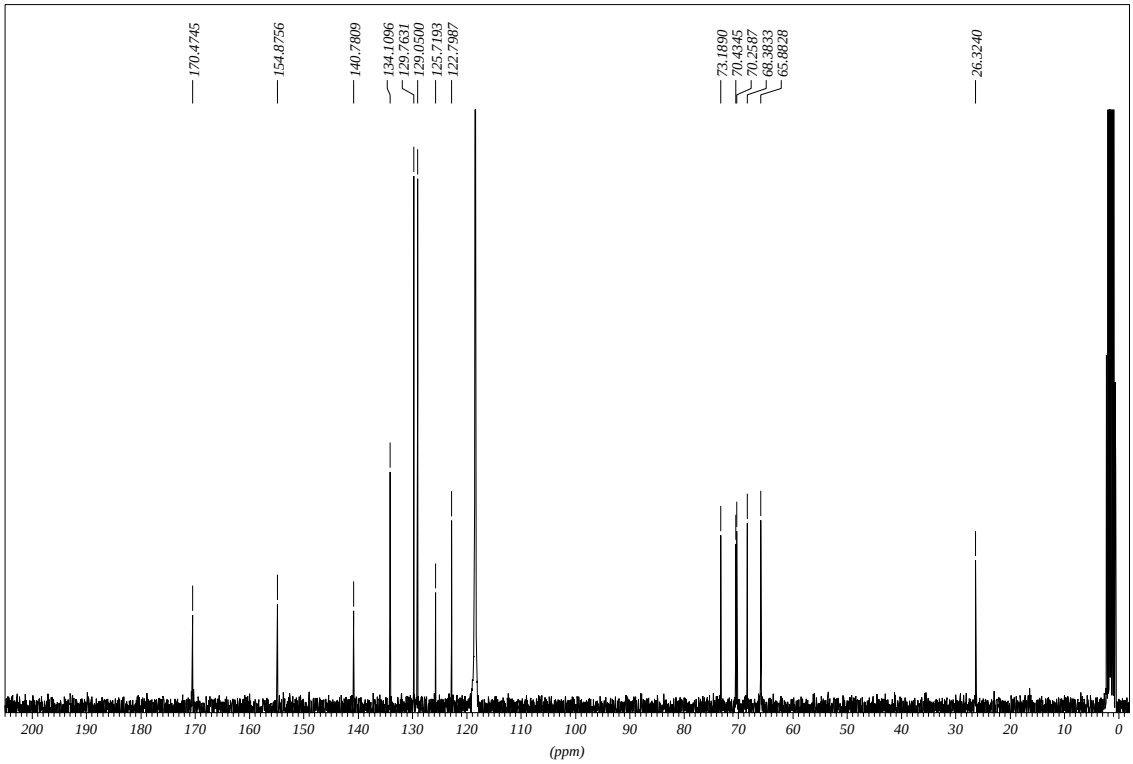

[Ru(2b)(?)]Cl_n and [Ru(2b)Cl]Cl

^{1}H-NMR (600 MHz, $CDCl_3$)

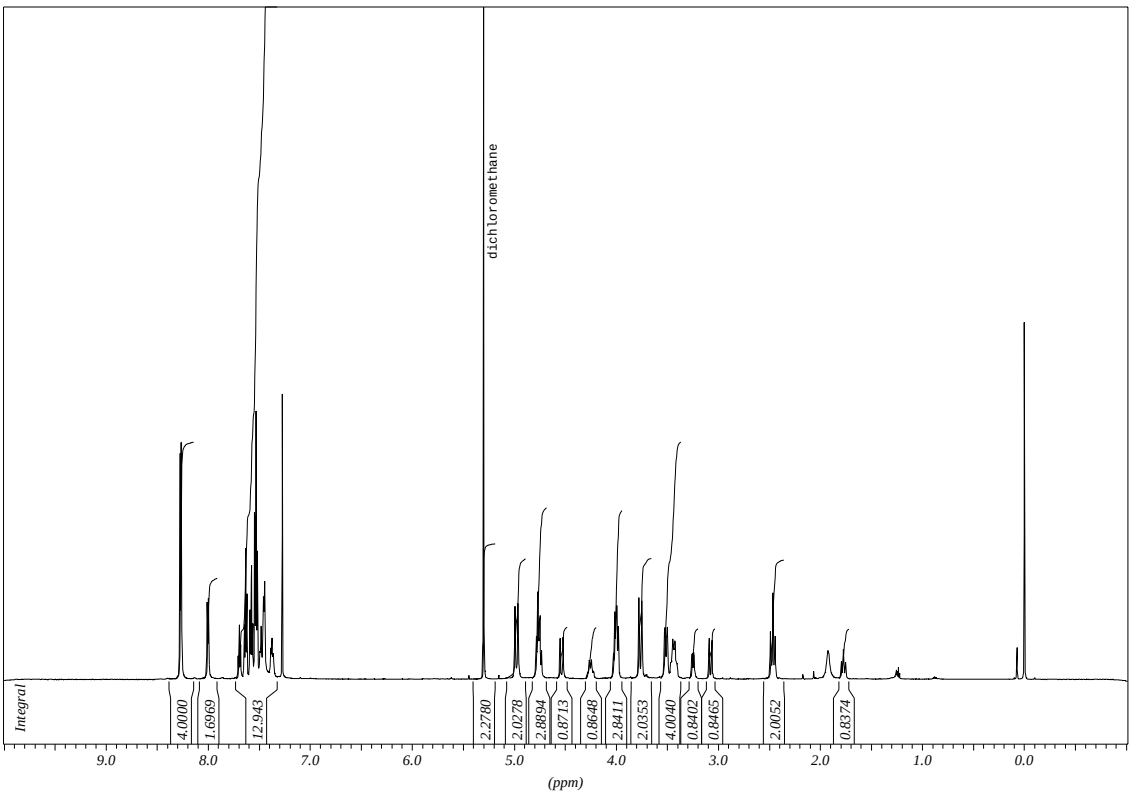

$_{\infty}$[Cd(2a)Cl_4Cd] (19)

^{1}H-NMR (300 MHz, CD_3CN)

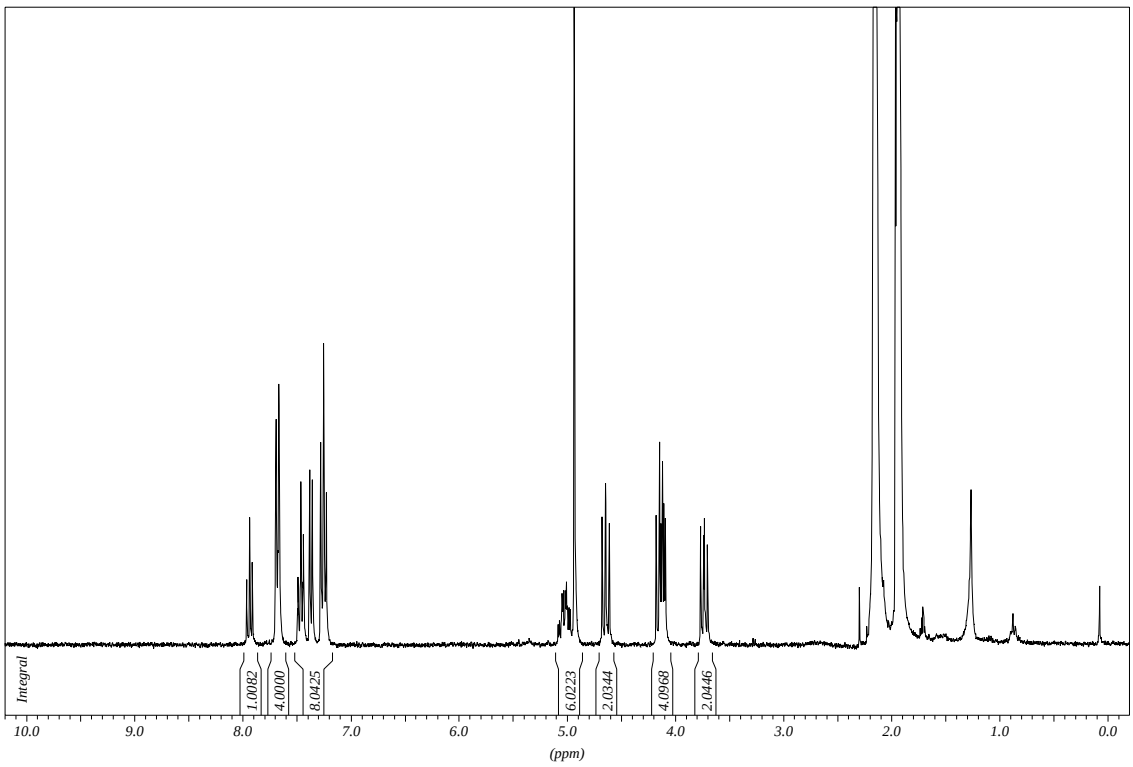

$_{\infty}$[Cd(2a)Br$_4$Cd] (20)

^{1}H-NMR (300 MHz, CD_3CN)

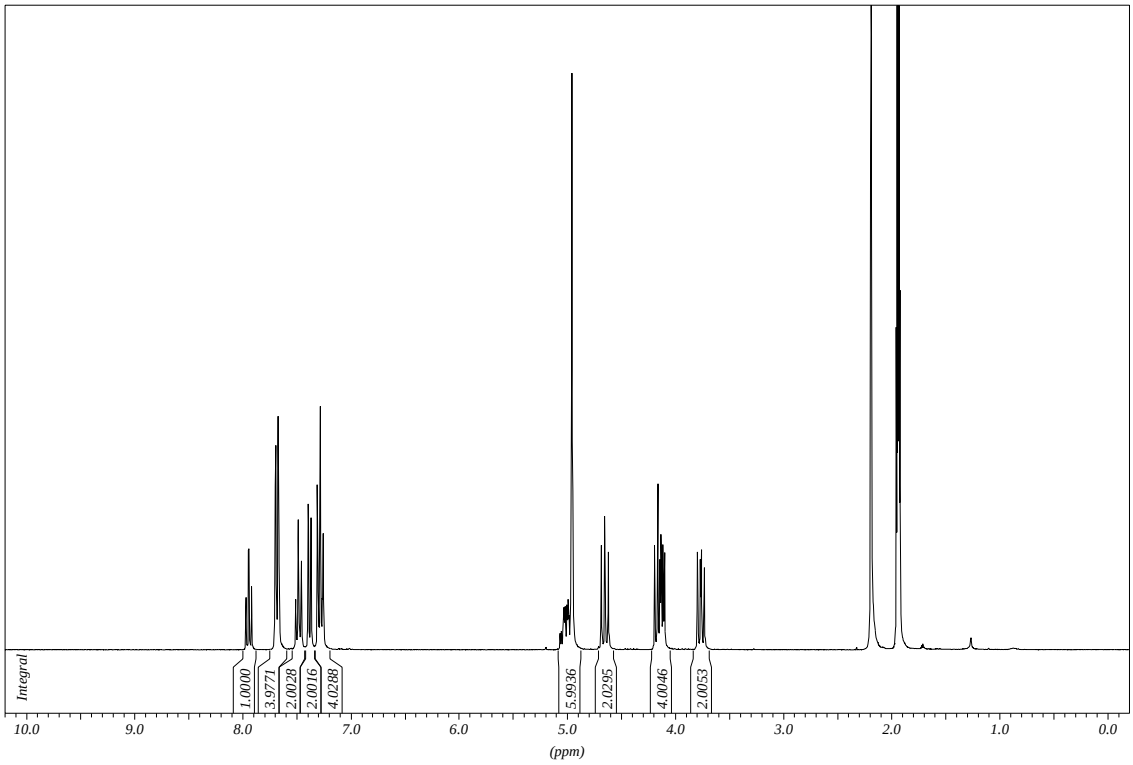

^{13}C-NMR (75.5 MHz, CD_3CN)

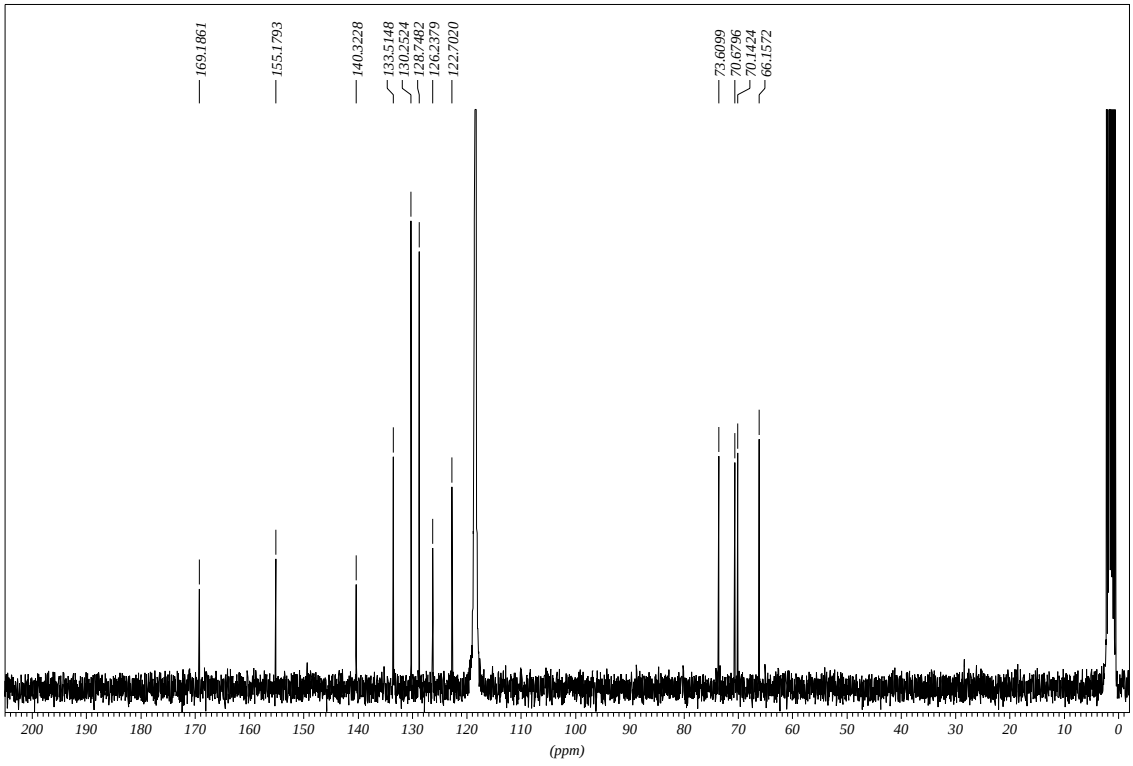

9.2 Crystal Structures – Selected Data

Selected bond lengths [Å] and angles [°]

$[Fe(2a)(H_2O)_2](ClO_4)_2$*THF

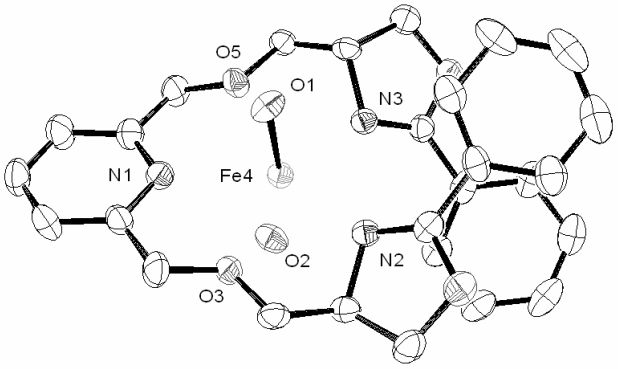

ORTEP-plot of $[Fe(\mathbf{2a})(H_2O)_2]^{2+}$ (50% probability level, hydrogens omitted for clarity) with atom numbering scheme.

Fe(4)-O(1)	2.111(3)
Fe(4)-O(2)	2.148(3)
Fe(4)-O(3)	2.332(3)
Fe(4)-O(5)	2.336(3)
Fe(4)-N(1)	2.339(3)
Fe(4)-N(2)	2.268(3)
Fe(4)-N(3)	2.232(3)

O(1)-Fe(4)-O(2)	168.99(14)
O(1)-Fe(4)-O(3)	91.46(10)
O(1)-Fe(4)-O(5)	82.45(10)
O(1)-Fe(4)-N(1)	86.02(11)
O(1)-Fe(4)-N(2)	87.57(12)
O(1)-Fe(4)-N(3)	98.82(14)
O(2)-Fe(4)-O(3)	83.94(12)
O(2)-Fe(4)-O(5)	93.41(12)
O(2)-Fe(4)-N(1)	82.98(14)
O(2)-Fe(4)-N(2)	100.26(14)
O(2)-Fe(4)-N(3)	89.48(15)
O(3)-Fe(4)-O(5)	133.29(10)
O(3)-Fe(4)-N(1)	66.92(10)
O(3)-Fe(4)-N(2)	70.68(10)
O(3)-Fe(4)-N(3)	154.32(10)
O(5)-Fe(4)-N(1)	66.47(10)
O(5)-Fe(4)-N(2)	153.96(10)
O(5)-Fe(4)-N(3)	71.75(10)
N(1)-Fe(4)-N(2)	136.89(10)
N(1)-Fe(4)-N(3)	136.89(10)
N(2)-Fe(4)-N(3)	86.22(10)

[Co(2b)(THF)](OTf)$_2$

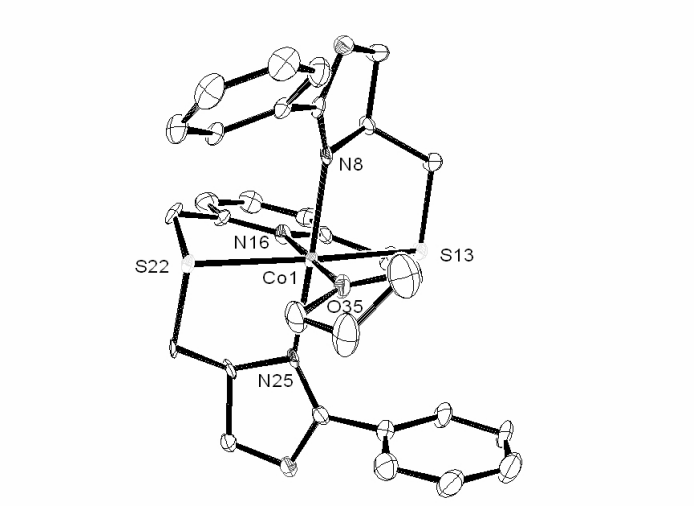

ORTEP-plot of [Co(**2b**)(THF)]$^{2+}$ (50% probability level, hydrogens omitted for clarity) with atom numbering scheme.

Co(1)-O(35)	2.066(4)
Co(1)-N(16)	2.106(5)
Co(1)-N(25)	2.124(5)
Co(1)-N(8)	2.143(5)
Co(1)-S(13)	2.4631(17)
Co(1)-S(22)	2.4800(17)

O(35)-Co(1)-N(16)	179.7(2)
O(35)-Co(1)-N(25)	92.89(18)
N(16)-Co(1)-N(25)	87.26(19)
O(35)-Co(1)-N(8)	92.56(18)
N(16)-Co(1)-N(8)	87.29(19)
N(25)-Co(1)-N(8)	174.5(2)
O(35)-Co(1)-S(13)	97.19(14)
N(16)-Co(1)-S(13)	82.51(17)
N(25)-Co(1)-S(13)	97.14(15)
N(8)-Co(1)-S(13)	82.20(15)
O(35)-Co(1)-S(22)	97.72(14)
N(16)-Co(1)-S(22)	82.59(17)
N(25)-Co(1)-S(22)	80.61(15)
N(8)-Co(1)-S(22)	98.63(15)
S(13)-Co(1)-S(22)	165.02(6)

[Co(2c)(H_2O)]($OTf)_2$

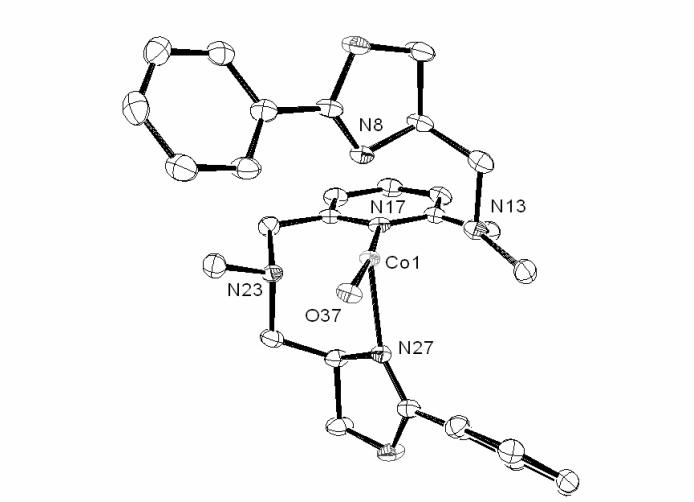

ORTEP-plot of [Co(**2c**)(H_2O)]$^{2+}$ (50% probability level, hydrogens omitted for clarity) with atom numbering scheme.

Co(1)-O(37)	2.0250(18)
Co(1)-N(17)	2.065(2)
Co(1)-N(27)	2.167(2)
Co(1)-N(8)	2.220(2)
Co(1)-N(23)	2.255(2)
Co(1)-N(13)	2.263(2)

O(37)-Co(1)-N(17)	174.42(9)
O(37)-Co(1)-N(27)	91.99(7)
N(17)-Co(1)-N(27)	89.02(8)
O(37)-Co(1)-N(8)	90.66(7)
N(17)-Co(1)-N(8)	88.51(7)
N(27)-Co(1)-N(8)	176.83(9)
O(37)-Co(1)-N(23)	97.39(8)
N(17)-Co(1)-N(23)	77.36(9)
N(27)-Co(1)-N(23)	80.28(8)
N(8)-Co(1)-N(23)	101.11(8)
O(37)-Co(1)-N(13)	107.83(8)
N(17)-Co(1)-N(13)	77.47(9)
N(27)-Co(1)-N(13)	97.15(8)
N(8)-Co(1)-N(13)	80.36(8)
N(23)-Co(1)-N(13)	154.74(8)

[Zn(2a)](ClO$_4$)$_2$

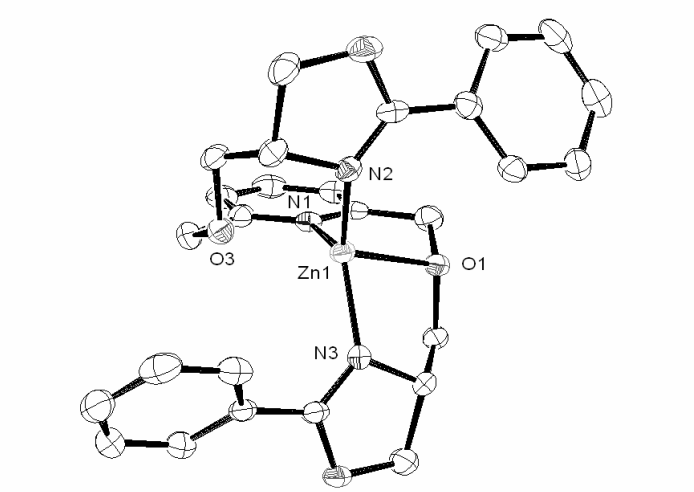

ORTEP-plot of [Zn(**2a**)]$^{2+}$ (50% probability level, hydrogens omitted for clarity) with atom numbering scheme.

Zn(1)-O(1)	2.220
Zn(1)-O(3)	2.275
Zn(1)-N(1)	2.031
Zn(1)-N(2)	1.961
Zn(1)-N(3)	1.953

O(1)-Zn(1)-O(3)	152.56
O(1)-Zn(1)-N(1)	76.93
O(1)-Zn(1)-N(2)	115.31
O(1)-Zn(1)-N(3)	80.64
O(3)-Zn(1)-N(1)	76.07
O(3)-Zn(1)-N(2)	80.43
O(3)-Zn(1)-N(3)	107.30
N(1)-Zn(1)-N(2)	113.74
N(1)-Zn(1)-N(3)	116.45
N(2)-Zn(1)-N(3)	129.62

[Zn(2a)](OTf)$_2$*CH$_2$Cl$_2$

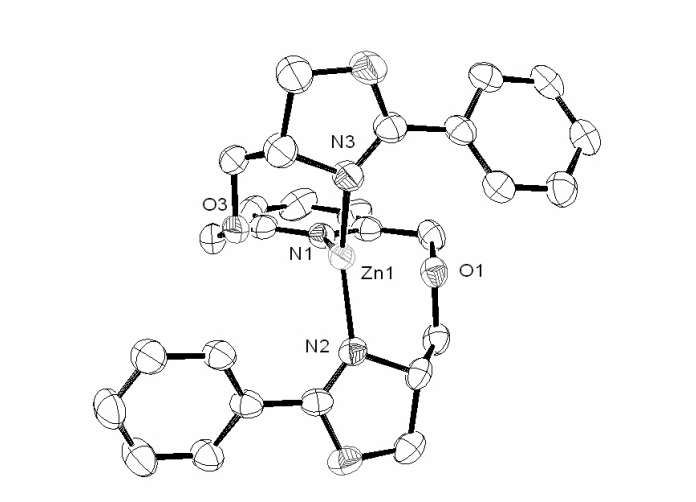

ORTEP-plot of [Zn(**2a**)]$^{2+}$ (50% probability level, hydrogens omitted for clarity) with atom numbering scheme.

Zn(1)-O(1)	2.261(2)
Zn(1)-O(3)	2.251(2)
Zn(1)-N(1)	2.031(3)
Zn(1)-N(2)	1.978(3)
Zn(1)-N(3)	1.969(3)

O(1)-Zn(1)-O(3)	152.76(9)
O(1)-Zn(1)-N(1)	76.31(9)
O(1)-Zn(1)-N(2)	80.22(9)
O(1)-Zn(1)-N(3)	109.84(9)
O(3)-Zn(1)-N(1)	76.45(10)
O(3)-Zn(1)-N(2)	110.96(10)
O(3)-Zn(1)-N(3)	80.82(10)
N(1)-Zn(1)-N(2)	113.55(11)
N(1)-Zn(1)-N(3)	112.44(12)
N(2)-Zn(1)-N(3)	134.00(12)

[Zn(2b)]$(ClO_4)_2$*H_2O

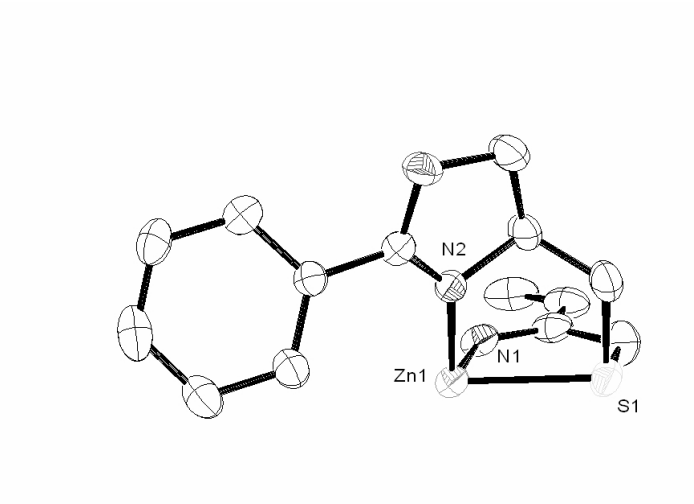

ORTEP-plot of [Zn(**2b**)]$^{2+}$ (50% probability level, hydrogens omitted for clarity) with atom numbering scheme.

Zn(1)-S(1)	2.5299(8)
Zn(1)-N(1)	2.096(3)
Zn(1)-N(2)	1.981(3)

S(1)-Zn(1)-N(1)	84.43(2)
S(1)-Zn(1)-N(2)	83.84(7)
S(1)-Zn(1)-S(1)#1	168.86(3)
S(1)-Zn(1)-N(2)#1	100.02(7)
N(1)-Zn(1)-N(2)	110.12(7)
S(1)#1-Zn(1)-N(1)	84.43(2)
N(1)-Zn(1)-N(2)#1	110.12(7)
S(1)#1-Zn(1)-N(2)	100.02(7)
N(2)-Zn(1)-N(2)#1	139.76(10)
S(1)#1-Zn(1)-N(2)#1	83.84(7)

[Zn(2c)]$(ClO_4)_2$*CH_3CN*H_2O

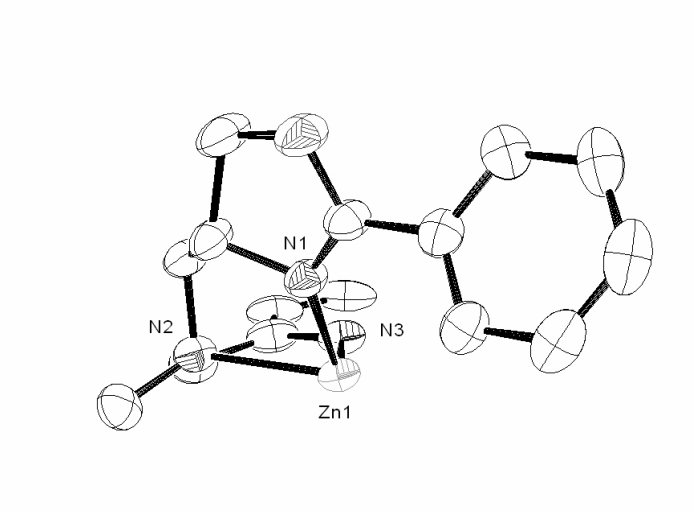

ORTEP-plot of [Zn(**2c**)]$^{2+}$ (50% probability level, hydrogens omitted for clarity) with atom numbering scheme.

Zn(1)-N(1)	2.025(2)
Zn(1)-N(2)	2.286(2)
Zn(1)-N(3)	2.108(2)

N(1)-Zn(1)-N(2)	81.77(9)
N(1)-Zn(1)-N(3)	119.00(6)
N(1)-Zn(1)-N(1)#1	122.01(9)
N(1)-Zn(1)-N(2)#1	112.84(9)
N(2)-Zn(1)-N(3)	75.36(6)
N(1)#1-Zn(1)-N(2)	112.84(9)
N(2)-Zn(1)-N(2)#1	150.73(9)
N(1)#1-Zn(1)-N(3)	119.00(6)
N(2)#1-Zn(1)-N(3)	75.36(6)
N(1)#1-Zn(1)-N(2)#1	81.77(9)

{[Cd(2b)(ClO_4)](ClO_4)}$_3$*CH_3CN

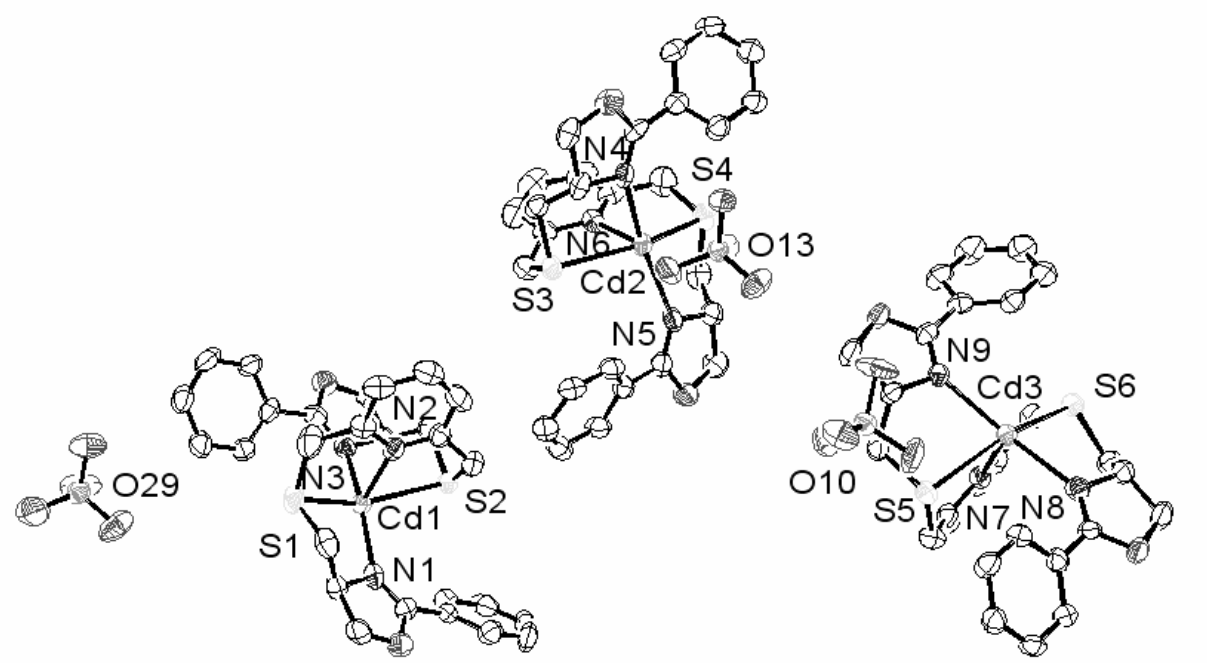

ORTEP-plot of the three unique units of [Cd(**2b**)(ClO_4)]$^+$ (50% probability level, hydrogens omitted for clarity) with atom numbering scheme.

Cd(1)-S(1)	2.6530(17)	Cd(2)-S(3)	2.6454(19)	Cd(3)-S(5)	2.6729(15)
Cd(1)-S(2)	2.6790(18)	Cd(2)-S(4)	2.6747(18)	Cd(3)-S(6)	2.6838(17)
Cd(1)-N(1)	2.277(5)	Cd(2)-N(4)	2.347(5)	Cd(3)-N(8)	2.333(5)
Cd(1)-N(2)	2.416(5)	Cd(2)-N(6)	2.402(5)	Cd(3)-N(7)	2.403(5)
Cd(1)-N(3)	2.297(5)	Cd(2)-N(5)	2.310(5	Cd(3)-N(9)	2.343(5)
Cd(1)-O(10)#1	2.609(5)	Cd(2)-O(13)	2.581(5)	Cd(3)-O(29)#2	2.392(6)
S(1)-Cd(1)-S(2)	150.16(5)	S(3)-Cd(2)-S(4)	151.36(6)	S(5)-Cd(3)-S(6)	151.62(5)
S(1)-Cd(1)-N(1)	80.59(14)	S(3)-Cd(2)-N(4)	79.69(12)	S(5)-Cd(3)-N(7)	77.26(12)
S(1)-Cd(1)-N(2)	74.78(13)	S(3)-Cd(2)-N(6)	77.44(13)	S(5)-Cd(3)-N(9)	78.61(12)
S(1)-Cd(1)-N(3)	108.46(14)	S(3)-Cd(2)-N(5)	102.11(13)	S(5)-Cd(3)-N(8)	101.40(13)
S(1)-Cd(1)-O(10)#1	80.79(12)	S(3)-Cd(2)-O(13)	128.40(13)	S(5)-Cd(3)-O(29)#2	122.49(17)
S(2)-Cd(1)-N(1)	101.93(13)	S(4)-Cd(2)-N(4)	108.60(13)	S(6)-Cd(3)-N(8)	79.54(13)
S(2)-Cd(1)-N(2)	75.63(13)	S(4)-Cd(2)-N(6)	74.38(13)	S(6)-Cd(3)-N(7)	74.49(12)
S(2)-Cd(1)-N(3)	78.49(13)	S(4)-Cd(2)-N(5)	79.68(13)	S(6)-Cd(3)-N(9)	106.20(13)
S(2)-Cd(1)-O(10)#1	128.96(12)	S(4)-Cd(2)-O(13)	80.16(12)	S(6)-Cd(3)-O(29)#2	85.88(17)
N(1)-Cd(1)-N(2)	101.89(17)	N(4)-Cd(2)-N(6)	96.99(18)	N(7)-Cd(3)-N(8)	96.83(17)
N(1)-Cd(1)-N(3)	161.40(18)	N(4)-Cd(2)-N(5)	159.62(17)	N(8)-Cd(3)-N(9)	168.13(18)
N(2)-Cd(1)-N(3)	96.24(17)	N(5)-Cd(2)-N(6)	103.23(18)	N(7)-Cd(3)-N(9)	94.74(16)
O(10)#1-Cd(1)-N(1)	77.06(16)	O(13)-Cd(2)-N(4)	84.72(16)	O(29)#2-Cd(3)-N(8)	85.66(17)
O(10)#1-Cd(1)-N(2)	155.33(17)	O(13)-Cd(2)-N(6)	153.68(17)	O(29)#2-Cd(3)-N(7)	159.3(2)
O(10)#1-Cd(1)-N(3)	88.19(17)	O(13)-Cd(2)-N(5)	78.30(16)	O(29)#2-Cd(3)-N(9)	84.43(17)

$_{\infty}$[Cd(2a)Cl_4Cd] (19)

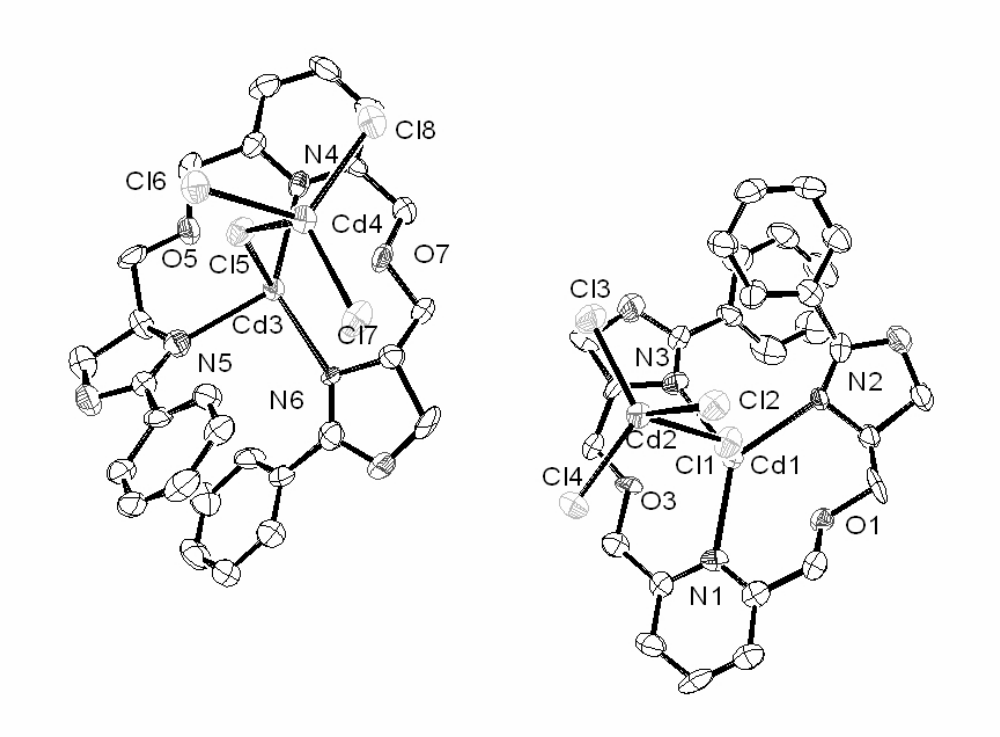

ORTEP-plot of the two unique units of $_{\infty}$[Cd(**2a**)Cl_4Cd] (**19**) (50% probability level, hydrogens omitted for clarity) with atom numbering scheme.

Cd3-N4	2.444(13)	Cd1-N1	2.424(13)
Cd3-O5	2.527(12)	Cd1-O1	2.503(9)
Cd3-O7	2.471(10)	Cd1-O3	2.458(9)
Cd3-N5	2.402(12)	Cd1-N2	2.410(11)
Cd3-N6	2.363(12)	Cd1-N3	2.319(12)
Cd3-Cl5	2.596(4)	Cd1-Cl1	2.601(4)
Cd4-Cl5	2.514(4)	Cd2-Cl1	2.503(4)
Cd4-Cl6	2.520(4)	Cd2-Cl2	2.517(4)
Cd4-Cl7	2.390(5)	Cd2-Cl3	2.401(5)
Cd4-Cl8	2.417(5)	Cd2-Cl4	2.407(5)
Cl5-Cd3-O5	86.6(2)	Cl1-Cd1-O1	86.5(2)
Cl5-Cd3-O7	90.1(2)	Cl1-Cd1-O3	90.3(2)
Cl5-Cd3-N4	80.9(2)	Cl1-Cd1-N1	83.0(3)
Cl5-Cd3-N5	88.0(2)	Cl1-Cd1-N2	87.4(2)
Cl5-Cd3-N6	103.7(3)	Cl1-Cd1-N3	101.8(3)
O5-Cd3-O7	128.8(4)	O1-Cd1-O3	130.0(4)
O5-Cd3-N4	65.0(4)	O1-Cd1-N1	64.1(4)
O5-Cd3-N5	68.1(4)	O1-Cd1-N2	69.2(4)
O5-Cd3-N6	158.4(4)	O1-Cd1-N3	160.0(4)
O7-Cd3-N4	64.1(4)	O3-Cd1-N1	66.0(4)
O7-Cd3-N5	162.9(4)	O3-Cd1-N2	160.5(3)
O7-Cd3-N6	70.9(4)	O3-Cd1-N3	68.7(4)
N4-Cd3-N5	132.2(4)	N1-Cd1-N2	132.7(4)
N4-Cd3-N6	134.7(4)	N1-Cd1-N3	134.4(4)
N5-Cd3-N6	93.0(4)	N2-Cd1-N3	92.9(4)
Cl5-Cd4-Cl6	89.24(13)	Cl1-Cd2-Cl2	89.03(13)
Cl5-Cd4-Cl7	116.38(17)	Cl1-Cd2-Cl3	115.07(16)
Cl5-Cd4-Cl8	108.32(17)	Cl1-Cd2-Cl4	110.53(17)
Cl6-Cd4-Cl7	113.92(17)	Cl2-Cd2-Cl3	111.97(16)
Cl6-Cd4-Cl8	108.59(17)	Cl2-Cd2-Cl4	107.45(17)
Cl7-Cd4-Cl8	116.92(19)	Cl3-Cd2-Cl4	118.67(17)
Cd3-Cl5-Cd4	128.78(16)	Cd1-Cl1-Cd2	131.01(16)
Cd3-Cl6-Cd4	132.92(17)	Cd1-Cl2-Cd2	130.67(17)

$_{\infty}$[Cd(2a)Br_4Cd] (20)

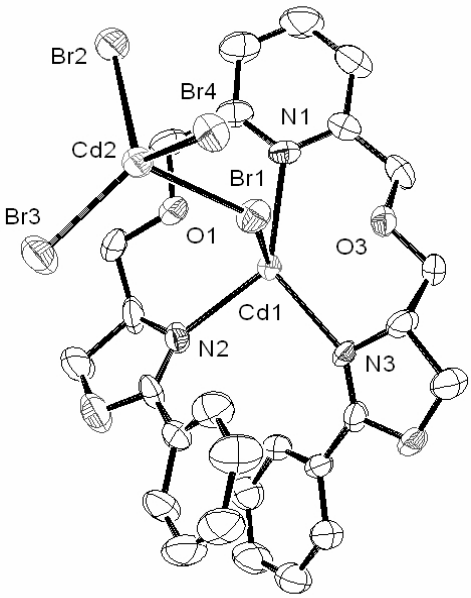

ORTEP-plot of the two unique units of $_{\infty}$[Cd(**2a**)Br_4Cd] (**20**) (50% probability level, hydrogens omitted for clarity) with atom numbering scheme.

Cd1-N1	2.445(5)
Cd1-O1	2.459(5)
Cd1-O3	2.507(4)
Cd1-N2	2.356(6)
Cd1-N3	2.408(5)
Cd1-Br1	2.7137(10)
Cd2-Br1	2.6362(12)
Cd2-Br2	2.5449(9)
Cd2-Br3	2.5246(11)
Cd2-Br4	2.6466(12)

Br1-Cd1-O1	93.65(19)
Br1-Cd1-O3	80.02(17)
Br1-Cd1-N1	84.24(19)
Br1-Cd1-N2	96.7(2)
Br1-Cd1-N3	92.78(15)
O1-Cd1-O3	128.49(16)
O1-Cd1-N1	64.05(18)
O1-Cd1-N2	69.59(19)
O1-Cd1-N3	162.28(19)
O3-Cd1-N1	64.46(18)
O3-Cd1-N2	161.59(19)
O3-Cd1-N3	68.96(18)
N1-Cd1-N2	133.6(2)
N1-Cd1-N3	133.14(19)
N2-Cd1-N3	93.3(2)
Br1-Cd2-Br2	110.07(4)
Br1-Cd2-Br3	111.08(4)
Br1-Cd2-Br4	88.29(3)
Br2-Cd2-Br3	118.78(4)
Br2-Cd2-Br4	106.54(4)
Br3-Cd2-Br4	117.89(4)

Cd1-Br1-Cd2	128.66(5)
Cd1-Br2-Cd2	129.36(5)

9.3 List of Publications

Research Articles

1) Marina Schinnerl, Michael Seitz, Anja Kaiser, Oliver Reiser, *Org. Lett.* **2001**, *3*, 4259-4262:
New Applications for Bis(oxazoline) Ligands in Catalysis: Asymmetric 1,2- and 1,4-Addition of ZnR_2 to Carbonyl Compounds.

2) Rakeshwar B. Chhor, Bernd Nosse, Sebastian Sörgel, Claudius Böhm, Michael Seitz, Oliver Reiser, *Chem. Eur. J.* **2003**, *9*, 260-270:
Enantioselective Synthesis of Paraconic Acids.

3) Marina Schinnerl, Claudius Böhm, Michael Seitz, Oliver Reiser, *Tetrahedron: Asymmetry* **2003**, *14*, 765-771:
New bis(oxazoline) ligands with secondary binding sites for the asymmetric cyclopropanation of furans.

4) Michael Seitz, Anja Kaiser, Douglas R. Powell, Andrew S. Borovik, Oliver Reiser, *Adv. Synth. Catal.* **2004**, *346*, 737-741:
Predetermined helical chirality in octahedral complexes with a novel pentadentate C_2-symmetric chiral bis(oxazoline) ligand

5) Michael Seitz, Anja Kaiser, Sabine Stempfhuber, Manfred Zabel, Oliver Reiser, submitted:
Helical, non-racemic inorganic-organic hybrid polymers of cadmium halides with pentadentate bis(oxazoline) ligands

6) Michael Seitz, Sabine Stempfhuber, Manfred Zabel, Oliver Reiser, submitted:
Predetermined helical chirality in pentacoordinate zinc complexes – First selective access to both pseudo-enantiomers with one ligand-stereochemistry

Miscellaneous

7) Michael Seitz, *Angew. Chem. Int. Ed.* **2001**, *40*, 3922:
Principles and Applications of Asymmetric Synthesis. By Guo-Qiang Lin, Yue-Ming Li and Albert S.C. Chan (Book Review)

10 Acknowledgement

Ich danke Prof. Dr. O. Reiser für die interessante Themenstellung, die beständige Unterstützung in jeglicher Hinsicht und das entgegengebrachte Vertrauen.

Ebenso schulde ich Prof. Dr. A. S. Borovik (University of Kansas, Lawrence, USA) und seiner Familie Dank für die herzliche Aufnahme, die sehr angenehme und interessante Zeit im Mittleren Westen und nicht zuletzt für die Möglichkeit, ein paar neue wissenschaftliche Perspektiven zu erhalten.

Der Deutschen Forschungsgemeinschaft danke ich für die finanzielle Unterstützung der Arbeit und speziell für die grosszügige Gewährung von Reisemitteln für meinen USA-Aufenthalt.

Ausserdem bin ich folgenden Leuten zu Dank verpflichtet (in beliebiger Reihenfolge):

Dr. Peter Kreitmeier für Allwissenheit und Hilfsbereischaft in jeglicher Hinsicht.

Frau Kratochvil, Frau Rotermund und Frau Ohli für grosse Hilfbereitschaft.

Herrn Dr. Burgemeister, Frau Stühler, Frau Schramm und Herrn Kastner für die Aufnahme von NMR-Spektren und immer ein offenes Ohr, auch für knifflige Fragen.

Herrn Dr. Zabel, Herrn Dr. Powell (University of Kansas, Lawrence, USA) und Frau Stempfhuber für die Lösung der Röngtenstrukturen und die geduldige Hilfsbereitschaft, auch wenn die Kristalle einmal nicht so optimal waren.

Herrn Dr. Mayer, Herrn Söllner und Herrn Kiermaier für die Aufnahme von Massenspektren.

Herrn Wandinger und seinen Mitarbeitern für die Durchführung der Elementaranalysen.

Brigitte Eichenseher, Georg Adolin, Klaus Döring, Robert Tomahogh und Andrea Roithmaier für grosse Hilfsbereitschaft, immer lustige Gespräche und den lebenswichtigen Cola-Nachschub.

Allen aktuellen und ehemaligen Mitstreitern der Lehrstühle Prof. Reiser und Prof. Borovik für ein gutes Arbeitsklima, gegenseitige Hilfbereitschaft und eine Menge Spass im Laufe der langen Jahre.

Den Mitstudenten meines Semesters für eine phänomenale Zeit und einige der lustigsten Erinnerungen meines Lebens.

Allen meinen Freunden für die geschenkte Zeit, gute Gespräche und das Teilen von Freud´ und Leid.